

# THE TECHNICAL COOPERATION PROGRAM

SUBCOMMITTEE ON NON-ATOMIC MILITARY RESEARCH AND DEVELOPMENT

SUBGROUP W

PROCEEDING OF THE WORKSHOP ON THE  
MICROCALORIMETRY OF ENERGETIC MATERIALS

7 - 9th APRIL 1997

LEEDS, UNITED KINGDOM

19980102 076

**DISTRIBUTION STATEMENT A**

Approved for public release;  
Distribution Unlimited

DTIC QUALITY INSPECTED 4

**THE TECHNICAL COOPERATION PROGRAMME**

**SUBCOMMITTEE ON NON-NUCLEAR RESEARCH AND DEVELOPMENT**

**SUBGROUP W**

**PROCEEDINGS OF THE WORKSHOP ON THE  
MICROCALORIMETRY OF ENERGETIC MATERIALS**

**7 - 9th APRIL  
LEEDS, UNITED KINGDOM**

**APRIL 1997**

**PUBLISHED BY  
DEFENCE RESEARCH AGENCY  
WX3 PYROTECHNICS GROUP  
ELECTRO-OPTIC WARFARE DEPARTMENT  
FORT HALSTEAD  
SEVENOAKS  
KENT TN14 7BP  
UNITED KINGDOM**

## TABLE OF CONTENTS

PREFACE	i
MICROCALORIMETRY: AN ANALYTICAL TOOL FOR MONITORING STABILITY, COMPATIBILITY AND AGING.	A1 - 2
B E DOUDA	
MICROCALORIMETRIC INVESTIGATION OF ENERGETIC MATERIALS : A REVIEW OF METHODIC DEVELOPMENT AT BICT.	B1 - 15
S WILKER, G PANTEL, U TICAMUS, P GUILLAME	
DETERMINATION OF INTERACTION PROFILES IN COMPATIBILITY TESTING.	C1 - 9
L G SVENSSON	
MICROCALORIMETRIC CRITERIA FOR EVALUATION OF CORROSIVE LIQUID PROPELLANT ON METAL CONTAINERS.	D1 - 11
A CHIN, D S ELLISON, D R CROWLEY, H A FARMER	
PRELIMINARY MICROCALORIMETRY STUDIES OF ADVANCED GUN PROPELLANTS.	E1 - 15
A WHITE, R M KEMPSON, P BERRY	
THE USE OF MICROCALORIMETRY IN THE PREDICTIVE SURVEILLANCE PROGRAM.	F1 - 9
J A WILSON, A CHIN	
KINETIC DESCRIPTION OF THE AGEING OF GUN AND ROCKET PROPELLANTS FOR THE PREDICTION OF THEIR SERVICE LIFETIME.	G1 - 31
A BOHN	
20MM GUN PROPELLANT SAFETY SERVICE LIFE STUDY USING MICROCALORIMETRY/ HPLC CORRELATION DIAGRAMS.	H1 - 12
A CHIN, D S ELLISON	
AN ASSESSMENT OF THE STABILITY OF NITRATE ESTER BASED PROPELLANTS USING HEAT FLOW CALORIMETRY.	J1 - 12
R G JEFFREY, M McPARLAND, M ELLIOT, D J WOOD, P BARNES, N TURNER.	
INFLUENCE OF ENVIRONMENTAL FACTORS ON THE LIFETIME OF GUN PROPELLANTS INVESTIGATED WITH HEAT FLOW MICROCALORIMETRY.	K1 - 9
B J Van der MEER, W P C de KLERK	
MICROCALORIMETRIC DETERMINATION OF THE CURE REACTION IN SOME FLUORINATED POLYETHER RUBBERS.	L1 - 10
P F BUNYAN, A V CUNLIFFE	

- USE OF ISOTHERMAL MICROCALORIMETRY IN THE EARLY  
DETECTION OF DRUG FORMULATION INCOMPATIBILITIES. M1 - 14  
M A PHIPPS, R A WINNIKE
- COMPARISONS OF PYROTECHNIC WHISTLE COMPOSITIONS BY  
DIFFERENTIAL SCANNING CALORIMETRY. N1 - 5  
J A DOMANICO G V TRACY, M N GERBER
- MICROCALORIMETRY: PRELIMINARY INVESTIGATION OF  
DICHROMATED MAGNESIUM AND COMPATIBILITY STUDIES OF  
THE ENERGETIC BINDER POLYNIMMO. P1 - 13  
D BLAZER T T GRIFFITHS
- AGEING STUDIES ON THE BORON-POTASSIUM DICHROMATE  
SYSTEM. Q1 - 29  
E L CHARSLEY, H S FIELDHOUSE, J J ROONEY,  
S B WARRINGTON, T T GRIFFITHS
- PHENOMENON OF AUTOCATALYSIS IN DECOMPOSITION OF  
ENERGETIC CHEMICALS. R1 - 16  
S CHERVIN G T BODMAN
- THE DECOMPOSITION OF BRANCHED GAP BY THERMO-  
ANALYTICAL TECHNIQUES. S1 - 17  
D E G JONES, R A AUGSTEN, H FENG, K J MINTZ
- THERMAL STABILITY OF AMMONIUM DINITAMIDE AND  
AMMONIUM DINITAMIDE CONTAINING VARIOUS TABILIZERS. T1 - 7  
R F BOSWELL, A S TOMPA
- COMMON FACTORS THAT MAY AFFECT THE ACCURACY OF  
MICROCALORIMETRIC DATA. U1 - 10  
D S ELLISON, A CHIN
- PRACTICAL APPLICATION OF MICROCALORIMETRY TO THE  
STABILITY STUDIES OF PROPELLANTS. V1 - 18  
M RAT, P GUILLAUME, S WILKER, G PANTEL
- APPLICATION OF MICROCALORIMETRY AND GAS FLOW  
AMPOULE SYSTEM TO STUDY THE SHELF LIFE OF  
PYROTECHNICS. W1 - 8  
A CHIN, D S ELLISON, BR HUBBLE, R G SHORTRIDGE
- ADVANCES IN MICROCALORIMETRY. X1 -  
E A LEWIS, L F LEWIS, D J RUSSELL, C R JOHNSON
- VARIOUS CALORIMETRIC TECHNIQUES APPLIED TO THE  
CHARACTERISATION OF ENERGETIC MATERIALS. Y1 - 15  
S MOREAU, P Le PARLOUER



MICROCALORIMETRIC PERFORMANCE NOW AND IN THE  
FUTURE: ITS USE IN SOLID STATE KINETICS.

Z1 -1

J SUURKUUSK

QUESTION AND DISCUSSION

P LAYE

LIST OF ATTENDESS

DISTRIBUTION LIST

## PREFACE

This document compiles papers presented at the Workshop on Microcalorimetry as applied to propellants and pyrotechnics and held between the 7 - 9th April 1997 in Leeds UK. The Workshop was conducted under the auspices of KTA 4-21 of TTCP Subgroup WTP4. The Technical Cooperation Program is an intergovernmental programme involving Australia, Canada, New Zealand, United Kingdom and the United States, however, for this Workshop permission was sought and granted for it to be an open meeting. Consequently, the Workshop was attended by 58 participants, from 12 countries and 24 papers were presented. Attendees represented government, industry academia and three of the instrument manufactures.

No Workshop can be successful without the backing and support from various organisations and individuals therefore I would like to acknowledge the following. Firstly I would like to thank TTCP, Subgroup WTP and the Pyrotechnic Area Focus Officers for recognising the importance of the subject, for allowing the Workshop to be open to non TTCP members and to run under the auspices of TTCP. I would like to thank DERA for its support and in particular Dr Paul Reip for suggesting and financing the first evenings "mixer". Also to CINO and Dr P Barnes for their support and who have contributed towards the cost of publishing the Proceedings.

I personally would like to thank those who physically helped me to organise the Workshop and gave unstinting support. Among these are Leeds Metropolitan University and in particular Professor Ted Charsley and his staff, Ms Heidi Fieldhouse and Mr Jim Rooney. Since they were in the vicinity of the Workshop location they had the onerous job of finding a suitable venue and of arranging a social programme. The success of the Workshop is a monument to their judgement and hard work. It is appropriate at this point to thank the Chevin Lodge Hotel for the lecture facilities, comfortable accommodation, good food and for sending us away a few pounds heavier. Also the staff of Harewood House and the Cavendish Pavilion, Bolton Abbey for making our precious few hours of leisure so enjoyable.

Other individuals I would like to thank are Mr Tony Cardell for his assistance and helpful discussions on organising the Workshop and putting together the Workshop Programme. Thanks to Mr Jim Queay who has collated the papers ready for publishing and without whom I may have on occasions been lost for words. I wish to recognise the work of Mrs Janet Smith of DERA who typed all the sections which were not papers.

I wish to thank, on behalf of myself and everyone associated with organising the Workshop, Dr Peter Laye who did a magnificent job in leading the final discussion and highlighting the conclusions of the delegates.

Finally I would like to thank all the authors who submitted papers, which resulted in an interesting technical programme, and especially all the delegates for making the effort to attend for without you there would have been no Workshop.

A handwritten signature in cursive script, appearing to read 'T T Griffiths'.

T T Griffiths  
(Workshop Chairman)

## MICROCALORIMETRY

### An Analytical Tool for Monitoring Stability, Compatibility, and Aging

Bernard E. Douda  
Naval Surface Warfare Center  
Crane Division  
Crane, Indiana 47522-5001 U.S.A.

As early as 1969, and perhaps earlier, there are reports of bacterial calorimetry. This type of work accelerated during the 1970's. In 1980, I visited Mr. J. Isler at GERPy, the pyrotechnics R&D group, in Toulon, France. He described his aging study on a single base propellant and the use of a microcalorimeter made for him, if I recall correctly, by Professor Patin at the University of Marseilles. Through the mid-1980's Mr. Isler presented and published several articles on his work. This was my first introduction to microcalorimetry.

Up until then, thermal methods such as DSC, DTA and TG had been used to study stability, compatibility and aging, but the most serious limitation was that they were not sensitive enough. The main advantage of microcalorimetry was the increase in sensitivity.

Throughout the 1980's, projects using microcalorimetry to study energetic materials expanded into many countries and many organizations, primarily sponsored by government military agencies. Some leaders in Europe in this field were Elmquist, Lagerkvist Svensson and Gellerstedt in Bofors, Sweden and Isler in GERPy, France. The technique spread quickly to the UK, Germany, and the US for evaluation of not only energetics but also pharmaceuticals (Lilly Research Laboratories, US), and battery materials (Venture Technology, UK).

In 1986, Dr. Jan Hansson of the National Defense Research Institute, Sweden, arranged for me to visit Professor Wadso at the University of Lund. Prof. Wadso is credited with the invention of the apparatus later to become the LKB instrument. Seeing the instrument and its capabilities convinced me we needed to initiate energetic materials aging studies at Crane. Others in the US such as Picatinny Arsenal and the Naval Ordnance Station Indian Head did likewise. Australia at the Materials Research Laboratory (MRL) at Melbourne and Canada at the Defense Research Establishment, Valcartier (DREV), and the Defense Research Agency (DRA), UK joined in.

In the late 1980's and early 1990's, the microcalorimetry technique was being applied extensively by defense agencies to the study of energetic materials. The Technical Cooperation Program (TTCP) had initiated a Key Task Area (KTA) to explore techniques and exchange information on the degradation of pyrotechnic fuels. This work confirmed microcalorimetry as a promising technique to monitor the aging process. It was obvious that there was insufficient cross-communication between workers in this very specialized field. To remedy this situation, the TTCP leaders sanctioned a Workshop on microcalorimetry which would include academia, industry, instrument manufacturers and Government agencies.

This TTCP sponsored Workshop on Microcalorimetry will be the focus of our interest for the next three days. There are eleven countries represented from twenty four different organizations. The fifty delegates with varied backgrounds will have the opportunity to exchange information and communicate with colleagues to share common successes, problems and solutions. This is an opportunity, afforded to us by the TTCP organization, to share our experiences involving the application of microcalorimetry to a variety of materials studies.

# MICROCALORIMETRIC INVESTIGATION OF ENERGETIC MATERIALS - A REVIEW OF METHODIC DEVELOPMENT AT BICT

Stephan Wilker<sup>\*</sup>, Gabriele Pantel<sup>\*</sup>, Uldis Ticmanis<sup>\*</sup>, Pierre Guillaume<sup>^</sup>

<sup>\*</sup>Bundesinstitut für chem.-techn. Untersuchungen beim BWB, Großes Cent, D-53913 Swisttal

<sup>^</sup>PB Clermont S.A., Rue de Clermont, B-4480 Engis

## Abstract

Heat flow calorimetry (HFC) or microcalorimetry is one of the most important and promising tools in the application of stability of energetic materials, especially propellants. With the aim of microcalorimetry it is easy to estimate such important things as storage life time, the service life time, and the compatibility of propellants. At BICT the microcalorimetry has been used for 20 years and a huge amount of knowledge arose during this period.

In this paper the calculation of the service life of propellants from Arrhenius plots of double base propellants is presented. The quality and the reliability of the received data can be concluded by the fact that multiple measurements in different laboratories show the same values of the heat production rate.

HFC investigations of the decomposition reaction of a double base propellant were combined with HPLC (stabiliser loss) and GPC (molecular mass depletion) measurements under different atmospheres. By doing this the typical shape of the microcalorimetric curve can be interpreted.

The decomposition of primitive masses can be followed easily by HFC measurements. After an initial peak a very fast exothermic and extremely autocatalytic reaction can be observed with maxima of about 200  $\mu\text{W/g}$  and a total energy release of 2000 J/g. HFC is the best method to calculate critical diameters and/or critical temperatures.

Compatibility experiments can also be easily run by HFC. The advantage of this method is that all chemical reactions can be observed and not only gas generating ones (like in the vacuum stability test) or reactions that lower the decomposition temperature (like in DTA experiments). We also experienced with different mixture ratios, different sample preparations and different measuring temperatures in order to get a clear insight into the chemical processes that deliver huge amount of heat and gas.

## 1 Introduction

Heat flow calorimetry (or microcalorimetry) is one of the most useful techniques in the field of prediction of the service life of (rocket) propellants<sup>1</sup>. In comparison to other tests there are three advantages:

- a) The sensitivity of modern calorimeters is very high, so that heat flows at or even below 1  $\mu$ W can be measured reproducibly;
- b) The high sensitivity allows measurements at low temperatures (80-30°C), which are much lower than those of the „classical“ stability tests like Bergmann-Junk, Dutch weight loss or Abel test;
- c) The fundamental principle that all chemical or physical reactions, which produce heat are recorded during the whole measuring time.

From measurements at several temperatures the activation energy and the pre-exponential factor of the decomposition reaction can be calculated. It can be observed that for NC-based propellants normally a change in the activation energy and the pre-exponential factor occurs at about 60°C. Some examples of this are presented in chapter 2.

Although the kinetics of the decomposition reaction can be calculated very precisely it is difficult to evaluate the ballistic life time based only upon these data, because one has to know the maximum loss of energy of the propellant that still delivers an acceptable ballistic behaviour. For gun propellants normally a value of 3 % energy loss is estimated<sup>2</sup> but there is much work to do to make exact estimations if it is ever possible.

Heat flow calorimetry is not a useful tool for the estimation of the service life when other processes in the propellant than chemical degradation rule the life time of propellants, such as loss in mechanical behaviour, or migration phenomena or if phase changes of the material take place. In these cases other tests in addition to HFC must be conducted to make estimations of the life time of propellants.

For the estimation of compatibility heat flow calorimetry can be easily used. It has the advantage that all chemical reactions can be observed and not only gas generating ones (like in the vacuum stability test) or only reactions that are fast enough to lower the decomposition temperature (like in DTA experiments). Details of this are given in chapter 4.

At BICT heat flow calorimetric (HFC) measurements have been performed since the mid 1970's. Since 1993 we work with modern TAM calorimeters that make HFC measurements much more convenient and reliable. Fig. 1 shows the measuring principle of the TAM heat flow calorimeter. Because most of the participants of this meeting are familiar with it and detailed description of the measuring principle are published elsewhere<sup>1</sup>, it's not necessary to give detailed information at this point.

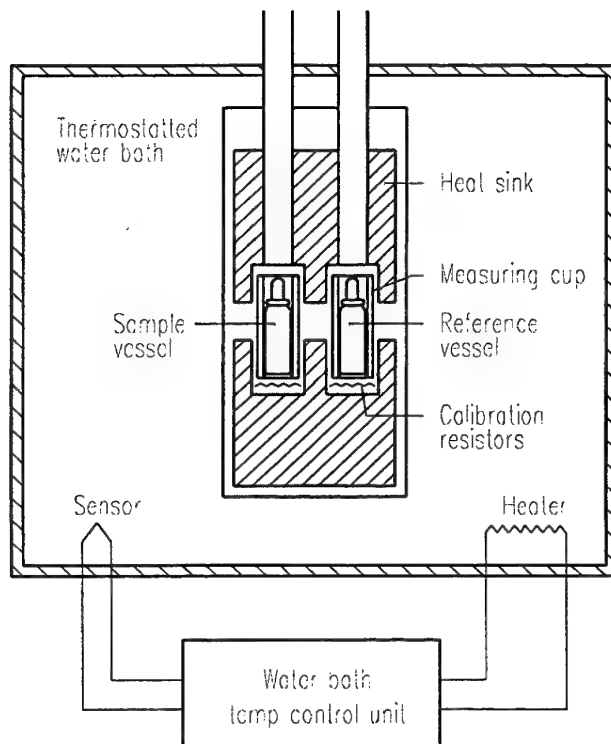


**Fig. 1.** Measuring principle of heat flow calorimetry

## 2 Determination of service life of propellants

To calculate the service life of a propellant (which means the time until 3% of its energy content is lost) it is necessary to measure its heat flow at different constant temperatures in the range between 80 and 30°C and to establish an Arrhenius plot. Usually the sample is at first measured at 80°C to give initial reactions the possibility to complete rapidly. After they are finished the constant rate decomposition of the propellant gives a constant HFC signal that is used for evaluation of the kinetic parameters. In the following example it is done for a 14 year old propellant which didn't show any decomposition behaviour in the classical tests. The values of P (constant heat flow) are collected in table 1.

Another series of HFC measurements with double base propellant K 6210 is presented in tables 5 and 6.

**Table 1:** Constant heat flow measurements (double measurements) of propellant H 5180

Temperature [°C]	80	70	60	50	40	30
Heat flow [μW/g]	17,2/18,8	4,8/4,8	1,62/1,57	0,70/0,77	0,43/0,42	0,19/0,15

As can be seen the double measurements are within a small range (max. ± 20% in the lower temperature area). If this doesn't occur then the measurement series has to be remade.

The Arrhenius plot is depicted in figure 2.



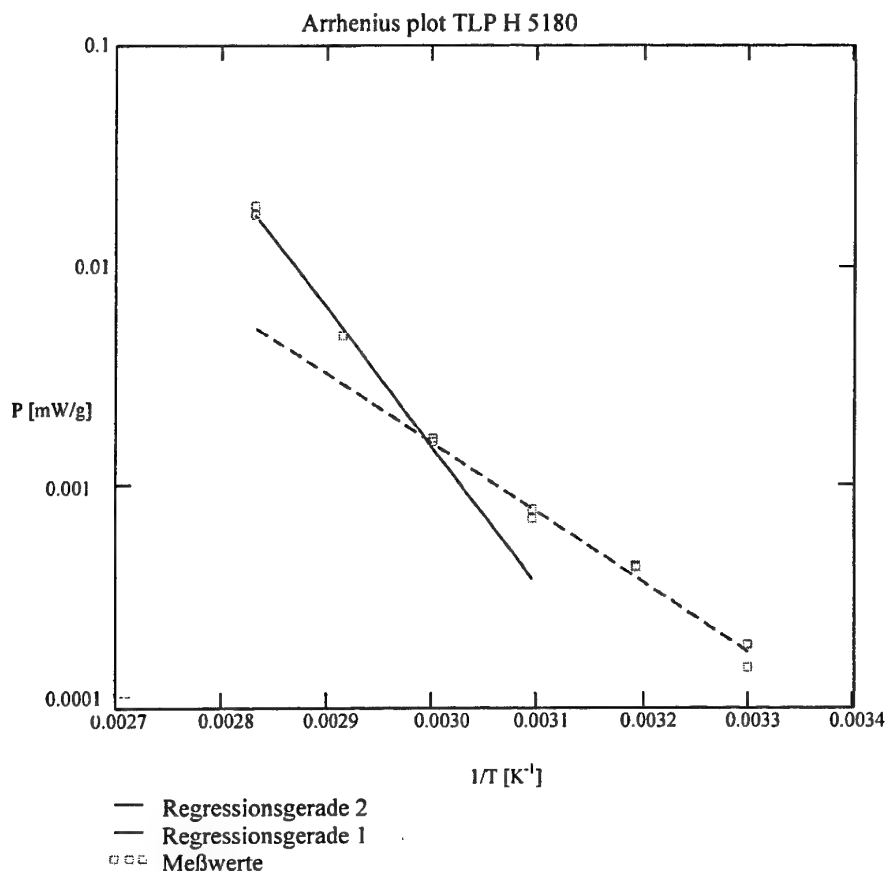


**Fig. 2:** Arrhenius plot of double base propellant H 5180

It's obvious that a change in the slope of the Arrhenius plot occurs at about 60°C (0.0030 K<sup>-1</sup>). It is not yet clear why this happens but probably there are changes in the mobility of the smaller molecules in the nitrocellulose matrix. This change is not always as sharp as in fig. 2 and in some cases it doesn't occur at all. But if it occurs then it is necessary to take the low-temperature values for the calculation of activation energy and pre-exponential factor. The high temperature kinetics would predict an unrealistic long service life time.

Therefore it is very important to get reliable values of the specific heat production rates in this temperature range because small changes (e.g. 0.2 instead of 0.4 μW/g) would have a big effect on the slope and thus on the service life calculation of the propellant.

In this case it could be shown that the activation energy (60 kJ/mole) and the pre-exponential factor (3,9·10<sup>6</sup> W/kg) are at the lower end of the range of double base propellants. The complete output of this measurement is given in table 2.<sup>3</sup>

**Table 2:** Results of heat flow measurements of a 14 year old propellant

E <sub>a</sub> H.T.	E <sub>a</sub> N.T.	vF H.T.	vF N.T.	r <sup>2</sup> H.T.	r <sup>2</sup> N.T.
[kJ/mol]	[kJ/mol]	[W/kg]	[W/kg]		
121	60	1,4*10 <sup>16</sup>	3,9*10 <sup>6</sup>	0,984	0,997

Remarks:

$E_a$  = Activation energy

$vF$  = pre-exponential factor (according to the frequency factor)

H.T. = high temperature area ( $> 60^\circ\text{C}$ )

N.T. = lower temperature area ( $< 60^\circ\text{C}$ )

$r^2$  = correlation coefficient

**Table 3: service life time of propellant H 5180 at different temperatures**

Ambient temperature	[°C]	50	40	30	20	10
Ballistic service life	[years]	6,4	13,1	28	63	150

service life: time until 3% of the energy content of the propellant (according to heat of explosion) is lost

The ability of HFC measurements to show reproducible values can be demonstrated by a series of measurements of different lots of the double base propellant K 6210<sup>4</sup>. Whereas the degradation of the stabiliser occurs with a different rate (table 4; the time until the 2<sup>nd</sup> maximum is reached is the time when nearly all of the DPA is used up; see chapter 6) the final constant heat flow value are comparable within all the different lots measured. This leads to nearly the same values of activation energy and of the pre-exponential factor (see table 6).

**Table 4: Important values of HFC measurements of different lots of propellant K 6210-13<sup>a)</sup>**

Lot		216	218	219	220	221	222	223
1 <sup>st</sup> maximum	[μW/g]	65	105	104	80	83	58	70
1 <sup>st</sup> minimum	[μW/g]	18	28	33	22	20	22	30
2 <sup>nd</sup> maximum	[days]	4,7	3,5	1,7	3,9	3,4	3,5	2,8
2 <sup>nd</sup> maximum	[μW/g]	94	116	83	95	115	78	90

a) averages of double or multiple measurements

**Table 5: HFC measurements of lots 218 to 223 (propellant K 6210-13, niveau 2)<sup>a)</sup>**

temperature	lot 218	lot 219 <sup>c)</sup>		lot 220	lot 221	lot 222	lot 223 <sup>c)</sup>	
[°C]	P [μW/g]	P [μW/g]		P [μW/g]	P [μW/g]	P [μW/g]	P [μW/g]	
80	100	71 <sup>b)</sup>	79	77 <sup>b)</sup>	77 <sup>b)</sup>	67	76	80 <sup>b)</sup>
70	28.2	29.5	23.5	-	-	-	-	-
60	7.5	6.4	6.8	7.1	6.5	6.0	6.3	7.0
50	2.07	2.05	2.16	1.98	1.97	1.92	1.99	2.01
40	0.63	0.66	0.62	0.61	0.63	0.64	0.61	0.63

a) averages of double or multiple measurements

b) value not constant because of endothermic peaks due to gas evolution

c) right side: values measured by PB Clermont, left side: values measured by BICT

-) not measured

The measurements of lots 219, 220, 221, and 223 were run both at BICT and PB Clermont and show nearly no difference. That means that sample preparation and measuring performance are comparable in both laboratories. Only the value of the lot 218 is somewhat higher than the others; the reason for this might be the higher moisture content.

The indices niveau 1 and niveau 2 refer to the first and the second constant niveau of heat generation, respectively, and can be seen in figure 10 (points 2 and 4). The higher value of the ballistic service life of the niveau 1 measurements is due to the lower pre-exponential factor. As this niveau is not constant throughout the whole first three per cent energy loss it is not allowed to take this value for life time calculation.

**Table 6:** Kinetic data of lots 218 to 223

lot		218 (niveau 1)	218 (niveau 2)	219 (niveau 2)	220 (niveau 2)	221 (niveau 2)	223 (niveau 2)
T-range	[°C]	60-40	60-40	60-40	60-40	60-40	60-40
activation energy	[kJ/mol]	97	107	100	107	102	103
pre-exp. factor	[W/kg]	$3.6 \cdot 10^{12}$	$5.1 \cdot 10^{14}$	$2.8 \cdot 10^{13}$	$4.8 \cdot 10^{14}$	$5.7 \cdot 10^{13}$	$9.4 \cdot 10^{13}$
heat of explosion	[J/g]	4047	4047	4094	4054	4056	4038
ballistic service life at 40°C	[years]	15.0	6.2	6.1	6.6	6.2	6.3

service life: time until 3% of the energy content of the propellant (according to heat of explosion) is lost

### 3 Autocatalytic decomposition reactions of nitrocellulose and primitive masses

Another important field of the application of heat flow calorimetry is the prediction of the storage safety of explosive materials. In several examples we investigated the autocatalytic decomposition reaction of dried unstabilized nitrocellulose and primitive masses (mixtures of nitrocellulose and nitroglycerin or DEGN, respectively). Normally they are only stored wet (that means a water or alcohol content of about 30 wgt-%), those samples don't show any exothermic or autocatalytic behaviour until the volatiles are lost.

Fig. 3 shows the rapid decomposition of a dried primitive mass containing about 20% of nitroglycerin and 15% of DEGN at 80°C. The higher the amount of material in a fixed total volume the sooner the reaction begins due to the autocatalytic effect of nitrogen oxides, the first and most important product in the chain of degradation reactions. More details of this investigation are given in <sup>5</sup>.

As the normal maximum value in the TAM calorimeter is 3015 µW/sample the heat flow in the maximum of the reaction can't be measured and so the reaction path can't be followed correctly. With a new potentiometer the range is 10 times higher and thus the whole reaction can be seen (fig. 4). The dotted line is the heat flow (left axis), the solid one symbolizes the integration (values on the right axis). With a total energy release of about 2000 J/g nearly the same value is reached that is obtained from dynamic DSC experiments.

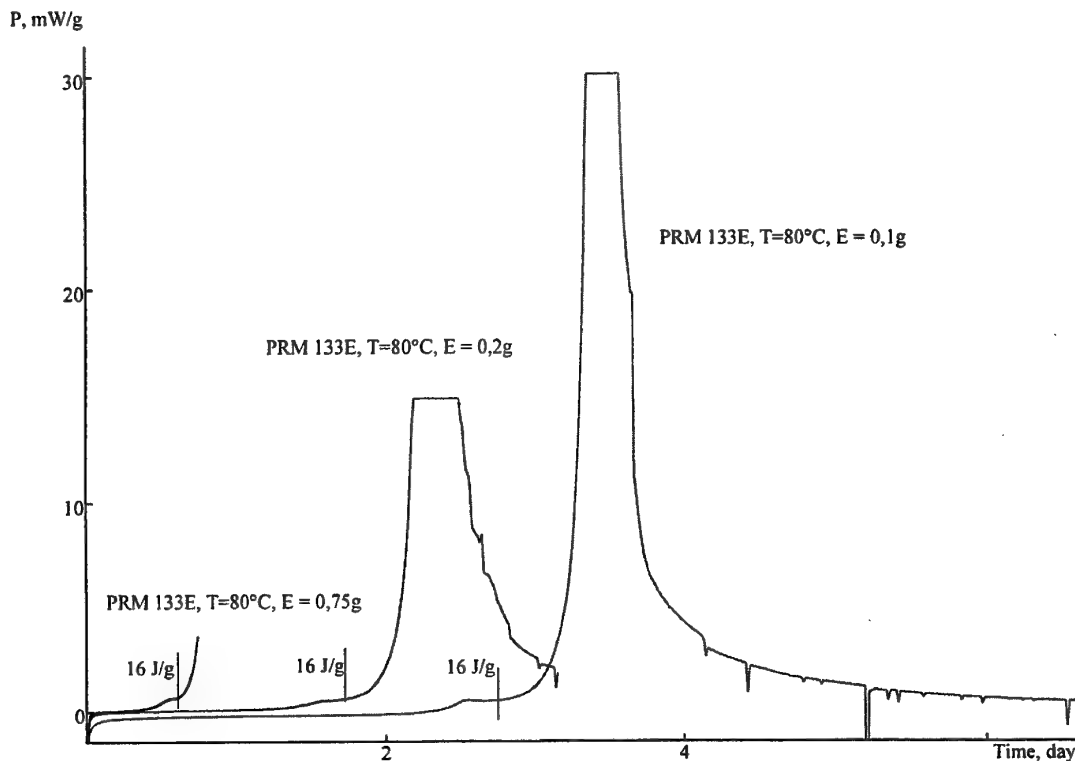


**Fig. 3:** Degradation of PRM 133E at 80°C with different amounts of primitive mass

The calculation of safe storage time of dried samples is done by taking the time until an energy release of 16 J/g is reached at different temperatures (this is the point after the first small peak before the rapid increase of heat flow starts). Table 7 gives the result of the storage time at ambient temperatures of 12°C of dried primitive masses under the assumption of a constant activation energy between 80 and 10°C (it is constant for 80-60°C).

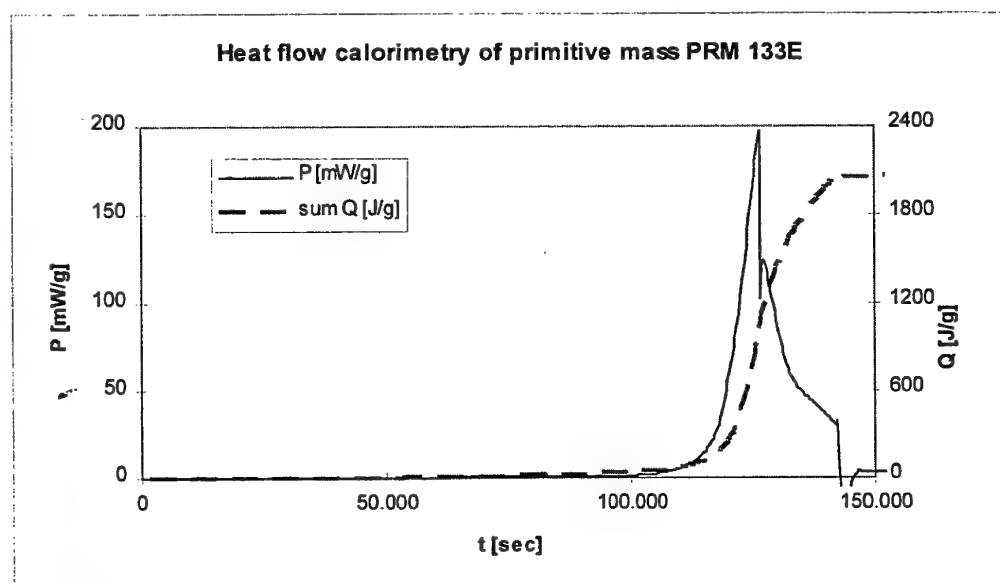


**Fig. 4:** Complete decomposition of PRM at 80°C including integration (right axis)

**Table 7:** Storage time of dried primitive masses containing 20% of nitroglycerin and 15% of DEGN. Calculated for totally filled vessels.

ambient temperature [°C]	time until 16 J/g are reached [days]
60	3,2
50	8,0
40	21
30	60
20	180
12	470

With the knowledge of heat conductivity, the geometry of the sample and the storage temperature also the critical diameter (and with a given diameter the critical temperature) for a thermal explosion can be calculated. This makes HFC a useful tool for the calculation of these important values (risk analyses).

#### 4 Compatibility experiments

Chemical compatibility is one of the most important things to prove when using new or changed compounds for an ammunition system. In Germany the test usually is run as reactivity test, where the evolution of evolved gas is measured using a mercury apparatus. Also the decrease in melting and/or decomposition temperature is routinely determined using DTA. But incompatibility leading to other reactions than gas evolution or decomposition temperature reduction can't be measured by these classical methods<sup>6</sup>. So we looked for modern thermo-analytical methods for the determination of compatibility. For primers a thermogravimetric method proved to be successful<sup>7</sup>. For propellants heat flow calorimetry is chosen as useful method, because all chemical and physical reactions that produce or consume heat can be detected very sensitively.

For the compatibility we used small glass vessels that were totally filled with different mixtures of propellants and contact materials as shown in table 8. The contact material was dried and afterwards cut into very small pieces and vigorously mixed with the propellant.

The calculation of compatibility is done by comparing the amount of heat generated by the mixture divided by the theoretical amount (addition of single values). If the amount of both components is the same, then the formula (2) according to STANAG 4147 Annex D is used.

$$D' = \frac{(P_1 + P_2) * M}{P_1 * K_1 + P_2 * K_2} \quad (1)$$

$$D = \frac{2 * M}{K_1 + K_2} \quad (2)$$

using

D or D' = relative compatibility

M = energy release of the mixture until time t (according to<sup>6</sup> 7 days at 85°C)

P<sub>1</sub> = amount of component 1

P<sub>2</sub> = amount of component 2

K<sub>1</sub> = energy release of component 1 (propellant)

K<sub>2</sub> = energy release of component 2 (contact material)

If D ≤ 2 the contact pair is compatible

If 2 < D < 3 the contact pair is probably incompatible, further investigation is necessary

If D > 3 the contact pair is incompatible

As can be seen there is a nearly linear dependence of the D value from the amount of contact material when its content is higher than 5 wgt %. The higher D value after 4.8 days in comparison to that of 7 days is due to the total absence of the first minimum when the contact material has a content of > 25 % (see also figure 5.)

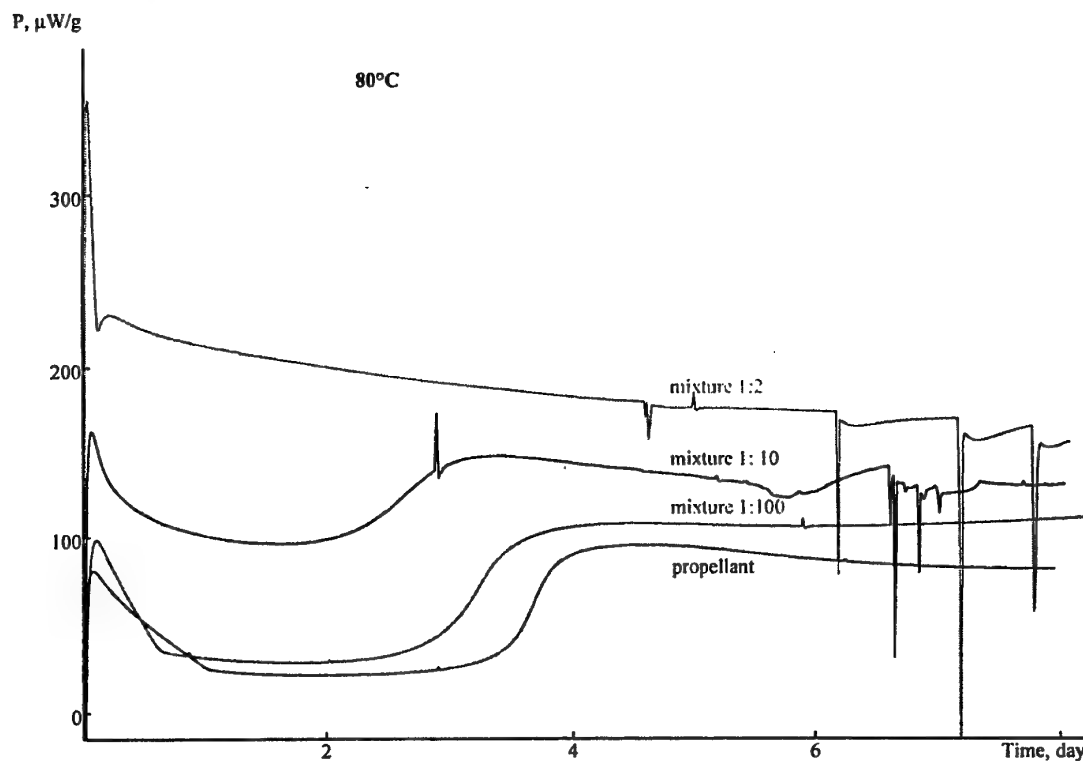


Fig. 6: Compatibility experiments with propellant K 6210 and bitumen lacquer (method B). The 1:2 mixture curve has a totally different shape.

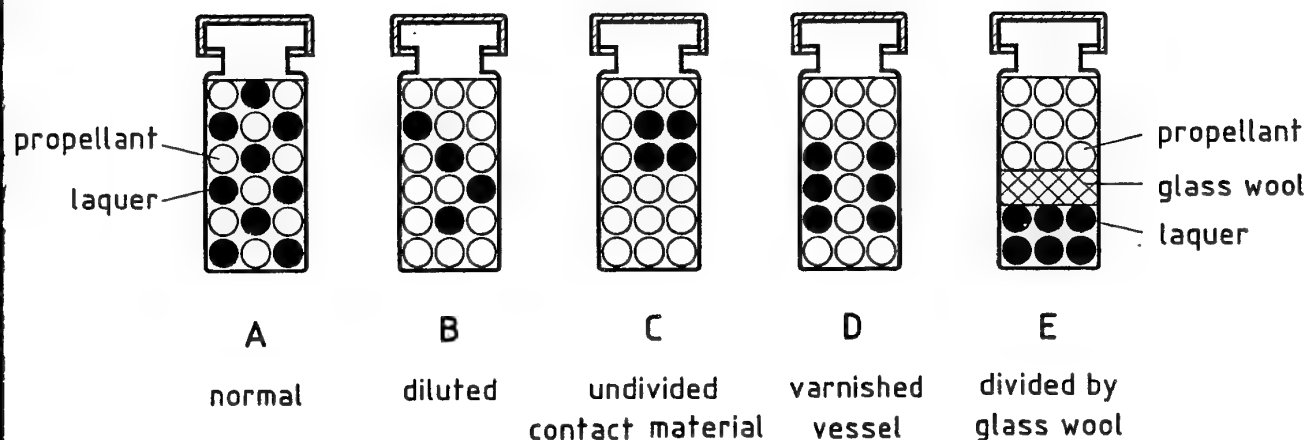


Fig. 7: Compatibility experiments – different arrangements

The relative compatibility factor D as a function of contact material content is presented in figure 5.

**Table 8:** Compatibility testing of double base ball propellant K6210-13 with contact material

Sample	contact material	Q (4,8 d)	Q (7,0 d)	P <sub>const</sub> (7,0 d)	D (4,8d)	D (7,0d)
	[%]	[J/g]	[J/g]	[μW/g]		
propellant	0	16,5	33,3	83,9	1,78	1,87
	0	16,5	33,3	84,6	1,78	1,87
mixture 1:100	1	20,6	41,9	107,0	1,26	1,28
	1	24,8	45,0	115,5	1,52	1,35
mixture 1:50	2	16,5	38,4	115,4	1,02	1,17
	2	17,9	38,4	112,3	1,10	1,17
mixture 1:20	4,8	29,1	-	-	1,84	-
mixture 1:10	9,1	41,5	65,0	129,7	2,73	2,13
	9,1	50,9	75,2	135,0	3,35	2,47
mixture 1:5	16,7	65,5	98,6	174,7	4,65	3,51
	16,7	61,9	94,2	170,3	4,39	3,35
mixture 1:2	33,3	82,0	114,4	173,0	7,02	4,98
	33,3	74,6	101,0	161,0	6,39	4,40
mixture 1:1	50	87,7	115,8	181,0	9,47	6,51
	50	91,0	123,0	152,0	9,82	6,92
contact material	100	1,21	1,47	0,96	-	-
	100	2,85	3,05	3,60	-	-

explanation: contact material [%]: amount of contact material in the mixture; Q (4.8d): total energy released within 4.8 or 7 days, respectively; P<sub>const</sub>: constant heat production rate at the end of the experiment; D/D': D-value after 4.8 or 7 days according to (1) or (2; STANAG definition<sup>8)</sup>)

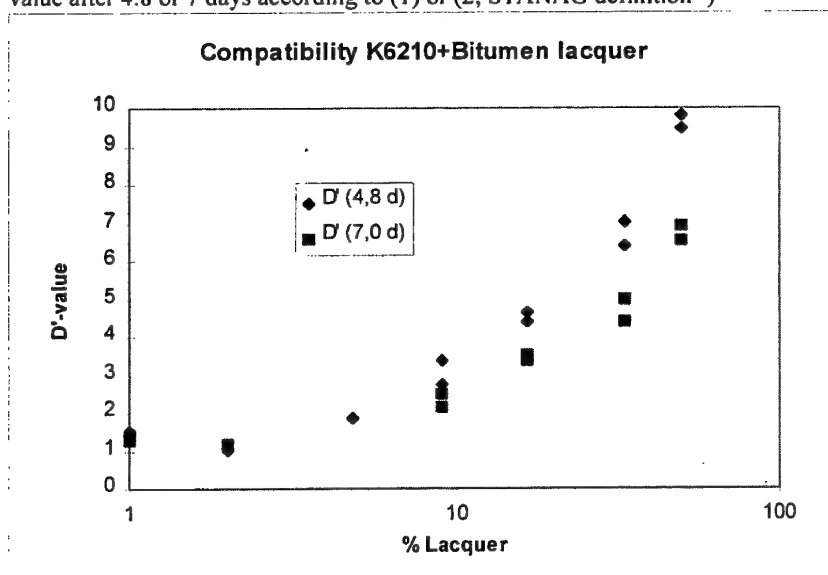


**Fig. 5:** Relative compatibility factor D' in dependence of amount of the contact material in the mixture.

With a different arrangement of sample and contact material (see fig. 7) one can find out which type of contact is responsible for the strong exothermic effects of this incompatible couple. To do that we separated the lacquer and the propellant by a layer of glass wool. We observed even with a 1:1 mixture ratio only an increase of the heat generation but, in contrast to the direct contact pair, the shape of the curve is comparable but all reactions go on faster. That means that the reaction is only in parts a gas phase reaction. The major incompatibility is due to a surface contact reaction. When the surface is reduced markedly by using bigger pieces of lacquer (arrangement C) or varnished vessels (arrangement D) the heat production rate is also much lower than before. Details of this investigations are reported in <sup>9</sup>.

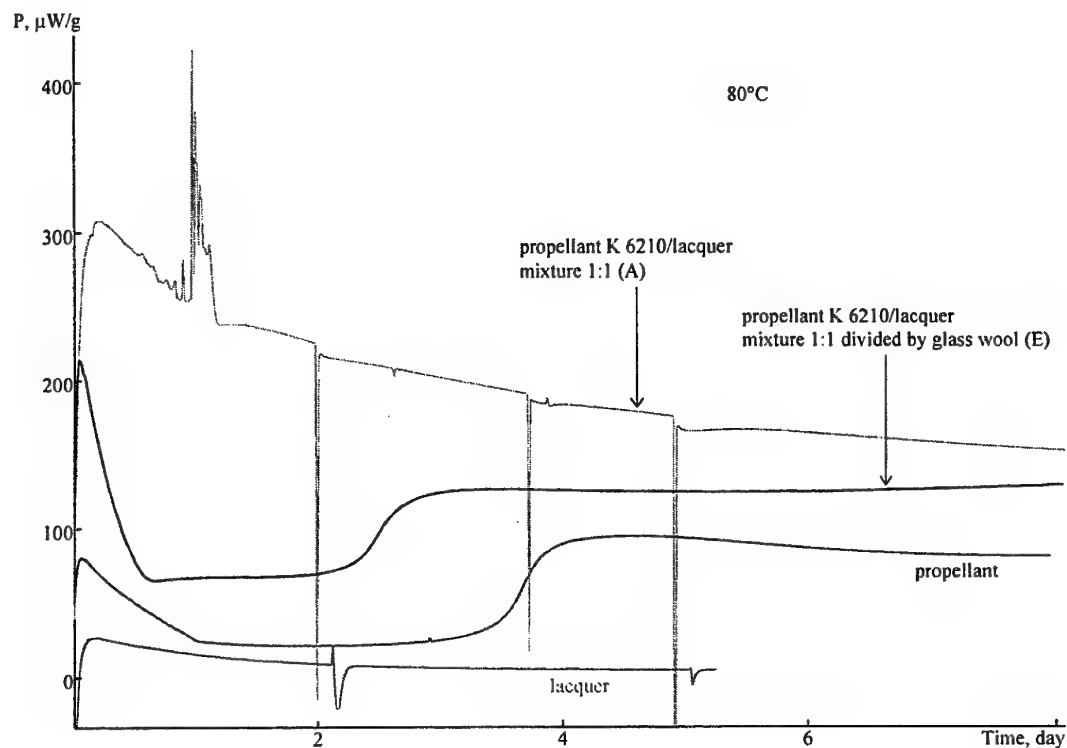


**Fig. 8:** Compatibility experiments – additional results using different sample preparation techniques

## 5 Experiments at lower temperatures (e.g. 30 or 40°C)

To run those experiments it is necessary to give the calorimeter enough time to get equilibrated. It is useful to wait for at least 30 hours after the temperature of the water bath had been changed. The correctness of the base line must be looked at by recording it. The calibration has to be performed carefully and long enough. Because of the fact that the lower temperature values are so important (see fig. 2) and the values are very small these precautions have to be made.

During the measurements one can use the switch technique, that means the sample and the reference vessel are changed, and the recording the heat flow is continued. If a perfect calibration had been done and if you let the switched sample/reference equilibrate long enough one should obtain the negative value. So it should be possible to control the base line, and



shifts could be detected easily. But as the sample and reference channel differ a little bit in their thermal environment the zero point is never exact at  $0.000 \mu\text{W}$  but lies in the range between  $-50$  and  $+50 \text{ nW}$ . Whether this is a mistake in our calibration process or a systematic error due to the geometry of the TAM calorimeter should be discussed. Fig. 7 shows an example of measurements using the switch technique.

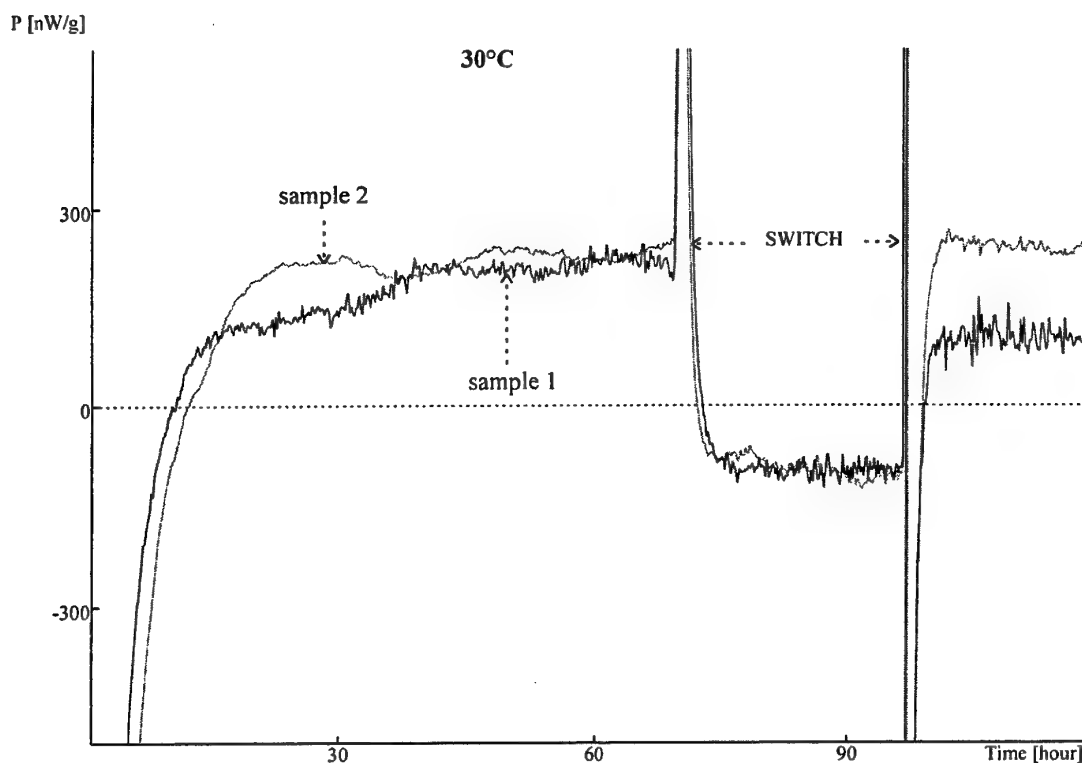


**Fig. 9:** Experiment at  $30^\circ\text{C}$  using the switch technique. Only one sample shows the same positive and negative value

## 6 Combination of methods that describe the degradation of propellants (HFC, HPLC and GPC)

It is very important to know what chemically happens during the HFC measurement of a propellant. In the case of double base propellants we have a certain and reproduceable structure of the curve which can be described by (see solid line in fig. 10)

- a first maximum
- a first minimum
- a second maximum
- a final nearly constant value

The same shape appears also at lower temperatures (e.g.  $60$  or  $50^\circ\text{C}$ ) when a fresh sample is introduced, and, as expected, the time to reach the different stages is much longer and the values are much lower; but the energy release is comparable. That means that the decomposition mechanism is unchanged for all these temperatures and the extrapolation from higher to ambient temperatures is possible [if one assumes that there is no change in kinetics below  $50^\circ\text{C}$ ].

We analysed the samples after the above mentioned stages in the reaction and looked at the stabiliser products and the molecular mass distribution at each point (see tables 8 and 9).

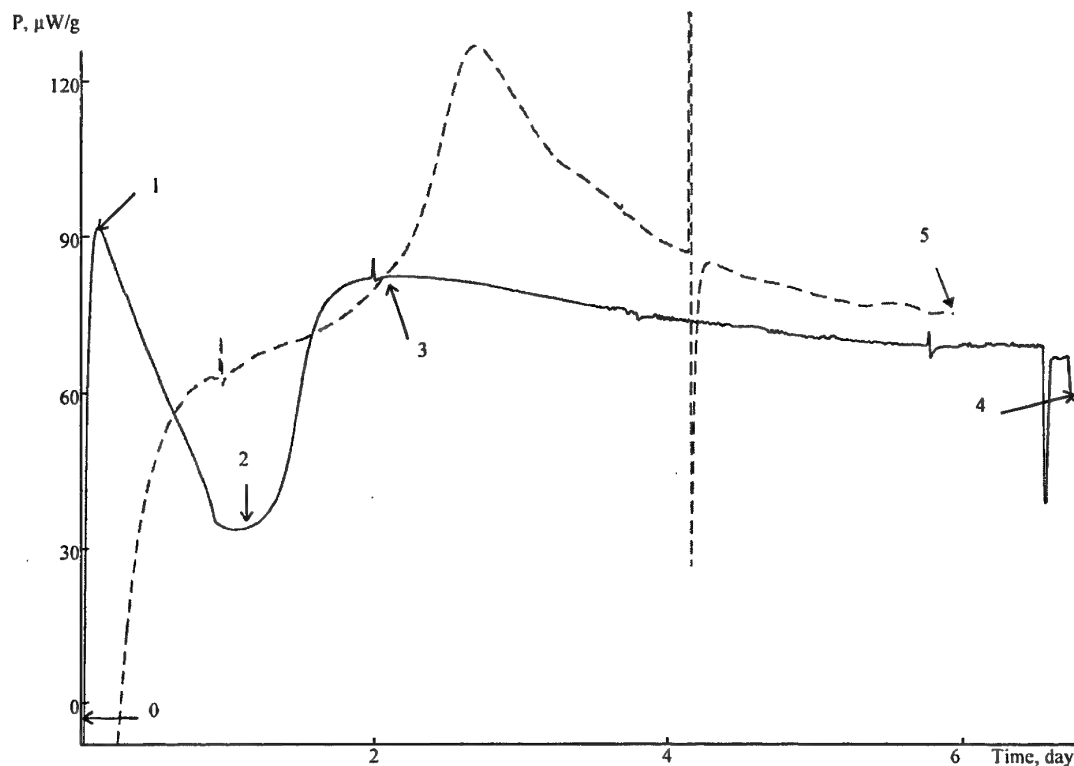


**Fig. 8:** Heat flow calorimetry of propellant K6210 at 80°C combined with stabilizer loss

**Table 9:** Stabiliser depletion at different stages of the HFC measurements

sample	N°	DPA	N-NO-DPA	2-N-DPA	4-N-DPA	2,2'-DN-DPA	2,4'-DN-DPA	4,4'-DN-DPA
		[%]	[%]	[%]	[%]	[%]	[%]	[%]
before meas.	0	45.9	48.7	2.7	2.7	0.0	0.0	0.0
1. maximum	1	32.4	61.9	3.0	2.7	0.0	0.0	0.0
1. minimum	2	4.1	89.6	3.5	2.8	0.0	0.0	0.0
2. maximum	3	0.6	96.8	1.8	0.8	0.0	0.0	0.0
end of meas.	4	0.0	97.1	0.0	1.4	1.5	0.0	0.0
sample not closed (end of meas.)	5	0.0	33.7	7.5	0.0	3.2	29.2	26.0

As can easily be seen, the DPA concentration decreases while the measurement goes on. In the minimum it is only 10% of the original value while the amount of N-NO-DPA is increasing rapidly above 90% of the total stabiliser content. Because no additional oxygen is available the reaction of N-NO-DPA to nitro derivatives of DPA according to (2) is not pos-

sible and most of the DPA remains as the N-NO derivative while the heat production rate is much higher than with DPA available.

If you allow oxygen to come into the measuring vessel then the oxidation of N-NO-DPA is possible and more than 50% of the DPA is transformed into the DN-derivatives (last entry).

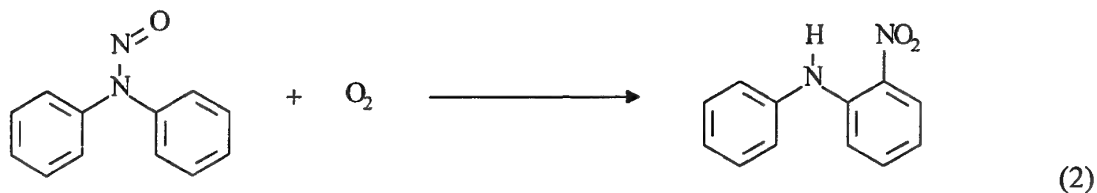


**Table 10:** Molecular mass distribution at different stages of the HFC measurements <sup>a)</sup>

sample	N°	M <sub>n</sub>	M <sub>w</sub>	M <sub>p</sub>	D
		[g/mol]	[g/mol]	[g/mol]	-
1. maximum	1	78.000	184.000	154.000	2,36
1. minimum	2	60.500	186.000	146.000	3,08
2. maximum	3	40.500	168.000	131.500	4,14
end of measurement	4	35.500	142.000	103.000	3,99

a) all values refer to polystyrene standards. The numbers 1-4 refer to the same points as given in fig. 10.

M<sub>n</sub> is reduced from the beginning on and in the second maximum it fell on nearly half of the original value. At this point also M<sub>w</sub> is beginning to decrease (which means the polydispersity D is rising from the beginning to the second maximum).

## 7 Conclusion

Heat flow calorimetry is a very sensitive method to determine the decomposition process of nitrate ester propellants. The temperature dependent heat production rate allows to make an Arrhenius plot from which the time until 3% energy at ambient temperatures is lost can be calculated. This time is usually taken as the service life of the propellant. Due to the change in the kinetics the small low temperature values are much more important than the high temperature ones which makes an accurate calibration necessary.

A calculation of service life time only from one method independently is always difficult. But a combination of heat flow calorimetry results which give you the speed with which the reaction is going forward and stabilizer consumption or molar mass degradation experiments that define the actual stage of the decomposition reaction allow to look inside of what is going on. For a life time determination all limiting factors must be known, e.g. the „allowed“ loss of energy, the „allowed“ consumption of stabilizers or the „allowed“ loss in average molecular weight <sup>10</sup>. For double base propellants in general all migration processes of nitroglycerine must be taken into account additionally.

In the field of storage safety prediction HFC is the best method because the relevant data (the heat production) is the data you get. With knowledge of heat conductivity, sample geometry

and ambient temperature reliable calculations of critical diameter and/or temperature can be made.

The use of HFC to determine the compatibility of propellants with contact material becomes more and more fashionable. Simple variations in sample preparation additionally allow to make conclusions which type of reaction is going on (gas phase or solid phase reactions).

---

## References and Notes

<sup>1</sup> C.J. Elmqvist, P.E. Lagerkvist, L.G. Svensson, „Stability and Compatibility Testing Using a Microcalorimetric Method“, *J. Haz. Mat.* **7**, 281-285 (1983); L.G. Svensson, C.K. Forsgren, P.O. Backman, „Microcalorimetric Methods in Shelf Life Technology“, *Proc. ADPA Symp. on Compatibility of Plastics and Other Materials with Explosives, Propellants and Pyrotechnics*, New Orleans 1988, p. 132-137; S. Wilker, G. Pantel, U. Ticmanis, „Wärmeflußkalorimetrische Untersuchungen an Anzündhütchen“, *Proc. Int. Annu. Conf. ICT* **26**, 84 (1995).

<sup>2</sup> H.P.J. Jongeneelen, „Investigation into the ballistic stability of nitrate ester propellants“, *TNO Report Ass. TL 7980-II* (1971); van Geel, J.L.C., „Ergebnisse des Deutsch-Niederländischen Ringversuchs zur Voraussage der Lebensdauer bei 338,5 K von vier TLP“, *TNO Ass.* 5059 (1977).

<sup>3</sup> S. Wilker, G. Pantel, „Ermittlung der chemischen Stabilität des TLP H 5180-12“, *BICT-Bericht* 110/16154/96.

<sup>4</sup> S. Wilker, G. Pantel, P. Guillaume, A. Fantin, M. Rat, „Stabilität TLP K 6210“, *BICT-Bericht* 810/15777/97; P. Guillaume, A. Fantin, M. Rat, S. Wilker, G. Pantel, „Stability Studies of Spherical Propellants“, *Proc. Int. Annu. Conf. ICT* **27**, 16-1 - 16-14 (1996).

<sup>5</sup> S. Wilker, G. Pantel, U. Ticmanis, M. Kaiser, T. Fox, „Sicherheitslebensdauer von Pulverrohmassen“, *Proc. Int. Annu. Conf. ICT* **27**, 101-1 - 101-14 (1996).

<sup>6</sup> W. de Klerk, N. van der Meer, R. Eerligh, M. Leenders, „Compatibility testing of propellants with polymers using the vacuum stability test and the heat flow calorimeter“, *Proc. Int. Annu. Conf. ICT* **25**, 44-1 - 44-13 (1994).

<sup>7</sup> U. Ticmanis, „Direct reactivity analysis, a kinetic approach to compatibility“ *Symp. Chem. Probl. Conn. Stabil. Explos.* **10**, (1995), Margareterorp, Sverige.

<sup>8</sup> *STANAG 4147*, „Chemical Compatibility of Ammunition Components With Explosives (Non Nuclear Applications)“ AC/310 (SG1) (Draft Edition X-95), Annex D, Test 2.

<sup>9</sup> S. Wilker, G. Pantel, A. Sommer, „Chemische Verträglichkeit von Treibladungspulver mit Kontaktmaterialien“, *Proc. Int. Annu. Conf. ICT* **28** (1997).

<sup>10</sup> Comparable studies were successfully done for the determination of the service life time of primers in the last years in BICT by Scheunemann and Ticmanis.

# DETERMINATION OF INTERACTION PROFILES IN COMPATIBILITY TESTING

L. G. Svensson

Celsius Materialteknik Karlskoga AB, Gammelbackavägen 6, S-691 51 Karlskoga, Sweden

## INTRODUCTION

The usual purpose with a compatibility test is to predict how the stability properties of an explosive are affected when being exposed to other substances, e. g. plastics, rubbers, sealants, adhesives or other explosives. With the increasing use of polymeric materials in the design of advanced weapon systems the "inverse process", i. e. the influence of the explosives on critical properties of the materials has become increasingly important. Many polymers, particularly those containing amine and amide groups have been found to interfere strongly with nitrate ester propellants and to some extent also with nitro compounds such as TNT, leading to more or less deteriorated mechanical properties [1]. When evaluating results from compatibility testing of such systems it should be emphasized, however, that a high level of chemical reactivity with the explosive is not a sufficient condition for deteriorated mechanical properties. Just as in all other chemical ageing processes where the material is attacked by surrounding aggressive components the interaction is comprised of two coupled processes — the transport of the reactive component into the material and the subsequent chemical reaction with the material [2]. Competition between these two processes leads to formation of a more or less pronounced interaction profile with the most severe degradation located to the surface of the material. The thickness of the profile depends on which of the two processes being the dominating one. "Severe incompatibility", i. e. a rapid chemical interaction usually results in a very thin degradation zone leaving the bulk of the material unaffected. Moderate interaction rates on the other hand give the reactive component a longer average time to migrate into the bulk before reaction takes place, and the interaction profile will therefore extend deeper into the material. From the viewpoint of mechanical strength the latter case is usually the most unfavourable.

Microcalorimetry (MC) has become a very useful tool in the testing of long-term compatibility of explosives and materials owing to its extreme measuring sensitivity combined with a broad applicability. Degradation rates down to a few percent per year can normally be measured with acceptable accuracy. In this work MC is used for estimation of interaction profiles in a frequently used structural adhesive, Araldite 2011, when exposed to a standard double base propellant for mortar ammunition. Araldite 2011 is an epoxy material containing functional groups of amine as well as amide type and is therefore expected to be strongly "incompatible" with propellants. The study includes determination of the temperature influence on the depth of the interaction profile. This influence can be of great importance for a correct interpretation of results from accelerated ageing tests in term of natural storage conditions.

## THEORY

The incompatibility of Araldite 2011 is assumed to be caused by reactions with nitroglycerine and various (nitrated) degradation products migrating from the propellant into the adhesive. As a first approximation we assume that all these substances affect the polymer in a similar way,

i. e. that they can be treated as one single reactant. The time dependence of the concentration ( $c$ ) of this reactant in the bulk of the adhesive is given by the equation

$$\frac{dc}{dt} = D \cdot \frac{d^2c}{dx^2} + I(c, T, \alpha) \quad (1)$$

where the first term represents Fick's second law for diffusion and the other term the rate by which the reactant is consumed [2].  $D$  is the diffusion coefficient and  $x$  the distance from the surface of the sample (we have adopted a simple one-dimensional model). The reaction term  $I$  can be separated in an Arrhenius factor and a concentration function,

$$I(c, T, \alpha) = A \cdot \exp\left[\frac{-E_a}{RT}\right] \cdot f(c, \alpha) \quad (2)$$

where  $A$  and  $E_a$  represent the pre-exponential factor and activation energy, respectively.  $\alpha$  is a reaction parameter representing the fraction of already consumed reactive sites in the adhesive. The activation energy can readily be obtained from MC experiments at different temperatures [3]. However, in order to obtain the true  $E_a$  value for the chemical interaction the adhesive/propellant mixture sample has to be prepared in such a way that diffusion effects can be neglected. In practice this implies that the adhesive thickness must be (much) smaller than the thickness of the interaction profile and that an excess of propellant should be used to guarantee an unlimited supply of reactive gases. The function  $f(c, \alpha)$  can also, at least theoretically, be derived from MC measurements at different reactant concentrations and different degrees of sample degradation.

Equations (1) and (2) can be used e. g. in simple finite element calculation models for obtaining accurate concentration gradients and interaction profiles in the bulk of the adhesive. For practical purposes, however, a crude estimation of the profile thickness is usually sufficient for judging if the incompatibility can affect the performance of the adhesive. Such estimations can be made by comparing MC data for mixtures of propellant with a solid body and with a very finely ground adhesive sample, respectively. If both samples yield equal heatflow levels after normalisation to unit mass of adhesive, then the interaction must be uniform throughout the bulk of the adhesive, i. e. not limited by diffusion barriers. Every reduction in heatflow of the solid sample compared to the milled is an indication of diffusion controlled interaction.

An approximate interaction profile thickness  $x$  can be calculated from the volume  $V$  and surface area  $A$  of the solid sample using the equation

$$x \approx \frac{V}{A} \cdot \frac{P_s}{P_o} \quad (3)$$

where  $P_s$  and  $P_o$  represent the interaction heatflow of the solid and the finely milled adhesive, respectively, normalised to unit mass (1 g). Equation (3) is acceptably valid for a profile up to, say,  $x = 10\%$  of the solid sample thickness, provided that the ground sample can be considered as uniformly reactive. For "deeper" interaction a more complicated expression based on the geometry of the solid sample must be employed.

## EXPERIMENTAL

### Preparation of samples

Araldite A2011 is a room temperature curing adhesive, but to ensure complete hardening (for minimum heatflow and low risk for unreacted amines to migrate into the propellant) the adhesive was cured at 80°C for 24 h. A solid piece, 36 mm long and with a rectangular cross section area of 3.8 x 4.6 mm was cut from the cured sample and the surfaces were smoothed using an ultra fine emery cloth. A powdered sample was obtained by grating the cured material and passing it through a 250 µm sieve. These two samples were used in mixtures with propellant. The residual grated material > 250 µm was used as the reference sample for pure adhesive. Propellant samples were obtained from 0.5 mm thick sheets by cutting ~ 3 mm wide strips of variable length 3 - 35 mm. See Table 1 for details about the samples.

**Table 1 -- List of samples**

Sample No.	Sample	Amount (g)	Approximate dimensions (mm)
1	Double base propellant m/84	1.665	Strips 0.5 x 3 x 25
2	Adhesive Araldite 2011	0.388	Grated, grain size > 0.25
3	Propellant + solid Araldite 2011	2.073 + 0.672	Propellant strips 0.5 x 3 x 35 Araldite 3.8 x 4.6 x 36
4	Propellant + grated/sieved Araldite 2011	2.020 + 0.045	Propellant strips 0.5 x 3 x 3 Araldite powder < 0.25

An excess of propellant was used in both mixture samples to ensure that the interaction with the adhesive would not be limited by lack of reactive gases. Adhesive and propellant were thoroughly mixed in sample 4.

All samples were packed in sealed glass vials of 3 or 4 cm<sup>3</sup> volume, depending on the size of the sample. Prior to sealing the vials were purged with nitrogen gas in order to suppress interference from oxidation reactions.

### MC measurements

The MC measurements were carried out with a 4-channel heat flux calorimeter of type 2277 Thermal Activity Monitor (TAM) from ThermoMetric AB, Järfälla, Sweden. The instrument was equipped with four 2277-201 Ampoule measuring cylinders. TAM is originally developed at the Department of Thermochemistry, University of Lund, Sweden. For details regarding instrument design and measuring principles see Ref [4].

All four samples were tested simultaneously, and with continuous recording of the heat flow. The temperature was changed in steps during the measurement according to the sequence 30 → 20 → 10 → 30 → 45°C. At the lower temperatures the sample and the (inert) reference sample (high purity sea sand, Merck 7712) were temporarily swapped to obtain a "mirror image" of the heatflow signal centered around the true baseline, see Figure 1. With this so-called switch technique it is possible to determine the baseline position accurately and hence to improve the measuring sensitivity considerably.

### Calculation of activation energy ( $E_a$ )

The usual way to obtain activation energies is to make a plot of  $\ln(\text{rate constant})$  vs.  $1/T$  in an Arrhenius diagram and calculate  $E_a$  from the slope of the straight line fitted to the data points. For most slow reactions studied with MC the rate constant can be substituted by the heatflow, i. e. with a quantity proportional to the reaction rate. Such a replacement is legitimate as long as the reaction rate is so slow that the concentration-dependent part  $f(c, \alpha)$  of the rate expression (Eq. 2) can be treated as a constant over the time interval of the experiment. This condition is practically always fulfilled for the so-called step method [5] used for determination of  $E_a$  in this work. The step method, which is based on comparison of the heatflow immediately before and after a temperature step, is particularly useful when the heatflow changes with time. If the step method is applied to several consecutive temperature steps in an experiment it is important that the heatflow drift arises solely from changes in reactant concentrations and not from a change in the reaction mechanism.

## RESULTS AND DISCUSSION

### Interaction profiles

Figure 1 shows the interaction heatflow curves for the two propellant/adhesive mixtures. Interaction curves are simply obtained by subtracting the heatflow contributions from the pure propellant and Araldite 2011 samples (not shown in Figure 1) from the heatflow curves of the mixture samples. Curve 1 representing the solid adhesive sample is normalized to 1 g of Araldite while curve 2 for the milled adhesive only corresponds to 0.05 g of Araldite. The actual difference in interaction heat per gram of epoxy is therefore 20 times larger than shown in Figure 1. The result clearly shows that the interaction must be mainly located to the surface of the adhesive. If the bulk of the material had been involved in the interaction the heatflow level of the solid sample should have been much closer to curve 2.

The interaction rate changes with temperature, as expected, but it is obvious from Figure 1 that the temperature dependence is different for the two samples. Thus, at 20°C the level of curve 2 is approximately twice as high as for curve 1 (i. e. ~ 40 times higher interaction) while the corresponding difference at 30°C amounts to roughly to a factor 3 (~ 60 times higher interaction). A magnification of the 10°C interval (not shown here) shows that the curves practically coincide at this temperature (~ 20 times higher interaction). The average heatflow ratio between curve 1 and 2 at the different temperatures are summarized in Table 2. Since these values are equivalent with the quotient  $P_s/P_0$  in Eq. (3) they can be directly used to estimate the thickness of the interaction profile. With  $V/A = 0.98$  mm (calculated from the dimensions of the solid sample, see Table 1) we obtain the result shown in Figure 2.  $T = 10^\circ\text{C}$  thus yields an interaction zone extending approximately 60  $\mu\text{m}$  into the bulk of the adhesive. At 20 and 30°C the profile thickness is reduced to roughly 50% and 25% of its value at 10°C, respectively. Above 30°C only minor changes seem to occur.

Table 2 -- Interaction heatflow quotients  $P_s/P_0$  at different temperatures

Temperature ( $^\circ\text{C}$ )	10	20	30	45
$P_s/P_0$	0.060	0.027	0.015	0.013



A decrease in the slope of the curve in Figure 2 is of course expected since the profile thickness can theoretically never reach zero regardless of the choice of temperature. However, we suspect that the curvature to some extent can be affected by the interaction profile itself. When the temperature is raised one must sooner or later reach a point where the size of the interaction zone becomes comparable with the average grain diameter of the milled adhesive sample. At this point the milled material is no longer representative for a uniform (100%) interaction which implies that Eq. (3) yields too large x-values. No attempt has been made to accurately determine the grain size but microscopy shows that the "effective particle diameter" must be much smaller than the 250  $\mu\text{m}$  sieve grid due to a highly irregular shape of the grains.

### Activation energy

Figure 3 shows Arrhenius plots based on the heatflow steps in Figure 1. Both systems display a non-linear relationship between  $\ln P$  and  $1/T$  presumably due to a vast difference in activation energy between the diffusion and the chemical reaction contributions to the interaction process. Furthermore, the average  $E_a$  value for the interaction of the solid adhesive (79 kJ/mol according to the slope of the straight line) is significantly smaller than for the milled sample (104 kJ/mol) indicating that the influence of the diffusion is most pronounced in the solid sample. This result was of course expected.

### Degradation calculus

A very crude estimation of the degradation rate ( $d\alpha/dt$ ) of the epoxy material at full interaction, i. e. without diffusion barriers, has been made from the interaction heatflow ( $P$ ) of the milled sample (curve 2) in Figure 1 using the equation

$$\frac{d\alpha}{dt} = \frac{P}{\Delta H} \quad (4)$$

With  $\Delta H \approx 3$  kJ/g of epoxy as a reasonable enthalpy value for the interaction and  $P \approx 400$   $\mu\text{W/g}$  we obtain a degradation rate of  $\alpha = 1.3 \cdot 10^{-7} \text{ s}^{-1}$ , i. e. typically 1% per day at 20°C. This is of course a very severe incompatibility from a purely chemical viewpoint but with respect to its extreme location to the surface of the adhesive it is not necessarily immediately crucial for the strength of an adhesive joint.

## SUMMARY AND CONCLUSIONS

For a complete characterization of the compatibility of (polymeric) materials with the atmosphere from explosives or other substances the chemical reactivity as well as the diffusion of the reactive gases shall be considered. The competition between these processes gives rise to a more or less pronounced interaction profile, i. e. a surface zone where the interaction takes place.

Microcalorimetry is a suitable technique for estimation of the thickness of interaction profiles. The method is based on comparison of the interaction heatflow from mixture samples containing solid and finely milled material, respectively.

The difference in activation energy between chemical reactions and diffusion processes normally leads to an increase in the profile thickness at lower temperatures. The temperature dependence can readily be studied with the microcalorimetric method.

From the chemical viewpoint the epoxy adhesive Araldite 2011 is severely incompatible with the double base propellant m/42 for mortar ammunition (and most likely with other double base propellants as well). The degradation rate of the adhesive is estimated to typically 1% per day at 20°C. The interaction is however limited to a thin surface layer not exceeding 0.1 mm thickness at room temperature and will therefore not necessarily jeopardize the performance of adhesive joints.

## REFERENCES

1. L. G. Svensson, D. E. Taylor, C. K. Forsgren, P. O. Backman, Proc. of the ADPA Symp. on Compatibility of Plastics and Other Materials with Explosives, Propellants and Pyrotechnics, Long Beach, CA, USA (1986) 86
2. A.V. Cunliffe, A.A. Davis, Polym. Deg. and Stab. 4 (1982) 17
3. L. G. Svensson, Proc. of 11:th ICTAC Conference, Philadelphia, USA (1996)  
To be Published in J. Thermal Anal. 49 (1997)
4. J. Suurkuusk, I. Wadsö, Chemica Scripta (Sweden) 20 (1982) 155
5. Swedish Defence Standard FSD-0214, Appendix 3, Method 113.1

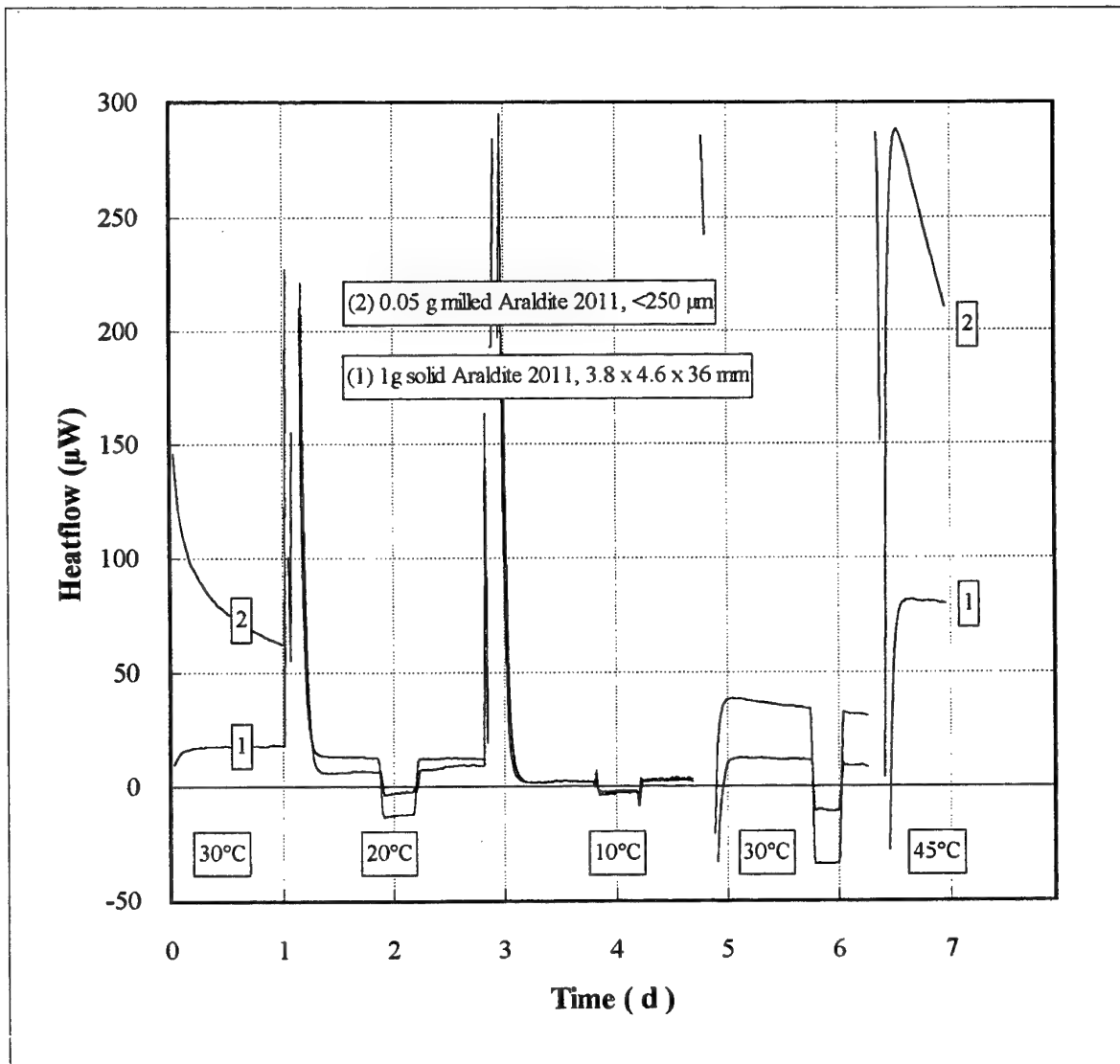


**FIGURE 1**

Interaction curves for 1 g of solid (curve 1) and 0.05 g of milled (curve 2) epoxy exposed to a double base propellant at different temperatures. The temporary changes to negative heatflow values represent the so-called switch technique for accurate determination of the baseline position.

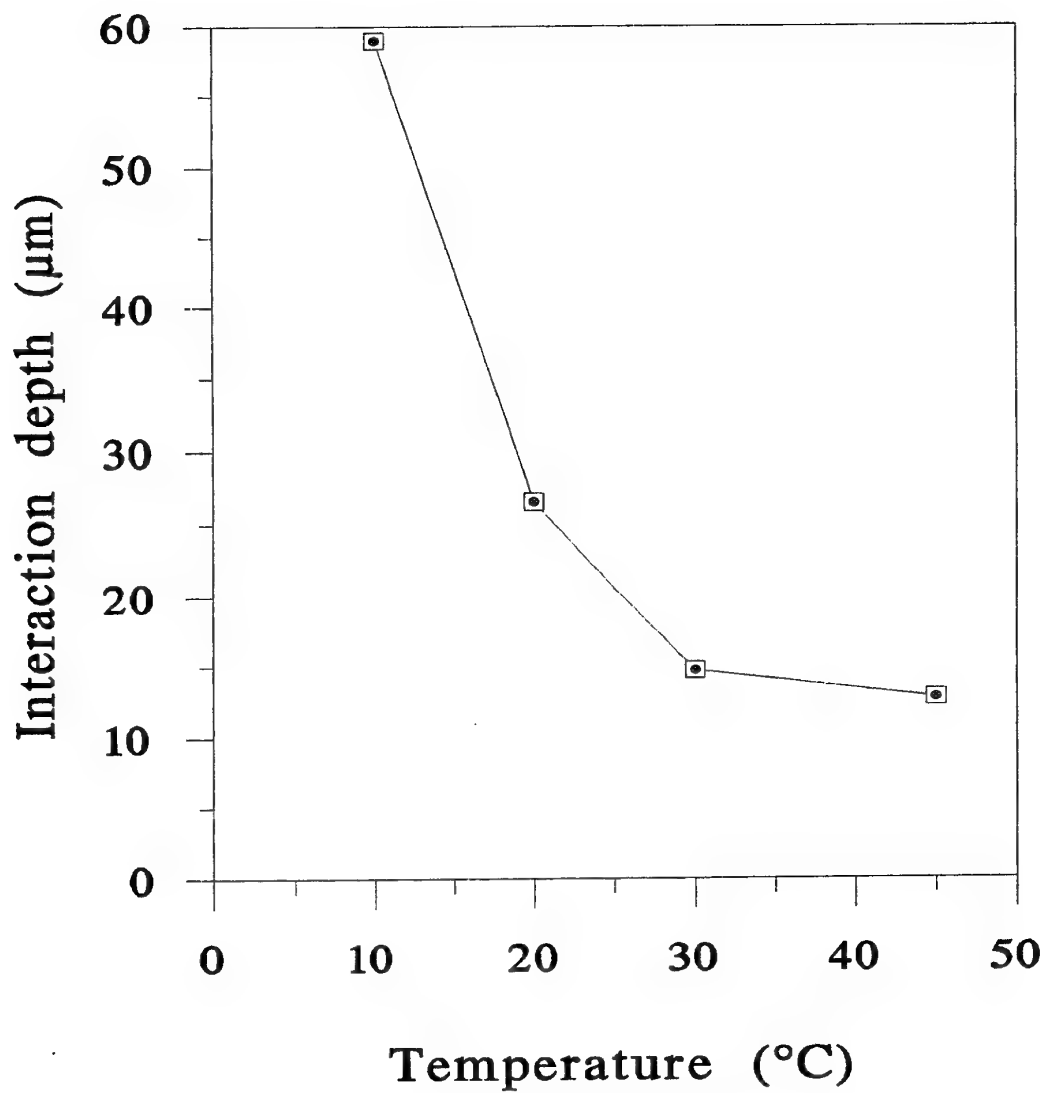


**FIGURE 2**

Interaction profile thickness as a function of temperature, calculated from Eq. (3). The calculation is based on the assumption that the finely milled epoxy sample is 100% reactive. This is not necessarily true at the highest temperatures where the interaction depth is of the same order of magnitude as the average thickness of the epoxy grains.

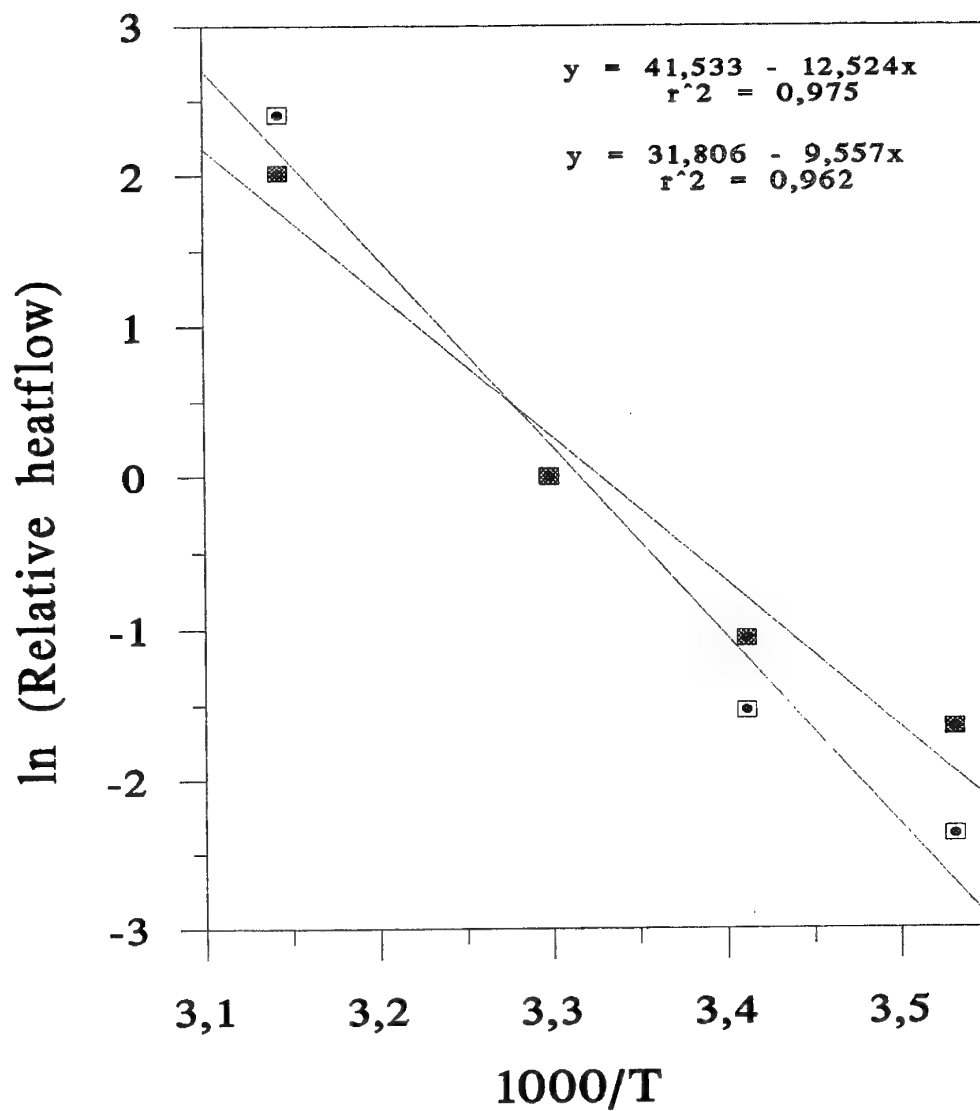


**FIGURE 3**

Arrhenius plots for the interaction of milled (□) and solid (■) Araldite 2011 with double base propellant. The linearity is poor for both plots indicating that the interaction is complex.

$E_a$  (average, milled) = 104 kJ/mol

$E_a$  (average, solid) = 79 kJ/mol

# MICROCALORIMETRIC CRITERIA FOR EVALUATION OF CORROSIVE LIQUID PROPELLANT ON METAL CONTAINERS

Anton Chin, Daniel S. Ellison Daniel R. Crowley and Harry A. Farmer  
Test & Evaluation Department  
Ordnance Engineering Directorate  
Crane Division, Naval Surface Warfare Center  
Crane, Indiana 47522-5001 USA

## ABSTRACT

Corrosive liquid propellants such as red fuming nitric acid and hydrazines are often used in the missile propulsion system. During storage at various environmental stimuli, some types of the metal containers may corrode to a point that accidents can occur. In order to accurately test the rate of corrosion, a special metal container was designed and developed to fit the detector of the TAM Model 2277 microcalorimeter.

The sample cell assembly, including inner cell for holding the sample and outer cell for protecting the microcalorimeter in case the inner cell cracks, was made at NSWC, Crane. Both inner and outer cell were made by machining the same alloy metal used for the actual container (17-7 PH stainless steel). The proportion of the dimensions of the sample cell was made as closed as possible to that of the tank under investigation.

In this paper, the completed design of the test apparatus, methods used to determine the corrosion rate and the safety service life of the container will be presented.

## I. BACKGROUND

Inhibited red fuming nitric acid (oxidizer) and hydrazine derivatives (fuel) are widely used in the liquid propulsion system of training and target missiles. Due to the nature of the ingredients, the metal container may corrode and etch to a point that accident can occur. Spontaneous explosion of the container was reported sometime ago in the tropical country such as Philippine.

Preliminary results from failure analysis indicated that the major cause for the explosion was probably due to the over-pressure from the oxidizer tank containing the inhibited red fuming nitric acid. It was concluded that the burst tank was overfilled when originally charged with inhibited red fuming nitric acid. On the basis of these findings, The shelf life of the units filled with the acid was reduced to no more than two years.

## II. RATIONALE FOR EXTENSION OF SHELF LIFE

Due to the current two year shelf life restriction of the devices, the realistic production or operational requirements of the program can not be met. Therefore, an effective test method is urgently needed to reinvestigate the actual shelf life of the devices and to extend it realistically without compromising safety. Based on the failure report issued after the accident, the recommendation for 2 year shelf life was an action of emergency, not on sufficient and well proved scientific evidence. Although there were test data to verify that the oxidizer tank had successfully passed the 2 year test, no tests were conducted to prove or disapprove that the tank can not pass five years or longer safe storage time. After visiting the tank manufacturer and fuel/oxidizer filling facility at the contractor's warehouse, there was a stronger believe that the shelf life of the devices can be extended using the microcalorimetric technology.

## III. HISTORY AND BASIC PRINCIPLE OF MICROCALORIMETRY IN CORROSION STUDY

History: Early microcalorimetric method for determination of the shelf life of any substance or composition was focused primarily on the pharmaceutical and biochemical. In 1980, AB Bofor Sweden, was the first pioneer to apply the same technology to study the compatibility and aging processes of propellants, explosives, and pyrotechnics (PEP). Today the technique opens more new application fields to include characterization of moisture sensitive PEP, corrosion process, and material aging, just to name a few. NSWC, Crane Division adapted the same technique in 1988 and developed it extensively to suit the need of surveillance work on the aging trend and shelf life of PEP.

Basic Principle: Practically all chemical and/or physical reactions known today are accompanied with heat production or consumption. Metal corrosion reaction is no exception to this rule. A metal is considered corrosion-resistant if the corrosion rate is less than 0.1 mm/year. This is equal to a constant heat flow of approximately 20  $\mu\text{W}$  (microwatts) per  $\text{cm}^2$  of the sample's surface area [1]. Such a small heat flow is often difficult to measure using the conventional thermal analyzers such as DSC (Differential Scanning Calorimetry) and DTA (Differential Thermal Analysis). One method that has proven to be very useful in a variety of applications concerning the aging trend and shelf life of energetic compositions is microcalorimetry. Microcalorimeter is known to be the world's most sensitive heat detecting instrument (detectability limit  $< 0.2 \mu\text{W}$ ) for measuring the degradation rate in terms of heat flow. Figure 1 shows the sketches of microcalorimeter cross section and measuring cylinder. Figure 2 shows the close-up view of the detector. It should be noted that the amount of heat flow associated with a energetic reaction is always a function of temperature. Temperature dependent rate constant (k) can be obtained by the well known Arrhenius Equation:

$$k = A \exp(-E_a/RT)$$

R = gas constant (1.987 cal/mole-°C)  
E<sub>a</sub> = energy of activation  
T = absolute testing or storage temperature (K°)  
A = frequency factor (pre-exponential factor)

Integration between T<sub>1</sub> and T<sub>2</sub>, the equation can be modified as:

$$\ln k_2/k_1 = - \frac{E_a}{R} (1/T_2 - 1/T_1)$$

Measuring the heat flows of a energetic system (i.e. metal + acid) at different temperatures will establish the database for tabulating the accelerating factors. Accelerating factor is defined as the ratio of rate of reaction (k<sub>2</sub>/k<sub>1</sub>) or degradation (corrosion, etc.) at any two different temperatures (T<sub>2</sub> and T<sub>1</sub>). Accelerating factor by far is the most important single number for providing guidelines for an accurate and successful accelerating aging test. To conduct the accelerating aging test at the highest temperature, without compromising safety and/or changing course of degradation mechanism, microcalorimetry is the best method to achieve the longest aging equivalent within the shortest possible time.

#### IV. TECHNICAL APPROACHES

##### 1. SAMPLES:

Oxidizer - Freshly made IRFNA (inhibited red fuming nitric acid) stored in a inert container should be used.

Fuel - A pre-mixed MAF-4 fuel which contains 60% 1,1-dimethylhydrazine, and 40% diethylenetriamine stored in a proper container should be used.

Sheet Metal Plates - A total of 4 pieces approximately 1" x 1" x 0.06" sheet metal from standard tank material are needed from the contractor. The first two are plain tank metal which will be used as models to calibrate the surface condition of the test cells made at Crane. The other two are actually two separate pieces of 1" x 0.5" tank metal welded together by a electron beam. These two plates are intended to be used in the controlled experiments. All 4 metal plates should be heat treated before shipping to Crane.

Sample Cell - Sample cells will be made at NSW Crane by machining the same alloy metal block (17-7 PH stainless steel from Allegheny Ludlum) to the dimensions as illustrated in



Figures 3a - 3c. The proportion of dimensions of the small scale sample cell will be made as closed as possible to that of the actual tank. Gold gaskets are custom-made to fit and to prevent the acid from leaking into the microcalorimeter detector. The inside portion of the cell cover will be gold-plated to obtain more controllable reaction. After completion, the sample cells will be sent to the contractor for electron beam welding (simulate) and heat treatment before use. These processes are necessary to assure that the sample cell have similar mechanical property to that of the actual liquid propellant tank.

Pressure Transducer - HPLC fittings will be used to connect between the sample cell and high performance pressure transducer (>2000 psi).

## 2. TESTING:

Microcalorimetry - Thermometric (TAM Model 2277): Isothermal microcalorimeter will be used for the analysis. Initial tests will be conducted at 25, 35, and 45°C. Different temperatures may be used depending upon the initial results. In general, the basic kinetic approach to determine the shelf life of the corrosion process follows the guidelines listed below [2].

- a. Define the end of induction time.
- b. Establish critical properties at zero aging time. This requires historical information and database analysis.
- c. Obtain heat flow ( $\mu\text{W}$ ) as function of temperature.
- d. Identify limiting reactions (Reagents) which control the major aging and degradation processes (rate determine step).
- e. Develop quantitative model for properties as a function of time.
- f. Determine orders of reaction and rate constants for property changes.
- g. Fit rate constants to the Arrhenius Equation and determine the activation energy and accelerating factors of the corrosion process in a temperature interval between the natural storage and test temperatures.
- h. Define critical property value (end of service life) of the item under test by calculating the maximum acceptable heat flow for the prevailing storage conditions (temperature, material quantity, etc.), using standard models for thermal runaway reactions.
- i. Time to reach critical property value at various temperatures (Service life or shelf life) will then be determined.

#### Other Supporting Tests:

- a. Surface Area Analysis - Used to determine the surface area differences between the sample cell and the actual fuel/oxidizer tank, per  $\text{cm}^2$ .
- b. Fuel and Oxidizer Samples - Samples of each will be filled into the sample cell to a point that the volume of ullage to sample ratio is proportional to the actual device.
- c. Scanning Electron Microscopy (SEM): Amray Model 3200S, ECO SEM will be used. The SEM will provide qualitative information on the corrosion by-product during the testing. The morphology information provided by SEM will allow insight into the growth rate and method of corrosion.
- d. Leco Neophot Optical Metallograph (LNOM): LNOM will be performed on a cross-sectioned sample of the corroded material. The sample will be polished and etched in accordance with ASTM procedures. The depth of pitting and corrosion mode, intergranular or transgranular, will show the potential failure mode of the material due to corrosion.
- e. Stress Analysis and Hydro-burst Test: When two pressure cylinders of different size subjected to the same internal pressure, the distribution of radial and tangential stress to the vessel wall are a function of the ratio of radius to wall thickness. In order to compensate the difference, higher pressure has to be applied to the smaller cell. A computer stress study will be conducted to compensate the difference before the actual hydro-burst test take place.

#### **V. INFORMATION OBTAINED**

Microcalorimetry is the most effective thermal technique to perform the accelerating aging test and measuring the real time aging processes in one instrument. Use this method, a ten years aging equivalent of corrosion process at ambient temperature can be achieved in less than 2 or 3 months at higher temperatures, depending upon the accelerating factor. This means a substantial cost saving in time and money. The following three important information can be obtained when all the tests are completed.

1. Maximum Acceptable Heat Flow and Stability: The heat generated in terms of heat flow ( $\mu\text{W}$ ) will provide valuable information about how stable the oxidizer/fuel and tank system are when subject to the temperature at test. If the observed heat flow does not exceed the maximum limit at any time during the measurement, and shows no autocatalytic tendencies, then the risk for potential thermal hazards or self-explosion accidents should be negligible. The maximum acceptable heat flow can be calculated for the prevailing storage or processing conditions (temperature, fuel/oxidizer quantities, etc.), using standard models for thermal runaway reactions [3]. This information may provide some vital clue about actually how the oxidizer tank of the

target missile exploded in Philippine.

2. Three-way Correlation Diagram of Corrosion rate, Temperature and Pressure: A three-way real time temperature, pressure, and degradation rate correlation chart will be established to predict the shelf life of fuel/oxidizer container systems at various storage temperatures. This chart will be the most important information for the responsible safety officer (RSO) to overview the entire relationship of degradation rate as a function of temperature and pressure over a known period of time. At a normal or emergency situation, the RSO will be able to know the exact safety condition of the tank and make a quick and best judgement of it.

3. Aging Trend and Shelf Life: Based on the information in the previous sections., the shelf lives within the test temperature range (i.e. 25, 35, 45°C) can be determined. Shelf lives beyond this region has to be extrapolated by an Arrhenius Plot (Ln rate vs. reciprocal of test temperatures). The program manager (APML) and RSO will determine the final safety margin of extension of shelf life.

## VI. CONCLUSION

A question will surely be asked if the microcalorimetric data is truly representing the data from testing the actual scale device. The answer is positive for the following three reasons; a). corrosion rate is measured in the unit of depth of corrosion per time (mm/year) which is independent of size, shape, and total surface area of the container, b). the test cell is nearly a true replica made of the same tank material and later heat treated according to the manufacturer's specification, c). all theories and test methods are based on science and existing procedures. Since the data from the hydro-burst test of the smaller container has to be compensated by using higher pressure (>1500 psia), therefore an higher deviation is expected.

## VII. REFERENCES

1. L.E.Paulsson, L. G. Svensson, and C. K. Forsgren, "Microcalorimetric Methods for Corrosion Rate Measurement". ThermoMetric Application Note #TM001. Department of Explosive Technology, AB Bofor, Bofors, Sweden. (1989).
2. A. Chin and D. S. Ellison, "New Microcalorimetric Approaches In Shelf Life Technology". Proceedings of ADPA Predictive Technology Symposium, p-238 (1993)
3. L. G. Svensson, L. E. Paulsson, and T. Lindblom, "A Microcalorimetric Study Of Temperature and Stabilizer Effects On The Heat Generation In Gun Propellants". 4<sup>th</sup> Gun Propellant Conference, Mulwala, Australia, (1990).

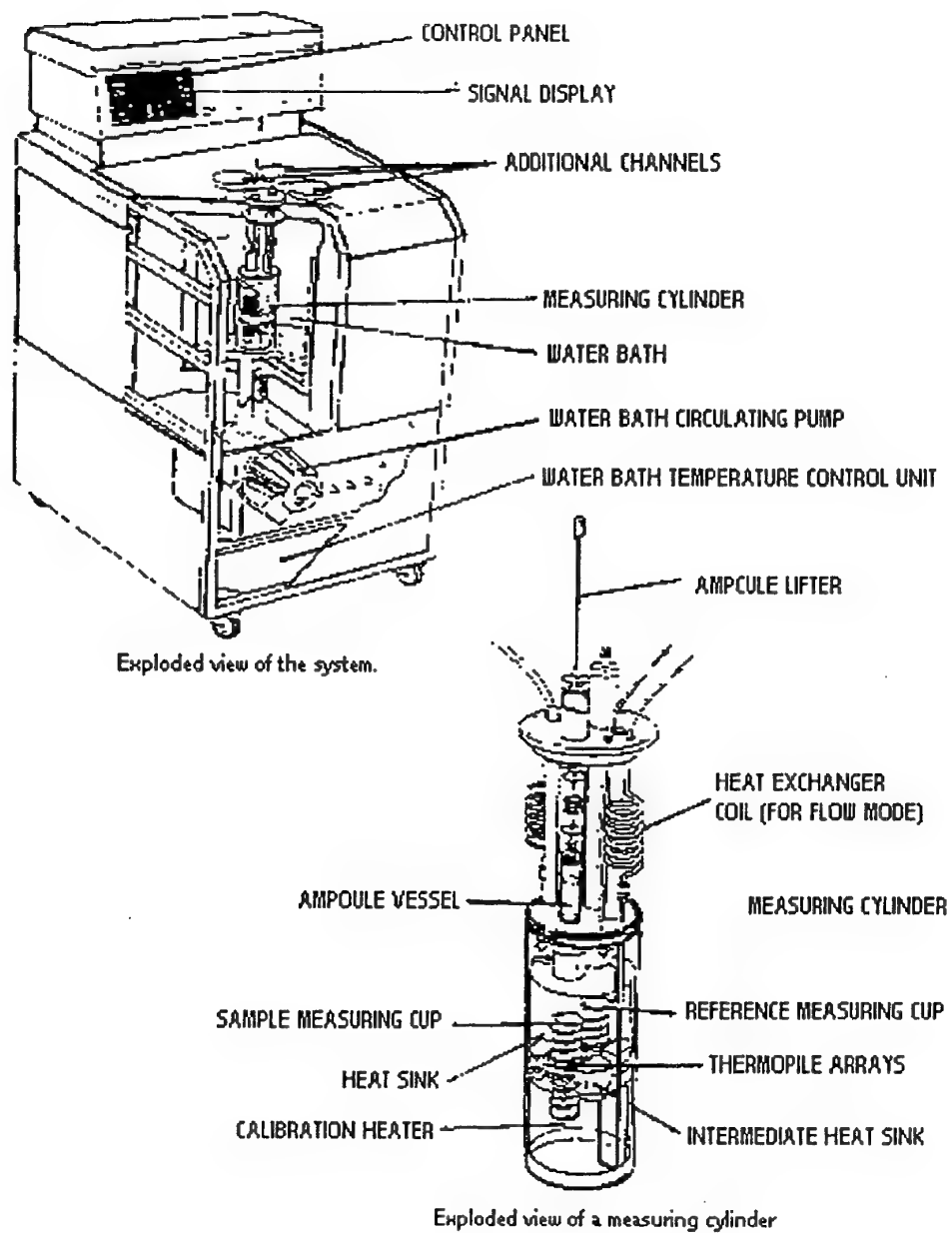
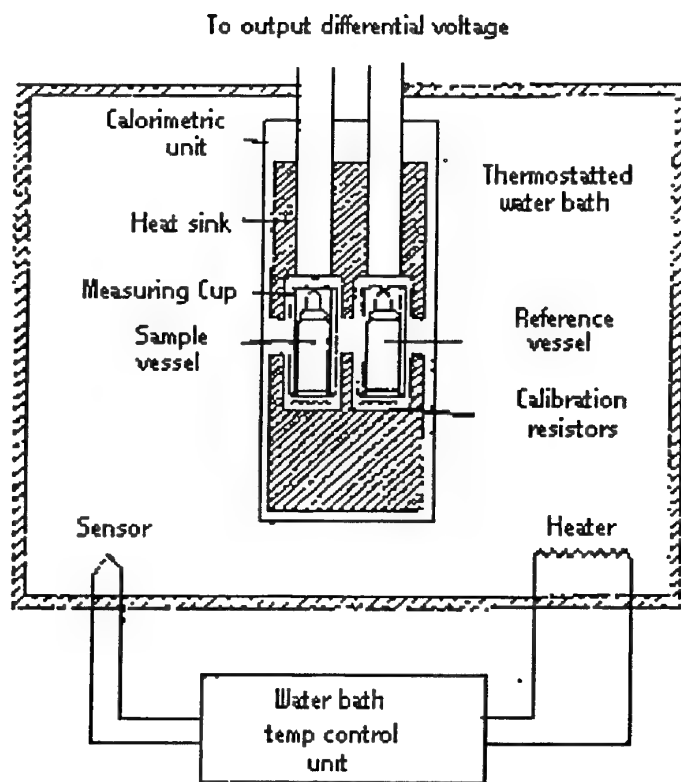


**Figure 1.** Sketches of Microcalorimeter Cross Section (top and Measuring Cylinder (bottom)).



Basic Microcalorimeter cell,  
sample side

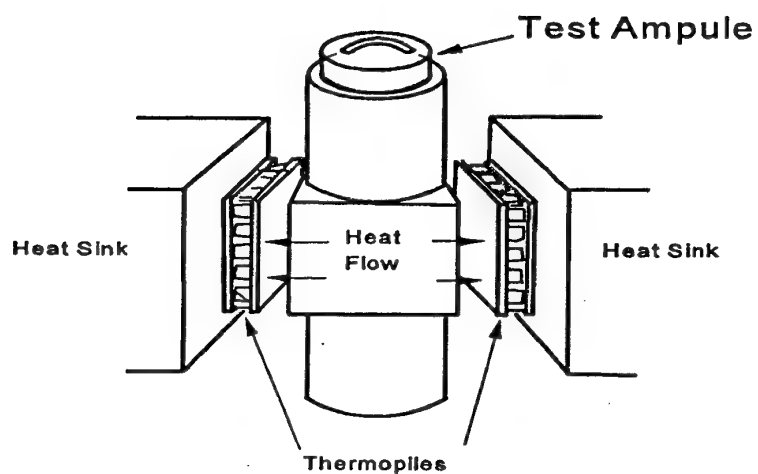


Figure 2. A Closer Look at the Detection and Measurement Unit (top) and  
a Much Closer View of the Detection Unit (bottom)

TEST AMPOULE  
17-7 PH STAINLESS  
STEEL

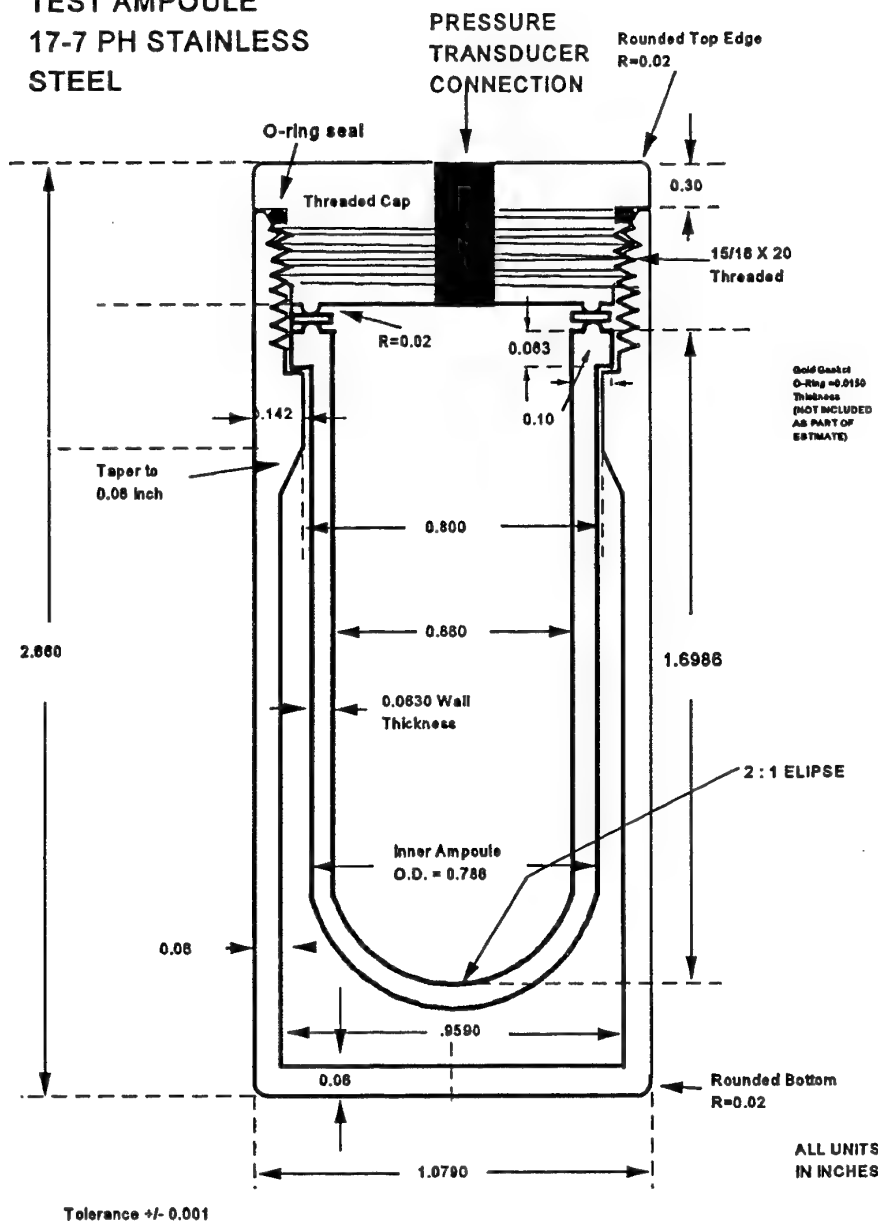
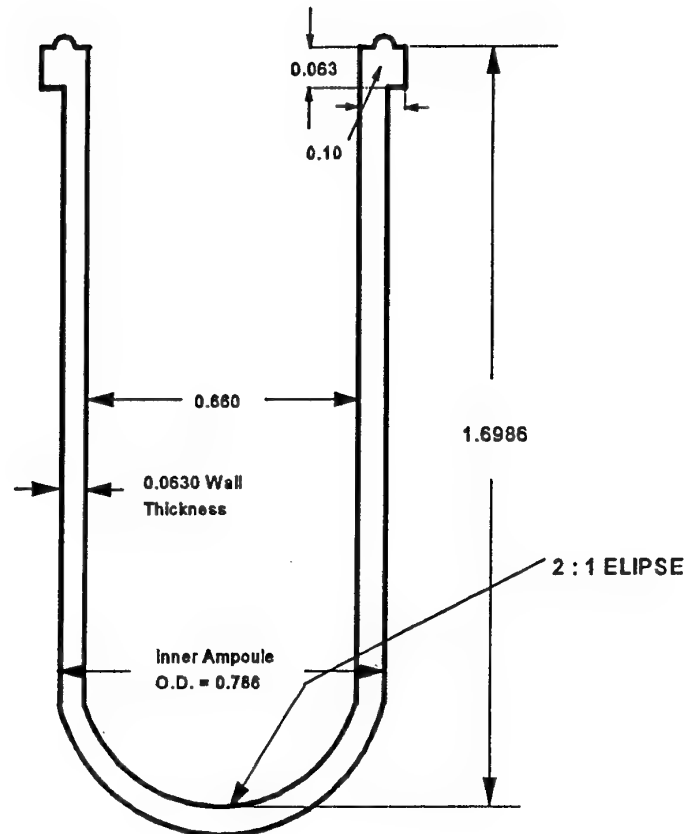


Figure 3a. Overall View of Microcalorimetric Test Cell for Corrosion Rate and Shelf Life Analysis of AQM-37 Fuel/Oxidizer Tank

INNER TEST AMPOULE  
17-7 PH STAINLESS  
STEEL



ALL UNITS  
IN INCHES  
Tolerance +/- 0.001

Figure 3b. The Dimesions of Inner Sample Cell for Oxidizer or Fuel.

PROTECTIVE OUTER TEST AMPOULE  
17-7 PH STAINLESS STEEL

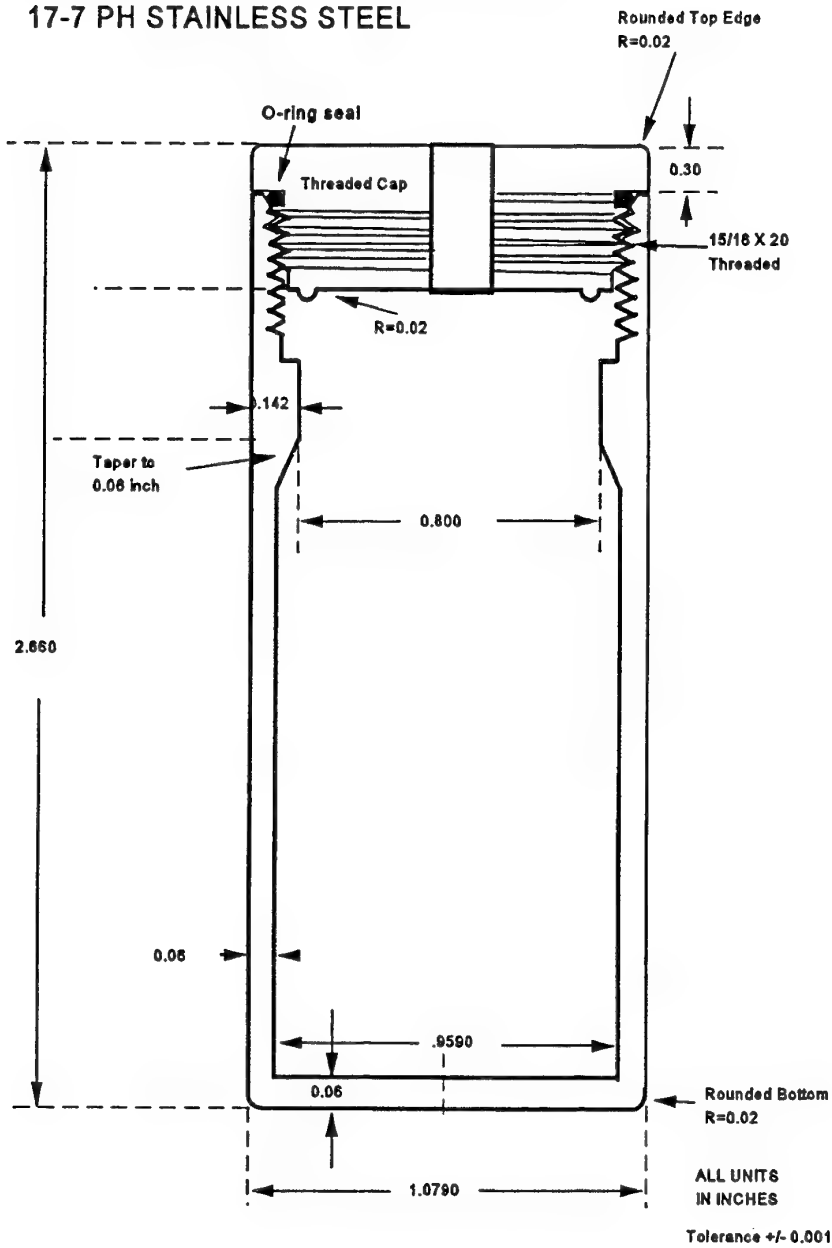


Figure 3c. The Dimensions of Outer Protecting Cell. The Purpose of This Cell is to Protect the Microcalorimeter Detector in Case the Inner Sample Cell Burst.



## PRELIMINARY MICROCALORIMETRIC STUDIES OF ADVANCED GUN PROPELLANTS

A. White, R.M. Kempson and P. Berry  
(presented by J. Adams)

Weapons Systems Division, Aeronautical and Maritime Research Laboratory,  
Defence Science and Technology Organisation, PO Box 1500, Salisbury,  
South Australia, Australia.

### 1. INTRODUCTION

Conventional gun propellants contain nitrocellulose (NC) as a major energetic component. NC is inherently unstable, decomposing with the release of oxides of nitrogen. These oxides themselves may react with the NC, causing further denitration and subsequent degradation of the cellulose chain itself. This ultimately results in a degradation of physical and ballistic properties and a consequent reduction in service-life. If these reactions are not retarded, autocatalysis of the decomposition ensues, possibly resulting in spontaneous deflagration. Stabilisers are introduced into these propellants during manufacture to react with the oxides of nitrogen as they are produced, hindering further reactions, thereby extending service-life and safe-life.

In recent years, advanced gun propellants have been developed with a view to improving performance, reducing sensitivity and replacing or reducing the amount of NC found in conventional gun propellants. These propellants may contain energetic ingredients such as hexahydro-1,3,5-trinitro-1,3,5-triazine (RDX), triaminoguanidine nitrate (TAGN) and 1,5-diazido-3-nitrazapentane (DANPE).

At present all gun propellants contained in munitions in service with the Australian Defence Force are of the conventional type. However, it is likely that munitions containing advanced propellants will be introduced into Australian service in the foreseeable future. Consequently, Weapons Systems Division (WSD) has been investigating chemical, ballistic and thermal properties of these propellants. In particular, attention has been focused on suitable stabilisers for these types of propellants [1, 2, 3] and the safe-life and service-life implications of introducing them into service [4].

Several methods have been applied to study the stability of advanced gun propellants, including stabiliser loss and molecular weight degradation during accelerated ageing [1, 2, 3]. The availability of modern commercial microcalorimetry instruments has introduced another technique which may provide

additional information on the processes occurring in these propellants. This paper describes the application of this technique to several advanced gun propellants. The results obtained are compared with those from stabiliser content measurements, the Abel heat test and the vacuum stability test. Differences in the results from these tests after accelerated ageing of the propellants are also discussed.

## 2. EXPERIMENTAL

### 2.1 Propellant manufacture

Advanced gun propellants were manufactured using the WSD gun propellant batch processing facility using conventional solvent processing techniques [5]. All propellants were processed using ethyl acetate/ethanol solvent (however, the ratio varied according to the formulation) in incorporators of either 3 or 6 L nominal capacity. Propellants were extruded in 7 perforate form using dies with a diameter/pin size of 5.27 mm/ 0.50 mm). From previous work [1, 2, 3] the most appropriate stabiliser was chosen for each formulation. The propellant cords were granulated to 8 mm length and stoved to reduce total volatile matter (water plus residual processing solvents) levels to less than 2% (m/m) of the finished propellant. The finished propellants ranged in length from 7.8 to 8.6 mm and in diameter from 4.5 to 4.9 mm. Propellant formulations are given in Table 1 (a glossary of acronyms and abbreviations is provided in section 6).

*Table 1: Nominal propellant formulations.*

Lot	Formulation					
	NC (%)	Polymer	Plasticiser	Energetic filler	Stabiliser (%)	TVM (%)
1253	37.5	Etocel	DOS	RDX	0.7 EC	0.18
1254	4.0	CAB	ATEC	RDX	0.4 EC	0.01
1255	4.0	CAB	BDNPA/F	RDX	0.4 EC	0.28
1256	30.0	-	DOP	RDX/TAGN	1.0 RES	1.13
1257	26.5	-	DANPE	RDX/TAGN	1.0 RES	1.49
1258	33.0	-	DANPE	RDX/TAGN	1.0 2NDPA	1.37
1259	30.0	-	DANPE	RDX	1.0 2NDPA	1.64

### 2.2 Accelerated ageing

Unground samples were heated at 65.5°C for 60 days in loosely stoppered test-tubes (Method 403 [6]). This method is adapted from that used in NATO Stanag 4117 and is the standard accelerated ageing test employed for the sentencing of propellants in Australian service.

### 2.3 Stabiliser analysis

EC and 2NDPA were determined by reverse phase high performance liquid chromatography (HPLC) [7]. A 0.6 g sample was extracted with dichloromethane and 2-4-dinitrotoluene (DNT) was added as internal standard. The analysis was carried out using a Waters chromatograph (Model 600E pump, 717 WISP Autosampler and 490E UV detector) fitted with a Radpak Resolve C18 column, using UV detection at 270 nm and an isocratic solvent system of water/acetonitrile (35/65) at a flow rate of 1.6 mL/min.

Resorcinol was determined by gas chromatography (GC). A 2.0 g sample was extracted with dichloromethane, DNT was added as internal standard and the analysis was carried out using an SGE BP10 Megabore column (25 m long  $\times$  0.53 mm ID). The initial oven temperature was 120°C followed by a temperature ramp, a flame ionisation detector and nitrogen as carrier gas.

### 2.4 Abel heat test

The Abel heat test is a simple traditional test, subjective in nature, that relies on the detection of low concentrations of nitrogen oxides from a heated propellant by a starch/iodide paper. The test was conducted at 82.2°C (Method 401 [6]), the test temperature usually employed in UK and Australian specifications for acceptance of single base propellants.

### 2.5 Vacuum stability test

Five gram samples were placed in vacuum stability tubes fitted with pressure transducers. The tubes were evacuated, placed in a metal heating block at 100°C and allowed to equilibrate for one hour. The volume of gas evolved over the next 40 hours was determined.

### 2.6 Microcalorimetry

#### 2.6.1 Instrumentation

Heat flow measurements were obtained using a Thermometrics thermal activity monitor (TAM) model 2277. Samples were run in glass ampoules sealed with Teflon-faced butyl rubber septa. The TAM was run at a nominal temperature of 65°C controlled to  $\pm 0.001^\circ\text{C}$ .

#### 2.6.2 Sample preparation

Septa were conditioned in an oven at 65°C for 48 hours prior to use and were only used once. Specially cleaned dry glass beads (0.5 mm) were used in the reference ampoules. Propellant samples consisted of  $1 \pm 0.05$  g samples (weighed to 1 mg) ground to Abel heat test size (passes 2.0 mm sieve but retained on 1.0 mm sieve). Ampoules containing propellants and glass beads

(reference) were conditioned in an oven for 24 hours at 65°C prior to being placed in the TAM.

#### 2.6.3 Analysis procedure

After a 30 minute time lapse, baselines were recorded for 30 minutes. A 60 minute pause phase was then initiated. At the commencement of the pause, the ampoules were introduced and lowered to the equilibration position (halfway down). After 20 minutes in this position, the ampoules were lowered the rest of the way to the measuring position. After the pause phase, curves were recorded for a period of 24 hours, after which the ampoule was removed during another 60 minute pause phase and a further 30 minute baseline was recorded. In all cases, baseline correction was found to be unnecessary. All data were normalised for one gram samples. All samples were run in duplicate.

### 3. RESULTS AND DISCUSSION

If it is assumed that stabiliser depletion during accelerated ageing of propellants containing NC occurs through reaction of the stabiliser with the oxides of nitrogen evolved from the decomposition of the NC in these propellants, then it would be expected that the stabiliser would deplete more rapidly in propellants with higher NC contents. Given two propellants with different stabilisers but the same NC content, a more rapid rate of stabiliser depletion in one during accelerated ageing may mean that that stabiliser is performing better and more quickly reacting with the nitrogen oxides as they are produced by the self-decomposing NC, preventing them causing further decomposition of the NC. On the other hand, a rapid rate of stabiliser depletion may mean that the stabiliser is reacting directly with another component in the formulation, possibly the NC, causing its premature decomposition. Other tests, apart from stabiliser depletion, are required to differentiate between these effects. Such tests include the Abel heat test, the vacuum stability test, microcalorimetry and gel permeation chromatography (by which degradation of the nitrocellulose in a propellant can be monitored by measurement of changes in its molecular weight).

#### 3.1 Stabiliser analysis

Stabiliser levels, and  $(\text{stabiliser level} / \text{NC content}) \times 100$ , before and after accelerated ageing are given in Table 2. Lots 1254 and 1255 were manufactured with a lower percentage of stabiliser than the other advanced propellants (Table 2) because of their very low NC contents [4]. However, because of these very low NC levels, these propellants contain higher ratios of stabiliser to NC than the other propellants (Table 2).

On accelerated ageing, the stabiliser levels in samples stabilised with EC (lots 1253 - 1255) are depleted by a small amount, ranging from 0.03% for lot 1254 to 0.08% for lot 1253 (Table 2). However, relative to the amount of NC present in each propellant, the stabiliser in lot 1255 is depleted most rapidly. It should be noted that lot 1255 is similar in composition to lot 1254 except that lot 1255 contains an energetic plasticiser (BDNPA/F) while lot 1254 contains ATEC (Table 1). The effects of this will be discussed later.

Lots 1256 and 1257, stabilised with resorcinol, lose practically all their primary stabiliser on accelerated ageing. No difference is apparent between the propellant plasticised with the energetic plasticiser DANPE (lot 1256) and that plasticised with DOP (lot 1257), although this may be due to the very little stabiliser remaining. Only the primary stabiliser (resorcinol) is measured by GC, and not the levels of derivatives resulting from its reaction with oxides of nitrogen. Some of these derivatives may still be present and may act as secondary stabilisers. It is intended that a method will be developed for the determination of the derivatives of resorcinol by HPLC.

Stabiliser levels in propellants stabilised with 2NDPA (lots 1258 and 1259) are depleted by amounts intermediate between those of the propellants stabilised with resorcinol and those stabilised with EC. Note that, apart from different stabilisers, lot 1258 contains similar ingredients to that of lot 1257, albeit in different proportions. Lot 1258 is also similar in composition to lot 1259 except that lot 1258 contains TAGN and lot 1259 does not. Again, the effect of these differences will be discussed below.

*Table 2: Stabiliser levels, and (stabiliser level/NC content)  $\times$  100, before and after accelerated ageing at 65.5°C for 60 days.*

Lot	Stabiliser	Stabiliser (%)			(Stabiliser (%)/NC (%)) $\times$ 100		
		Unaged	Aged	Dec.	Unaged	Aged	Dec.
1253	EC	0.65	0.57	0.08	1.73	1.52	0.21
1254	EC	0.36	0.33	0.03	9.00	8.25	0.75
1255	EC	0.35	0.30	0.05	8.75	7.50	1.25
1256	RES	0.81	0.02	0.79	2.70	0.07	2.63
1257	RES	0.81	0.02	0.79	3.06	0.08	2.98
1258	2NDPA	0.96	0.78	0.18	2.91	2.36	0.55
1259	2NDPA	0.93	0.75	0.18	3.10	2.50	0.60

### 3.2 Abel heat test

In conventional single-base propellants, Abel heat test times are an indication of the rate of evolution of nitrogen oxides from the propellant under test, a higher test time indicating a lower rate of evolution. These nitrogen oxides are products from the decomposition of the NC in the propellant on heating. The nitrogen oxides measured in the test are those that escape from the propellant, ie those that do

not react with the stabiliser in the propellant. Thus, it would be expected that propellants with lower NC contents and/or better stabilisers should perform better on the Abel heat test.

Abel heat test times measured at 82.2°C are given in Table 3. In the unaged samples, lot 1253 performs better than lots 1254 and 1255, even though the latter two propellants have much lower NC contents. On ageing, all three of these lots perform poorly on this test, even though they all have a significant amount of stabiliser remaining. On the other hand, the propellants stabilised with resorcinol (lots 1256 and 1257) perform relatively well, both before and after ageing, despite there being very little primary stabiliser left in either propellant after ageing. For the propellants stabilised with 2NDPA, lot 1258 performs poorly before ageing but well after ageing, while lot 1259 performs well before ageing but relatively poorly after ageing.

It appears that the results from the Abel heat test for these advanced propellants should be treated with caution, particularly those from samples which have been aged. If only the unaged samples are considered, it would appear that lots 1254 and 1258 are of inferior stability to the other lots tested.

*Table 3: Abel heat test times at 82.2°C before and after accelerated ageing at 65.5°C for 60 days.*

Lot	Stabiliser	Abel heat test time at 82.2°C (minutes)		
		Unaged	Aged	Diff.
1253	EC	30	7	-23
1254	EC	9	11	2
1255	EC	16	6	-10
1256	RES	30	25	-5
1257	RES	23	20	-3
1258	2NDPA	7	27	20
1259	2NDPA	28	11	-17

### 3.3 Vacuum stability test

The vacuum stability test determines the amount of gas released on heating of a sample during a certain time period. Thus it is an indication of the rate of the reactions causing the gas evolution and can be used to determine compatibility between ingredients in a propellant formulation. In these samples, the primary source of gas evolution (after the residual solvent has been driven off, see Table 1) is expected to be the degradation of nitrocellulose. It should be noted that the test is rather severe, involving heating at 100°C for a period of 40 hours (however, when an excessive reaction was evident the tube was removed from the block before the full duration of the test).

Results from the advanced gun propellants are shown in Table 4. In the unaged samples, lots 1258 shows a particularly high rate of gas evolution with 9.3 mL being evolved after only 3 hours when it was removed from the block. This appears to be in accord with the results from the Abel heat test (Table 3). When the NC content is also taken into consideration (Table 4), lot 1257 also performs poorly, although this is not evident in the Abel heat test results. These propellants contain NC, DANPE, RDX and TAGN as energetic ingredients. As the volume of gas evolved from lot 1259 (containing NC, DANPE and RDX) is relatively low, the poor behaviour of lots 1257 and 1258 appear to indicate some incompatibility between DANPE and TAGN. For the aged samples, lots 1256 and 1257 perform very poorly, as might be expected from their low levels of remaining stabiliser (Table 2). The aged sample of lot 1258 was not tested for safety reasons.

*Table 4: Vacuum stability data for 5 g samples heated for 40 hours at 100°C before and after accelerated ageing at 65.5°C for 60 days.*

Lot	Volume of gas evolved (mL)			Gas volume evolved (mL) / NC (%)		
	Unaged	Aged	Diff.	Unaged	Aged	Diff.
1253	3.5	4.6	1.1	0.09	0.12	0.03
1254	0.3	0.4	0.1	0.08	0.10	0.02
1255	0.7	0.6	0.1	0.18	0.15	0.03
1256	5.8	10.1 <sup>1</sup>	>>4	0.19	0.33 <sup>1</sup>	>>0.13
1257	6.7	10.8 <sup>2</sup>	>>4	0.25	0.40 <sup>2</sup>	>>0.15
1258	9.3 <sup>3</sup>	Not done <sup>4</sup>	-	0.28 <sup>3</sup>	Not done <sup>4</sup>	-
1259	3.7	4.1	0.4	0.12	0.14	0.02
<sup>1</sup> after 6 hours, tube then removed from block <sup>2</sup> after 10 hours, tube then removed from block <sup>3</sup> after 3 hours, tube then removed from block <sup>4</sup> not done due to excessive reaction by the unaged sample						

### 3.4 Microcalorimetry

Microcalorimetry was used to obtain heat flow measurements ( $\mu\text{W/g}$ ). A positive heat flow is a measure of the exothermic reactions occurring in the propellant. The main exothermic reaction in conventional propellants during accelerated ageing is degradation of the NC. Thus the heat output is a measure of the rate of NC degradation. Again, higher heat outputs should be expected from propellants with higher NC contents. In advanced propellants containing other energetic ingredients, other reactions may occur in the propellant, which would have an effect on the results obtained by microcalorimetry.

Heat flows measured by microcalorimetry are shown in Figures 1 - 7. Traces shown include the initial time lapse, baseline and pause phase during which the samples were introduced. In general, the traces for the unaged samples have a negative slope (except for lot 1256 which has a negligible slope) while those for

the aged samples show very little or no slope. Why this is so is not known, however as the aged samples often show lower heat outputs than the unaged samples (Figs. 1 - 7), it is possible that the sample is ageing in the TAM and the heat output is approaching that of the aged sample. It is intended that this will be investigated further, with samples being measured in the TAM for longer durations. The directions of the initial excursions as the sample is introduced into the TAM in two stages appear to be arbitrary, with some negative and some positive.

Heat flows recorded 16 hours into the run (an arbitrary time chosen for comparison purposes, where the trace is almost linear and well past the large excursion that can occur for several hours after lowering the vial into the TAM) are given in Table 5. Again, as the heat flow is expected to be affected by the level of NC in the propellant, the heat flow divided by the NC content is also shown in Table 5 for comparative purposes.

*Table 5: Heat flows, and heat flow/NC content, measured by microcalorimetry (at 65°C and 16 hours into run) before and after accelerated ageing at 65.5°C for 60 days.*

Lot number	Heat flow ( $\mu\text{W/g}$ )			Heat flow ( $\mu\text{W/g}$ )/NC (%)		
	Unaged	Aged	Diff.	Unaged	Aged	Diff.
1253	3.7	1.6	-2.1	0.10	0.04	-0.06
1254	3.0	0.3	-2.7	0.75	0.08	-0.68
1255	0.3	0.3	0.0	0.08	0.08	0.00
1256	15.3	40.8	25.5	0.51	1.36	0.85
1257	10.8	14.8	4.0	0.41	0.56	0.15
1258	27.0	6.2	-20.8	0.82	0.19	-0.63
1259	3.3	2.2	-1.1	0.11	0.07	-0.04

The heat flows recorded for the unaged samples of propellants stabilised with EC (lots 1253, 1254 and 1255, Figures 1 - 3, Table 5) show that lots 1253 and 1254 have a higher heat output than lot 1255. However, relative to the NC content (Table 5), the unaged sample of lot 1254 has a much higher heat output for its NC content than the other two lots, indicating that the NC appears to be degrading at a faster rate in this sample than the others. This also accounts for the poor Abel heat test for this sample (Table 3), although this does not appear to be reflected in the results from the vacuum stability test (Table 4).



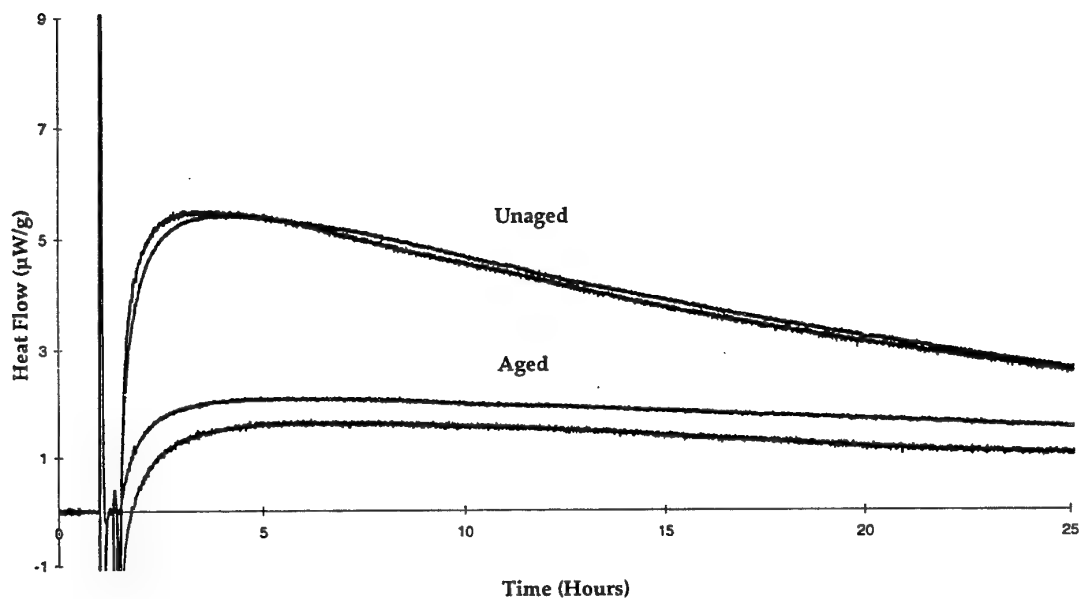


Figure 1: Heat flows ( $\mu\text{W/g}$ ) for lot 1253 before and after accelerated ageing at  $65.5^\circ\text{C}$  for 60 days.

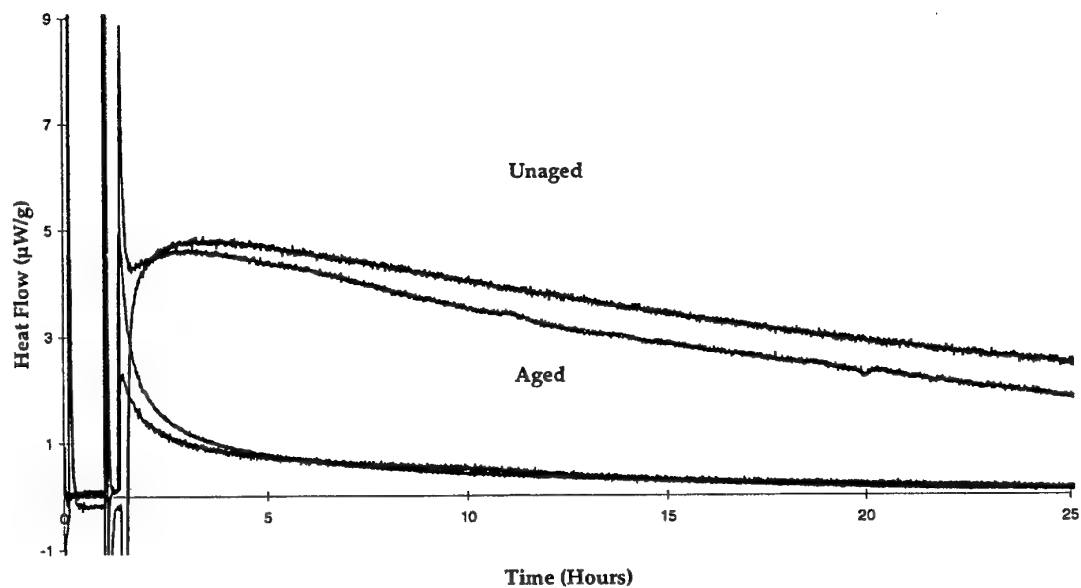


Figure 2: Heat flows ( $\mu\text{W/g}$ ) for lot 1254 before and after accelerated ageing at  $65.5^\circ\text{C}$  for 60 days.

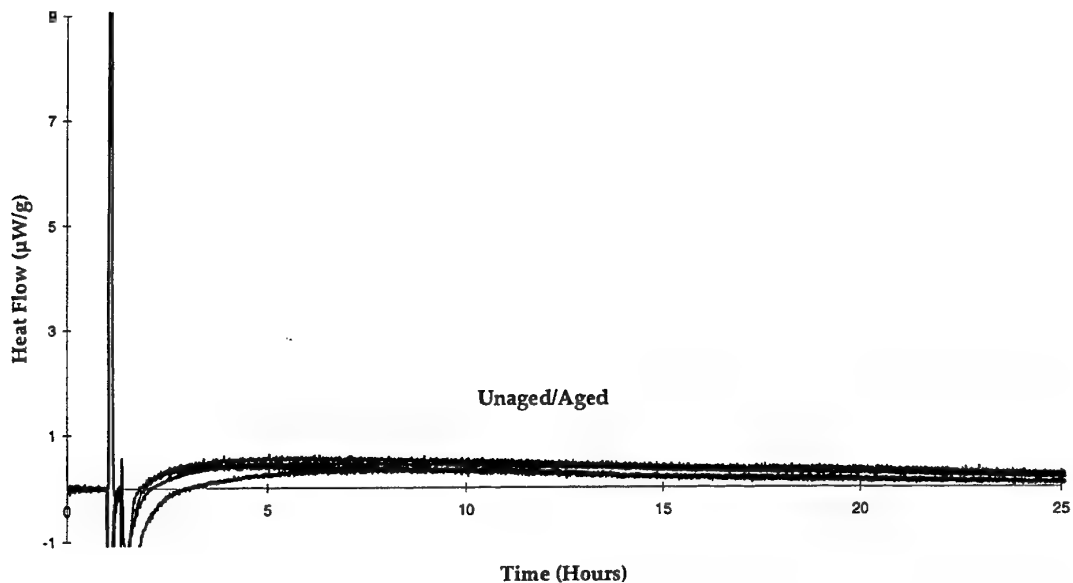


Figure 3: Heat flows ( $\mu\text{W/g}$ ) for lot 1255 before and after accelerated ageing at  $65.5^\circ\text{C}$  for 60 days.

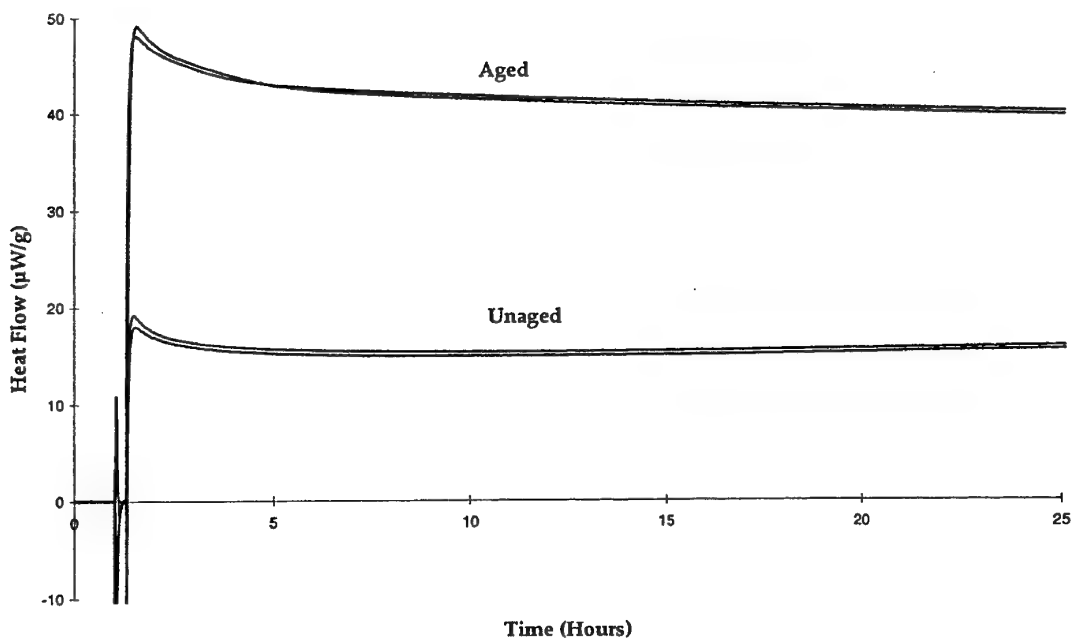


Figure 4: Heat flows ( $\mu\text{W/g}$ ) for lot 1256 before and after accelerated ageing at  $65.5^\circ\text{C}$  for 60 days.

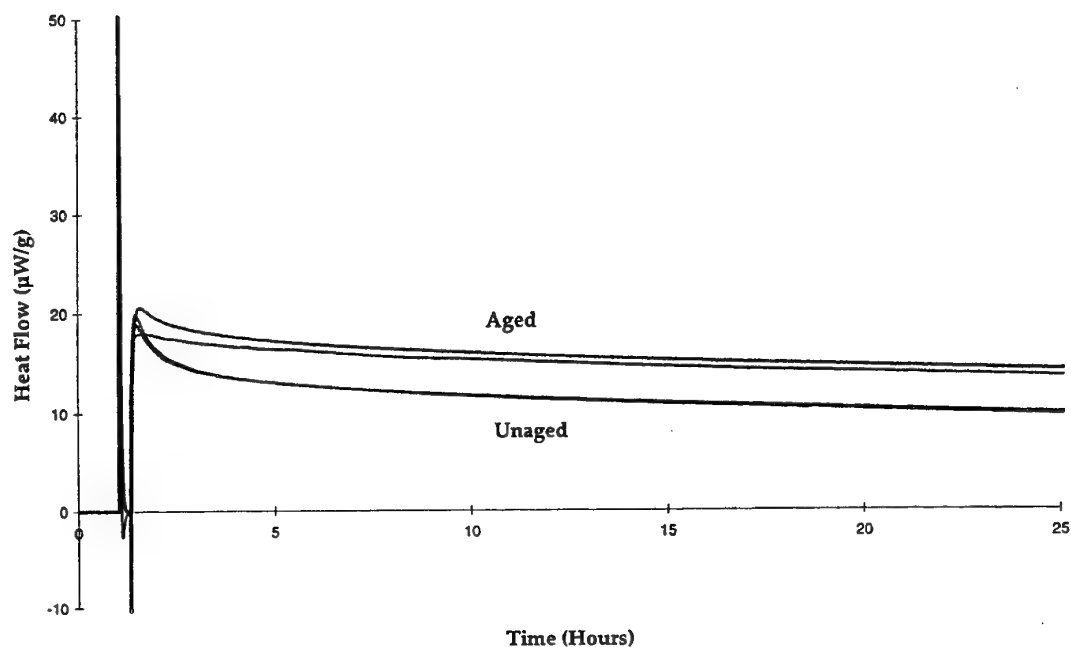


Figure 5: Heat flows ( $\mu\text{W/g}$ ) for lot 1257 before and after accelerated ageing at  $65.5^\circ\text{C}$  for 60 days.

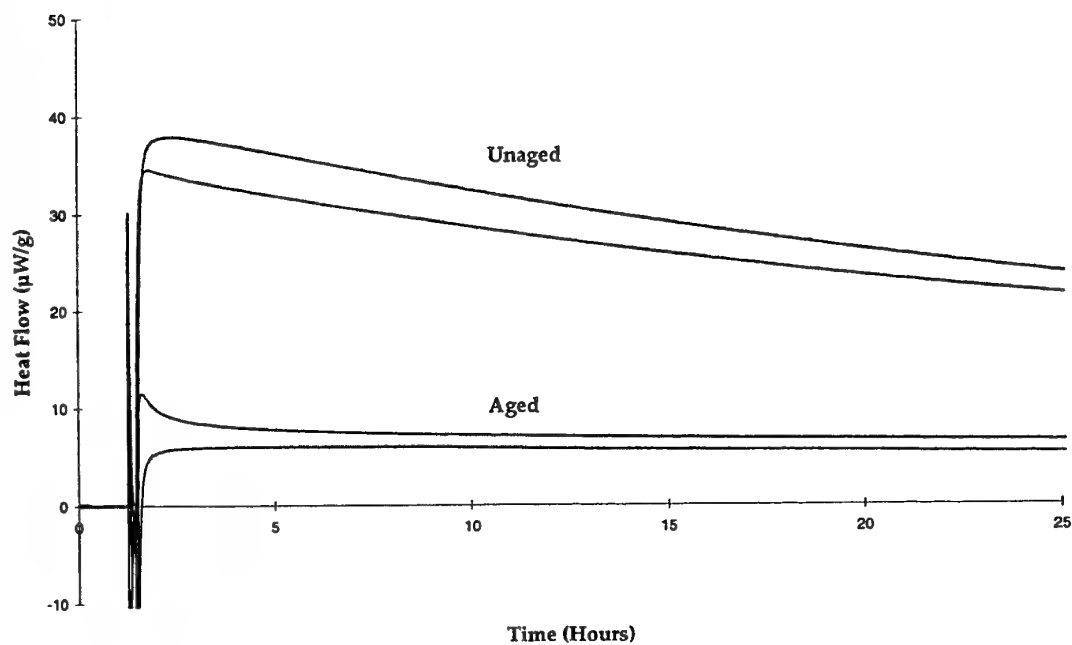


Figure 6: Heat flows ( $\mu\text{W/g}$ ) for lot 1258 before and after accelerated ageing at  $65.5^\circ\text{C}$  for 60 days.

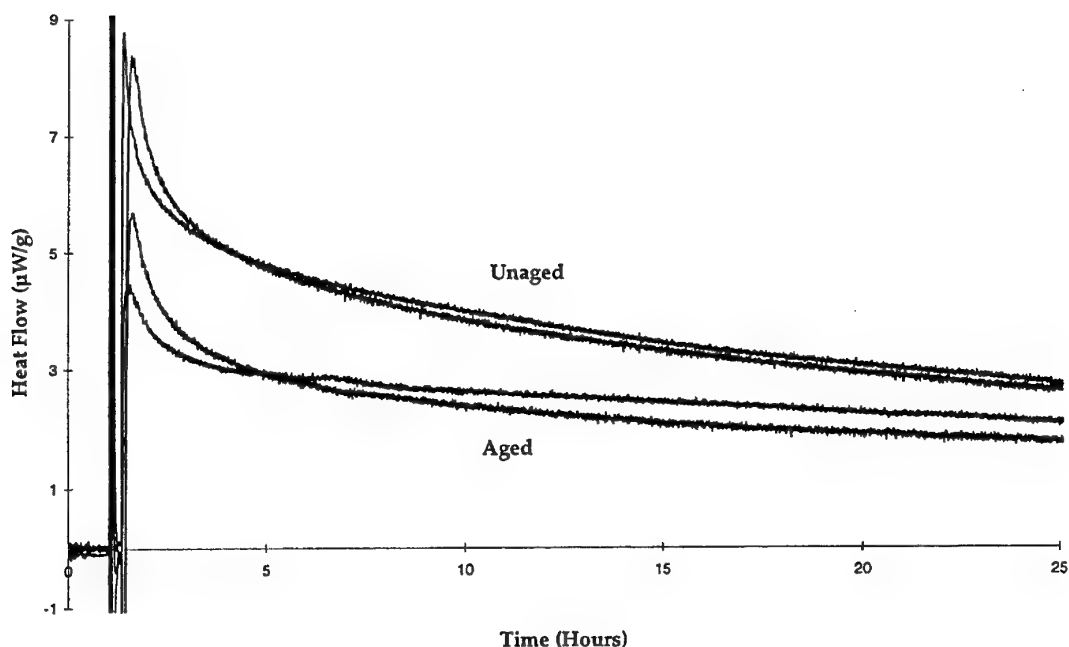


Figure 7: Heat flows ( $\mu\text{W/g}$ ) for lot 1259 before and after accelerated ageing at  $65.5^\circ\text{C}$  for 60 days.

It was noted above that lots 1254 and 1255 are similar in composition except that they contain different plasticisers (ATEC and BDNPA/F respectively). It appears that lot 1255 containing the energetic BDNPA/F is more stable than lot 1254, containing ATEC. Why this should be so is not known at this stage. It is possible that some impurity is introduced with the ATEC (such as citric acid) which causes a reaction in the propellant. Further work is required to resolve this issue. The heat output from the unaged sample of lot 1255 is low, consistent with the low NC content, indicating that nothing unexpected appears to be occurring in this propellant. On ageing, the heat output of lot 1255 does not change, again indicating that nothing untoward appears to be occurring in this sample. On ageing of lots 1253 and 1254, there is a small decrease in the heat output. This also occurs on ageing of the 2NDPA stabilised lots 1258 and 1259. This is similar to that observed in some conventional single base propellants [8, 9].

For the unaged propellant samples stabilised with resorcinol (lots 1256 and 1257, Figures 4 and 5, Table 5), the heat output is higher than those found for the EC stabilised propellants, possibly indicating that the NC is degrading faster in these propellants. These propellants are the only ones of those tested that showed a higher heat output in the aged samples than in the unaged samples. This is probably because practically all the primary stabiliser has been consumed in these propellants, thus the oxides of nitrogen produced by the degrading NC are not being taken up by the stabiliser and are free to react further with the NC, accelerating its degradation.

Unaged samples of lots 1254 and 1258 show very high heat flows relative to their NC contents, even higher than those obtained for the resorcinol stabilised propellants (Table 5). This is consistent with the poor Abel heat test times observed for these samples (Table 3). Although the stabiliser depletion during accelerated ageing is not excessive in these propellants, the poor Abel heat test and heat flow results are a cause for concern about their long term stability, particularly for lot 1258 which also performed very poorly in the vacuum stability test (Table 4). The application of gel permeation chromatography would be useful to observe any excessive NC degradation in these propellants during ageing.

Lot 1257 and lot 1258 also have similar components (although again in different proportions) except for the different stabilisers. Lot 1258 shows much higher heat output relative to the NC content (Table 5). Although resorcinol is depleted very rapidly on accelerated ageing it appears to be a better stabiliser than 2NDPA in this formulation on the basis of heat output. It is likely that the primary degradation products of resorcinol function as effective stabilisers. This rapid stabiliser loss has been observed previously in propellants containing RDX and TAGN, although from stabiliser measurements of propellants stabilised with resorcinol stored under ambient conditions, safe-lives of 10 years or more are indicated [1]. Thus, in regard to stabiliser depletion, these propellants appear to behave in a similar manner to some conventional double base propellants stabilised with EC (eg type M9 with 0.8% EC), in that they give poor results on accelerated ageing but behave adequately under ambient conditions.

Lot 1258 is also similar in composition to lot 1259 except that the former contains TAGN and the latter does not. Again, the higher heat flow, poor Abel heat test time and poor vacuum stability test result for lot 1258 appears to indicate that TAGN has an adverse effect on the stability of these propellants. Problems with propellants containing TAGN have been noted before [3].

#### 4. CONCLUSIONS

Microcalorimetry shows promise in the evaluation of the stability of advanced propellants, both freshly manufactured and during accelerated ageing. The Abel heat test and the vacuum stability test appear to be of little quantitative value, except possibly to indicate exceptionally bad propellant lots.

Further work is required to clarify the results obtained in this work and to understand the underlying processes occurring in advanced propellants. More extensive microcalorimetry and stabiliser derivitisation measurements are required coupled with gel permeation chromatography to observe changes in the molecular weight of the NC in the propellant. A more extensive database of the microcalorimetric behaviour of conventional and advanced propellants is also required. Microcalorimetry at various temperatures to obtain kinetic data is also proposed.

## 5. ACKNOWLEDGMENTS

The authors wish to acknowledge the contributions of A. Turner for stability testing and S. Odgers, J. Ackers, A. Starks and R. Cockerill for propellant manufacture.

## 6. GLOSSARY

ATEC	acetyl triethyl citrate
BDNPA/F	bis-2,2-dinitropropyl acetal / bis-2,2-dinitropropyl formal
CAB	cellulose acetate butyrate
DANPE	1,5-diazido-3-nitrazapentane
DNT	2,4-dinitrotoluene
DOP	dioctyl phthalate
DOS	dioctyl sebacate
EC	ethyl centralite (1,3-diethyl-1,3-diphenyl urea)
ETOCCEL	ethyl cellulose
NC	nitrocellulose
2NDPA	2-nitro diphenylamine
RDX	hexahydro-1,3,5-trinitro-1,3,5-triazine
RES	resorcinol
TAGN	triaminoguanidine nitrate

## REFERENCES

1. White, A. and Odgers, S.G. (1991).  
Stabiliser depletion and gel permeation chromatography studies of stabilised nitrocellulose - application to high energy propellants. Paper presented to 16th meeting TTCP Technical Panel W-4.
2. White, A. and Bellerby, J.M. (1992).  
Stabilisers for high performance gun propellants. Paper presented to 17th meeting TTCP Technical Panel W-4.
3. White, A., Turner, A.R. and Bellerby, J.M. (1993).  
Stabilisers for propellants containing new energetic ingredients. Proceedings of the 24th International ICT Conference, Karlsruhe, pp. 7-1 - 7-14.
4. Odgers, S.G. and Kempson, R.M. (1996).  
Safety and service life aspects of advanced gun propellants. Paper presented to 21st meeting TTCP Technical Panel W-4.
5. Docking, J.T. and James, B.H. (1984).

A small scale manufacturing facility for gun propellant research. Proceedings of the ICT Conference, Karlsruhe, pp. 767-775.

6. Defence Standardisation Committee, Department of Defence (1983). Methods of test for propellants. DEF(AUST) 5623.
7. Turner, A.R. and White, A. (1994). Determination of stabiliser contents in advanced gun propellants by reverse phase high performance liquid chromatography. DSTO Technical Note MRL-TN-663.
8. Lindblom, T.; Lagerkvist, P. and Svensson, L.-G. (1985). Comparison and evaluation of modern analytical methods used for stability testing of a single base propellant. Symp. Chem. Probl. Connected Stabil. Explos., 7th.
9. Paulsson, L.-E., Svensson, L.-G. and Lindblom, T. (1992). Degradation of nitrocellulose. Some microcalorimetric studies. Symp. Chem. Probl. Connected Stabil. Explos., 9th.

## **The use of Microcalorimetry in the Predictive Surveillance Program**

James A. Wilson and Anton Chin  
Test & Evaluation Department  
Ordnance Engineering Directorate  
Crane Division, Naval Surface Warfare Center  
Crane, Indiana 47522-5001 USA

### **ABSTRACT**

The ability to predict how long an ordnance item will remain serviceable (i.e., safe and functional) has been the goal of the US Navy's surveillance program [1] since the program's inception in 1944. Historically, surveillance programs have provided very limited (normally 5 - 6 years) service life projections for energetic materials. The primary cause of this short coming is the results of using statistical projections as a basis of service life extension. There are built-in confidence limits to all statistical projections which constrains any long range projections.

A number of attempts to artificially age items so that true predictive analysis could be accomplished have been attempted. Most of these attempts were done based on some general assumptions about the material's kinetic aging properties and the results were not very satisfactory. With the development and incorporation of the microcalorimeter as a standard evaluation tool for energetics, an extremely accurate kinetics measurement tool has been placed into the hands of surveillance engineer.

This paper will not deal with the processes used to acquire the microcalorimetry data, but rather how the microcalorimetry data is used in concert with other test data to provide the customer with the information they need for more effective stockpile management decisions.

### **INTRODUCTION**

After a less than auspicious start for the US torpedo warfare effort during World War II, the US Navy decided that it was important that all ordnance items should be periodically tested to assure that they were safe and would perform their intended function. For more than fifty years this mission has been assigned to various Naval laboratories located across the United States. While programmatic success is a difficult thing to quantify, most individuals who have first hand knowledge of the program would agree that the surveillance program has been a significant factor in assuring the Fleet both safe and reliable weapons. To be certain, there have been highly publicized exceptions to this general success, however, most of these anomalies resulted from a random and/or isolated manufacturing defect or an unplanned evaluation slippage.

In recent years, most of the surveillance work could be accurately classified as "projective" in nature. The heart of this process is the collection of pertinent variables data which reflects the end items critical parameters, i.e., those parameters which must be met for the item to be safe and



reliable. By comparing the results of previous test data to the current test data, it is possible to make statistical projections on the affects of age on the critical parameters. Obviously there are a number of potential pit falls related to this scheme; 1. Did the proper test variables get selected ?, 2. Is there a close correlation between item age and shifts in performance ?, 3. Is the true degradation slope a linear function ?, and 4. The confidence in the accuracy of any projections beyond 4 to 5 years into the future --- is very questionable.

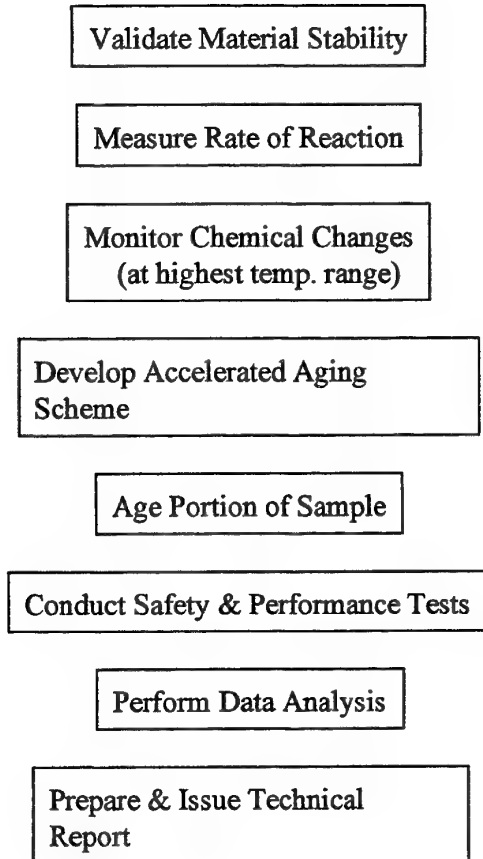
It has been apparent to most surveillance engineers that the key to improving the surveillance program was the ability to artificially age the energetic items. However, any process developed would have to be highly accurate, relatively quick, and reasonably economical if it is to be successful. There have been a number of attempts to conduct accelerated aging programs in the past, however, these experienced a number of problems. Most of these programs would attempt to accelerate the aging process by exposing the test item to relatively long term, moderately elevated temperature conditions. The guideline for most of these programs was to accomplish a two to one compression ratio, i.e., one year of storage would equal two years of in-service life.

While these programs had a modest level of success in predicting what the eventual life limiting defect would be, their cost was high and the ability to provide logistic managers with long term service life predictions was very limited.

### **PROGRAM GENESIS**

With the advent of the microcalorimeter a number of barriers have been overcome. This new tool has provided that missing element essential which measures the rate of heat reaction at real world temperature ranges. The data generated lays the foundation of the first truly accurate long range accelerated aging program. The basic flow of the Predictive Surveillance program is shown in Figure 1.

While it is valid to say that the microcalorimeter is the genesis of the Predictive Surveillance program, it is also true that it is only one element of the program. All too often when new technologies become available there is a tendency to use it to the exclusion of all other techniques or processes. The strength of the Predictive Surveillance program is that it does not see the microcalorimeter as a panacea, but rather, it is a very powerful starting point. It is only through a wide ranging and comprehensive evaluation program that true safety, reliability and service life of any energetic item can be identified.



### **PARADIGMS** **(You've got to love em)**

Anytime that changes in the status quo are initiated or even suggested, barriers immediately go up. The introduction of the Predictive Surveillance program is no exception to that phenomenon. At the same time, one of the risks associated with implementing new programs is that there can be an over-reaction which results in elimination of older but essential elements of a program. In an attempt to change the status quo while keeping that which was productive, a number of rules were used. Rules for breaking paradigms:

**Rule 1** If we have done it this way for many years, it's more than likely the wrong way to do it! This should be self evident.

**Rule 2** Assume stockpile homogeneity — always! Until shown statistically otherwise, all stockpiles should be considered homogenous. Due to the very constrained procurement specifications, it is extremely rare that stockpiles are found to be multi-modal.

**Rule 3** Since safety is the most important surveillance product, there **MUST** be a data point which measures! Too often, safety is rationalized as the lack of a hazardous event. If we are truly going to say that surveillance monitors safety, then we need to monitor and measure those attributes which constitute item safety.

The other side of breaking old paradigms is the establishment of new paradigms which support program objectives. My rules for accomplishing this task are as follows:

**Rule 1** Apply the latest technology whenever possible. Try to avoid the temptation to keep with the old technology because it makes correlation with older data easier. Twenty years from now, that decision will look dumb.

**Rule 2** Apply the Surveillance results to all similar items. If two or more items are comprised of the same energetic material, the results of the surveillance program for one should be applicable to all.

**Rule 3** No single test or piece of equipment can provide complete service life data. There are NO silver bullets in the service life assessment business.

While there could be an almost endless number of rules to make and break paradigms, the six that have been outlined here have truly helped in establishing the foundation for the new Predictive Surveillance program.

## THE PREDICTIVE PROCESS

The processes of the Predictive Surveillance program are more easily understood by analyzing in it's three fundamental stages as separate elements. These elements are:

- a. the Kinetics study
- b. the aging program and
- c. the safety / performance test element.

**The Kinetic Study Element** - The goal of this program element is to gather data on the long term chemical stability, the total available energy, the heat of reaction at various temperatures, and a profile of how the material under test will change chemically as it ages. There are three primary tools used to accomplish this sub-program: 1. the Differential Scanning Calorimetry (DSC), 2. the High Pressure Liquid Chromatography (HPLC), and 3. the Microcalorimeter

**DSC** - in the Predictive Surveillance program the DSC is used for two important functions. The first use of this tool is to act as a screening agent. If the material under investigation is already at the point of chemical instability, the DSC will detect this and the kinetics work can be terminated before it becomes a hazard to any individuals or

equipment. The second function of this equipment is to provide a measurement of the total energy available per unit of mass. This reading is obtained by Iso-DSC measurement

and is used in conjunction with other data generated by the microcalorimeter to determine the percent of degradation per year.

**HPLC** - as with all applications of the HPLC, the primary function of this separation tool is to determine the chemical constituents of the material under investigation. In the case of Predictive Surveillance, this process is used in conjunction with the microcalorimeter.

A relatively large sample of the material under test is placed in an oven at the same temperature as the highest microcalorimeter sample. Small portions of this material are then periodically removed from the oven and run through the HPLC. This provides a running history of how the material under investigation changes chemically as it undergoes aging. While this information is not essential for the Predictive Surveillance program in the strictest sense, it provides data which can be critical to future Engineering and/or Incident Investigations. Since this is a relatively low cost addition to the program and the potential return is so significant, the investment in this effort is highly recommended. Clearly, this data also provides a more complete understanding of the aging process and thus helps to determine causes in safety or performance shifts.

**Microcalorimeter** - the microcalorimeter is obviously the new player in the Kinetics arena. The Predictive Surveillance program uses this new technology for a number of reasons; the results are very reproducible, highly accurate, obtained at near ambient temperature ranges and utilizes relatively large samples which can be highly representative of the end item [2]. The output of the microcalorimeter is used for two very different objectives:

1. The first objective is to determine how long the material will remain chemically stable.
2. The second is to solve the Arrhenius equation and establish the activation energy of the test material.

These two objectives are the lynch pins to the Predictive Surveillance program. Without this information no real predictive service life program for energetic material is possible.

*Since the subject of this paper is Predictive Surveillance, the methodology and application techniques for the tools mentioned above will not comprehensively addressed in this document. The writer is confident that other papers will speak to these matters more eloquently and in depth than this author possibly could.*

Once completed, the Kinetics portion of the Predictive Surveillance program provides a prodigious amount of information on how rapidly the material ages, how it changes chemically, how long it can be expected to remain chemically stable, the rate of reaction heat at ambient

temperature levels and a measure of the rate of degradation per year. Until the advent of the microcalorimeter, there was no method which was capable of measuring all of the degradation products in the 75 to 45 degrees C temperature ranges. By measuring reaction heat at low temperatures, the calculation of the Arrhenius equation is far more meaningful for normal ambient conditions. Once this hurdle was breeched, the establishment of an accurate accelerated aging scheme became relatively simple.

**The Aging Program** - Since the primary aging mechanism for almost all modern ordnance items is storage temperature, the actual process of aging is extremely simple, i.e., raise the temperature above ambient levels and ---- you accelerate the aging process. The trick is knowing what temperature to use and how long to expose the material.

Because of the cost of actually conducting the aging as well as the costs associated testing, the typical Predictive Surveillance program will restrain this process to one or two accelerated ages.

In most cases this means a portion of the test sample will be aged to 10 years and another portion to 20 years. Obviously, there are an infinite number of temperatures that can be used for accelerating the aging process. It would be nice to say that the temperature selected was done based on some highly quantifiable and/or scientific basis, the reality is that the temperature used is arrived at based on two very non-scientific reasons; 1. the amount of time available to conduct the total program (usually well less than one year) and 2. the most important of all reasons --- the funding available.

Whenever possible, it is preferable to obtain both baseline and aging samples from the same end item or at least the same container. This is done to limit the possible effects of production variability. Examples of items from which multiple samples can be obtained from the same end item are components such as warheads and rocket motors. For smaller items such as squibs, CADs, and small pyro items, using the same production strata is the best selection criteria for the predictive process.

**NOTE:**

*Currently one of the primary assumptions of the Predictive Surveillance process is — that while there will be production lot to lot variance, the fundamental aging processes are applicable to the entire stockpile. This assumption will be held as factual until statistically proven invalid.*

**The Safety / Performance Test Element** - It is essential to understand that prior to initiating any safety or performance testing, a large portion of the test sample will be aged to predetermined ages. By having the same identical energetic material tested at three different ages, a true age to performance degradation rate can be established.

The safety / performance test portion of the Predictive Surveillance program is the most open forum of the three program elements. The type of test used is in most cases dependent on the size and complexity of the item under test. Small items such as small caliber ammunition, cartridge activated devices and small pyrotechnic devices are normally aged and functionally

tested as all-up-rounds. Larger items such as rocket motors, warheads and large pyrotechnic devices are evaluated using small scale test methods. The following is an abbreviated compilation of the types of tests used to test both groups:

**All-up-round testing** - In most cases the test used to test smaller items can best be described as lot acceptance testing without the environmental conditioning. Examples of this type of testing are: 1) gun firing of ammunition, 2) static (pressure bomb) firing of CADs, 3) field firing of decoy flares, 4) witness block testing of squibs, etc..

**Small scale testing** - Small scale testing, using representative samples of the item's energetic material, is normally more closely associated with initial item validation testing [3]. The items which utilize small scale testing tend to be the larger energetic item such as rocket motors, warheads and large pyro items. Examples of the types of tests are: 1) card gap, 2) cook-off, 3) strand burn, 4) Dynamic Mechanical Analysis, 5) detonation velocity, etc..

It is important to reiterate that a portion of each test sample will be artificially aged prior to testing. This allows an early and accurate assessment of the effect of item aging on safety and performance.

#### EXAMPLE OUTCOME

Due to the fact that this is a new and still evolving process, there is not an abundance of published material available. One of the best examples currently available is from the 1996 evaluation of the PGU-28/B 20 mm ammunition test. These are new items in the US inventory and this was the first surveillance iteration. Since these items are fundamentally pure energetic items without substantial mechanical or electronic components, the Predictive Surveillance processes were recommended to the item manager. Due to a paucity in funding, the aging portion of the Predictive Surveillance was not undertaken. However, the baseline kinetics work was accomplished with some rather meaningful data supplied to the item manager. The following is part of a table extracted from the report:

Lot No.	Initial Stabilizer Content (%)	Activation Energy (Ea) (Kcal/mole)	Estimated Safe Service Life (in years)			
			77°F	95°F	113°F	122°F
OL93H005-014	0.6169	29.948	67.8	13.2	3.02	1.27
LC92L000E-001	0.5721	31.730	66.9	11.7	2.31	1.08
OL-85G001-007	0.4402	30.262	40.4	7.7	1.63	0.78

From a casual perusal of the information provided above, a number of very significant concepts are clear:

1. **Keep your propellant cool.** While we have always known that temperature

dramatically effects the service life of propellant, this information, presented in this finite manner, brings this concept home to the item logistic manager.

**2. Optimized Stockpile Utilization is possible.** When the kinetics data is provided in a clear and understandable manner, the non-scientific manager is able comprehend and utilize the information to optimize stockpile utilization. Question: which of the three above lots would you expend first?

There are other logistic system advantages of the Predictive Surveillance Program that are not as readily seen as the two above. This would include the ability to quickly determine the effects of some unique storage environment, i.e., if this information had been available prior to Desert Storm, the effects of that exposure would have been quick and accurate.

## **CONCLUSION**

While the Predictive Surveillance program is still in it's infancy, the initial results are extremely exciting. The use of the microcalorimeter has provided the missing element for the establishment of a Predictive Surveillance program. When the microcalorimeter is used in conjunction with a robust aging and performance testing discipline, highly accurate and cost effective service life predictions become possible. It is our opinion that this process will replace all of the conventional evaluation programs which currently monitor the safety and reliability of our aging U.S. weapon stockpiles.

Though this new approach is primarily applicable to the true / pure energetic items, it has caused many of the old paradigms to be shaken to their roots. We believe that irreversibly change to the thought processes related to the evaluation of more complex items has already begun.

## **ACKNOWLEDGMENTS**

The authors wish to thank both Ms. D. Bolton, Naval Ordnance Center, and Col. Robinette, United States Marine Corp, for their unwavering support of this process. Without their moral and sponsorship support of our efforts, the Predictive Surveillance Program would only be a dream and not a reality.

## **REFERENCES**

1. The Naval Airborne Weapons Maintenance Program (MAWMP), OPNAVINST 8600.2B, chapter 4.7
2. R.G. Shortridge, A. Chin and D. Ellison, "Microcalorimetric Studies of Pyrotechnic Compositions" NSWCCR/RDTN-94/003 of 31 Aug 1994, TTCP Workshop on

**Aging/Degradation of Pyrotechnic Devices.**

3. M. N. Plooster, "Subscale Tests of Energetic Material Performance" NSWCCR/RDTN-94/003 of 31 Aug 1994, TTCP Workshop on Aging/Degradation of Pyrotechnic Devices.





# KINETIC DESCRIPTION OF THE AGEING OF GUN AND ROCKET PROPELLANTS FOR THE PREDICTION OF THEIR SERVICE LIFETIME

Manfred A. Bohn

Fraunhofer-Institut für Chemische Technologie (ICT)  
Postfach 1240, D-76318 Pfinztal-Berghausen, Germany  
fax: +49-721-4640-111, e-mail: bo@ict.fhg.de

## 1. Abstract

Ageing of gun and rocket propellants is not only a safety problem. It is necessary that after a time-temperature stress the relevant properties of the propellants are still in the range of tolerance, and that the designed conditions of operation are still fulfilled. Therefore one must quantify the ageing by (1) measuring the relevant properties as function of time and temperature, if necessary of further variables, and (2) describe the measured data with appropriate mathematical equations. The description in form of a rate equation is first given in a general way and then specified for some properties. The rate expressions may be of an empirical type or may be based on a mechanistic concept. Both ways are equivalent as long as the description achieves a separation of the variables time and temperature, reproduces the measured data very well and is able to extrapolate the data correctly along the time axis. Additionally the right temperature dependence of the rate constant must be found. These are the basic conditions for a reliable prediction of service lifetime in operation and in storage. By introducing a 'degree of property degradation'  $y_P$  as the ratio of the allowed limit value  $P_L$  to the original value  $P(0)$  of the property  $P$ , the service lifetimes can be calculated with the integrated form of the rate equation as the times  $ty_P(T)$  to reach  $y_P$ .

This reaction kinetic procedure will be exemplified with the following properties: stabilizer consumption, mass loss and heat generation, including autocatalysis. The connection between mass loss and heat generation is worked out. All the mathematical descriptions given can be applied for operational temperature conditions and one needs only representative temperature-time profiles for the operational conditions. Experimental results are shown for normal and autocatalytic situations in mass loss and in heat generation of nitrocellulose, gun propellant KN6540 and of several rocket propellants based on AN/GAP. The kinetic parameters are given to make lifetime predictions.

## 2. Introduction

Gun propellants (GP) and rocket propellants (RP) contain substances with so-called energetic groups, the most frequent are:

		B [kJ/mol]	weakest bond
nitric acid ester	C-ONO <sub>2</sub>	155 - 163	CO-NO <sub>2</sub>
azide group	C - N <sub>3</sub>	170	CN - NNI
nitramine group	N - NO <sub>2</sub>	193	N-NO <sub>2</sub>
nitro group (aromatic)	C - NO <sub>2</sub>	297 (152)	C - NO <sub>2</sub>
nitro group in CH <sub>3</sub> NO <sub>2</sub>	C - NO <sub>2</sub>	250	C-NO <sub>2</sub>

shown with the bond energy B of the weakest chemical bond in the groups. These values are relatively low, typical values of C-H bonds are 415 kJ/mol, and of C-C bonds 344 kJ/mol. The most stable energetic group is the so-called aromatic nitro group bonded to the benzene ring. The bond energy of the nitro group in aliphatic nitro compounds such as in nitromethane, CH<sub>3</sub>NO<sub>2</sub>, has smaller values. It can also have different values to those given, they can be reduced by catalysts. The smaller value for the aromatic nitro group given in brackets applies to situations with the possibility of hydrogen transfer to the NO<sub>2</sub> group.

Bonds with such low bond energies can be split easily thermally (thermolysis). The NO<sub>2</sub> radical is split off from the nitric acid ester group (also named as nitrate group, nitrate ester group) already at moderately high temperatures ( $\geq 40^{\circ}\text{C}$ ). The azide group easily releases molecular nitrogen. The activation energy for the decomposition of energetic groups is usually between 90 kJ/mol and 200 kJ/mol. These low values for bond and activation energies cause an increased ageing rate of energetic substances.

The chemical degradation reactions cannot be prevented directly. Their effect can be greatly reduced using stabilizers as it is done with nitrocellulose, PolyNIMMO, PolyGLYN, ADN, GPs and RPs, HTPB-bonded propellants and explosives. Stabilizers are used to catch reactive molecules such as nitrogen dioxide, NO<sub>2</sub>, and oxygen O<sub>2</sub>. The formation of NO<sub>2</sub> usually leads to autocatalytic decomposition not only for nitrocellulose and blasting oils. The primary decomposition of NC and similar substances cannot be prevented.

Apart from ageing due to chemical reactions, there is also an ageing due to physical and physical-chemical processes. This includes the diffusion or migration of low molecular constituents such as blasting oils, phlegmatizers, plasticizers, burning catalysts. Examples are the exudation of blasting oils, the migration of the above mentioned substances from the propellant into the liner and the isolation or the diffusion of surface treatment agents from the surface of a GP grain into its interior. These processes change the ballistic behaviour, which is also referred to as ballistic ageing.

Ageing of the propellant due to chemical reactions as well as through physical effects change the following mechanical properties: tensile strength, strain at break (strain capacity), elasticity modulus, shear modulus, morphology and thermomechanical properties such as glass transition temperature and embrittlement temperature (brittle-ductile transition temperature). During use this can result in dangerous failures as breech blow or motor explosion. Rocket motors are also subjected to an ageing due to crack formation and crack propagation in the propellant, which is triggered by a changing tempera-

ture load. Different thermal expansion behaviour of the motor case and the propellant can cause tensile stresses higher than the tensile strength of the RP.

Therefore it is necessary (1) to recognize the ageing processes, (2) to determine their rate and (3) to quantify them as accurately as possible using mathematical descriptions based on chemical-kinetic and physical as well as physical-chemical models. Reliable predictions of the ageing and therefore of safe use time, which means service lifetime, is in this way possible /1/. These are necessary for reasons of safety (protection against auto-ignition, dangerous failure), compliance with the designed functions (burning rate, muzzle velocity, target picture) and also because of economics. An increase of safe operational service lifetime due to more precise predictions helps to save costs.

If used in different regions of the earth with different climates (hot, cold and hot, humid regions), the stress on the GPs and RPs increase. Better information regarding the types of stresses and in the form of temperature-time profiles are required to make predictions about the operational service lifetime. Inaccurate data or estimates about the temperature load can only provide rough predictions. On the one hand this can lead to a disposal of still usable ammunition (costs), on the other hand it can lead to a dangerous mis-judgement (safety). The reliable way to achieve temperature-time information is the 'on-line' determination using small data recording equipment taken along with the propellant in the ammunition. The following Table 1 shows where the method 'prediction' is situated among the other methods to judge service life or stability and what degree of reliability they achieve.

**Table 1:** Methods to judge service life and stability.

<b>method to judge service life</b>	<b>objective</b>	<b>degree of reliability</b>
assumption	synthesis of a new energetic substance	low
estimation based on stability tests	formulation of a new propellant	low to medium
estimation based on limited time-temp. data	qualification for the next 5 to 10 years	low to medium
prediction	assessment with a quantitative description of measured data	medium to high
surveillance	guarantee of safe service life	high

It must be pointed out that the well-known stability tests are not suitable to make a prediction of service lifetime or of the ageing behaviour at the temperature-time situations during service. The stability tests are useful and necessary to determine the momentary quality of the constituting components of a formulation and their compatibility. For a

prediction of the ageing behaviour one needs temperature-time data of performance determining quantities of the propellant formulation, which cover a representative degree of property change.

### 3. Quantitative description of ageing

#### 3.2.1 Description with rate constants

In order to make reliable predictions of the service lifetime, it is necessary to describe the change in a measured property or quantity as function of time and temperature quantitatively, that means using a mathematical form. Oxygen access and humidity are included, if necessary. The data are always a group of curves, if they are represented as function of time with temperature as a parameter. The description is carried out in two steps:

- description of each individual curve as a function of time
- introduction of a time-independent but temperature dependent parameter, the rate constant, to separate the two variables time and temperature.

A great number of this type of description is known from chemical kinetics. They can be applied directly if the changing property is connected with a chemical reaction. In eq.(1), this procedure has been generally formulated as the rate equation of a property P.

$$(1) \quad \left( \frac{dP(t, T)}{dt} \right) \Big|_T = V_p = S \cdot k_p(T) \cdot f(P(t, T); g(t, T))$$

$$\left( \frac{dP(t, T)}{dt} \right) \Big|_T \quad \text{change in time (rate) of property } P(t, T)$$

$$k_p(T) \quad \text{rate constant, only a function of temperature}$$

$$g(t, T) \quad \text{parameter and quantities which influence } V_p$$

$$f(P(t, T); g(t, T)) \quad \text{specification of the kinetic formulation}$$

$$S \quad +1: P \text{ increases with time}$$

$$-1: P \text{ decreases with time}$$

The temperature dependence of  $k_p$  is mostly exponential and represented by equations of the Arrhenius type, eq.(2):

$$(2) \quad k_p(T) = Z_p \cdot \exp(-E_{a_p} / R / T)$$

$$Z_p \quad \text{preexponential factor}$$

$$E_{a_p} \quad \text{activation energy}$$

$$R \quad \text{general gas constant (8.3144 J/mol/K)}$$

$$T \quad \text{absolute temperature}$$

The so-called Arrhenius parameters  $Z_p$  and  $Ea_p$  are determined with eq.(2) from the experimental  $k_p$  values. Then the rate constants can be calculated for any operational service temperature and together with the integrated form of eq.(1), the times can be determined until a given degree of change of property P or of the measured quantity P,  $y_p$ , has been reached. This defines the searched for service lifetimes  $ty_p(T)$  according to eq.(3).

$$(3) \quad y_p = \frac{\text{limit value for P}}{\text{starting value of P}} = \frac{P_L}{P(0)} = \frac{P(ty_p(T))}{P(0)}$$

The 'degree of degradation', 'degree of consumption' or 'degree of change' are described by  $y_p$ , the 'degree of loss' is then  $(1-y_p)$ .  $P(0)$  is the value of the property or quantity P after the GP or RP has been manufactured or at the beginning of the measurements. The limit value  $P_L$  depends on the composition and formulation of the propellant, on the property P, the measurement accuracy for P and on the safety factor desired.

In order to achieve a reliable prediction of the lifetime, the following conditions must be fulfilled:

- the suitable propellant properties P must be selected (properties and values which are connected with ageing processes)
- the properties or measurement quantities P must be measured with a high degree of accuracy
- the mathematical description must represent the measurements very well
- the mathematical description must be able to extrapolate the measurements along the time axes very well, that means it must have an inherent ability for extrapolation
- the appropriate temperature dependence of the rate constant  $k_p(T)$  must be determined
- the suitable temperature range for the accelerated ageing must be used
- the accuracy and constancy of the oven temperatures, tolerance limits are  $\leq \pm 0.3^\circ\text{C}$ , for the isothermally accelerated ageing must be very good and this applies for long measurement periods over weeks and months, even over years.

Finding the correct description with an inherent extrapolation ability also helps to save costs as in further investigations fewer measurements are necessary, that means it is no longer necessary to measure down to small degrees of degradation  $y_p$  or in general to the limit value  $P_L$ .

### 3.2.2 Description with 'model-free' formulations

In the differential form, the usual kinetic formulations do not include time as an explicit variable on the right hand side. There are ageing processes which cannot be described very well using this type of approach, for example mechanical properties and the diffusion, see /1,6/. These formulations can be more of an empirical type. For the purpose of prediction, empirical equations are equivalent to those which are based on a modelling concept in so far as they can extrapolate the experimental data correctly along the time axis and can reproduce the data well.

Another empirical method is to determine the time until a set degree of change of the quantity  $P$  is reached, for example a decrease to 30% of the initial value  $P(0)$ , i.e.  $y_P = 0.3$ . This is also known as a 'model-free description'. The reciprocal times until this set limit has been reached are proportional to the corresponding reaction rate constants, if the rate constant  $k_P$  and  $t$  are coupled linearly in the associated rate equation. At the first moment, this method seems equal to the method with the rate constants. However, this is not the case as the associated rate equation is not known. If there is not a linear relationship between  $t$  and  $k_P$ , a too high or too low activation energy would be determined assuming a linear one [1,6]. This means that purely empirical descriptions can lead to wrong judgements. In addition, a model-free method requires more measurements, because they must be performed to small values of  $y_P$  or to the set limit  $P_L$ , as no inherently correct extrapolation is possible with a model-free description.

#### **4. Description of ageing of gun and rocket propellants using the quantities stabilizer consumption, mass loss and heat generation.**

The four quantities molar mass degradation, stabilizer consumption, mass loss (corresponds with gas formation) and heat generation are coupled together in GPs and RPs based on nitric acid esters. Thermally triggered decomposition of nitrocellulose (NC) and blasting oils initially result in the  $\text{NO}_2$  radical being split off from the  $\text{CO-NO}_2$  group. In consecutive reactions the radical function formed on the cellulose backbone is stabilized by rearrangement reactions and splitting off of small stable molecules. The affected anhydridoglucopyranose ring (chain element of cellulose) is destroyed, which leads to a chain scission. This explains the molar mass degradation of NC. The experimental results so far support this [2,3,4]. This primary decomposition reaction of NC cannot be prevented, it also takes place with stabilized NC and in GPs and RPs. The stabilizers catch the  $\text{NO}_2$  so that it can not catalyze the decomposition of NC in further reactions. That means  $\text{NO}_2$  is autocatalytically effective via acid formation (nitric acid, nitrous acid) and thereby catalyze the  $\text{CONO}_2$ -ester fission and the chain scission. As  $\text{NO}_2$  is a strong oxidating agent, it also reacts directly with the cellulose backbone, which in turn forms radical functions or other molecular damages arise, which lead again to a degradation in subsequent reactions. Catching  $\text{NO}_2$  consumes stabilizer, at the same time the molar mass distribution function is also changed according to this mechanistic approach. Permanent gases such as  $\text{CO}$ ,  $\text{CO}_2$ ,  $\text{N}_2\text{O}$ , water and other volatile compounds are formed during these cellulose backbone stabilizing reactions, the result is a loss in mass. Each reaction has an exothermal or endothermal heat of reaction. The total sum is an exothermal reaction which can be measured as heat generation using microcalorimeters. Molar mass decrease and stabilizer consumption are more detailed quantities than mass loss and heat generation.

The mean molar mass  $M_w$  or  $M_n$  of polymers also determines their mechanical properties. The decrease of the mean molar mass of nitrocellulose results in a decrease in tensile stress [4] and in the compressive strength of the gun propellant grains, which shifts the embrittlement temperature or brittle-ductile transition temperature towards higher temperatures. This can result in crumbling grain fracture with subsequent dangerous increase in burning rate and the build-up of pressure waves. A detailed description of a kinetic model for the decrease of the mean molar masses  $M_n$ ,  $M_w$  and  $M_z$  of NC can be found in [1,3,5,6].

## 4.1 Consumption of stabilizer

In a first step only the content of the primary stabilizer, as DPA, Acradite II, is considered with the degree of stabilizer consumption  $y_s$ . However, some consecutive products of the primary stabilizer, the mononitrated and dinitrated primary stabilizers, possibly also trinitrated ones, have a stabilizing effect [7,8,9]. These consecutive stabilizing products are called secondary stabilizers. At a higher nitration level the reactivity to bind the  $\text{NO}_2$  and  $\text{NO}$  decreases fast towards zero compared with the reactivity of the primary stabilizer [9], so that their stabilizing effect at higher temperatures with higher  $\text{NO}_2$  formation rates can no longer prevent catalytic decomposition. The stabilizing effect of consecutive stabilizer products is a reason for the difference between safe use time or safe service lifetime and safe storage time, the latter is therefore longer. The decrease in molar mass  $M_w$  of the NC and thereby a possible embrittlement of the GP grain can be a further reason for this difference. Stabilizers without forming consecutive stabilizing products also exist. A further developed evaluation should include the low nitrated consecutive stabilizer products in the prediction of service lifetime. In order to do this, the reactivities of the subsequent stabilizer products related to the reactivity of the primary stabilizer can be established, this in turn results in an effective stabilizer concentration, which is dealt with in the same way as the primary stabilizer as far as the application of a model for the description of the stabilizer consumption is concerned [9].

The degree of stabilizer consumption  $y_s$  is:

$$(4) \quad y_s = \frac{\text{lower limit of stabilizer content}}{\text{starting stabilizer content}} = \frac{S_L}{S(0)}$$

The original or starting stabilizer content is the value after production. If only the value is known at a time after this, the service lifetime and safe storage time are determined as from that point in time on. The value for  $y_s$  can range from  $0.0 \leq y_s \leq 0.5$  and is determined by:

- the prediction method used ( $y_s = 0.5$  using the half-time (half-value) method)
- the accuracy of the experimental data
- the type of stabilizer (if no secondary or consecutive stabilizers are formed,  $y_s = 0$  is not allowed)
- the composition of the propellant
- the desired safety factor

The literature states a number of examples for the modelling of the stabilizer consumption, from the reaction of zero order to a complete modelling and to the evaluation without reference to reaction models. The kinetic expressions and therefore the molecular processes, which consume the stabilizer, are very complex [9,10,11]. They do not need to be taken into consideration in detail here, as for the prediction of service lifetime only the decrease of stabilizer as a function of temperature and time is required. From the type of stabilizer decrease, a reaction of the first order would be suitable at a first glance.



#### 4.1.1 Reaction of the first order

This kinetic formulation is known and will be only mentioned briefly here. The change in stabilizer concentration in time is proportional to the momentary concentration, eq.(5). The reaction rate constant  $k_s(T)$  is described according to Arrhenius, eq.(6). Integrating eq.(5) results in eq.(7).

$$(5) \quad \left( \frac{dS(t,T)}{dt} \right) \Big|_T = -k_s(T) \cdot S(t,T)$$

$$(6) \quad k_s(T) = Z_s \cdot \exp(-E_{a_s}/RT)$$

$$(7) \quad S(t,T) = S(0) \cdot \exp(-k_s(T) \cdot t) \quad \text{or} \quad \ln(S(t,T)) = \ln(S(0)) - k_s(T) \cdot t$$

$S(0)$  is the initial concentration after production or at the beginning of the investigations and is equal for all temperatures of the investigation and in the evaluation. The time  $ty_s(T)$  until the degree of stabilizer consumption  $y_s$  is reached is:

$$(8) \quad ty_s(T) = \frac{1}{k_s(T)} \cdot \ln \frac{1}{y_s} \quad \text{with} \quad y_s = \frac{S_L}{S(0)} = \frac{S(ty_s(T))}{S(0)}$$

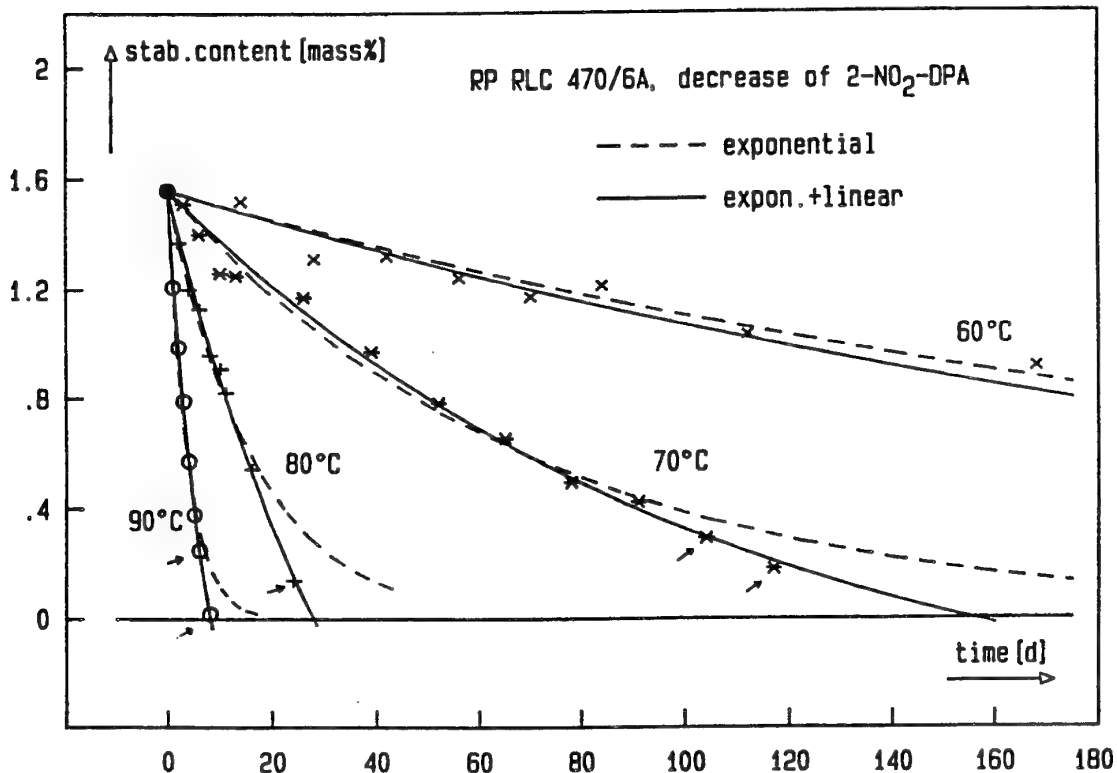


Fig. 1: Description of the decrease of stabilizer 2-NO<sub>2</sub>-DPA in the doublebase RP RLC 470/6A with the models 'exponential' and 'exponential. + linear'.

The times  $t_0(T)$  until the stabilizer content  $S(t,T) = 0$  has been reached are infinite, which does not agree with the reality for GPs and RPs. This model will be referred to as 'model 1' or 'exponential' model. An evaluation with this model is shown in Fig. 1. The broken curves have been obtained by a linear least squares fit procedure with eq.(7). Usually the logarithmic form is taken and then one calculates back to  $S(t,T)$ . The measurements marked with small arrows could not be taken into consideration, as they deviate too much from the given exponential decrease. In a logarithmic visual representation of the data this may not so obvious to recognize. Including the marked data the description is bad with this model. It is only sensible to use this model for degrees of stabilizer consumption  $y_s \geq$  about 0.3.

#### 4.1.2 Reaction of the first and zero order

A formal combination of the reactions of first and zero order should represent the type of stabilizer decrease more accurately as it includes the reaching of  $S(t,T) = 0$  in a finite time period. The evaluation using this kinetic formulation, also referred to as 'model 2' or 'exponential + linear' model can be seen by the solid lines in Fig. 1. All measured data, also the marked ones, have been included now in the evaluation. The reproduction of the measurements is very good. A detailed description of this kinetic model is given in /12/. A short derivation is given below.

The change of concentration  $S(t,T)$  in time is proportional to the momentary concentration and a constant  $k_s^2(T)$ , the part of the zero order reaction in this formulation, eq.(9).

$$(9) \quad \left( \frac{dS(t,T)}{dt} \right) \Big|_T = -k_s^1(T) \cdot S(t,T) - k_s^2(T)$$

Arrhenius behaviour applies to both reaction rate constants, eq.(10).

$$(10) \quad \begin{aligned} k_s^1(T) &= Z_s^1 \cdot \exp(-Ea_s^1 / RT) \\ k_s^2(T) &= Z_s^2 \cdot \exp(-Ea_s^2 / RT) \end{aligned}$$

The dimension of  $k_s^1$  is the reciprocal time, that of  $k_s^2$  is that of the stabilizer content and the reciprocal time. Integrating eq.(9) results in eq.(11).

$$(11) \quad S(t,T) = \left( S(0) + \frac{k_s^2(T)}{k_s^1(T)} \right) \cdot \exp(-k_s^1(T) \cdot t) - \frac{k_s^2(T)}{k_s^1(T)}$$

The times  $ty_s(T)$  can be calculated using eq.(12).

$$(12) \quad ty_s(T) = \frac{1}{k_s^1(T)} \cdot \ln \left( \frac{1 + \frac{k_s^2(T)}{S(0) \cdot k_s^1(T)}}{y_s + \frac{k_s^2(T)}{S(0) \cdot k_s^1(T)}} \right)$$

For  $y_s = 0$ , the  $t_0$  values are

$$(13) \quad t_0(T) = \frac{1}{k_s^1(T)} \cdot \ln \left( \frac{S(0) \cdot k_s^1(T)}{k_s^2(T)} + 1 \right)$$

A detailed analysis of the stabilizer consumption of the GP A5020 and the RP RLC 470/6A can be found in /12c/.

The function according to eq.(11) shows a simple behaviour. It starts at  $S(0)$  (the same for all temperatures) and falls monotonously to the limit ' $-k_s^2(T)/k_s^1(T)$ '. This is the reason for the good inherent extrapolation ability of this equation. It is not necessary to store and measure until the stabilizer content is zero. The extrapolation of the stabilizer consumption is good from  $y_s = S(t,T)/S(0) \approx 0.5$  on. But how far the measurements must go towards zero is also a question of the accuracy of the measurements and the scattering of the measured data.

Eq.(11) describes the decrease in stabilizer concentration very well for all stabilizers used, DPA, 2-NO<sub>2</sub>-DPA, Acardite II, Ethylcentralite, MNA, in every type of propellant, singlebase, doublebase, triplebase GP, doublebase RP. This is always the case if the propellant contains only one primary stabilizer. If mixed stabilizer systems are used, such as MNA and 2-NO<sub>2</sub>-DPA, DPA and Acardite II, DPA and Ethylcentralite, it is also possible to use eq.(46), as their reactivities are so different from one another that the curves are well separated. Each stabilizer is considered by itself. However, the procedure described in /9/ is the most accurate one, as it takes into account the consecutive stabilizer products also.

#### 4.1.3 Reaction of zero order

This formulation only considers the linear part of the stabilizer decrease. It also determines a finite time to reach  $S(t,T) = 0$ . One main disadvantage of this evaluation is that the measurements must be made up to the same degree of stabilizer consumption  $y_s$  for all temperatures, with  $y_s$  preferably less than 0.3.  $y_s$  must be equal for all temperatures, otherwise a wide ranging scattering occurs in determining the reaction rate constants, because the measurements do not result in a straight line or to be more precise, the course of the stabilizer decrease cannot be in a straight line from the point of view of the chemical reactions which take place /9/. Conditions might arise where a straight line might be the most sensible description, but also in this case applies what was said above. The equations given below correspond to those given for the other two models.

$$(14) \quad \left( \frac{dS(t,T)}{dt} \right) \Big|_T = -k_s^0(T)$$

$$(15) \quad k_s^0(T) = Z_s^0 \cdot \exp(-Ea_s^0 / RT)$$

$$(16) \quad S(t,T) = S(0) - k_s^0(T) \cdot t$$

$$(17) \quad ty_s(T) = \frac{S(0)}{k_s^0(T)} \cdot (1 - y_s)$$

$$(18) \quad t_0(T) = \frac{S(0)}{k_s^0(T)}$$

#### 4.1.4 Service lifetime prediction with stabilizer decrease under temperature-time profile stress.

If the propellants are exposed to changing temperatures, temperature-time data are required in order to establish a temperature-time profile for either the entire service lifetime or a representative period of time e.g. one year. Using eq.(11) in the form of eq.(19), the profile is run through section by section.

$$(19) \quad S(\Delta t_i, T_i) = \left( S(\Delta t_{i-1}, T_{i-1}) + \frac{k_s^2(T_i)}{k_s^1(T_i)} \right) \cdot \exp(-k_s^1(T_i) \cdot \Delta t_i) - \frac{k_s^2(T_i)}{k_s^1(T_i)}$$

$i = 1, 2, 3 \dots n$       number of profile section  $i$   
for  $i = 1$        $S(\Delta t_{i-1}, T_{i-1}) = S(0)$  or the respective end value after the profile cycle  $j$  for profile cycle  $(j+1)$   
 $\Delta t_i$       time interval of profile section  $i$   
 $T_i$       temperature of profile section  $i$

The service lifetime after one profile cycle, that means after a full run through, is

$$(20) \quad t(\text{profile cycle}) = \sum_{j=1}^n \Delta t_i$$

Using eq.(20), the profile is run through in a loop until the set degree of consumption  $y_s$  has been achieved. The entire service lifetime adds up to

$$(21) \quad ty_s(\text{profile}) = j \cdot \sum_{j=1}^n \Delta t_i$$

whereby  $j$  is the number of full profile runs until  $y_s$  or a value slightly above  $y_s$  has been reached. If the profile has been generated for the overall service lifetime, eq.(21) is not necessary.

Examples of results with temperature profiles have been listed in Table 2. For the degree of stabilizer consumption  $y_s = 0.1$ , the times are given for the doublebase RP RLC 470/6A and the singlebase GP A5020 under isothermal storage conditions between 20°C and 50°C and for three temperature profiles. Profile STANAG 2895 /13/, M1-IDM (maritime hot, induced daily maximum values), profile STANAG 2895, M1-EDM (maritime hot, environmental daily maximum values) as well as for profile Phoenix (very

hot and dry), which is used in the automotive industry for the airbag qualification. All three profiles have a total time period of one year. The time-temperature data of the STANAG profiles were taken from sum curves. The service lifetimes are considerably reduced by the temperature-time profile stress. The RP RLC 470/6A would not be suitable as airbag propellant as a service lifetime of 15 years is demanded according to the Phoenix profile.

**Table 2:** Time in years to reach the degree of stabilizer consumption  $y_s = 0.1$  at different thermal stresses, isothermal and at temperature-time profiles for the doublebase RP RLC 470/6A and the singlebase GP A5020.

thermal stress	RP RLC 470/6A		GP A5020		
	expon. 60°C - 90°C	exp.+ linear 60°C - 90°C	expon. 60°C - 90°C	exp.+ linear 60°C - 90°C	expon. 40 -60 -90°C
20°C	2408	930	1080	787	60.5
30°C	338	170	150	116	19
40°C	54	33.5	24	19.1	6.4
50°C	9.6	7.0	4.2	3.5	2.3
ST.-M1-IDM	3-4	3	1-2	1-1.5	1-1.5
ST.-M1-EDM	80	51	35	29	10
Phoenix-AMI	3	2-2.5	1-1.5	1-1.5	1-1.5

STANAG M1-IDM: STANAG 2895, maritime hot, induced daily maximum values,  
 $T_{max} = 69^\circ\text{C}$ ,  $T_{tav} = 51.6^\circ\text{C}$ .

STANAG M1-EDM: STANAG 2895, maritime hot, environmental daily maximum values  
in air,  
 $T_{max} = 48^\circ\text{C}$ ,  $T_{tav} = 32.5^\circ\text{C}$ .

Phoenix-AMI: profile of the automotive industry for airbag qualification  
 $T_{max} = 80^\circ\text{C}$ ,  $T_{tav} = 37.7^\circ\text{C}$ .

$$\text{time averaged temperature } T_{tav} = \frac{\sum T_i \cdot t_i}{\sum t_i}$$

The calculations are done with the following Arrhenius parameters ( $Z_s^1$  in 1/s,  $Z_s^2$  in mass-%/s):

	RP RLC 470/6A (S(0)=1.56 mass-%)		GP A5020 (S(0)=0.67 mass-%)	
temp. range [°C]	$E_{as}$ [kJ/mol]	$Z_s$ [1/s]	$E_{as}$ [kJ/mol]	$Z_s$ [1/s]
40 - 60 ( $k_{s2}$ )	-	-	85.7 ( $E_{s2}$ )	2.25 E+6 ( $Z_{s1}$ )
60 - 100 ( $k_{s1}$ )	145.0 ( $E_{s1}$ )	2.08 E+15 ( $Z_{s2}$ )	145.7 ( $E_{s1}$ )	6.18 E+15 ( $Z_{s2}$ )
60 - 100 ( $k_s^1$ )	123.7 ( $E_s^1$ )	8.434 E+11 ( $Z_s^1$ )	138.2 ( $E_s^1$ )	3.078 E+14 ( $Z_s^1$ )
60 - 100 ( $k_s^2$ )	184.6 ( $E_s^2$ )	5.580 E+20 ( $Z_s^2$ )	152.1 ( $E_s^2$ )	5.446 E+15 ( $Z_s^2$ )

As these temperature profiles include higher temperatures, for GP A5020 the smaller activation energy in the lower temperature range (40°C to 60°C) /14/ (this corresponds to higher reaction rates compared to the extrapolation only with the higher temperature range, 60°C to 90°C) has no effect under the Phoenix profile stress and the STANAG M1 IDM stress, all three calculation types result in the same storage time for GP A5020.

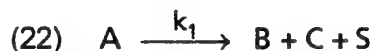
Nearly the same applies to RP RLC 470/6A. The influence of the STANAG-M1-EDM-profile can be seen clearly, however. The relative differences in the calculated times are considerably smaller than at 20°C. An equivalent isothermal load with regard to these relative differences would be found at temperatures about 40°C.

## 4.2 Mass loss

Mass loss measurements are part of the quality tests and quality evaluation of GPs and RPs and are carried out in standardized chemically resistant glass vials with a standard ground-in joint and loosely inserted ground-in stopper. This permits a certain amount of gaseous exchange to take place, so that oxygen is present above the sample. The water content of the atmosphere is not pre-set. In the case of singlebase and doublebase GPs and doublebase RPs a linear increase in mass loss (ML) can be observed after an initial fast rise due to the loss of water and residual solvents, until the ML accelerates increasingly when the so-called "brown fume" ( $\text{NO}_x$  formation, can be recognized by red-brown-yellow  $\text{NO}_2$ ) occur. This stage is referred to as autocatalysis. Usually no visible  $\text{NO}_x$  is formed in the case of triplebase (NC, blasting oils, nitroguanidin) GPs and there is no such obvious autocatalytical increase of mass loss. If the ratio of nitroguanidin - nitric acid ester is low, an accelerated increase of ML can be observed. Autocatalysis of NC has been investigated earlier [15,16,17]. Mass loss measurements are also performed using thermogravimetric devices as thermogravimetric analysis, TGA. The amounts used in these methods range from 1mg to 20mg and frequently are not representative in the case of complex samples, so that sample masses of 1g to 20g are necessary for the investigation of GP and RP, also for the reasons to use complete propellant grains and to observe morphological changes of the grains.

### 4.2.1 Mass loss without autocatalysis

A linear increase of mass loss is equivalent to a reaction of zero order for the decrease of the substance  $A(t, T)$ , eq.(22). The kinetic formulation is eq.(23).



$$(23) \quad \left( \frac{dA(t, T)}{dt} \right) \bigg|_T = -k_1(T) \quad \text{reaction of zero order}$$

C includes all volatile and escaping products, S the remaining solid reaction products. B is a product with a smaller molecular mass than the starting substance A and also remains in the residue. The eq.(22) and eq.(23) are defined in amounts of particles, with the unit mol. According to eq.(24) one has

$$(24) \quad \begin{array}{ll} M_A(t, T) = A(t, T) m_A & M_B(t, T) = B(t, T) m_B \\ M_C(t, T) = C(t, T) m_C & M_S(t, T) = S(t, T) m_S \end{array}$$

where  $m_i$  is molar mass of A, B, C and S. In eq.(25) this is applied to the mass decrease with  $A(t, T) = M_A(t, T)/m_A$ . The equation for the mass  $M_A(t, T)$  normalized with  $M_A(0)$  is also stated. The integration of eq.(25) results in eq.(26).

$$(25) \quad \left( \frac{dM_A(t, T)}{dt} \right) \Big|_T = -k_1(T) \cdot m_A$$

$$\left( \frac{d \left( \frac{M_A(t, T)}{M_A(0)} \right)}{dt} \right) \Big|_T = -\frac{k_1(T)}{A(0)} = -k_{ML}^1(T) \quad \text{with} \quad \frac{M_A(t, T)}{M_A(0)} = M_{Ar}(t, T)$$

$$(26) \quad M_A(t, T) = M_A(0) - k_1(T) \cdot m_A \cdot t$$

$$M_{Ar}(t, T) = M_{Ar}(0) - \frac{k_1(T)}{A(0)} \cdot t = 1 - k_{ML}^1(T) \cdot t$$

In the normalized form, all reaction rate constants have the dimensions 1/time and can be compared directly amongst the different methods, by taking into consideration possible additional scaling factors. But the measured quantity is not  $M_A(t, T)$ ,  $M(t, T)$  is determined, eq.(27), whereby in a complete formulation initial contents  $\neq 0$  of B and S must be admitted.  $M_N$  is a non-reacting component in the reaction mixture or propellant formulation.

$$(27) \quad \begin{aligned} M(t, T) &= M_N + M_A(t, T) + M_B(t, T) + M_S(t, T) \\ &= M(0) - M_C(t, T) \end{aligned} \quad \text{with} \quad M(0) = M_N + M_A(0) + M_B(0) + M_S(0)$$

The amounts in mol of B(t, T) is formed according to eq.(28) from A(t, T).

$$(28) \quad B(t, T) = B(0) + A(0) - A(t, T)$$

$A(0) - A(t, T)$  is the amount in mol of A, which has already reacted. For the mass  $M_B(t, T)$ , eq.(29) is valid.

$$(29) \quad M_B(t, T) = B(t, T) \cdot m_B = M_B(0) + \frac{m_B}{m_A} \cdot (M_A(0) - M_A(t, T))$$

Analogous to B(t, T),  $C(t, T) = A(0) - A(t, T)$ , and one gets for  $M_C(t, T)$  with  $M_C(0) = 0$  eq.(30).

$$(30) \quad M_C(t, T) = C(t, T) \cdot m_C = \frac{m_A - m_B - m_S}{m_A} \cdot (M_A(0) - M_A(t, T))$$

Using eq.(30) and eq.(27) one achieves at eq.(31),

$$M(t, T) = M(0) - \frac{m_A - m_B - m_S}{m_A} \cdot (M_A(0) - M_A(t, T))$$

(31)

$$M_r(t, T) = \frac{M(t, T)}{M(0)} = 1 - \frac{m_A - m_B - m_S}{m_A} \cdot \frac{M_A(0)}{M(0)} \cdot (1 - M_{Ar}(t, T))$$

whereby the normalized mass  $M_r(t, T) = M(t, T)/M(0)$  is also stated in eq.(31). Eq.(32) gives  $M_A(t, T)$  and  $M_{Ar}(t, T)$ .

$$M_A(t, T) = M_A(0) - \frac{m_A}{m_A - m_B - m_S} \cdot (M(0) - M(t, T))$$

(32)

$$M_{Ar}(t, T) = \frac{M_A(t, T)}{M_A(0)} = 1 - \frac{m_A}{m_A - m_B - m_S} \cdot \frac{M(0)}{M_A(0)} \cdot (1 - M_r(t, T))$$

Using eq.(31),  $M(t, T)$  and  $M_r(t, T)$  result in eq.(33) for a reaction of zero order.

$$M(t, T) = M(0) - k_1(T) \cdot (m_A - (m_B + m_S)) \cdot t$$

(33)

$$M_r(t, T) = 1 - k_1(T) \cdot \left( \frac{m_A - (m_B + m_S)}{M(0)} \right) \cdot t = 1 - k_{ML}^1(T) \cdot \left( \frac{1 - \frac{m_B + m_S}{m_A}}{1 + \frac{M_N + M_B(0) + M_S(0)}{M_A(0)}} \right) \cdot t$$

If  $m_A \gg (m_B + m_S)$ ,  $M_N = 0$ ,  $M_B(0) = 0$  and  $M_S(0) = 0$ , then  $M(t, T) = M_A(t, T)$  and  $M_r(t, T) = M_{Ar}(t, T)$  so that the following eq.(34) is derived from eq.(33).

$$(34) \quad M_r(t, T) = 1 - k_{ML}^1(T) \cdot t$$

The mass loss (ML) is calculated using eq.(35), whereby O is the initial mass loss (offset), which is not part of the decomposition reaction.

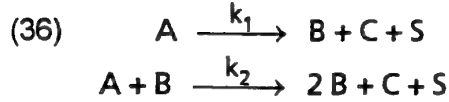
$$(35) \quad \begin{aligned} ML(t, T) &= O + 100\% \cdot \frac{M(0) - M(t, T)}{M(0)} = O + 100\% \cdot (1 - M_r(t, T)) \\ &= O + 100\% \cdot k_{ML}^1(T) \cdot t \end{aligned}$$

Eq.(33) or eq.(35) can be applied to the mass loss measurements for lifetime predictions. The k-values are determined from measurements at isothermal storage temperatures and these are then parameterised according to Arrhenius. Times up to 2% mass loss (ML) can also be used, whereby the reciprocal 'time to 2% ML' is proportional to a reaction rate constant. Examples of evaluations can be found in /7/ and /18,19,20/.



#### 4.2.2 Mass loss with autocatalysis

In the case of autocatalysis, the reaction product B is now introduced as autocatalytically effective and it reacts with the starting substance, reaction scheme eq.(36).



The following eq.(37) applies to the decrease of A.

$$(37) \quad \left( \frac{dA(t,T)}{dt} \right) \Big|_T = -k_1(T) - k_2(T) \cdot A(t,T) \cdot B(t,T)$$

Eq.(38) is derived from eq.(37) after division with A(0).

$$(38) \quad \left( \frac{d\left(\frac{A(t,T)}{A(0)}\right)}{dt} \right) \Big|_T = -\frac{k_1(T)}{A(0)} - k_2(T) \cdot A(0) \cdot \frac{A(t,T)}{A(0)} \cdot \left( \frac{B(0) + A(0) - A(t,T)}{A(0)} \right)$$

Eq.(39) results from equation (38) after the introduction of masses for A and B and using the abbreviations defined in eq.(40).

$$(39) \quad \left( \frac{dM_{Ar}(t,T)}{dt} \right) \Big|_T = -k_{ML}^1(T) - k_{ML}^2(T) \cdot M_{Ar}(t,T) \cdot (F + 1 - M_{Ar}(t,T))$$

whereby

$$(40) \quad k_{ML}^1(T) = \frac{k_1(T)}{A(0)} \quad \text{and} \quad k_{ML}^2(T) = k_2(T) \cdot A(0) \quad \text{and} \quad F = \frac{M_B(0)}{M_A(0)} \cdot \frac{m_A}{m_B}$$

Integration of the differential eq.(39) of the Riccati type with the initial condition  $M_{Ar}(0) = 1$  results in eq.(41).

$$(41) \quad M_{Ar}(t,T) = \frac{1}{2} + \frac{F}{2} + \frac{a}{2 \cdot k_{ML}^2(T)} \cdot \frac{(a + (1-F) \cdot k_{ML}^2(T)) \exp(-a \cdot t) - (a - (1-F) \cdot k_{ML}^2(T))}{(a + (1-F) \cdot k_{ML}^2(T)) \exp(-a \cdot t) + (a - (1-F) \cdot k_{ML}^2(T))}$$

$$\text{with } a = \sqrt{k_{ML}^2(T) \cdot (4 \cdot k_{ML}^1(T) + k_{ML}^2(T) \cdot (F+1)^2)}$$

For  $t \rightarrow \infty$ , one gets  $M_r(\infty) = \frac{1}{2} + \frac{F}{2} - \frac{a}{2 \cdot k_{ML}^2(T)} \approx 0$  if  $k_{ML}^1 \ll k_{ML}^2$ , which is the case

for GPs, RPs and nitrocellulose. Eq.(41) is called the 'zero order autocatalytic' model. If  $M_B(0) = 0$ , F is zero too. Using eq.(31),  $M(t,T)$  or  $M_r(t,T)$  can be determined.

If the non-autocatalytic decomposition reaction of A in eq.(36) proceeds according to a reaction of the first order, the following equations replace the eqs.(38), (39) and (40).

$$(42) \quad \left( \frac{d \left( \frac{A(t,T)}{A(0)} \right)}{dt} \right) \bigg|_T = -k_1(T) \cdot \frac{A(t,T)}{A(0)} - k_2(T) \cdot A(0) \cdot \frac{A(t,T)}{A(0)} \cdot \left( \frac{B(0) + A(0) - A(t,T)}{A(0)} \right)$$

$$(43) \quad \left( \frac{dM_{Ar}(t,T)}{dt} \right) \bigg|_T = -k_{ML}^1(T) \cdot M_{Ar}(t,T) - k_{ML}^2(T) \cdot M_{Ar}(t,T) \cdot (F + 1 - M_{Ar}(t,T))$$

$$(44) \quad k_{ML}^1(T) = k_1(T) \quad \text{and} \quad k_{ML}^2(T) = k_2(T) \cdot A(0) \quad \text{and} \quad F = \frac{M_B(0)}{M_A(0)} \cdot \frac{m_A}{m_B}$$

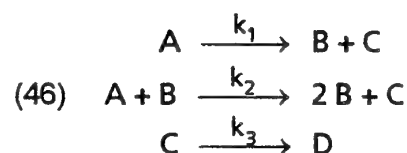
Eq.(43) is a differential equation of the Bernoulli type, integration results in eq.(45).

$$(45) \quad M_{Ar}(t,T) = \frac{k_{ML}^1(T) + (F+1) \cdot k_{ML}^2(T)}{k_{ML}^2(T) + (k_{ML}^1(T) + F \cdot k_{ML}^2(T)) \cdot \exp((k_{ML}^1(T) + (F+1) \cdot k_{ML}^2(T)) \cdot t)}$$

Eq.(45) is named 'first order autocatalytic' model.

Using eq.(41) with  $F = 0$ , Fig. 2, a good description was achieved for the autocatalytic mass loss of the in service triplebase GP KN6540 (M30 type). The mass loss commences already at the start of storage autocatalytically.

The autocatalytic mass loss of a plasticized nitrocellulose was described using the formulation according to reaction scheme eq.(46). In addition to the part 'zero order autocatalytic' there is a consecutive reaction of the product C, which is now non-volatile, to the volatile product D in a reaction of first order.



Eq.(47) (includes ML), which reproduces the data very well, is an approximated solution of the differential equation system of the reaction scheme eq.(46).  $M_r(t,T)$  is composed of two parts. The first part,  $M_{Ar}$ , describes the reaction of A and the autocatalytic reaction of A and B, the second part,  $M_{Cr}$ , approximates the reaction from C to D. The model 'zero order autocatalytic' or 'first order autocatalytic' can be used for  $f(t,T)$ .

$$(47) \quad ML(t,T) = O + (100\% - L) \cdot (1 - M_r(t,T))$$

$$M_r(t,T) = M_{Ar}(t,T) + M_{Cr}(t,T) = f(t,T) + (1 - f(t,T)) \cdot \exp(-k_{ML}^3(T) \cdot t)$$

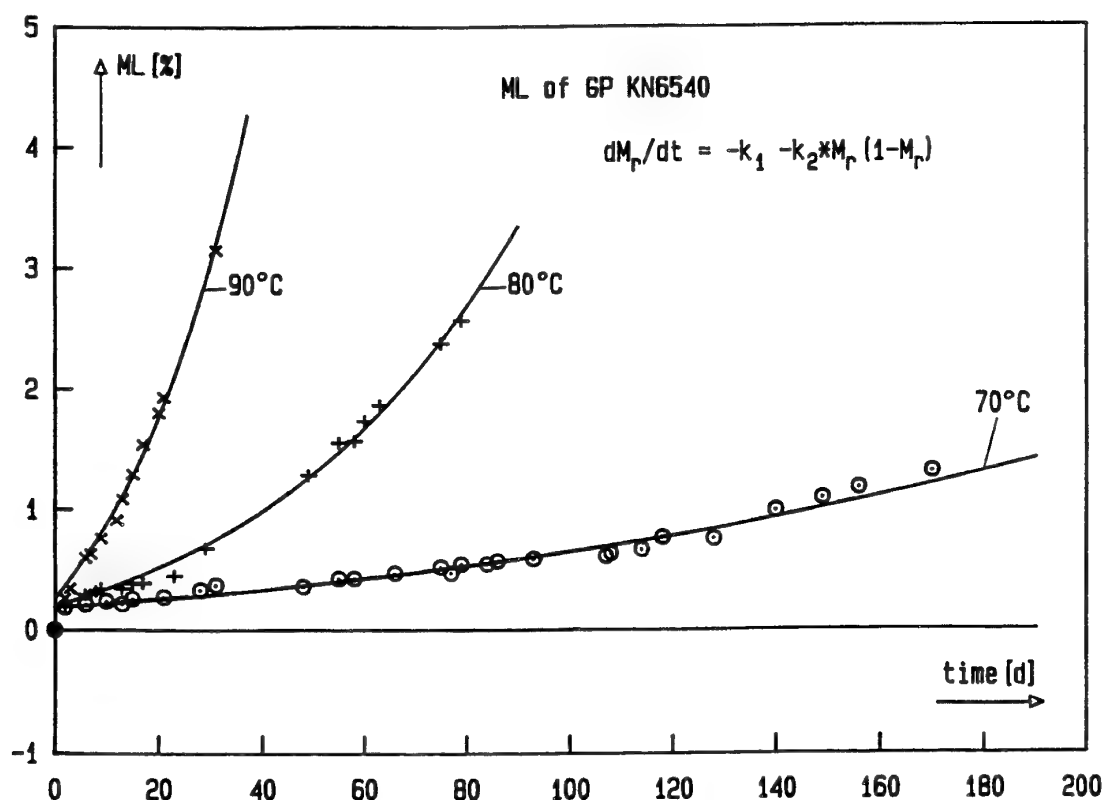


Fig 2: Mass loss of the triplebase GP KN6540. The curves are the description according to the 'zero order autocatalytic' model.

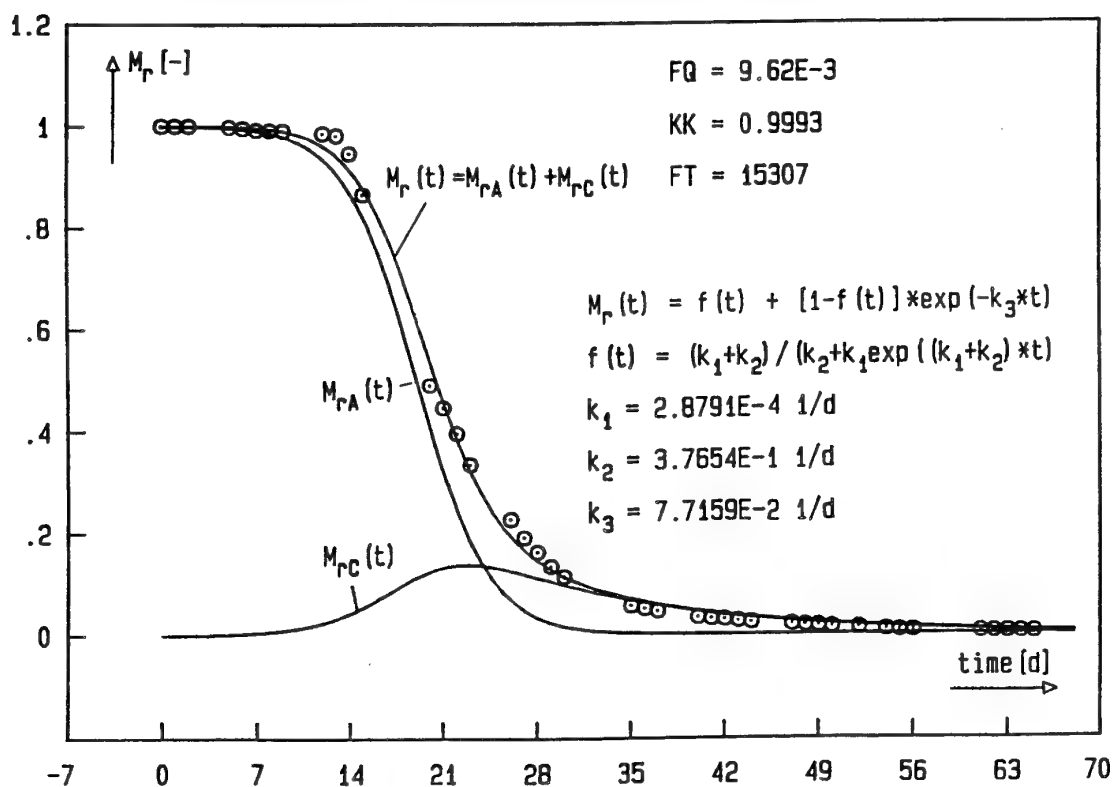


Fig. 3: Description of the autocatalytic course of the mass loss of a plasticized NC with the 'first order autocatalytic' model. KK is the correlation coeff. Mass loss re-scaled from the plateau value of 50.3% to 100%.

The eq.(47) take inert components into consideration by introducing the plateau value (100%-L). One can re-scale the mass loss to 100%. The re-scaling does not affect the values of the reaction rate constants /21/. This was done in Fig. 3. Here the model 'first order autocatalytic' was applied for  $f(t, T)$  with  $F = 0$ .

#### 4.2.3 Determining the service lifetime with mass loss

Analogous to the definition of the degree of degradation, eq.(48) applies to the 'degree of mass change'  $y_{ML}$ .

$$(48) \quad y_{ML} = \frac{M(ty_{ML}(T))}{M(0)} = M_r(ty_{ML}(T)) = \frac{M_L}{M(0)} = M_{r,L}$$

The 'degree of mass loss' is therefore  $(1-y_{ML})$ . According to eq.(34), the time  $ty_{ML}(T)$  to reach  $y_{ML}$  is given in eq.(49).

$$(49) \quad ty_{ML}(T) = \frac{1-y_{ML}}{k_{ML}^1(T)}$$

whereby here  $M_A(t, T) \approx M(t, T)$ .

As in general  $M(t, T)$  and  $M_A(t, T)$  are different, the associated degrees of change  $y_{ML}^M$  and  $y_{ML}^A$  are also different with the same  $ty_{ML}(T)$  (or the degrees of change are made equal with different times). According to eq.(31) and eq.(32), the following applies

$$(50) \quad y_{ML}^M = 1 - \frac{m_A - m_B - m_S}{m_A} \cdot \frac{M_A(0)}{M(0)} \cdot (1 - M_{Ar}(ty_{ML}(T))) = \frac{M(ty_{ML}(T))}{M(0)}$$

$$y_{ML}^A = 1 - \frac{m_A}{m_A - m_B - m_S} \cdot \frac{M(0)}{M_A(0)} \cdot (1 - M_r(ty_{ML}(T))) = \frac{M_A(ty_{ML}(T))}{M_A(0)}$$

In the case of autocatalytic mass loss according to eq.(41) and eq.(45), the expressions for  $ty_{ML}^A(T)$  are eq.(51) and eq.(52).

$$(51) \quad ty_{ML}(T) = \frac{1}{a} \cdot \ln \left( \frac{(a + (1-F) \cdot k_{ML}^2(T)) \cdot (1-K)}{(a - (1-F) \cdot k_{ML}^2(T)) \cdot (1+K)} \right) \quad \text{with} \quad K = \left( y_{ML}^A - \frac{1+F}{2} \right) \cdot \frac{2 \cdot k_{ML}^2(T)}{a}$$

with 'F',  $k_{ML}^1(T)$  and 'a' from equations (40) and (41)

$$(52) \quad t_{y_{ML}}(T) = \frac{1}{k_{ML}^1(T) + (F+1) \cdot k_{ML}^2(T)} \cdot \ln \left( \frac{\frac{1}{y_{ML}^A} \cdot (k_{ML}^1(T) + (F+1) \cdot k_{ML}^2(T)) - k_{ML}^2(T)}{k_{ML}^1(T) + F \cdot k_{ML}^2(T)} \right)$$

with 'F' and  $k_{ML}^i(T)$  from equation (44).

## 4.3 Heat generation

### 4.3.1 Description of heat generation data in principle

The basic relationship eq.(53) applies to the heat generation rate (heat flow)  $dQ/dt = \dot{q}$ .

$$(53) \quad \left( \frac{dQ_A(t, T)}{dt} \right) \Big|_T \equiv \dot{q}_A(t, T) = - \left( \frac{dA(t, T)}{dt} \right) \Big|_T \cdot (-\Delta H_R) = - \left( \frac{dM_A(t, T)}{dt} \right) \Big|_T \cdot \frac{1}{m_A} \cdot (-\Delta H_R)$$

$(-\Delta H_R)$  is the reaction heat (reaction enthalpy) per unit amount. The choice of the unit of concentration or of a quantity is optional: mol, mass-%, mol/l, mass. Eq.(53) is formulated in the unit mol for substance A and the mass  $M_A$  of A is obtained with  $m_A$  as molar mass of A. Eq.(53) can be transformed to the normalized quantities  $Q_{Ar}(t, T) = Q_A(t, T)/Q_A(te)$ ,  $A_r(t, T) = A(t, T)/A(0)$  and  $M_{Ar}(t, T) = M_A(t, T)/M_A(0)$ , whereby the normalization with  $Q_A(te) = A(0) \cdot (-\Delta H_R)$  is carried out for  $Q_{Ar}(t, T)$ , that means using the heat produced after the complete conversion of  $A(t, T)$ . Thus the following eq.(54) is derived from eq.(53):

$$(54) \quad \left( \frac{dQ_{Ar}(t, T)}{dt} \right) \Big|_T \equiv \dot{q}_{Ar}(t, T) = - \left( \frac{dA_r(t, T)}{dt} \right) \Big|_T = - \left( \frac{dM_{Ar}(t, T)}{dt} \right) \Big|_T$$

The integrated form of eq.(54) is:

$$(55) \quad Q_{Ar}(t, T) - Q_{Ar}(0) = 1 - A_r(t, T) = 1 - M_{Ar}(t, T)$$

$Q_{Ar}(0)$  is usually zero, however an offset can be taken into consideration, but this may not come from the conversion reaction of the reactant A. The following equations show the formulations for the heat generation rate and heat generation  $Q_A(t, T)$  and  $Q_{Ar}(t, T)$  respectively according to a reaction of first order for reactant A.

In a reaction of zero order, the heat generation rate is constant with time, in a reaction of the first order, it decreases exponentially with time and in a reaction of the 2nd order it decreases by  $(1/t)^2$ . In this way the reaction order can also be determined very well from the heat generation data.

$$(56) \left\{ \begin{array}{l} \left( \frac{dQ_A(t, T)}{dt} \right) \Big|_T = k_1(T) \cdot (-\Delta H_{R,1}) \cdot A(0) \cdot \exp(-k_1(T) \cdot t) \\ Q_A(t, T) - Q_A(0) = (-\Delta H_{R,1}) \cdot A(0) \cdot (1 - \exp(-k_1(T) \cdot t)) \\ Q_{Ar}(t, T) - Q_{Ar}(0) = (1 - \exp(-k_1(T) \cdot t)) \end{array} \right\}$$

### 4.3.2 Heat generation with autocatalysis

In contrast to mass loss as an integral quantity, The heat generation rate is a differential quantity so that in the case of autocatalysis a peak-type signal is found, Fig. 4.

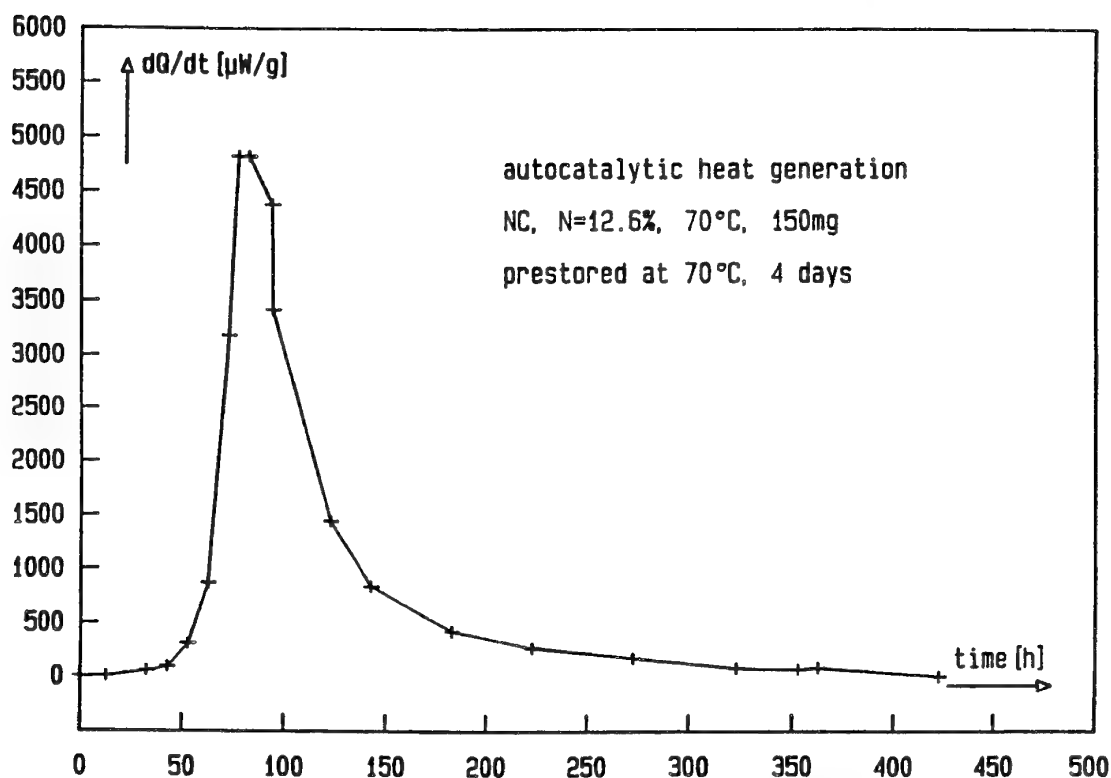
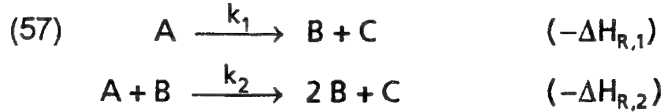


Fig. 4: Autocatalytic heat generation rate of a pure unstabilized NC.

Integration results in a curve analogous to that of mass loss. In this form the equations from section 4.2 can be taken over directly into eq.(54) and (55). For the reaction kinetic description of the reaction scheme eq.(57), the system of differential equations, eq.(58) must be considered.



$$\begin{aligned}
 (58) \quad & \left( \frac{dA(t,T)}{dt} \right) \Big|_T = -k_1(T) - k_2(T) \cdot A(t,T) \cdot B(t,T) \\
 & \left( \frac{dQ(t,T)}{dt} \right) \Big|_T = +k_1(T) \cdot (-\Delta H_{R,1}) + k_2(T) \cdot (-\Delta H_{R,2}) \cdot A(t,T) \cdot B(t,T)
 \end{aligned}$$

$$\text{with } B(t,T) = B(0) + A(0) - A(t,T)$$

The heat generation rate is normalized using the heat  $Q(te)$  released after A has been consumed, and which is formally set equal to  $A(0)(-\Delta H_R)$ , eq.(59).

$$(59) \quad \left( \frac{d \left( \frac{Q(t,T)}{Q(te)} \right)}{dt} \right) \Big|_T = k_Q^1(T) + k_Q^2(T) \cdot \frac{A(t,T)}{A(0)} \cdot \left( F + 1 - \frac{A(t,T)}{A(0)} \right)$$

where

$$(60) \quad k_Q^1(T) = \frac{k_1(T)}{A(0)} \cdot \frac{(-\Delta H_{R,1})}{(-\Delta H_R)}, \quad k_Q^2(T) = k_2(T) \cdot A(0) \cdot \frac{(-\Delta H_{R,2})}{(-\Delta H_R)} \quad \text{and} \quad F = \frac{B(0)}{A(0)}$$

As the heat generation rate is the measured quantity, eq.(59) can be applied directly. In order to determine the time  $ty_Q(T)$  to reach a set degree of energy consumption, the integrated form of eq.(59) is required. The expression  $A_r(t,T)$  is inserted into eq.(59), the form of which is equal to that of eq.(41), here given as eq.(41') and the integration of eq.(59) gives eq.(61).

$$(41') \quad A_r(t,T) = \frac{1}{2} + \frac{F}{2} + \frac{a}{2 \cdot k_A^2(T)} \cdot \frac{(a + (1-F) \cdot k_A^2(T)) \exp(-a \cdot t) - (a - (1-F) \cdot k_A^2(T))}{(a + (1-F) \cdot k_A^2(T)) \exp(-a \cdot t) + (a - (1-F) \cdot k_A^2(T))}$$

with

$$a = \sqrt{k_A^2(T) \cdot (4 \cdot k_A^1(T) + k_A^2(T) \cdot (F+1)^2)}$$

$$k_A^1(T) = \frac{k_1(T)}{A(0)} \quad \text{and} \quad k_A^2(T) = k_2(T) \cdot A(0) \quad \text{and} \quad F = \frac{B(0)}{A(0)}$$

$$(61) \quad Q_r(t,T) - Q_r(0) = k_Q^1(T) \cdot t + k_Q^2(T) \cdot (F+1) \int_0^t A_r(t,T) \cdot dt - k_Q^2(T) \int_0^t (A_r(t,T))^2 \cdot dt$$

The following equations apply in the case of a reaction of first order for the non-autocatalytic decomposition reaction of A in eq.(57).

$$(62) \quad \left( \frac{d \left( \frac{Q(t,T)}{Q(te)} \right)}{dt} \right) \bigg|_T = k_Q^1(T) \cdot \frac{A(t,T)}{A(0)} + k_Q^2(T) \cdot \frac{A(t,T)}{A(0)} \cdot \left( F + 1 - \frac{A(t,T)}{A(0)} \right)$$

where

$$(63) \quad k_Q^1(T) = k_1(T) \cdot \frac{(-\Delta H_{R,1})}{(-\Delta H_R)}, \quad k_Q^2(T) = k_2(T) \cdot A(0) \cdot \frac{(-\Delta H_{R,2})}{(-\Delta H_R)} \quad \text{and} \quad F = \frac{B(0)}{A(0)}$$

The integrals of eq.(61) can be solved analytically for both autocatalytic equations.

Fig. 5 shows the  $Q(t)$  values of the measurements from Fig. 4 and the description using eq.(61) with the conditions  $M_B(0) = 0$ , and  $(-\Delta H_{R,1}) = (-\Delta H_{R,2}) = (-\Delta H_R)$ , curve 1 in Fig. 5.

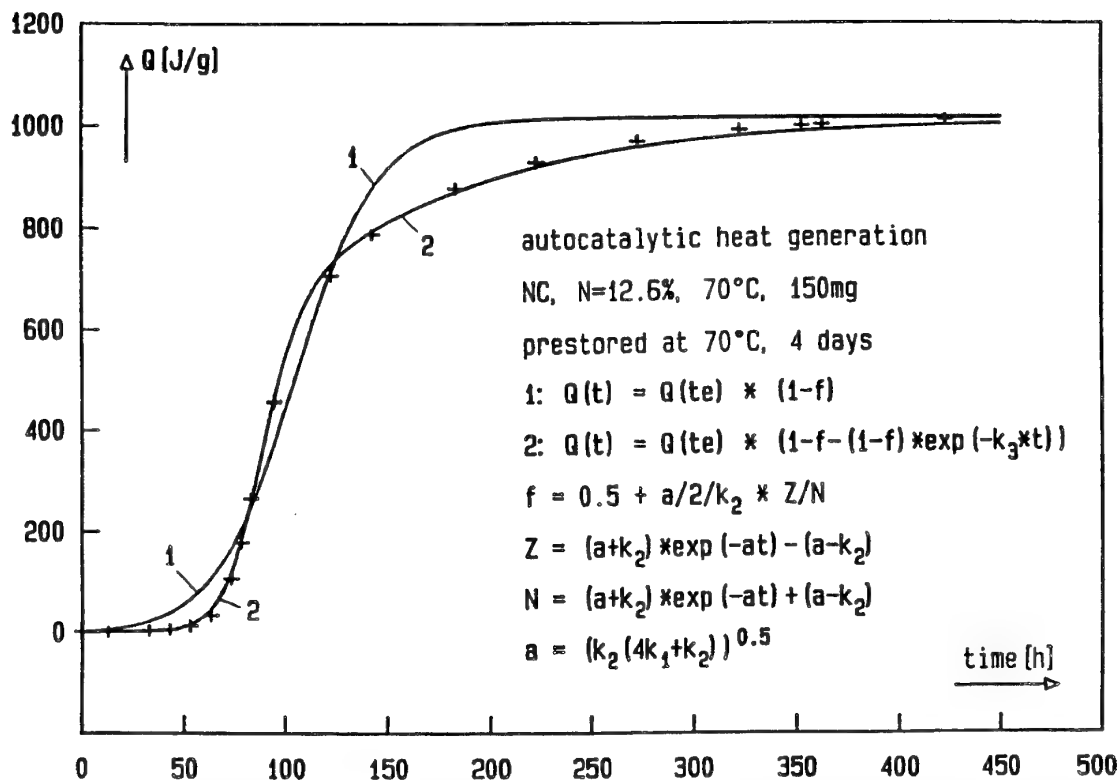
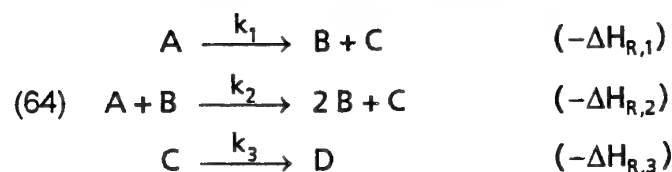


Fig. 5: Integrated heat generation rate from Fig. 4. Description with the model 'zero order autocatalytic', curve 1, and for curve 2 additionally with a consecutive reaction.

As  $Q(t)$  runs out on a plateau, it was possible to determine  $Q(te)$  as the final value of the plateau. Due to the asymmetry of the  $Q(t,T)$ -curves, also in  $M_i(t,T)$ -curves, see



/1,21/, the quantitative description is not very good with curve 1. Analogous to the example with the plasticized nitrocellulose, section 4.2.2, a subsequent reaction is introduced to supplement eq.(57) again as a reaction of first order, eq.(64).



Separating the two reactions, the autocatalytic and the subsequent reaction, according to eq.(65), curve 2 in Fig. 5,

$$(65) \quad Q_r(t, T) = 1 - f(t, T) - (1 - f(t, T)) \cdot \exp(-k_Q^3(T) \cdot t)$$

whereby  $f(t, T)$  stands for eq.(41'), a very good description and therefore parameterisation of the measurements is achieved similar to the example of mass loss of the plasticized nitrocellulose. Here too eq.(65) is only an approximation for the complete reaction scheme. The different reaction enthalpies of the reactions must also be taken into consideration.

The correct solution is obtained by numerically integrating the differential equation system eq.(66) together with the necessary experimental information.

$$\begin{array}{ll}
 \left( \frac{dA(t, T)}{dt} \right) \Big|_T &= -k_1(T) - k_2(T) \cdot A(t, T) \cdot B(t, T) \\
 \left( \frac{dB(t, T)}{dt} \right) \Big|_T &= +k_1(T) + k_2(T) \cdot A(t, T) \cdot B(t, T) \\
 (66) \quad \left( \frac{dC(t, T)}{dt} \right) \Big|_T &= +k_1(T) + k_2(T) \cdot A(t, T) \cdot B(t, T) - k_3(T) \cdot C(t, T) \\
 \left( \frac{dQ(t, T)}{dt} \right) \Big|_T &= +k_1(T) \cdot (-\Delta H_{R,1}) + k_2(T) \cdot (-\Delta H_{R,2}) \cdot A(t, T) \cdot B(t, T) \\
 &\quad + k_3(T) \cdot (-\Delta H_{R,3}) \cdot C(t, T)
 \end{array}$$

However, one must be aware that further reactions must be introduced into eq.(64), especially for GPs and RPs to achieve a full description and to reproduce the measured heat generation rates.

#### 4.3.3 Determining the service lifetime with heat generation

The heat generation rate  $dQ/dt$  is proportional to the momentary rate of the overall decomposition reaction weighed by the heat of reactions of the individual reactions. The integral  $Q(t)$  is the heat generated (released) up to the time  $t$ . It can be regarded as energy loss of the GPs and RPs. An analogous definition to that of mass loss can be made with the 'degree of energy consumption'  $y_Q$  or the 'degree of energy loss'  $(1 - y_Q)$ , which may not exceed a certain limit, e.g. 3% or 5% of a reference value  $Q_{ref}$ . Frequent-

ly the heat of explosion  $Q_{\text{ex}}$  of GPs or RPs after production is used as reference value. However, the reaction heat  $Q(\text{te})$  released up to the consumption of the reactants upon which the overall decomposition reaction is based, does not need to agree with  $Q_{\text{ex}}$  for GPs and RPs, as the reactions of the low-temperature decomposition are different to those of the burning reactions in operation. This is also shown by the significant residue in mass loss measurements of GPs and RPs. The plateau values are always significantly smaller than 100% ML.

In general, eq.(67) applies, from which the time  $ty_Q(T)$  to reach the degree of energy consumption  $y_Q$  is determined.

$$(67) \quad y_Q = \frac{Q_L}{Q_{\text{ref}}} = \frac{Q(ty_Q(T))}{Q_{\text{ref}}}$$

$$(1 - y_Q) \cdot Q_{\text{ref}} = \int_{t_0}^{ty_Q(T)} \dot{q}(t, T) \cdot dt$$

The starting time  $t_0$  can be a time offset or zero.

As already has been stated, GPs and RPs based on nitric acid esters often show a constant heat generation rate for a normal ageing state with sufficient stabilizer after an initial 'equilibration' period, which may last several days.  $dQ/dt$  is determined at some different temperatures, e.g. between 50°C and 90°C. The  $dQ(T)/dt$  data are parameterised according to Arrhenius, eq.(68).

$$(68) \quad \ln(\dot{q}(T)) = \ln(Z_Q) - E_{a_Q} / RT$$

According to eq.(69) the times  $ty_Q(T)$  can be calculated until the allowed 'degree of energy loss'  $(1 - y_Q)$  has been reached.

$$(69) \quad ty_Q(T) = \frac{(1 - y_Q) \cdot Q_{\text{ref}}}{\dot{q}(T)}$$

Eq.(69) assumes that the heat generation rates do not change with ageing, however, this does not apply in general, see /14/.

## 5. Mass loss and heat generation of AN/GAP propellants

In the connection with programmes to develop signature free (minimum smoke), less sensitive and high energetic rocket propellants, formulations are investigated based on ammonium nitrate (AN) and energetic binders like GAP and PolyGLYN. To achieve high specific impulses  $I_s$  energetic plasticizers have to be used. In the following results on the ageing of some formulations based on AN (64 mass-%), GAP (12 mass-%) and BTTN / TMETN blasting oil mixtures (22 mass-%) are shown. More details about the stability, compatibility and the choice of suitable ingredients can be found in /22/.

Fig. 6 show the mass losses as function of time and temperature of the two formulations AN 212 and AN 221. The mass losses starts from the beginning of the storage with a steadily increasing rate, this means they are autocatalytically accelerated. The data can be described very well with the model 'zero order autocatalytic', the curves in Fig. 6. In Table 3 the calculated times  $t_{ML}(T)$  to reach 2% mass loss are given for three AN/GAP formulations and compared to those of the in service GP KN6540. The absolute values of  $t_{ML}(T)$  at lower temperatures may be shorter in reality, because of only a higher temperature extrapolation. Here they are used for the purpose of comparison in order to assess, if a sufficient lifetime can be achieved with these AN/GAP formulations.

**Table 3:** Times  $t_{ML}(T)$  until 2% mass loss (ML) for three AN/GAP rocket propellant formulations and the GP KN6540 (M30 type, 105mm), determined with the model 'zero order autocatalytic'.

Temp.	AN 164		AN 212		AN 221		GP KN 6540	
[°C]	[d]	[a]	[d]	[a]	[d]	[a]	[d]	[a]
20		1224		990		998		1795
30		244		173		178		309
40		52		34		36		59
50		11.6		7.2		7.8		12.6
60	998	2.7	613	1.7	680	1.9	1066	2.9
70	249		156		177		269	
80	66		43		50		73	
90	18.3		12.5		15.0		21.5	
100	5.4		3.9		4.8		6.7	
$Ea_{ML}^1$ [kJ/mol]	110.7		122.3		135.0		135.8	
$Z_{ML}^1$ [1/d]	1.953 E+12		1.439 E+14		5.737 E+15		1.555 E+16	
$Ea_{ML}^2$ [kJ/mol]	151.9		135.7		124.7		125.4	
$Z_{ML}^2$ [1/d]	9.998 E+20		6.502 E+18		1.704 E+17		6.630 E+16	

**Table 4:** Comparison between the rate constants at 80°C obtained from the description of the mass loss and the heat generation of AN 212, in both cases with the kinetic model 'zero order autocatalytic'.

method	rate constant at 80°C	correlation coefficient
mass loss	$k_{ML}^1 = 1.39 \text{ E-4 d}^{-1}$	0.9966
	$k_{ML}^2 = 4.15 \text{ E-2 d}^{-1}$	
heat generation	$k_Q^1 = 4.74 \text{ E-4 d}^{-1}$	0.9996
	$k_Q^2 = 2.65 \text{ E-2 d}^{-1}$	

The heat generation rate of AN 212 at 80°C can be seen in Fig. 7, measured with a TAM-microcalorimeter from Thermometric, Sweden, as the data of Fig. 4. One recognizes two main parts. The first peak-type part indicates one autocatalytic overall reaction and in the second part the heat generation rate increases steadily with time. Therefore

an autocatalytic behaviour can be assumed also, which is shown to be the case in Fig. 8. There the integrated heat generation rate is presented, which can be reproduced well by the 'zero order autocatalytic' model formulated for heat generation. From these

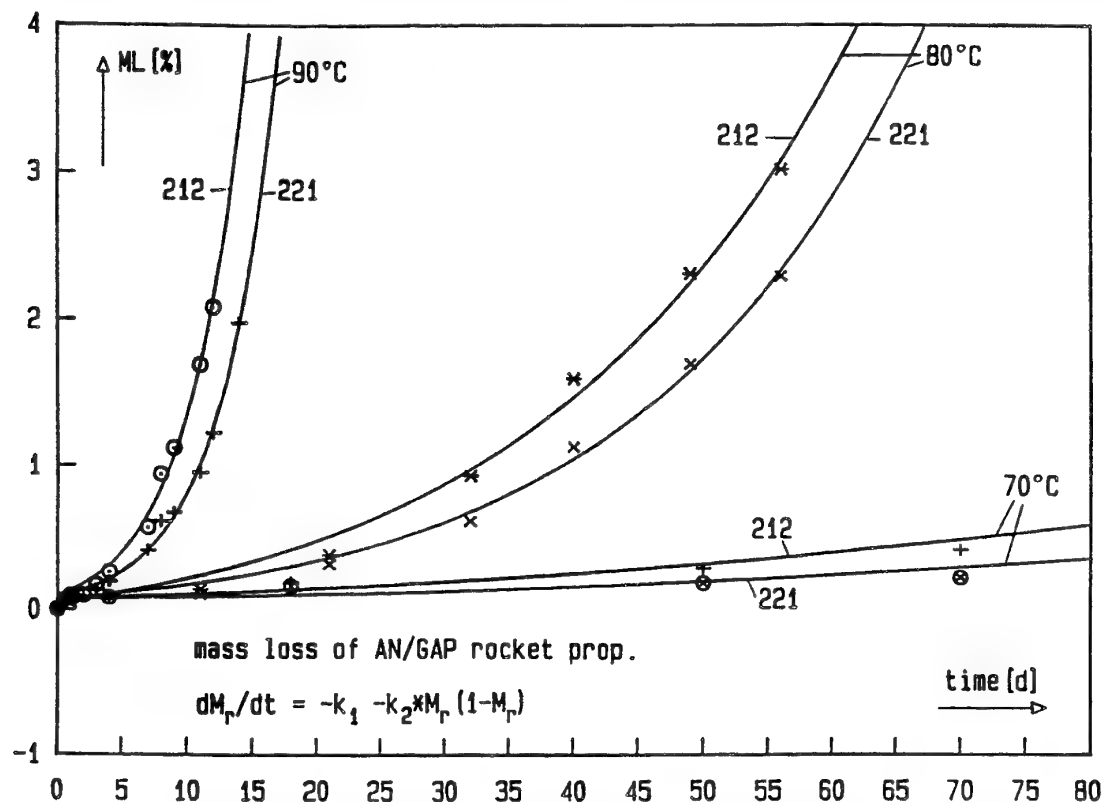


Fig. 6: Mass loss of AN/GAP formulations AN 212 and AN 221 at 70°C, 80°C and 90°C. the curves are the kinetic model 'zero order autocatalytic'.

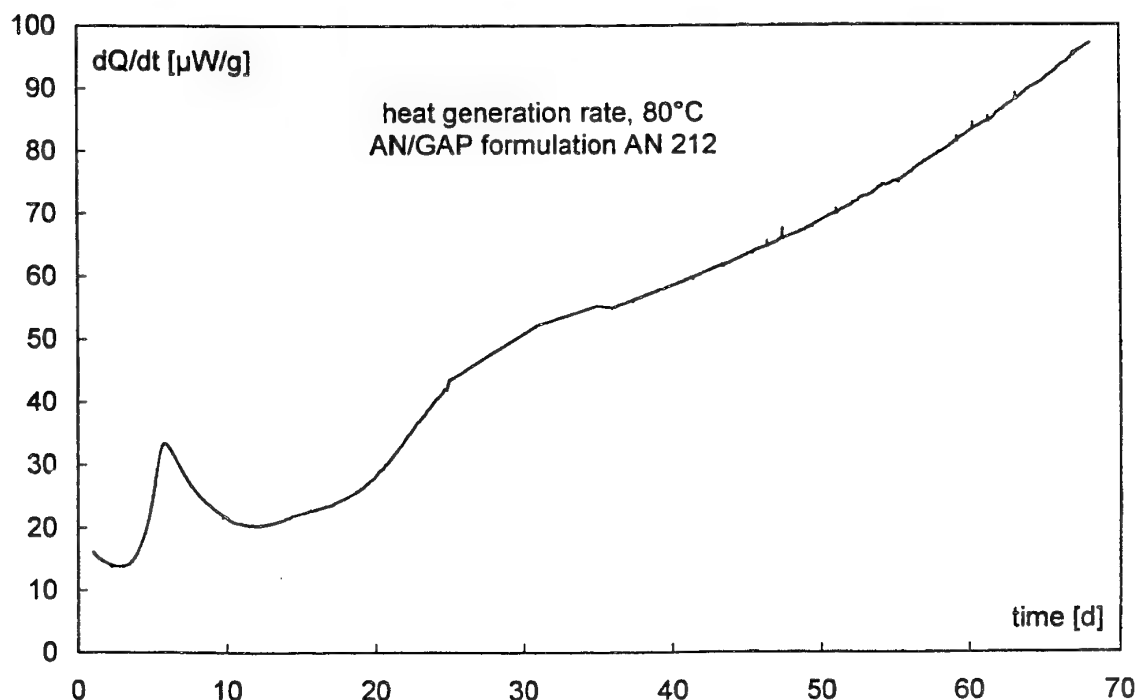


Fig. 7: Heat generation rate of AN/GAP formulation AN 212 at 80°C.

results one can conclude that the data of mass loss and heat generation measurements give basically the same information about the overall decomposition reaction in the AN/GAP formulations. The reaction rate constants are very similar, Table 4. For the normalization of the heat generation  $Q(t,T)$  the reference energy  $Q(te) = 3600\text{J/g}$  was taken. This is about 75% of the thermodynamically calculated heat of explosion of AN 212 and corresponds with the expected plateau value in mass loss of AN 212 at  $80^\circ\text{C}$ . An evaluation according to eq.(68) and eq.(69) is not possible. The reaction rate constants  $k_Q^1, k_Q^2$  are connected with  $k_A^1, k_A^2$  and  $k_{ML}^1, k_{ML}^2$  according to eq.(40), eq.(41'), eq.(60) and eq.(61).

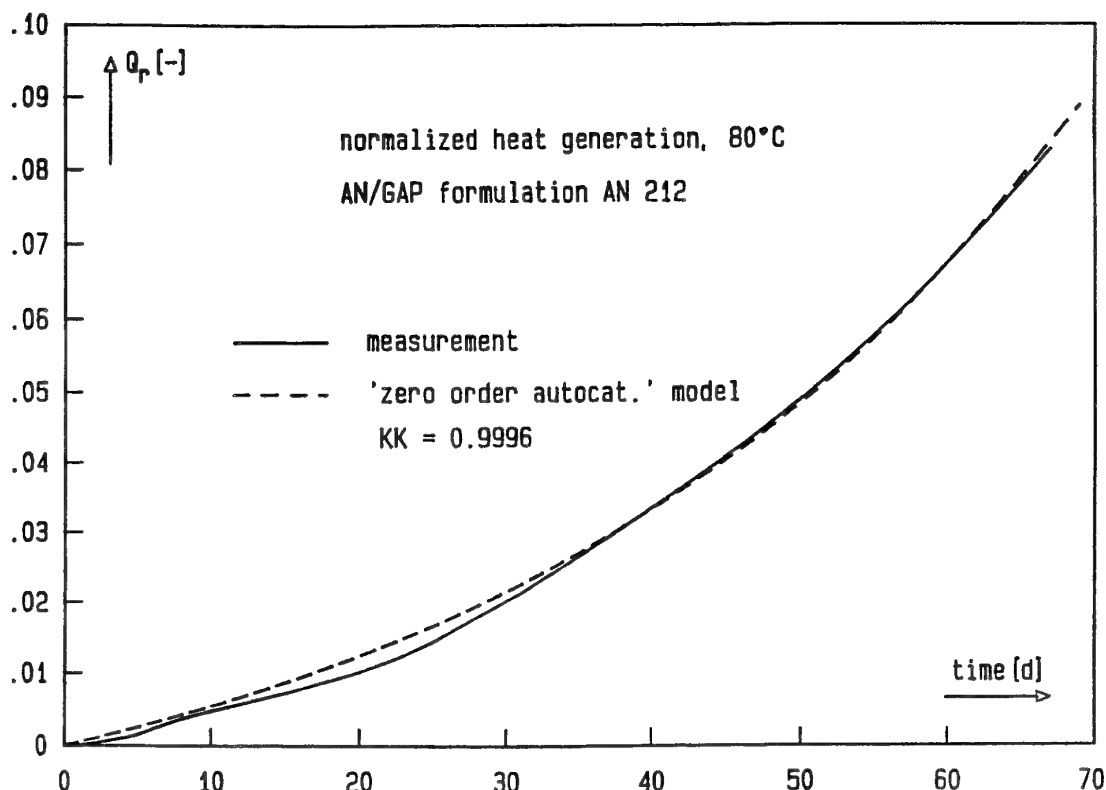


Fig. 8: Integrated rate of heat generation at  $80^\circ\text{C}$  of AN/GAP formulation AN 212. Description with the kinetic model 'zero order autocatalytic'.

## 6. Summary

Ageing processes in gun propellants (GP) and rocket propellants (RP) change important properties such as the contents of plasticizers, phlegmatizers, stabilizers and energy, mean mol masses  $M_n$ ,  $M_w$  and  $M_z$ , cross-link density, mechanical properties such as tensile strength, strain at break, elasticity modulus, shear modulus, glass transition temperature and embrittlement temperature. Therefore ageing processes limit the safe service lifetime and change the designed data of maximum pressure, vivacity, muzzle velocity and specific impulse, which subsequently declines the target picture.

In order to be able to predict after what time-temperature stress the tolerance limits have not yet been exceeded, ageing processes must be investigated and quantified. To

do this, the quantities or properties  $P$  connected with the ageing processes are measured as a function of time and temperature and the measurements are described mathematically using rate equations so that the dependence on time and temperature is separated. The temperature dependence is expressed using a pure temperature dependent coefficient, the rate constant. This type of mathematical formulation was given for the stabilizer consumption, mass loss and heat generation. By defining the degree of consumption or the degree of change  $y_P$  for the property  $P$ , the times  $ty_P(T)$  can be calculated until a set degree  $y_P = P_L/P(0)$  or the limit value  $P_L$  have been reached. These are the service lifetimes searched for. In order to make reliable predictions not only do the mathematical descriptions have to represent the measurements very well, they must also be able to extrapolate them appropriately along the time axis. The dependence of the rate constant on temperature must be parameterised in the correct way. On a possible different temperature dependence of the rate constants must be checked at investigation and application temperatures. Such differences are expressed by different Arrhenius parameters.

The model for stabilizer consumption, based on a combination of the reactions of zero and first order represent the measurements very well and can also extrapolate them very well. It can be used for reliable predictions. This model gives a much better description of the stabilizer consumption then the models based on a reaction of first order alone or on a reaction of zero order alone. The Arrhenius parameters of the stabilizer decrease of GP A5020 and RP RLC 470/6A were used to calculate the service lifetimes for temperature-time-profile stresses, whereby two STANAG profiles and a profile for the airbag qualification in the automotive industry were used.

For mass loss and heat generation, autocatalytic models have been formulated, which describe the measurements very well. The mass loss and heat generation data of AN/GAP rocket propellant formulations show that both methods can reveal the same overall decomposition reaction for these type of formulations. With both methods an autocatalytic decomposition behaviour was found, which could be described very well with the kinetic model 'zero order autocatalytic'. The ageing behaviour of some AN/GAP formulations was compared with that of the in service GP KN6540 (M30 type) using the times  $ty_{ML}(T)$  to reach 2% mass loss.

## 7. Literature

- /1/ M.A. Bohn  
*„Methods and Kinetic Models for the Lifetime Assessment of Solid Propellants“*, Paper 2 on the 87th Symp. of the Propulsion and Energetics Panel (PEP) of the AGARD (Advisory Group for Aerospace Research and Development), 'Service Life of Solid Propellant Systems', May 6-10, 1996, Athens, Greece. AGARD-Conference-Proceedings 586 (AGARD-CP-586), May 1997, F-92200 Neuilly sur Seine, France.
- /2/ F. Volk, G. Wunsch  
*„Determination of the Decomposition Behaviour of Double Base Propellants at Low Temperature“*, Propell. Expl. Pyrot. 10, 181 (1985).
- /3/ A. Pfeil, H.H. Krause, N. Eisenreich

- „The Consequences of Beginning Slow Thermal Decomposition on the Molecular Weight of Nitrated Cellulose“, Thermochim Acta 85, 395 (1985).*
- /4/ F. Volk, M.A. Bohn, G. Wunsch  
*„Determination of the Chemical and Mechanical Properties of Double Base Propellants During Aging“, Propell. Expl. Pyrot. 12, 81 (1987).*
- /5/ M.A. Bohn, F. Volk  
*„Prediction of the Lifetime of Propellants by Stabilizer Consumption and Molar Mass Decrease“, Proceed. ADPA Predictive Technology Symp., June 22-24, 1993, Orlando, FL, US-Army ARDEC, Picatinny Arsenal, New Jersey, USA.*
- /6/ M.A. Bohn  
*„Systematische Darstellung der Alterung von Rohrwaffentreibmitteln und Raketentreibstoffen“, Paper 109, Proceed. of the 28th Internat. Annual Conference of ICT, June 24-27, 1997, Karlsruhe, Germany, Fraunhofer-Institut für Chemische Technologie (ICT).*
- /7/ F. Volk  
*„Determining the Shelflife of Solid Propellants“, Propell. Expl. (Pyrot.) 1, 59 (1976).*
- /8/ F. Volk  
*„Determination of the Lifetime of Gun Propellants using Thin-Layer Chromatography“, Propell. Expl. (Pyrot.) 1, 90 (1976).*
- /9/ M.A. Bohn, N. Eisenreich  
*„Kinetic modelling of the stabilizer consumption and the consecutive products of the stabilizer in a gun propellant“, Propell. Expl. Pyrot., to be published in 1997.*
- /10/ N.J. Curtis  
*„Isomer Distribution of Nitro Derivatives of Diphenylamine in Gun Propellants: Nitrosamine Chemistry“, Propell. Expl. Pyrot. 15, 222 (1990).*
- /11/ R.A. Fifer  
*„Chemistry of Nitrate Ester and Nitramine Propellants“ in K.K. Kuo, M. Summerfield (eds.) 'Fundamentals of Solid Propellant Combustion', Progress in Astronautics and Aeronautics, Vol. 90, American Institute of Aeronautics and Astronautics, New York, USA, 1984.*
- /12/ M.A. Bohn  
*„Prediction of Life Times of Propellants - Improved Kinetic Description of the Stabilizer Consumption“, Propell. Expl. Pyrot. 19, 266 (1994).*
- M.A. Bohn  
*„Verbesserte kinetische Beschreibung der Stabilisatorabnahme zur Voraussage der Lagerzeiten von Treibmitteln“, ICT-Bericht 29/92, Dezember 1992, für BMVg, Bonn.*
- M.A. Bohn  
*„Modellierung des Stabilisatorverbrauchs in Treibmitteln“, Paper 42, Proceed. 25th Internat. Annual Conference of ICT, June 28-July 1, 1994, Karlsruhe, Ger-*

many, Fraunhofer-Institut für Chemische Technologie (ICT).

- /13/ STANAG (Standardization Agreement) 2895, „*Extreme climatic conditions and derived conditions for use in defining design and test criteria for NATO forces material*“, 1990, NATO Headquarters, Military Agency for Standardization, Bruxelles, Belgium.
- /14/ M.A. Bohn, F. Volk  
„*Aging Behavior of Propellants Investigated by Heat Generation, Stabilizer Consumption, and Molar Mass Degradation*“, Propell. Expl. Pyrot. 17, 171 (1992).
- /15/ S. Roginsky  
„*Über die Zersetzung von Sprengstoffen bei niedrigen Temperaturen*“, Physikal. Zeitschrift der Sowjetunion 1, 640 (1932).
- /16/ G.B. Manelis, Y.I. Rubtsov, L.B. Smimov, F.I. Dubovitskii  
„*Kinetics of the Thermal Decomposition of Pyroxilin*“, Kinetika i Katalis (Kinetics and Catalysis) 3, 42 (1962).
- /17/ N. Eisenreich, A. Pfeil  
„*Non-linear Least-Squares Fit of Non-Isothermal Thermoanalytical Curves. Reinvestigation of the Kinetics of the Autocatalytic Decomposition of Nitrated Cellulose*“, Thermochim. Acta 61, 13 (1983).
- /18/ M.A. Bohn, F. Volk, O. Brauer  
„*Bestimmung der sicheren Lagerzeit einer plastifizierten Nitrocellulose*“, Paper 62, Proceed. 25th Internat. Annual Conference of ICT, 1994, Karlsruhe, Fraunhofer-Institut für Chemische Technologie, (ICT).
- /19/ M.A. Bohn, F. Volk, O. Brauer  
„*Determining the Safe Lifetime of a Plasticized Nitrocellulose*“, in J.J. Mewis, H.J. Pasman, E.E. De Rademaeker (editors), Proceed. 8th Internat. Symp. on Loss Prevention and Safety Promotion in the Process Industries', June 6-9, 1995, Antwerp, Belgium, Vol. II, p. 483-494, Elsevier, Amsterdam, New York, 1995.
- /20/ F. Volk, M.A. Bohn  
„*Ageing Behaviour of Propellants Determined by Mass Loss, Heat Generation, Stabilizer Consumption and Molar Mass Decrease*“, Paper 20 on the 87th Symp. of the Propulsion and Energetics Panel (PEP) of the AGARD, 'Service Life of Solid Propellant Systems', May 6-10, 1996, Athens, Greece. AGARD-CP-586, May 1997.
- /21/ M.A. Bohn  
„*Bestimmung der Lebensdauer mit Massenverlustmessungen*“  
ICT-Bericht 13/94, März 1995, für BMVg, Bonn.
- /22/ M.A. Bohn, J. Böhnlein-Mauß, K. Menke  
„*Lifetime Assessment and Stability of AN/GAP Propellants*“, Paper 9 on the 87th Symp. of the Propulsion and Energetics Panel (PEP) of the AGARD, 'Service Life of Solid Propellant Systems', May 6-10, 1996, Athens, Greece. AGARD-CP-586, May 1997.



## 20 MM GUN PROPELLANT SAFETY SERVICE LIFE STUDY USING MICROCALORIMETRY/HPLC CORRELATION DIAGRAM

Anton Chin and Daniel S. Ellison  
Test & Evaluation Department  
Ordnance Engineering Directorate  
Crane Division, Naval Surface Warfare Center  
Crane, Indiana 47522-5001 USA

### ABSTRACT

In review of the world's gun propellant evaluation history for the last 75 years, it seems there has been a tremendous amount of frustration. The studies of fuming process of many type of propellants indicated that the time-to-fume test is simply a pass or fail test with no quantifiable content. The NATO test method has improved the capability of future life prediction by combining the HPLC analysis of the stabilizer levels before and after accelerating aging test. However, the complexity of the solid state kinetics used HPLC data alone may make it very difficult to derive a rate law truly representing the thermal safety and degradation process of the propellant.

Since 1988, NSWC Crane Division has been involving in developing a method which can determine the safety storage life of various energetic compositions. The method simplifies the interpretation of the data, and provide more realistic results for the prediction of thermal safety of the gun propellants. The method is Microcalorimetry. When used with HPLC, the combined HPLC/Microcalorimetry Correlation Diagram can provide a very accurate time frame for the remaining safety storage life of the gun propellants.

### I. INTRODUCTION AND BACKGROUND

Gun propellant contains nitrate esters (nitrocellulose, nitroglycerin, or both). Nitrate esters are unstable. During the course of storage, it slowly and spontaneously releases nitrogen oxides (a red color fume). Stabilizer is added to the propellant at the time of manufacturing to serve as a "trap" for the oxides. Without the stabilizer, or the stabilizer is consumed, the liberated nitrogen oxides can catalyze the decomposition of the original nitrate esters. This reaction is exothermic and can eventually lead to autocatalysis (self-ignition) of the gun propellant. Propellants are subjected to test throughout their life time to assure that they remain in a stable condition safe for storage and handling.

In review of the world's gun propellant evaluation history for the last 75 years, it seems there is nothing but a lot of frustration [1]. The studies of fuming process of many types of propellants indicated that the test is simply a pass or fail test with no quantifiable content [2]. Review the cause of one typical incident occurred in 1976, it was found that the red fume produced in the test could fade in a few days. At some time after the red fume fading, many of the samples would self-ignite. Therefore the time-to-fume test is clearly not an accurate and safe predictive test method.

Today the degradation process is understood greatly by routinely using HPLC (High Performance Liquid Chromatography) analysis to quantify the effective stabilizer contents remained in the propellant. The HPLC data is useful for assessment of the current stability condition, however, it does not predict the future safe storage life of the propellant.

The NATO test method has improved the capability of future shelf life prediction by combining the HPLC analysis of the stabilizer levels before and after accelerated aging test (65.5°C for 90 or 120 days). The NATO test method is based on a kinetic model established by the observed rate of stabilizer depletion. However, the complexity of the solid state kinetics may make it very difficult to derive a rate law truly representing the propellant degradation process.

Since 1988, NSWC Crane Division has been involving in developing a method which can determine the safe storage life of various energetic compositions with less complexity [3]. The method simplifies the calculation and provide more realistic results for the prediction. The method is Microcalorimetry. When use with HPLC, the combined HPLC/Microcalorimetry Correlation Diagram can provide very accurate time frame of the remaining shelf life of the energetic materials.

## **II. EXPERIMENTAL**

### **1. Samples:**

20 mm Semi-Armor Piecing High Explosive Incendiary (SAPHEI) cartridges were selected for safety, aging trend and shelf life tests. The cartridge contains typical double base gun propellant (i.e. WC-867). The selection was based on the year of product.

### **2. Instrumentation:**

DSC Analysis - For quick identification of adverse thermal behavior of the propellant, and provide guidelines for setting up the microcalorimetric test parameters.. TA Model 2100 DSC/DTA system was used.

Microcalorimetric Analysis: Three ThermoMetric Model 2277 Thermal Activity Monitor (TAM) and two Hart Model 4225 microcalorimeters were used in the analysis. The TAM model equipped with 4 ampoule calorimeters of differential type with a sample and a reference heat detector for effective suppression of thermal noise. The baseline stability over 8 hours at 25°C is within the  $\pm 0.05 \mu\text{W}$  in static mode, and  $\pm 0.5 \mu\text{W}$  in liquid flow mode. The sample container

capacity is between 4 to 25 ml. The TAM was used to perform the tests at 80, 75, 65.5, and 50 °C. Lower temperature test ( i.e. 45 °C) required larger sample quantity (> 30 grams) of samples to produce the heat flows within the detectability of the instrument. In this case, the Hart microcalorimeter with a larger sample cell (50 ml) was used to carry out the test.

HPLC Analysis - Waters Model 150C ALC/GPC system equipped with photo diode array variable wavelength detector was used. The objective of the HPLC is to support the microcalorimetry in the determination of degradation trend of the stabilizers. The rate of depletion and remaining effective stabilizers in the propellant can be determined.

### 3. Experimental Approaches:

Maximum sample size were used to maximize the detectability of the microcalorimeter. The sample was loaded in a way similar to the loading pattern of the actual propellant cartridge so the most realistic results can be obtained. Preconditioning of the samples at elevated temperatures must be performed inside the microcalorimeter so the early heat flow pattern can be recorded and studied. In most of the cases, important chemical kinetics are always taking place at the early stage of reaction at above 70 °C.

To begin with the frame work of the master HPLC/Microcalorimetry template, samples from lots of different aging levels would have to be initiated first. The microcalorimetric analyses were performed at the pre-selected temperatures. During the heating period, samples were periodically taken for stabilizer depletion analysis by HPLC. A HPLC chromatogram, in terms of percentage of stabilizers (DPA and daughter products) versus time was established and plotted against the heat flow curve of microcalorimetric analysis. The HPLC/Microcalorimetry correlation diagram will be used to determine the exact aging status and safe storage life in relation with stabilizer depletion and the time to thermal runaway (or the time to the MAHF - Maximum Allowable Heat Flow).

## III. RESULTS AND DISCUSSIONS

Microcalorimetric analysis and Arrhenius plot of the 1993 sample tested at 80, 75, 65.5 50 and 45°C are presented in Figure 1 and Figure 2. The propellant yields almost perfect straight line between 75 to 45°C temperature range. The linearity is extremely important, it means that the reaction mechanisms stays the same through out the entire test temperature ranges. It also means that the rate data obtained from the accelerating test at higher temperature (i.e. 75°C) can be used to calculate the rate of degradation of the propellant at ambient temperature with good accuracy. Figures 3 and 4 show the results of microcalorimetric analysis of 1992 and 1985 samples lots . The corresponding Arrhenius plots are shown in Figures 5 and 6, respectively. Due to the time limitation. The 1992 and 1985 lots were analyzed only at 3 temperatures (80, 75 and 65.5°C). However, based on the data from the 1993 lot, the linearity should be good also for the 1992 and 1985 lots from 80 to 25°C. A change in the slope of the Arrhenius plot has been

reported at below 60°C [4] [5]. This indicates that the different reaction mechanisms (i.e. rate of degradation) may be observed below 60°C for the same propellant. If this is the case, the temperature of the accelerating aging test should not be exceeding 60°C.

The HPLC analysis of the stabilizer depletion have also been carried out. The correlation diagram of the real time microcalorimetry and HPLC of WC-867 propellant has been established. The data shows that the thermal hazard indicator MAHF (Maximum Allowable Heat Flow) stays low through out the entire simulated accelerating aging test period. This result clearly indicates, even after all the parent DPA is consumed, the remaining daughter (effective) stabilizers will continue to protect the propellant from possible self-ignition for a long period of time. Figure 7 shows a typical example (1993 lot at 75°C) of the relationship between real time microcalorimetric heat flow data and HPLC stabilizer depletion data. Please note that even after the parent stabilizer (DPA) is totally depleted, the propellant is still protected by the remaining effective (daughter) stabilizers.

#### **IV. ESTIMATED SAFE STORAGE LIFE BASED ON THE MICROCALORIMETRY AND HPLC CORRELATION DIAGRAM**

The following table lists the current stabilizer levels, activation energies and estimated safe storage lives of the 1992 and 1993 propellant lots calculated from the correlation diagram. Data from 1985 lot is also included for reference purpose.

Lot #	Stabilizer (DPA) Content (%)	Activation Energy (Kcal/Mole)	Estimated Safe Storage Life (Yr)			
			25°C	35°C	45°C	50°C
1993	0.6169	29.948	67.8	13.2	3.02	1.27
1992	0.5721	31.730	66.9	11.7	2.31	1.08
1985	0.4402	30.262	40.4	7.70	1.63	0.78

#### **V. CONCLUSIONS**

1. Microcalorimetry/HPLC correlation diagram represents the true thermal behavior of the entire aging processes.
2. The correlation diagram shows that the remaining effective stabilizers will continue to protect the propellant from possible thermal hazards long after the parent DPA is completely depleted.

3. The tests report only the worst case scenario to provide extra zone for safety.

## VI. REFERENCES

1. T. Lindblom, P. E. Lagerkvist, L. G. Svensson, "Comparison and Evaluation of Modern Analytical Methods Used for Stability Testing of a Single Base Propellant", 7<sup>th</sup> Symp. On Chemical Problems Connected with the Stability of Explosives, Sweden, p-247 (1985).
2. Gail Stine, Susan Franklin and Joe Salama, "The Study of Stabilizer Content of Fumed heat test propellant". Naval Ordnance Station, Indian Head, MD. (1989).
3. A. Chin and D. S. Ellison, "The Applicability of Microcalorimetry as an Effective Surveillance technique for Stored Munitions", ADPA Symposium on Energetic Materials Technology, Orlando, Florida, p-399 (1994).
4. F. Volk and M. A. Bohn, "Ageing Behavior of Propellants by measuring Heat Generation, Stabilizer Consumption and Molar Mass Degradation", ADPA Symposium on Compatibility and Processes, Virginia Beach, Virginia. P-335 (1989).
5. L. G. Svensson, L. E. Paulson and T. Lindblom, "A Microcalorimetric Study of Temperature and Stabilizer Effects on the Heat Generation in Gun Propellants", 4<sup>th</sup> Gun Propellant Conference, Mulwala, Australia. (1990).

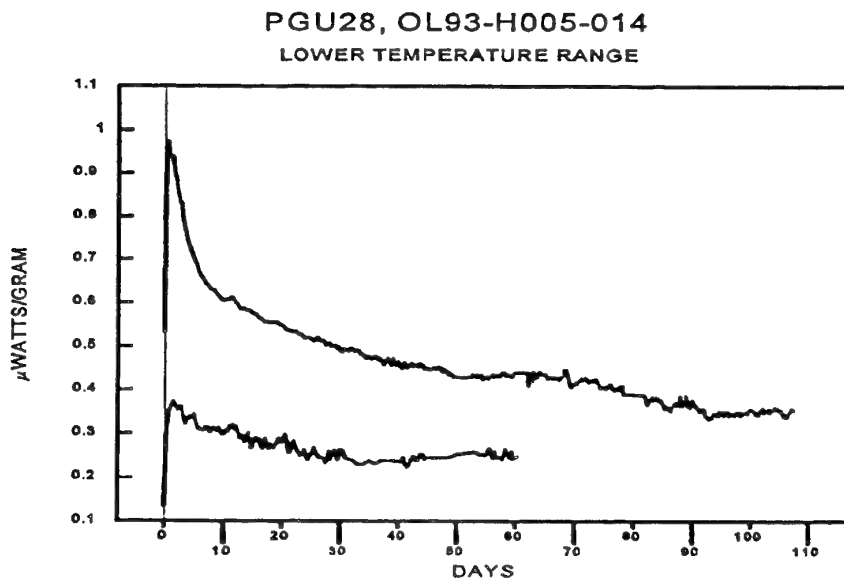
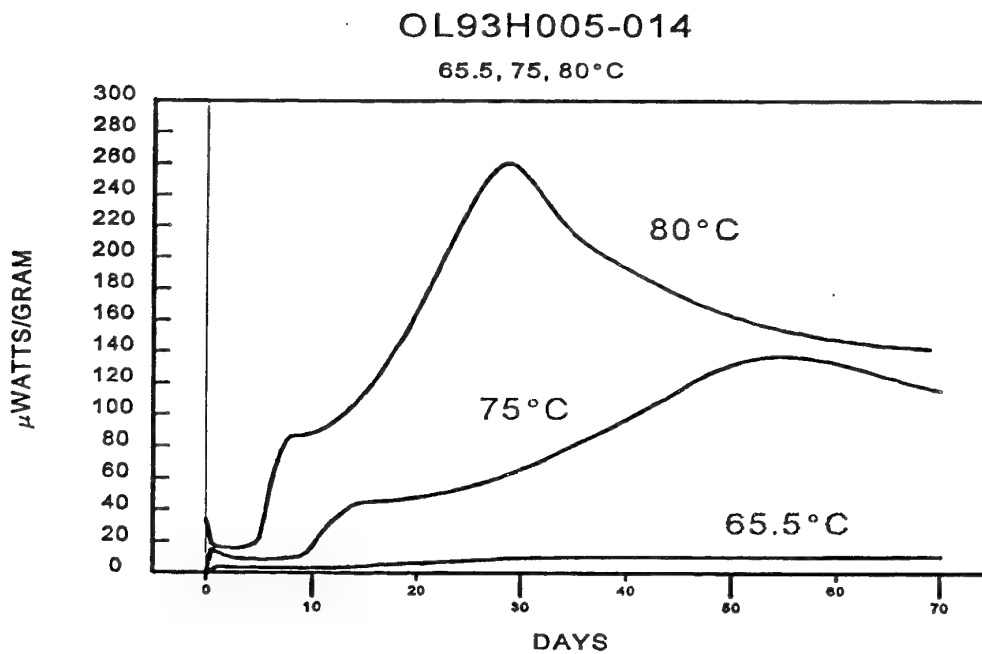


Figure 1. Heat flow curve of the microcalorimetric analysis of WC 867 propellant, Lot OL93H005-14, at 45, 50, 65.5, 75, and 80°C.

PGU28/B PROPELLANT  
ARRHENIUS PLOT  
OL93H005-014

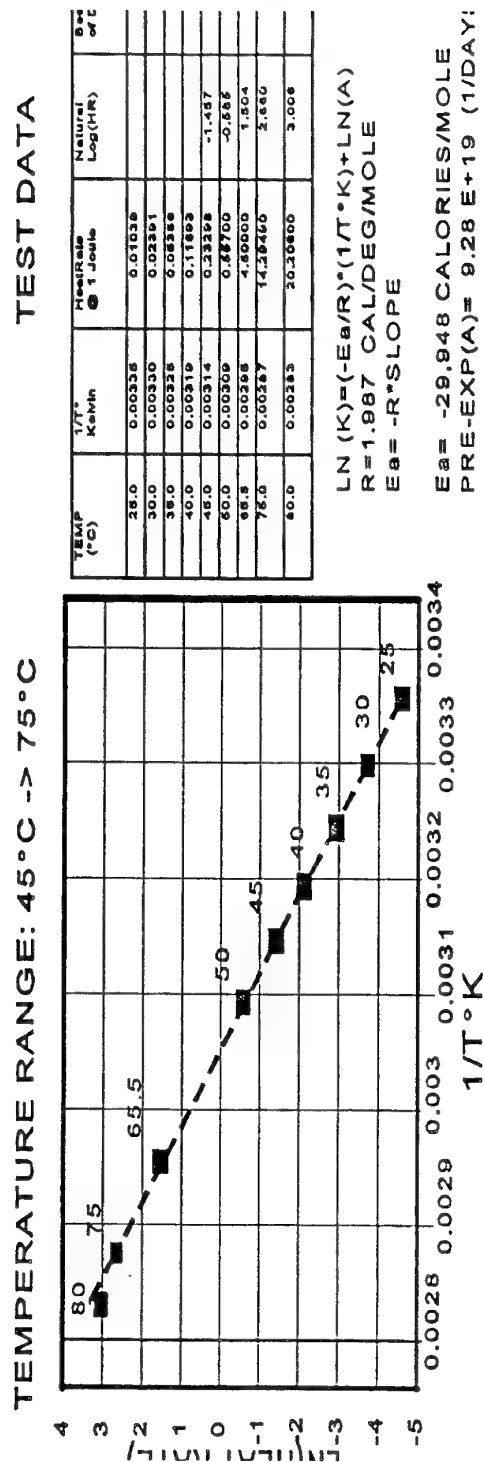


Figure 2. Arrhenius Plot of WC867 propellant, Lot OL93H005-014

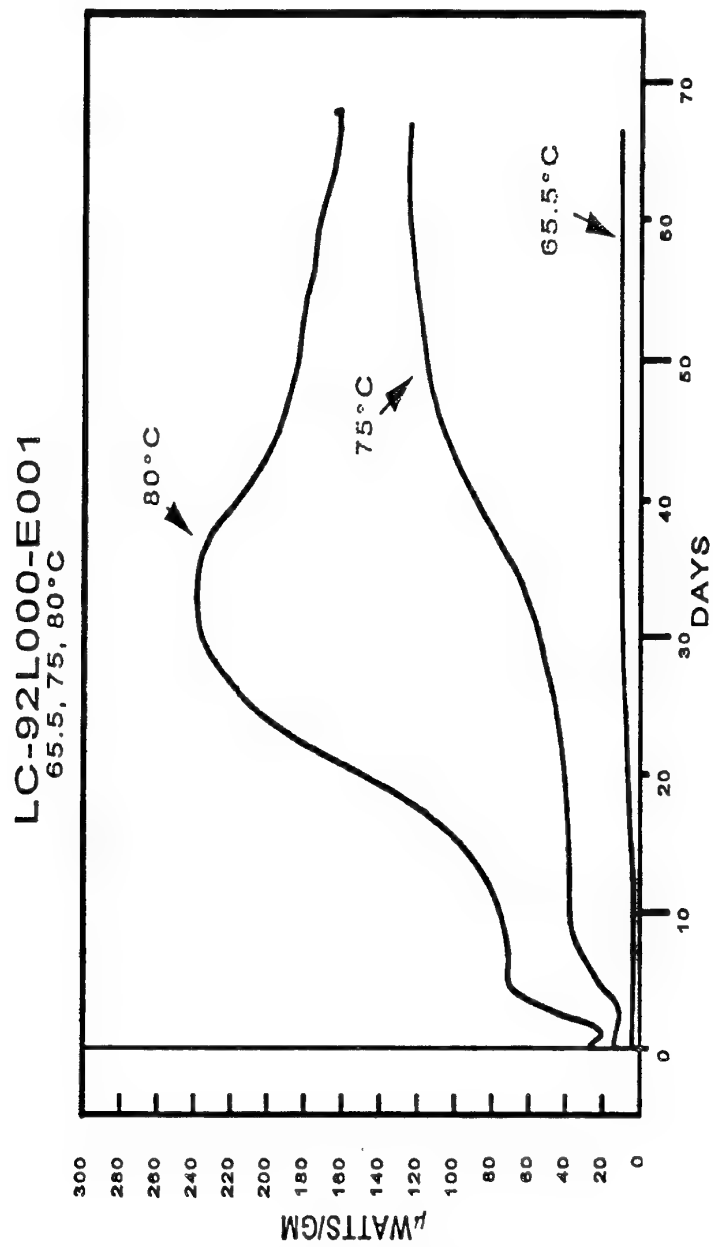


Figure 3. Heat flow curves of the microcalorimetric analysis of WC867 propellant, Lot LC-92L000-E001, at 65.5, 75, and 80°C.



PGU28/B PROPELLANT  
ARRHENIUS PLOT  
LC-92L000-E001

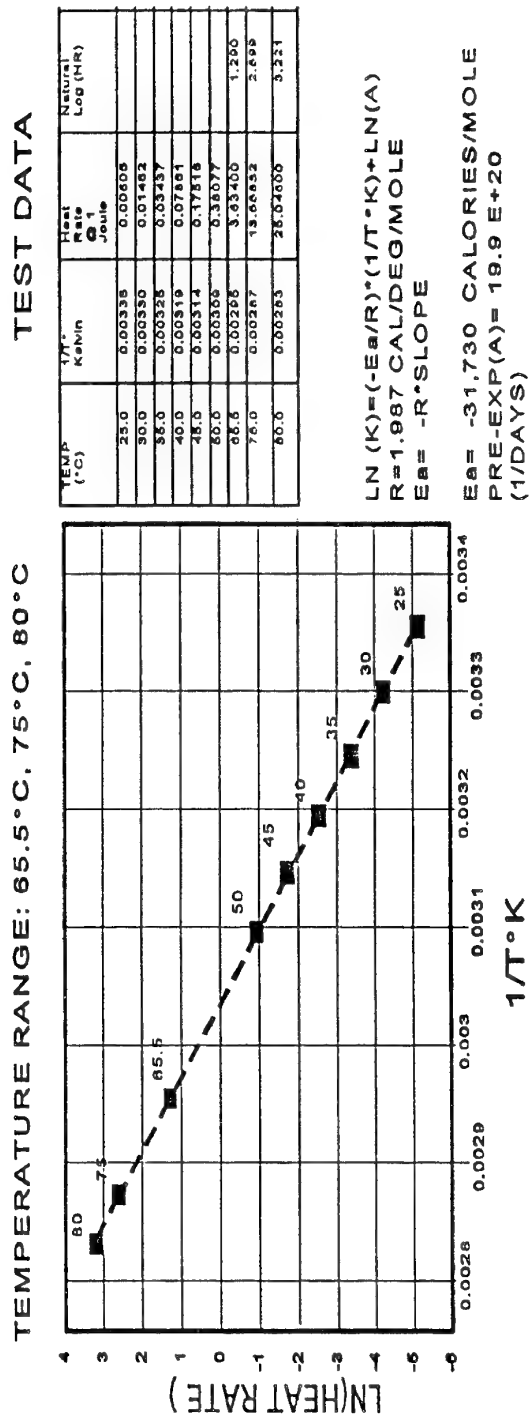


Figure 4. Arrhenius plot of WC867 propellant, Lot LC-92L000-E011

OL-85G001-007  
65.5, 75, 80°C

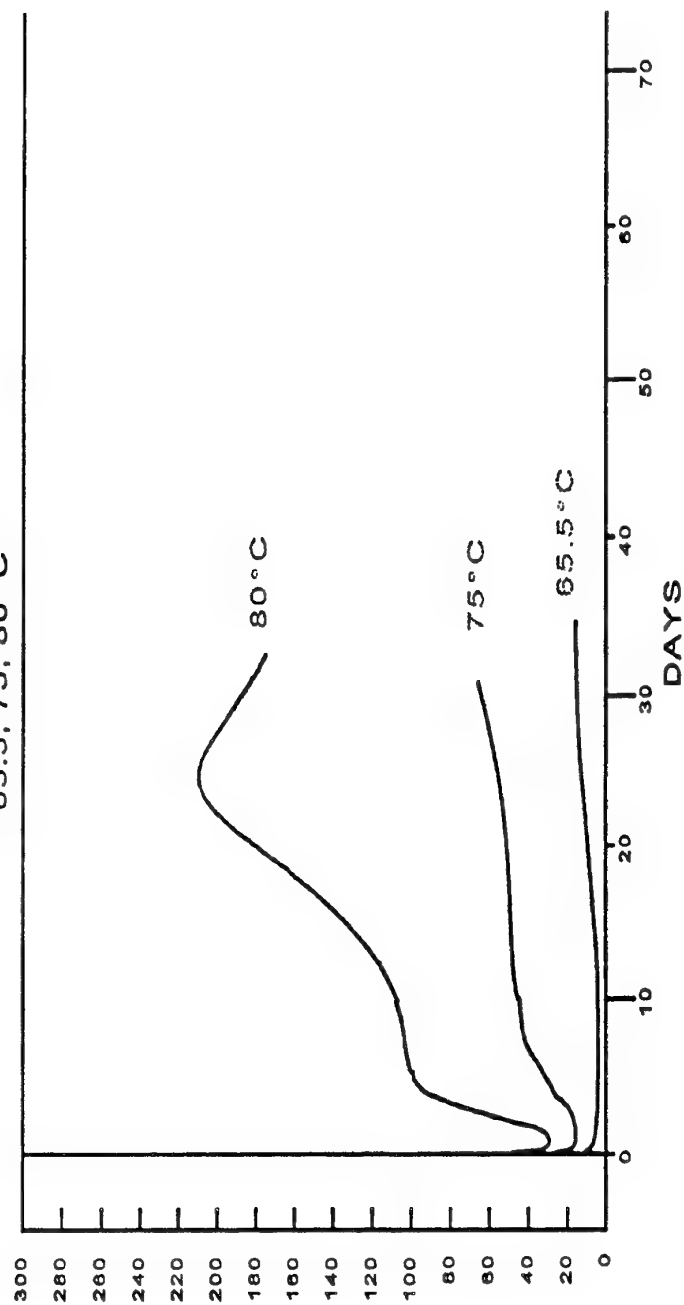


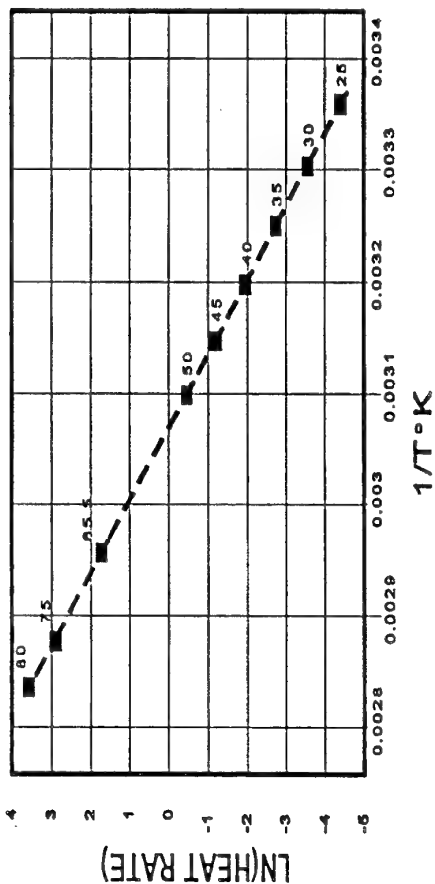
Figure 5. Heat flow curves of the microcalorimetric analysis of WC867 propellant, Lot OL85G001-007, at 65.5, 75, and 80°C

PGU28/B PROPELLANT  
ARRHENIUS PLOT  
OL85G001-007

TEMPERATURE RANGE: 65.5°C, 75°C, 80°C

TEST DATA

TEMP (°C)	1/T° Kelvin	Heat Rate Q 1 Joule	Natural Log(HR)
26.0	0.00338	0.01144	
30.0	0.00330	0.02858	
35.0	0.00325	0.08001	
40.0	0.00319	0.13210	
45.0	0.00314	0.28368	
50.0	0.00309	0.59486	
65.5	0.00288	5.21000	1.651
75.0	0.00287	18.8612	2.828
80.0	0.00283	39.4415	3.510



$$\begin{aligned} \text{LN (K)} &= (-E_a/R) \cdot (1/T^\circ\text{K}) + \text{LN(A)} \\ R &= 1.987 \text{ CAL/DEG/MOLE} \\ E_a &= -R \cdot \text{SLOPE} \end{aligned}$$

$$\begin{aligned} E_a &= -30,262 \text{ CALORIES/MOLE} \\ \text{PRE-EXP(A)} &= 17.4 \text{ E+19 (1/DAYS)} \end{aligned}$$

Figure 6. Arrhenius plot of WC867 propellant, Lot OL85G001-007

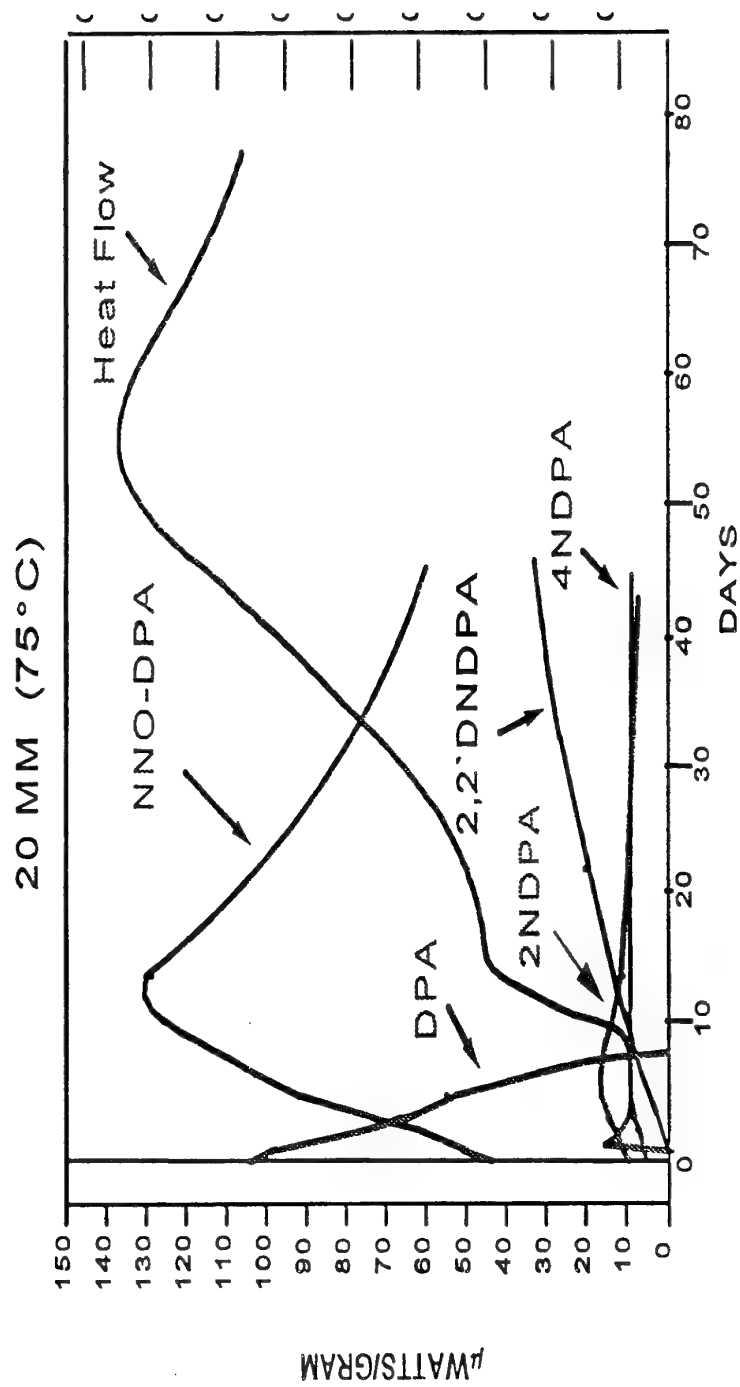


Figure 7. Example of HPLC/Microcal Correlation diagram of WC867 propellant

# AN ASSESSMENT OF THE STABILITY OF NITRATE ESTER BASED PROPELLANTS USING HEAT FLOW CALORIMETRY.

by

R.G. Jeffrey<sup>1</sup>, M. McParland<sup>1</sup>, M. Elliot<sup>1</sup>, D.J. Wood<sup>1</sup>, P. Barnes<sup>2</sup> and N. Turner<sup>2</sup>

1. DERA Bishopton, Station Road, Bishopton, Renfrewshire, PA7 5NJ, UK
2. CESO (N), Block B, Ensleigh, Bath, BA1 5AB, UK

## Abstract

DERA Bishopton has for many years assessed the stability of nitrate ester based propellants on behalf of UK service users. The techniques employed in these assessments have generally been the traditional heat test methods, measurement of stabiliser depletion and multi-temperature trials.

As an adjunct to this work an initial evaluation has been carried out on the potential for using micro-heat flow calorimetry to support the in-life surveillance programmes for Naval propellant stores. Kinetic parameters derived from the heat flow measurement of propellants artificially aged for different times and temperatures were compared with similar data from stabiliser consumption studies.

It was found that the heat output was strongly dependant on the micro-environment of the propellant and that, for use in assessment of ageing characteristics, careful control of the sample environment is required. Analysis of the kinetic data suggests that, as a result, care must be taken when comparing results for propellant stability to similar determinations obtained using stabiliser consumption rate.

Long term ageing of propellants at 80°C in the calorimeter has allowed the variation in heat outputs to be directly related to the formation of the stabiliser degradation products of diphenylamine and 2-nitrodiphenylamine stabilised propellant.

In addition, the results of a recent study comparing the time at which auto-catalytic decomposition occurs in the Silver Vessel Test and an exponential increase in heat flow for a F527/327 propellant, is also reported.

## Introduction

DERA Bishopton has for many years carried out the assessment on the safe shelf-life of nitrate ester based propellants for both UK Army and Navy ordnance stores. Nitrate ester propellants decompose with time (Figure 1) and at elevated temperatures reaction rates increase. Unless the material is properly stabilised premature ignition can occur.

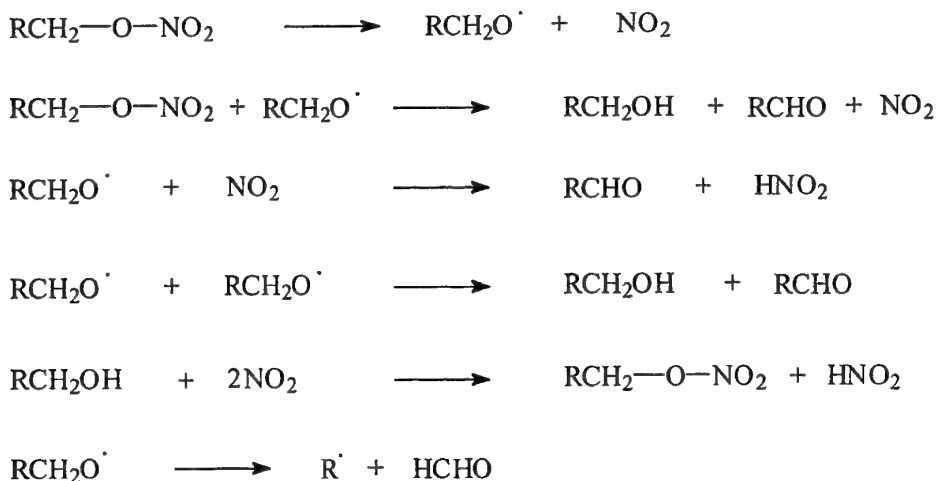


**Figure 1 - Breakdown of Nitrate Ester based Propellants.**

All propellant compositions in UK service or storage have to undergo periodic inspection and assessment to ensure that they have a safe shelf life.

Both DLSA and CESO (CINO) select samples from their stock records and submit them to DERA for analysis. This assessment programme is dependent on the type of store, its age and the storage conditions. From the results of the analysis a safe shelf life is then assigned to each store from a defined sentencing criteria.

## Methods of Analysis

The assessment of propellant stability can be carried out by a number of chemical techniques, see Table 1.

The measurement of gas evolution from the propellant is often the simplest method of assessing stability. Such techniques are quick and give a reasonable indication of the propellants stability.

A second stage assessment is the measurement of the stabiliser concentration to determine the "residual effective stabiliser" level in the propellant. This gives a better indication as to the degree of decomposition taking place, since in general loss of stabiliser and the amount of stabiliser degradation products is directly related to the stability of the propellant.

**TABLE 1 - THERMAL STABILITY TESTS**

TEST	METHOD	TEMPERATURE	TIME
Abel Heat Test	Time for evolved NO <sub>x</sub> to produce line on starch-iodide paper.	60°C to 82.2°C	30 mins
Methyl Violet Test	Time for evolved NO <sub>x</sub> to change methyl violet paper from violet to pink.	134.5°C single 120°C double	40 mins
B & J Test	Quantitative Test of acidity of evolved gases reported as ml of NaOH.	132°C single 120°C double	5 hours 3 hours
Dutch Test	Weight loss due to evolution of decomposition gases.	110°C single 105°C double	8 hours 64 hours
Woolwich Test	Consumption of DPA in single-base propellants	80°C	21 days
Silver Vessel Test	Time taken for self-heating to result in a temperature rise of 2°C	80°C	3 months
NATO Test	Determination of stabiliser consumption after artificial ageing.	65.5°C	60 or 120 days
Multi-Temperature Ageing	Determination of stabiliser consumption after artificial ageing over a range of temperatures	50-80°C	Up to 2 years

Stabiliser levels in propellants are measured by solvent extraction and subsequent analysis by HPLC or GLC. The concentration of stabiliser is then compared to the nominal values at manufacture which allows a shelf life of up to 5 years to be assigned.

To assign a longer safe shelf-life, accelerated ageing techniques such as the NATO Stanag 4117 test are used. In this test samples are heated at 65.5°C for 60 and 120 days and the difference in residual stabiliser levels before and after ageing used to assign a shelf life of up to 10 years. This test is also important where the propellant may have experienced non standard storage conditions or where the initial composition of the propellant is not known. The test is based on the assumption that an acceleration factor, i.e. the number of times the rate of reaction increases, for propellant degradation is 3 per 10°C increase in temperature. Experience shows that although this acceleration factor may be a good approximation for some propellants, it does not hold for all, especially the more recent high energy compositions.

DERA Bishopton have in recent years determined the actual acceleration factors for a number of propellant compositions on behalf of CESO. The acceleration factor is determined by multi-temperature ageing of the propellant for a varying time period.

Using the data obtained in this manner and assuming 1st Order Kinetics, the rate constant for the stabiliser consumption at each temperature can be calculated (1) and using the Arrhenius equation (2), the acceleration factor (3) can be found.

Assuming first order kinetics, the rate constant (k) is determined by,

$$t = 1/k \ln ([A_0]/[A_t]) \quad 1$$

t = time of ageing

[A<sub>0</sub>] = as received level of stabiliser

[A<sub>t</sub>] = concentration of stabiliser at time t

The gradient of the line is equal to (1/k).

Activation energy is the gradient of the line Ea/R.

$$\ln k = \ln A - \frac{E_a}{RT} \quad 2$$

where Ea = activation energy (J mole<sup>-1</sup>)

A = frequency factor

R = gas constant (8.3143 JK<sup>-1</sup> mole<sup>-1</sup>)

T = temperature (K)

$$R^{[(T_2 - T_1)/10]} = t_{1/2(1)}/t_{1/2(2)} \quad 3$$

Where R = Acceleration Factor

T<sub>2</sub> = 65.5°C

T<sub>1</sub> = 32°C

t<sub>1/2(1)</sub> = stabiliser half life at 32°C

t<sub>1/2(2)</sub> = stabiliser half life at 65.5°C



One test that warrants a special mention is the Silver Vessel Test (80°C Self Heating Test). In this test ~ 70-80g of propellant is heated at 80°C until the propellant begins to self heat (2°C temperature rise) or brown fumes are observed on visual inspection of the sample. This test is usually carried out on new propellant formulations, but is a specification requirement for many materials. It is often viewed as the final arbiter for propellant stability, but due to its severity, has in the past resulted in propellant ignition and destruction of test facilities.

Both DERA Bishopton and DERA Fort Halstead have over the years been funded by CINO to investigate propellant stability and to assess new techniques in an attempt to obtain better and more meaningful measures of propellant stability.

Heat Flow Calorimetry is one technique that over the last 10 years has been assessed by DERA and is increasingly throughout the world, being used as a tool to determine propellant stability.

### **Heat Flow Calorimetry**

The experimental apparatus initially used at DERA Bishopton was based on equipment developed at PERME Waltham Abbey. These heat flow calorimeters were based on an original design from the National Defence Research Organisation RVO-TNO in the Netherlands. In the early 1980's a number of propellant formulations were assessed using this equipment, but problems due to the sensitivity and interference from the environment resulted in investment by Bishopton in a new system.

In 1992 DERA Bishopton purchased a two channel Thermal Activity Monitor (TAM) system from ThermoMetric Ltd and a Bomic software package developed by Bofors, Sweden. This system was expanded to a four channel instrument by purchase of a twin ampoule calorimetric unit and amplifiers in 1993, thus giving the capability of comparing four samples at the one time.

### **Initial Studies**

Based on the experience of other users, a standard procedure was developed for conditioning the propellant samples prior to testing.

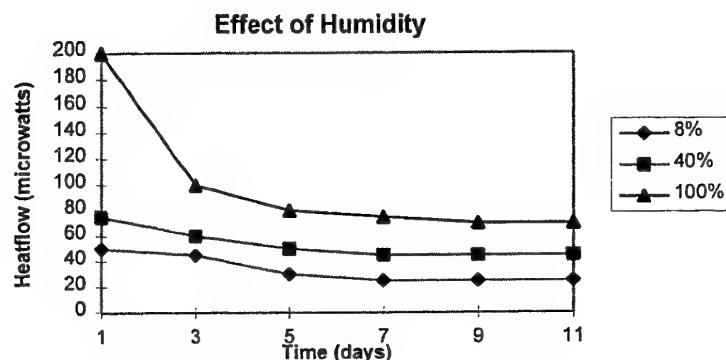
Initial studies at 50°C to 70°C were carried out, but these produced low heat flow values and the time scale for experiments was long, thus 80°C was chosen as the initial test temperature as it gave significant heat outputs in a short time scale.

As part of the initial study two propellant samples which were known to have wide differences in stability test results were examined. One sample had a low Abel Heat test result while the other gave a high test result. Both gave

identical levels of stabiliser and had undergone ageing trials. Heat Flow measurements confirmed as expected, that the sample with the low Abel Heat test gave the higher heat output and hence was the least stable.

### The Effect of Humidity on Heat Flow Measurements

This experiment was carried out without the use of a "flow through cell", hence it was only possible to control the humidity in the sample vial and the propellant at the start of the experiment. Ground propellant samples were conditioned in desiccators at 20°C and at humidities of 8%, 40% and 100% for three days. After conditioning the vials were sealed and placed in an oven at 80°C for two hours, then transferred to the calorimeter. Although the actual humidity within the vial and sample during the test is unknown the differing humidities still allow determination of the effect of moisture content on the heat flow profiles.

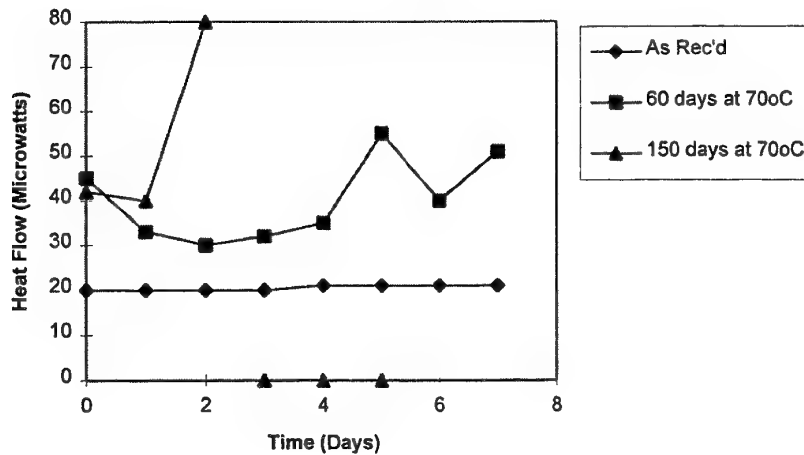


It is well known that the water content of a propellant has a significant influence on the degradation of nitrate esters and on the reaction of breakdown products, including the subsequent reaction with the stabiliser. From the heat flow outputs it can be clearly seen that the higher the moisture content in the vials, the higher the heat flow. This experiment indicates that sample conditioning is critical and must be carefully controlled to ensure that all calculations involving heat output are independent of moisture effects.

### Heat Flow Profiles of Naval Propellants

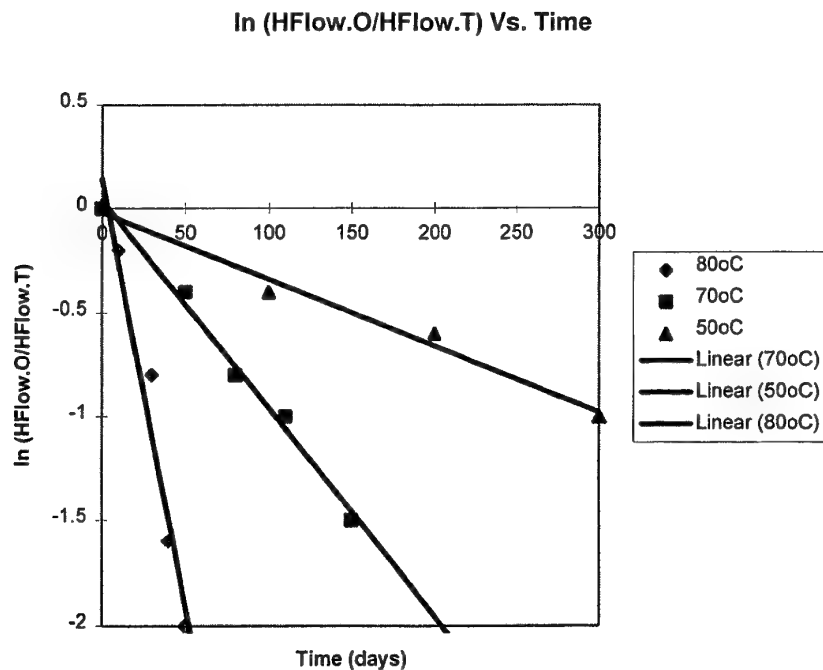
It was agreed with CINO that a database would be established on the thermal activity of Naval propellants from previous stabiliser consumption trials conducted recently at DERA Bishopton. Propellant samples artificially aged over a range of temperatures for different time intervals and containing varying stabiliser levels were tested by HFC.

### Heat Outputs of Aged Propellant



The samples were first conditioned at 80°C for 2 hours and then inserted into the calorimeter. The heat flow profiles indicate that the propellant in the "as received" condition was fairly stable with no major change in the heat output after a week. The sample with ~50% of the original stabiliser (60 days at 70°C) clearly shows that a reaction is occurring between 4 and 5 days, possibly relating to depletion of the remaining stabiliser. The sample containing no stabiliser (150 days at 70°C) after an initial period of steady heat flow, produced an exponential increase in the output after 2 days demonstrating a major change in its heat flow profile. This trend was found to be true in all the propellants tested indicating a relationship between HFC and stabiliser levels within the propellant matrix.

To allow data to be collected in a reasonable time scale samples from recent stabiliser consumption trials were studied. All samples were conditioned at 50% relative humidity at 20°C prior to test. All propellant samples were examined in their "as received" condition and after ageing at three temperatures (50, 70 and 80°C) for various time intervals. When the heat flow reached an equilibrium the values were recorded. The plot shows a typical output obtained for an NQ/S (triplebase) propellant.



As can be seen there is a strong relationship with the heat output, as expected, increasing with decreasing stabiliser levels. This relationship was found for all the samples studied suggesting that heat output is directly related to the stabiliser level. The data was used to calculate the activation energy using the Arrhenius equation as per the stabiliser consumption trial method substituting heat flow values in place of stabiliser levels.

#### ACTIVATION ENERGY RESULTS

PROPELLANT	STAB. CONS. KJ mol <sup>-1</sup>	HEAT FLOW KJ mol <sup>-1</sup>
NRN	142	141
MECHANITE	143	120
MNLF/2P	150	159
MNL	161	142
NQ/S	177	137

**ACCELERATION FACTORS per 10°C TEMPERATURE RISE**

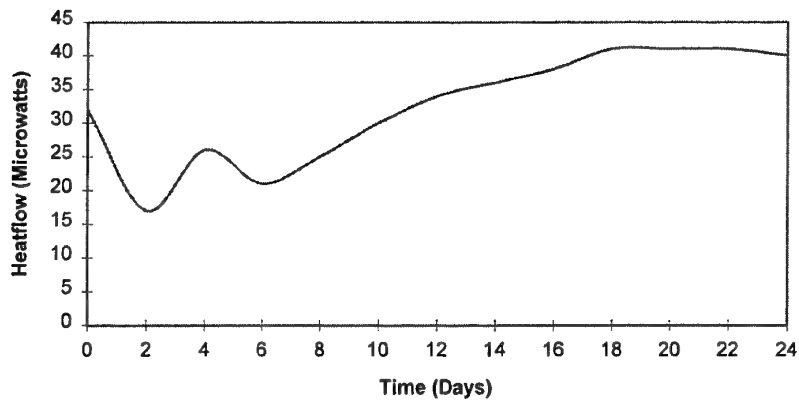
PROPELLANT	STAB. CONS.	HEAT FLOW
NRN	5.2	5.2
MECHANITE	5.3	4.0
MNLF/2P	5.7	6.4
MNL	6.5	5.2
NQ/S	7.9	4.9

The results for both kinetics by stabiliser depletion and heat output flow show a similar pattern, and agree well for some propellant compositions. The differences that do occur, indicate the importance of clearly defining and controlling the experimental conditions of the Calorimetry test.

**The study of HFC Profiles and Stabiliser Reactions**

Propellant samples were aged at 80°C in the HFC for various time intervals and were then analysed to determine the levels of stabiliser and stabiliser degradation products. This showed that in certain cases it was possible to relate variation in heat outputs directly to the reactions of the stabilisers and the production of the stabiliser degradation products. An example of this is the heat output increase between 2 to 6 days that appears to be due to the formation of N-nitroso-diphenylamine during the degradation of DPA.

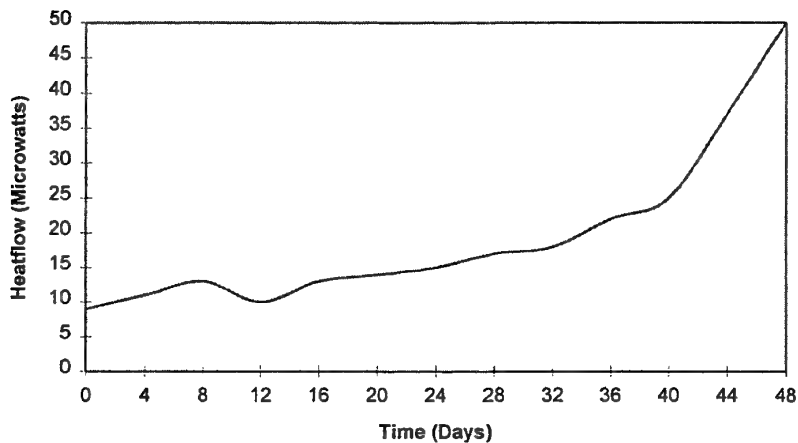
### Heat Flow Profile of DPA Stabilised Propellant.



### HFC Experiments to the Onset of Auto-catalytic Decomposition

A portion of the Silver Vessel Standard propellant was aged in the HFC until the onset of exponential heat output. The results agreed well with similar results for time to auto-catalytic decomposition obtained using the Silver Vessel test and indicate the HFC may be a suitable technique to predict the onset of auto-catalytic decomposition and potentially replace the Silver Vessel test for routine use.

### Silver Vessel Std Propellant at 80oC on HFC



## **Conclusion and Recommendations.**

The results reported in this work show that Heat Flow Calorimetry is potentially a powerful additional tool for the characterisation of the propellant ageing process. It has been shown that the results obtained from Heat Flow Calorimetry of propellants are highly dependant on the micro-environment within the sample during test. Where species, such as moisture are present that are consumed in the ageing reaction, this has a major impact on the result of the test. This confirms the findings of other workers who have shown the criticality of controlling both moisture and oxygen content during the ageing of explosives. It therefore appears that although Heat Flow Calorimetry has significant scope for use in the characterisation of the propellant ageing process it must be used with great care and it is recommended that at this stage it is used to compliment the information already received from the established stability methods. Future work is clearly required and should concentrate on establishing a data base of heat flow characteristics for a wide range of propellant types collected under carefully controlled conditions. The use of controlled environmental conditions during the test should also be explored as, in general, propellant can not be assumed to be hermetically sealed within its service container and in many cases will have unlimited access to ambient atmosphere during storage. Access to ambient atmospheric conditions during ageing will from the data obtained to date result in a higher heat flow and therefore data collected at lower moisture and oxygen content, such as during a sealed experiment, may give an overly optimistic view on the propellant stability.

It is recommended that further work be carried out to extend the database of information on propellant ageing from heat flow measurements and that this work includes further comparison with stabiliser depletion measurements. Work should also be extended to include a detailed study of the importance of the micro-environment surrounding the ageing propellant by use of controlled environment Heat Flow Calorimetry.

## 8. REFERENCES

- 1 Letter Brett, ST64, CINO dated 29th January 1993, ref D/ST64B/229/9/4
- 2 STANAG 4147 Annex D ( DERAft )  
Chemical Compatibility of Explosives and Propellants.
- 3 Def Stan 05-51/1 Annex C, dated 24th February 1978  
Available stabiliser limits of propellants.
- 4 STANAG 4117 Annex D ( DERAft ) 3rd Edition  
Limits of acceptance
- 5 Stabiliser consumption trials on various propellant stores, Part 1.  
C McPherson, Unpublished DERA Report.
- 6 Stabiliser consumption trials on various CINO propellant stores,  
Part 2. C McPherson, Unpublished DERA Report.
- 7 The design of a measurement and processing system for a  
propellant micro heat flow calorimeter.  
P Clarke, Unpublished DERA Report.
- 8 Technical specification for ThermoMetric Thermal Activity  
Monitor.
- 9 DERA Bishopton Operating Procedure No. 2 - Microcalorimetry  
Document No. BN0005, June 1993.
- 10 New Microcalorimetric Approaches in Shelf Life Technology.  
A. Chin and D.S. Ellison, Crane Division, NSWC Crane, Indiana,  
USA.



# THE INFLUENCE OF ENVIRONMENTAL FACTORS ON THE LIFETIME OF GUN PROPELLANTS INVESTIGATED WITH HEAT FLOW CALORIMETRY

B.J. van der Meer, W.P.C. de Klerk  
TNO Prins Maurits Laboratory  
P.O. Box 45, 2280 AA Rijswijk

## Introduction

For years the surveillance of gun propellants in the Netherlands is focused on the assessment of heat evolution, measured at 85 °C during a week in a heat flow calorimeter (HFC) of the van Geel type<sup>1</sup>. Based on a conservative value of the activation energy of 100 kJ/mole, the result allows for the determination of a safe storage period of about 8 years, at 30 °C, if the dimensions of the stored item are smaller than the critical dimensions under the given circumstances. After this period, the heat evolution should be determined again to assess if the propellant is thermally stable for another period.

However, since recently it was felt that the safe storage period should be extended to longer period, especially for the newly procured propellants. Using munition items for a more extended period or in military activities through out the world where the environmental load under the circumstances encountered by the munition items is more severe than in the well conditioned storage bunkers in many countries, requires insight into the thermal stability for a longer period. The maximum period of 50 years is considered to be sufficiently long.

To determine this longer period for safe storage, several factors, like reaction kinetics, temperature, moisture, relative humidity and gasses, need to be investigated before the extended life time could be estimated fairly accurately.

However the safe storage is not the only factor that determines the usefulness of propellants. The ballistic performance is just as important and, in fact, experimental results suggest that this life time is for some propellants a more limiting factor than thermal stability. To have some insight into the decrease of ballistic performance, the mass decrease during HFC measurement is determined as well.

Finally, the HFC results of propellants having been in store in the magazines of TNO-PML are compared with the identical propellants that has been subjected for a part of their life to the climatological conditions in Cambodia.

## Standard assessment of shelf life

The standard surveillance method is based on the calculation of the critical diameter<sup>2</sup> of the propellant. This diameter is the maximum dimension assuring a stationary heat production, conduction and transfer to the environment, without the occurrence of propellant ignition. A parameter needed to determine this dimension is the maximum heat evolution that will be developed during storage in the future period, in our case derived from the heat evolution at 85 °C.

---

<sup>1</sup> J.L.C. van Geel, Self ignition hazard of nitrate ester propellant, thesis, 1969

<sup>2</sup> J.L.C. van Geel, Ind. and Eng. Chemistry, vol 58, no. 1, 1966

Basically, to calculate the covered period at, let's say 25 °C, the acceleration factor should be known. Assuming an Arrhenius type, one step rate determining degradation of the propellant the acceleration factor is determined by the activation energy of that . In the past, the activation energy of several gun propellants have been determined, and it was shown that this energy was not only fairly constant to be about  $140 \pm 15$  kJ/mole for the conventional nitrate ester based propellants, but also for propellant conversions that occur during the period of the experiment of one week at 85 °C. To have a safety margin, the nominal value to calculate the critical diameter for safe storage has been fixed at 100 kJ/mole for all conventional propellants. Using this value for the activation energy, the covered period by a week at 85 °C is about 15 years at 25 °C. This is a very conservative shelf life and it is no surprise that many propellants have been repeatedly subjected to the one week at 85 °C period. If the 140 kJ/mole is used, it can be easily shown that the covered period at 25 °C is more than 200 years!

The maximum observed heat production is used to calculate the critical diameter based on the theory of Frank-Kamenetski<sup>3</sup>. This critical diameter does not only depend on the heat production, but also on the heat conduction coefficient and the mass density of the propellant.

Extending the maximum safe shelf life at 25 °C to 50 years, the activation energy needs to be constant for conversion of the propellant over 5 weeks at 85 °C in stead of over one week. The first aim was to investigate this. Secondly, as the new period at 25 °C is much longer than 10 years, environmental factors that may influence the heat evolution should be included as well and lifetime assessment should be performed under those realistic conditions. As the environmental factors throughout the world differ greatly and the storage conditions are not always well-defined, a start was made to investigate the influence of oxygen and of higher relative humidity on the heat production.

## **Extended lifetime of 50 years**

The advantage of HFC is that one don't need to be concerned with the complex degradation kinetics of some stabilisers. As long as the produced heat remains within the limits determined by the critical dimensions of the stored system, this system can be considered as thermally stable.

Though the shelf life for gun propellants is rarely determined for periods longer than about 10 years, it is known that the life time of many propellants is quite often much longer than that. This has been observed for both accelerated aged gun propellants as well as for naturally aged propellants that were in the inventory for more than 50 years. For example, a propellant stored for half a year at 85 °C didn't show thermal runaway. Using the standard activation energy of 100 kJ/mole, the acceleration factor amounts to be 866 at 25 °C covering a period of more than 400 years! An example of a propellant produced in 1916 which is still stable for week at 85 °C is shown below. These data give evidence that the shelf lifetime can be much longer than 10 years and that the assessment of a safe storage time of 50 year at 25 °C can be achieved for properly produced, good quality propellants.

To investigate if the activation energy is constant for the ongoing propellant decomposition over at least 5 weeks at 85 °C, the theory for analysing the non-constant heat production as

---

<sup>3</sup> P.C. Bowes, "Self-heating: evaluating and controlling the hazards", Elsevier, 1984

described in [1] is applied. In figure 1 the heat production of the double base propellant KBPH 6916 is shown at three different temperatures in a log-log plot. It is clear from this figure that during 2000 hours at 75 °C no thermal runaway was observed, though the maximum heat production is slowly increasing after 200 hours to about 200 uW/g. To calculate the activation energy, the points of intersection of a straight line having a slope of -1 with the

#### KB 6916 (DB)

100 hr in IST at 75 C = 68 year at 25 C

65 C = 15 year at 25 C

55 C = 3 year at 25 C

Ea = 150 kJ/mol

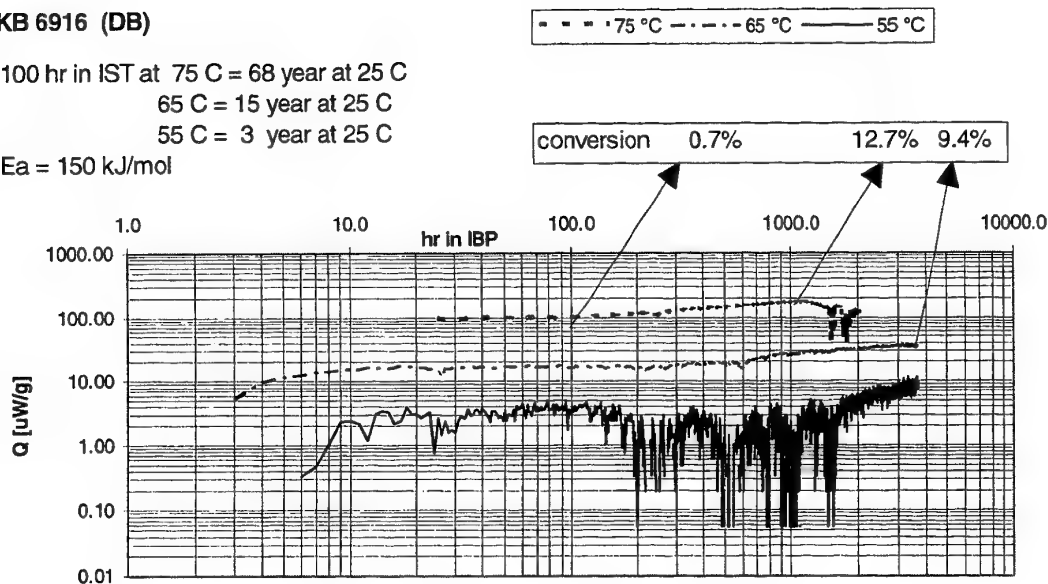


**Figure 1. Heat production of propellant KBPH 6916 at several temperatures**

time-axis and the heat production curves are used. These are points of equal propellant conversion at the indicated temperatures, according to [1]. The activation energy can be calculated if these heat productions are plotted against the reciprocal temperature  $1/T$ . The slope of the obtained straight line gives the activation energy. This analysis can be performed for any straight line, with slope -1, through the heat production curves as a function of residence time in the HFC, and therefore as a function of conversion. The activation energy as a function of conversion is shown in figure 2.

A fairly constant value of about 170 kJ/mole could be calculated from this figure. However, taking a safety margin account and using 150 kJ/mole for the activation energy, 100 hours at 75 °C correlates with 68 years at 25 °C. The extended residence time in the HFC for several hundreds of hours and the large value for the activation energy allows for the conclusion that this propellant can be safely stored for 50 years at conditions that are standard in many European storage bunkers.

The percentages shown in figure 1 indicate the amount of energy liberated in the microcalorimeter at 75 °C relative to the calorific value of the propellant as determined in a bomb calorimeter. It is clear that a significant portion of the energy as a result of decomposition is produced between 100 and 1000 hours at 75 °C. Usually, for a good ballistic behaviour the decrease in energy of the propellant is allowed to be less than a few percent. This means that the ballistic lifetime ends at about 200 hours at 75 °C, while the

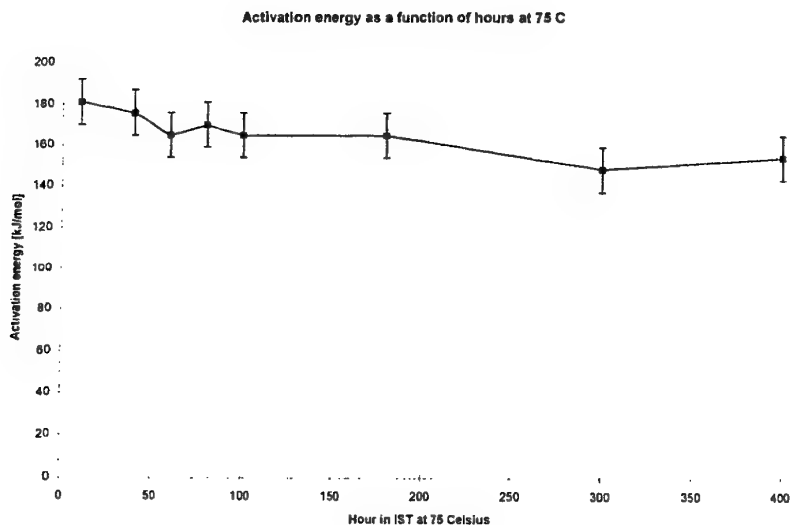


Figure 2. The activation energy as a function of conversion of the propellant

propellant is still thermally stable. Unfortunately, the mass decrease during this experiment is not known and a correlation between heat production and mass decrease could not be made.

It should be pointed out here that the heat production is indicated per unit mass. If the decomposed mass fraction is a significant fraction of the total mass, a correction to the heat production should be made. The curve of the heat production between 100 and 1000 hours at 75 °C is then somewhat steeper than the curve shown in figure 1.

100 hr in IBP at 95 C = 25 year at 25 C  
 85 C = 10 year at 25 C  
 75 C = 4 year at 25 C  
 65 C = 1.5 year at 25 C

$E_a = 100 \text{ kJ/mol}$

KB 6856 (SB)

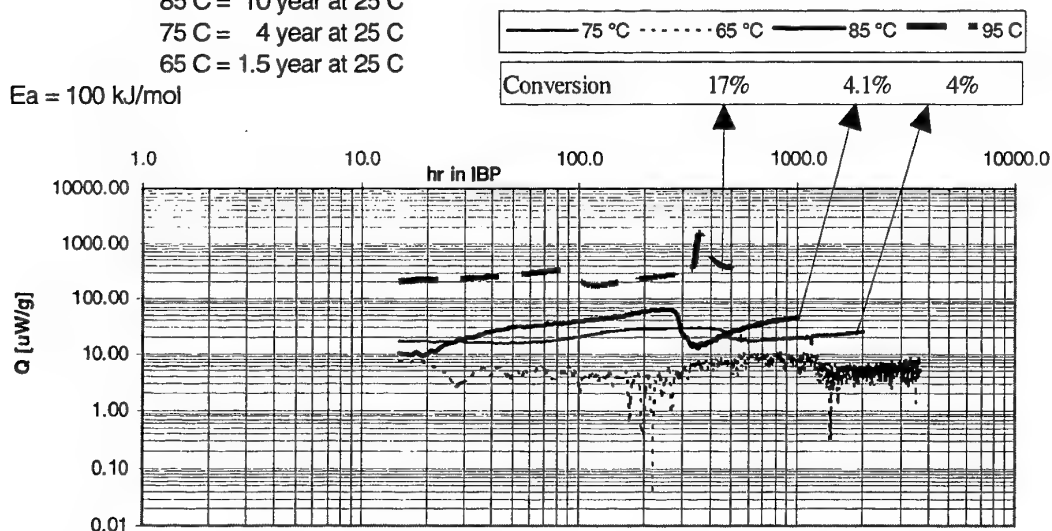
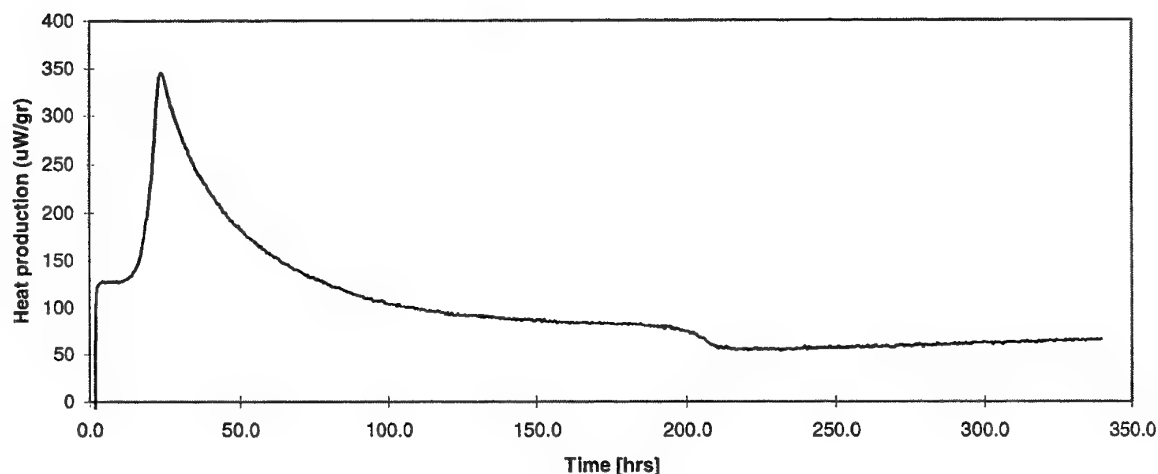


Figure 3. Heat production of propellant KBPH 6856 at several temperatures

A second example is shown in figure 3 for the single base propellant KBPH 6856. Though the heat evolution was measured during more than 1000 hours at 85 °C, again no runaway reaction was observed, but the reaction kinetics turn out to be more complex than in the first example. The heat evolution of the propellant at 75 °C Celsius crosses the heat evolution at 85 C temperatures. The heat production at 65 °C is rather low relative to the sensitivity HFC, but the shape of the measured heat production is similar to the one at 75 °C if a line with slope -1 is drawn.

As a final example, a propellant produced in 1916 has been subjected to storage at 85 °C for more than 300 hours, a period in which there was no thermal runaway observed. This means that the propellant is at least thermally stable for another 20 years adding up to the 80 years to a total safe storage life time of about 100 years. However, temporarily, the heat production is relatively large and therefore the critical diameter is small during that period of time. Though the propellant is stable for a longer period, the propellant is facing its final life time if the critical dimensions is smaller than the dimensions of the stored item and a thermal runaway can be expected.



**Figure 4. Heat production of a propellant produced in 1916**

An example of a propellant for which the end of its lifetime has been observed is shown in figure 5. After 500 hours at 85 °C a clear runaway reaction is observed. This limits its safe storage time to about 30 year maximum at 25 °C. To assess the end of the lifetime of a propellant, especially if the munition is still in the inventory, a more accurate assessment of the end of the propellants life time is needed. An example of how to investigate has been published<sup>4</sup>.

<sup>4</sup> C. Boyers, W.G. Gough, Analytical Chemistry vol. 27, no. 6, 1955

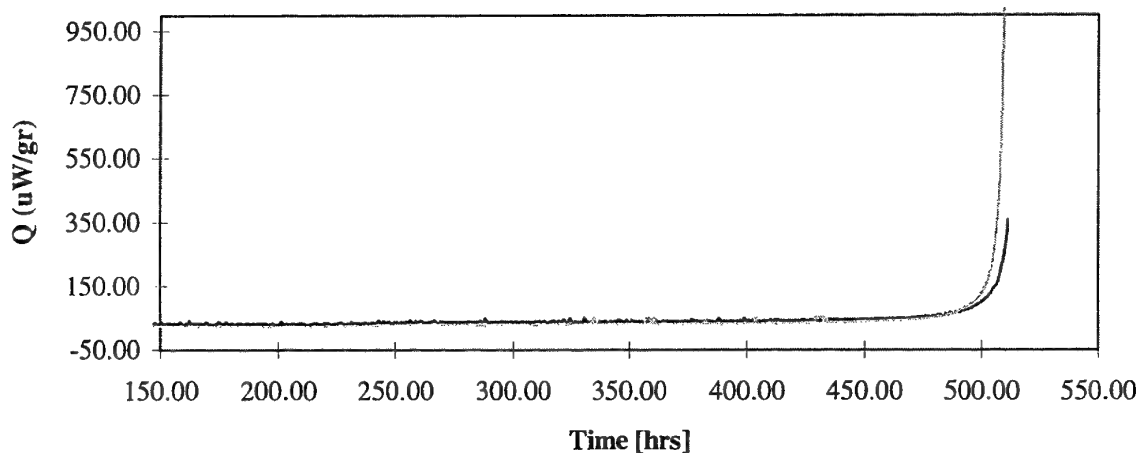


**Figure 5. Heat production of propellant KBPH 6981 facing the end of its thermally stable lifetime.**

### **Influence of moisture**

The relative humidity of the atmosphere over the sample is of influence on the heat production of the gun propellants. In general, the higher the relative humidity the larger the heat production. This holds for single, double base and rocket propellants. Also the moisture content of the propellant is expected to be of influence to the heat production. An example of the higher heat production at higher relative humidity is shown in figure 6.

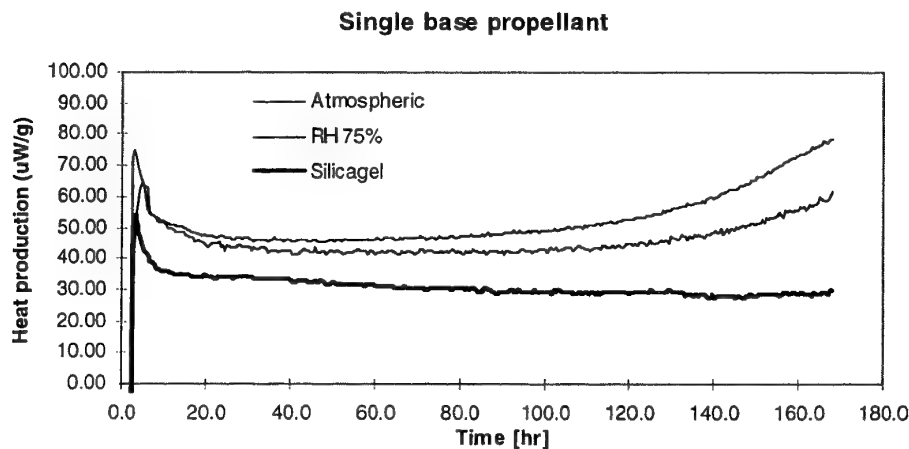


**Figure 6. Heat production as a function of relative humidity**

## Oxygen and nitrogen

The presence of oxygen is reported to increase the heat production of the propellant as NO can be oxidised to NO<sub>2</sub> which catalysis the decomposition of the propellant. In figure 7 the heat production of propellant 6981 is shown under atmospheric conditions and under 1 atmosphere of nitrogen.

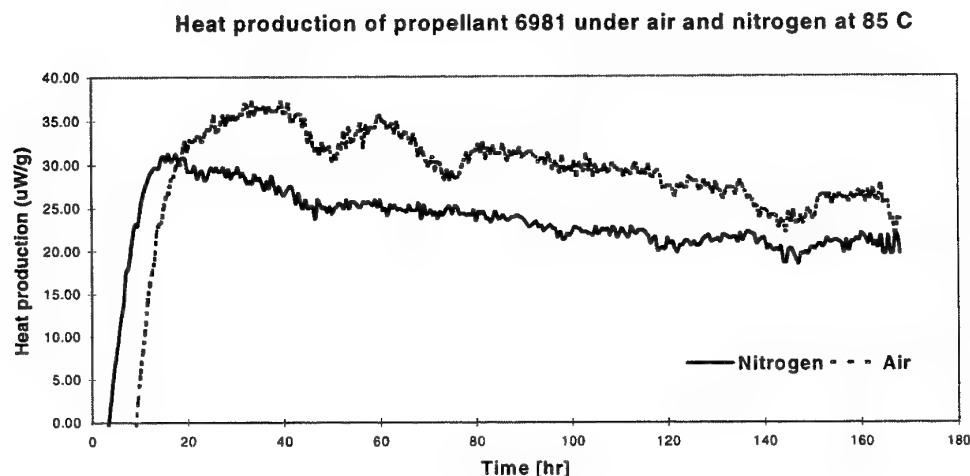


**Figure 7. Heat production of propellant 6981 at 85 °C under atmospheric conditions and under 1 atmosphere of nitrogen**

If the larger heat production is due to a higher decomposition rate or due to site reactions is not known. The propellant is stabilised by ethyl centralite (EC). Analysing the stabiliser content after ageing, a small difference is observed for ageing under 1 atmosphere of air and nitrogen. The primary stabiliser content for ageing under nitrogen was slightly larger than for ageing under air (0.177 mass% and 0.147 mass%, respectively). The content of 2-NEC was identical, and 4-NEC has decreased slightly more under air than under nitrogen.

## Analysis of Cambodia gun propellants

Several gun propellants has been in Cambodia from May 1992 till October 1993 (15 months) as shown in table 1. After being returned to and stored in the Netherlands the propellants arrived in March 1996 at TNO-PML. The propellants were of relatively young age as can be concluded from the production date. All propellants were of ball powder type. The fraction of their lifetime the propellants has been stored in Cambodia is indicated as well and ranged from 7% to 16 %. The circumstances the propellants were stored or used in Cambodia were unknown. Based on the encountered environmental conditions in Cambodia, the propellants were analysed on their water content, heat production, and stabiliser content. Focusing on the heat production as measured in the HFC at 85 °C, no significant difference was observed between the Cambodia propellants and the reference propellants that has been in store in the TNO-PML, except for one propellant. An example

of two propellants that showed the same heat production curve (in shape and in level) is given in figure 8 for propellant KBPH 6971 and 7222.

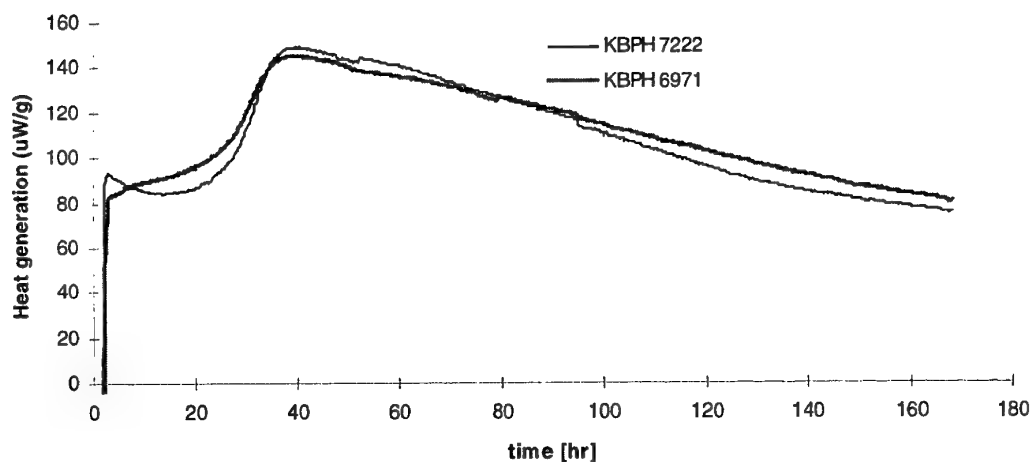


**Figure 8. Comparison of the heat production for a propellant that has been stored in Cambodia (KBPH 7222) and the reference propellant (KBPH 6971)**

The KBPH 6238 and 7219 show a slightly different heat production as can be seen in figure 9.

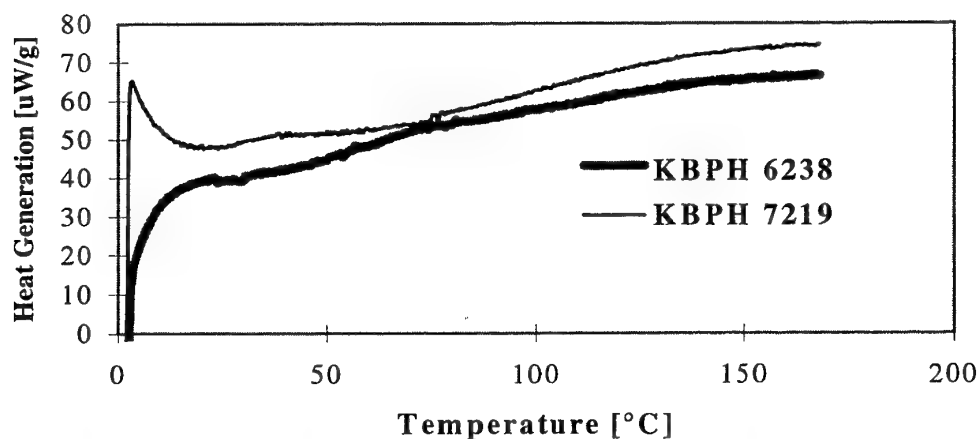


**Figure 9. Comparison of the heat production for a propellant that has been stored in Cambodia (KBPH 7219) and the reference propellant (KBPH 6238)**

For the latter propellant the primary and the secondary stabiliser content was assessed to see if the supposed accelerated ageing of the Cambodia propellants resulted in a difference in the stabiliser content relative to reference propellant. However, the primary and the



secondary stabiliser content were almost identical, indicating that the decomposition process was in the same phase for both propellants.

**Table 1: Data of investigated propellants.**

Reference propellant	MM/YY of production	Cambodia propellant	Fraction of life time in Cambodia
6238	10/1978	7219	7%
6510	??/1982*	7220	9%
6843	07/1986	7221	12%
6971	06/1988	7222	15%
6996	05/1989	7223	17%
7091	12/1989	7224	18%
7103	03/1989	7225	16%

\* No propellant data sheet

It was concluded that the storage conditions in Cambodia has been almost identical to those in the storage bunker at TNO-PML, which is a non-conditioned storage building showing a temperature fluctuation over the year of about 20 °C.

## Conclusion

It has been shown that the shelf for safe storage of good quality propellants can be extended to 50 years. To assess if this is possible for individual propellants, the activation should be determined under a high relative humidity and excess of oxygen. The activation energy for decomposition should be known for temperatures lower than 60 °C as well as higher than 60 °C as it is well known that the decomposition pathways change at that temperature while storage under practical circumstances can occur in both temperature regimes.

# **Microcalorimetric Determination of the Cure Reaction in Some Fluorinated Polyether Rubbers**

**P F Bunyan and A V Cunliffe**

**Defence Research Agency, Fort Halstead, Sevenoaks, Kent, TN14 7BP (UK).**

## **INTRODUCTION**

When mixed, hydroxyl and isocyanate end group functionalised fluorinated polyether prepolymers react together to give a crosslinked polyurethane rubber. An understanding of the kinetics of this curing reaction is desirable to allow the selection of suitable storage and processing conditions during manufacture of filled rubbers.

Differential scanning calorimetry has been used to describe the kinetics of the cure reaction in extensively crosslinked systems such as epoxy and polyester resins by monitoring the heat generated during bond formation at elevated temperatures [1,2]. However, these fluorinated urethane rubbers are relatively lightly crosslinked systems with a correspondingly smaller enthalpy of reaction. The maximum processing temperature that could be employed for the manufacture of filled rubbers was limited to around 80°C by the need to use a water jacket for reactor temperature control. DSC was found to be insufficiently sensitive to record the low levels of heat generated at these temperatures particularly during the later stages of the reaction.

Polyurethane cure reaction kinetics have also been studied by wet chemical analysis methods. For example, Yee and Adicoff [3] have described the cure of polybutadiene rubbers by aging several samples of mixed precursor over a range of temperatures with periodic removal and analysis. The reaction in each subsample was quenched by lowering the temperature, unreacted isocyanate was then extracted with a suitable solvent, reacted with an amine and finally excess amine was determined by titration. The number of separate stages involved makes the procedure labour intensive, time consuming and therefore costly. The poor solubility of fluorinated polymers in all common laboratory solvents would create additional problems if this procedure was applied to fluorinated rubbers.

The use of a more sensitive calorimetric method and its application to quantify the effect of various treatments on the cure rate of this type of rubber, are described here.

## **EQUIPMENT AND MATERIALS**

A Thermometric type 2277 Thermal Activity Monitor [TAM] was used to monitor the cure reaction by recording the associated heat generation. Rubber precursor samples were sealed prior to analysis in 3cm<sup>3</sup> glass ampoules.

Four polymers were used for this work. Each possessed a similar fluorinated, linear, random copolyether backbone, but were terminated with different functional groups.

Polymer A was nominally difunctional and terminated with isocyanate groups.

Polymer B was nominally difunctional and terminated with primary hydroxyl groups, adjacent to the fluorinated polymer backbone.

Polymer C was nominally difunctional and also terminated with hydroxy groups. Unlike polymer B, the end groups are separated from the fluorinated main chain by the insertion of short ethoxy blocks.

Polymer D was nominally tetrafunctional and terminated at each end with one primary and one secondary hydroxy group. Like polymer C the functional groups are isolated from the fluorinated main chain by the insertion of short ethoxy blocks.

The same batch of each material was used for all experimental work.

The temperature of the freezer employed for extended storage trial was monitored remotely using a Tinytalk-temp miniature data logger.

Gel times were measured with a Brookfield rotating spindle viscometer.

## EXPERIMENTAL AND RESULTS

### General Experimental Procedure

Rubber precursors were prepared by mixing one or more polyols with polymer A. The proportions were chosen to give mixtures which were stoichiometrically 1:1 in NCO:OH, based on the equivalent weight values supplied by the manufacturer. In practice, blending will be required to manufacture rubbers with a range of mechanical properties. In order to model these systems, a 3 component blend, consisting of a mixture of polymer D and polymer B cured stoichiometrically with isocyanate terminated polymer A, was also studied.

The components were mixed thoroughly, using a glass rod and a  $0.75 \pm 0.25\text{g}$  aliquot transferred to a TAM sample ampoule, sealed and lowered into the equilibration region of the TAM analytical cylinder. Since the curing reaction of interest commences as soon as the components come into contact, the entire process was performed with minimum delay to reduce errors caused by failure to record the initial stages of the reaction.

After a temperature equilibration period of 5 minutes, the sample was lowered into the TAM detection region and the power output recorded continuously. Where possible, the signal was monitored until it had dropped to an undetectable level and this was assumed to represent the complete reaction. Due to time constraints, this was not possible with the less reactive mixtures at the lower end of the temperature range studied and the experiments were terminated when the majority of the reaction had occurred. In these cases the area under the "tail" was estimated by consideration of the behaviour of identical mixtures when cured at higher temperatures, with the assumption that the total heat generated during the reaction was independent of cure temperature.

During the processing and interpretation of the resulting cure curves, the assumption was made that, at any point in the reaction, the cure reaction rate was proportional to the heat generation rate ( $q$ ) and the degree of advancement of the reaction ( $\alpha$ ) was equal to the heat evolved at that time as a fraction of the total heat detected during the entire cure.

### Relative Reaction Rates of Different Polymer Mixtures

The cures of 2 component mixtures of each of the 3 polyols with Polymer A were measured at a constant temperature of  $80^\circ\text{C}$ . The superimposed cure curves are shown in Figure 1.

It can be seen that Polymer A/B cures far slower than the other two mixtures and the reaction is obviously incomplete after 3 days. The other two mixtures appear to cure much faster by comparison - both decay to very low levels in about a day, the Polymer A/C mixture being slightly faster than Polymer A/D.

The cure curve of the 3 component blend, Polymer A/D/B is shown in Figure 2.

### Effect of Extent of Cure

Order plots were constructed for each of the 4 mixtures as follows.

Assuming the reaction can be described by a "power law" dependence of rate on concentration and that at any time during the reaction, the observed heat generation rate is directly proportional to the reaction rate.

$$\text{Then } cq = \frac{-d\alpha}{dt} = k(1-\alpha)^n \quad 1$$

Where  $\alpha$  = Fraction reacted  
 $q$  = Heat generation rate  
 $n$  = Reaction order  
 $t$  = Time  
 $c, k$  = Constants

Equation 1 can be rearranged to give the equation of a straight line.

$$q = k(1-\alpha)^n \Rightarrow \ln q = \ln k(1-\alpha)^n \Rightarrow \ln q = \ln k + n \ln(1-\alpha)$$

$$\Rightarrow \ln q = \ln k + n \ln(1-\alpha) \quad 2$$

From 2 the order of the reaction will be equal to the gradient of a plot of  $\ln(q)$  against  $\ln(1-\alpha)$ .

The cure curves for each mixture, recorded at 70°C, were processed in this way. Results are summarised in table 1 and figure 3. All show an approximately second order decay behaviour which may be used to obtain "working estimates" of the time to reach any point in the reaction. However, since each plot is curved, it will not be possible to describe the variation of rate with extent of these cure reactions precisely with any simple "power law" mechanism.

**TABLE 1** Variation of Reaction Rate With Extent of Cure - Reaction Curves Recorded at 70°C

*i Polymer A/C*

Time (hours)	Rate ( $\mu\text{W.g}^{-1}$ )	$\ln(\text{Rate})$	$\alpha^B$	$1-\alpha$	$\ln(1-\alpha)$
0.25	5122.6	8.541	0.195	0.805	-0.2175
0.5	3148.3	8.054	0.336	0.664	-0.4098
1	1725.8	7.453	0.499	0.501	-0.6929
2	828.4	6.719	0.669	0.331	-1.1062
3	495.0	6.204	0.760	0.230	-1.4292
4	329.1	5.796	0.818	0.182	-1.7043
5	233.4	5.452	0.857	0.143	-1.9491
6	171.7	5.145	0.886	0.114	-2.1744

Order of reaction indicated by slope of linear regression line of data plotted in Fig. 3 = 1.70

*ii Polymer A/D*

0.25	5706.0	8.649	0.159	0.841	-0.1741
0.5	3712.5	8.219	0.291	0.709	-0.3446
1	1960.2	7.580	0.443	0.557	-0.5866
2	972.0	6.879	0.599	0.401	-0.9153
3	621.1	6.431	0.688	0.312	-1.1669
4	441.7	6.090	0.748	0.252	-1.3815
5	332.4	5.806	0.792	0.208	-1.5741
6	258.7	5.555	0.826	0.174	-1.7521

Order of reaction indicated by slope of linear regression line of data plotted in Fig. 3 = 1.96

<sup>B</sup> Where  $\alpha$  is the integral of the cure curve up to that time as a fraction of the integral of the entire reaction curve

**TABLE 1 (Continued)** Variation of Reaction Rate With Extent of Cure - Reaction Curves  
Recorded at 70°C

Time (hours)	Rate ( $\mu\text{W.g}^{-1}$ )	$\ln(\text{Rate})$	$\alpha^B$	$1-\alpha$	$\ln(1-\alpha)$
<i>iii Polymer A/B</i>					
1	575.4	6.355	0.051	0.949	-0.0523
3	397.9	5.986	0.180	0.820	-0.1984
5	294.4	5.685	0.272	0.728	-0.3174
10	180.8	5.197	0.425	0.575	-0.5534
15	132.6	4.887	0.529	0.471	-0.7529
20	105.8	4.661	0.609	0.391	-0.9390
25	80.9	4.393	0.671	0.329	-1.1117
30	64.4	4.165	0.720	0.280	-1.2730
35	53.5	3.980	0.760	0.240	-1.4271
40	44.3	3.791	0.794	0.206	-1.5799
45	37.1	3.614	0.821	0.179	-1.7204

Order of reaction indicated by slope of linear regression line of data plotted in Fig. 3 = 1.591

*iv Polymer A/D/B*

0.25	3249.3	8.086	0.100	0.900	-0.1054
0.5	2098.2	7.649	0.176	0.824	-0.1936
0.75	1545.7	7.343	0.231	0.769	-0.2626
1	1228.0	7.113	0.272	0.728	-0.3175
3	482.0	6.178	0.452	0.548	-0.6015
5	303.7	5.716	0.545	0.455	-0.7875
10	152.2	5.025	0.676	0.324	-1.1270
15	94.6	4.550	0.750	0.250	-1.3863
20	66.5	4.197	0.799	0.201	-1.6045
25	45.3	3.813	0.833	0.167	-1.7898
30	34.4	3.538	0.857	0.143	-1.9449
35	24.1	3.182	0.875	0.125	-2.0794
40	18.3	2.906	0.889	0.111	-2.1982

Order of reaction indicated by slope of linear regression line of data plotted in Fig. 3 = 2.317

<sup>B</sup> Where  $\alpha$  is the integral of the cure curve up to that time as a fraction of the integral of the entire reaction curve

Effect of Temperature

A series of isothermal cure curves were recorded on samples of each of the 4 mixtures, over the temperature range 40-80°C. The curves for the Polymer A/B mixtures are illustrated in figure 4 - curves from the other three mixtures resembled these and are not shown. In the case of a calorimetry experiment where the heat generation rate was effectively constant throughout the duration of the test (kinetically zero order), it would be possible to obtain the activation energy by applying the Arrhenius equation:

$$q = A.e^{-E/RT} \quad 3$$

Where A = Arrhenius factor  
E = Activation energy  
R = The gas constant  
T = The absolute temperature

This implies a constant value of q for constant values of E and T - a condition which is clearly not met with these cure reactions and equation 3 cannot be used. However, it has been proposed by Van Geel [4] that, if the degree of reaction (as denoted by the quantity of heat evolved up to that point, Q) is taken into account, then a modified form of the equation:

$$q = F(Q).e^{-E/RT}$$

4

Where  $F(Q)$  is a function of  $Q$ , can give a value of  $E$  which is independent of the degree of reaction.

Equation 4 may be expressed as:

$$\ln q = -\frac{E}{RT} + \ln F(Q)$$

5

and a plot of  $\ln(q)$  vs  $1/T$  should be linear, with a gradient equal to  $-E/R$ .

In practice, this requires an accumulative integration of the rate vs time plot output from the TAM. Corresponding rates of heat generation at the points of identical total heat generation can then be selected from the tabulated data from several different isothermal experiments carried out over a range of temperatures. Results are summarised in Table 2 and Figure 5.

**TABLE 2** Temperature Dependence of Reaction Rate

Temperature/ $^{\circ}\text{C}$	1/Temperature/ $\text{K}^{-1}$	Heat Generation Rate ( $\mu\text{W.g}^{-1}$ ) when $\alpha=0.5$	$\ln(\text{RATE})/(\mu\text{W.g}^{-1})$
<i>i Polymer A/C</i>			
80	0.0028316	3291	8.0989
74	0.0028806	2545	7.8418
70	0.0029142	1955	7.5781
60	0.0030016	1927	7.5637
40	0.0031933	538.5	6.2887

From plot of  $\ln$  rate vs  $1/K$  (Fig 5), activation energy =  $39.75 \text{ kJ.mol}^{-1}$

*ii Polymer A/D*

80	0.0028316	2667	7.8887
74	0.0028806	2500	7.8240
70	0.0029142	1856.5	7.5264
60	0.0030016	1662	7.4157
40	0.0031933	512.5	6.2393

From plot of  $\ln$  rate vs  $1/K$  (Fig 5), activation energy =  $38.19 \text{ kJ.mol}^{-1}$

*iii Polymer A/B*

80	0.0028316	188.2	5.2375
74	0.0028806	128.0	4.8520
70	0.0029142	151.0	5.0173
60	0.0030016	45.6	3.8199
40	0.0031933	14.45	2.6707

From plot of  $\ln$  rate vs  $1/K$  (Fig 5), activation energy =  $61.37 \text{ kJ.mol}^{-1}$

*iv Polymer A/D/B*

80	0.0028316	554.7	6.3184
74	0.0028806	438.7	6.0838
70	0.0029142	374.8	5.9264
60	0.0030016	110.0	4.7005
40	0.0031933	47.4	3.8586

From plot of  $\ln$  rate vs  $1/K$  (Fig 5), activation energy =  $60.03 \text{ kJ.mol}^{-1}$

### Storage Life of Polymer Mixtures

The temperature of a storage deep-freezer was monitored for several days and found to maintain a temperature of  $-32^{\circ}\text{C} \pm 0.5^{\circ}\text{C}$ . An estimate of the expected half-lives of each of the 4 mixtures under consideration were made, using the descriptions of temperature dependence obtained in the previous section. In the case of the less reactive mixtures (A/B and A/D/B), these times were too long to allow them to be tested by experiment conveniently and expected half-lives at  $23^{\circ}\text{C}$  were estimated instead.

Given that the reaction half-life is proportional to the reciprocal of the initial rate.

$$\text{ie } r = \frac{k}{t_{0.5}} \quad 6$$

Where  $r$  = Initial rate  
 $t_{0.5}$  = Reaction half-life  
 $k$  = A constant

Assuming the reaction obeys an Arrhenius temperature dependence law.

$$\text{Then } \ln(r) = \ln \frac{k}{t_{0.5}} = C - \frac{E}{RT} \quad 7$$

Where C is a constant

On rearrangement, a straight line relationship is obtained.

$$\ln t_{0.5} = \frac{E}{RT} - B \quad 8$$

Where B is a constant (the sum of C and  $\ln k$ )

The value of the constant B must first be determined by substitution of an experimentally determined half-life and the temperature at which it was measured into equation 8. Half-lives at any other temperature can then be estimated by applying the same equation.

Curable mixtures were prepared, sealed in TAM ampoules and transferred either to the freezer, or a  $23^{\circ}\text{C}$  water bath without delay. After the predicted half life had elapsed, each sample was moved to the TAM and its remaining cure reaction recorded at  $80^{\circ}\text{C}$  and compared with the cure curve of a similar mixture analyzed immediately after mixing. A typical pair of curves, obtained from Polymer A/B, are illustrated in figure 6.

Results are summarised in table 3. The predicted and observed attenuation show reasonable agreement in the case of the less reactive mixtures at  $23^{\circ}\text{C}$ , but the half lives predicted for Polymer A/C and A/D at  $-32^{\circ}\text{C}$  appear pessimistic. A further storage trial on these two mixtures was therefore performed in a water bath at  $8^{\circ}\text{C}$ .

**TABLE 3** Partial Cure of Mixtures During Storage

Sample Description	Storage Temp/ $^{\circ}\text{C}$	Storage time /h*	Heat Evolved During Cure Reaction ( $\text{J.g}^{-1}$ ) <i>Freshly prepared</i>	<i>After Storage</i>	% Reduction
Polymer A/B	+23	420	26.7	12.5	53.2
Polymer A/D/B	+23	109	29.14	12.37	57.5
Polymer A/C	-32	279	27.34	18.05	33.9
Polymer A/D	-32	308	33.23	26.4	20.5
Polymer A/C	+8	16.4	27.34	15.26	44.2
Polymer A/D	+8	20.2	33.23	23.6	29.0

\* Storage time calculated to result in 50% cure reaction during storage

### Equating Heat Generation with Gel Time

The time for gelation to occur in these binders is of practical significance for deciding processing pot life, but the point where this occurs is not given by the calorimetric curve alone since it is not associated with any abrupt change in heat generation. Simultaneous calorimetry and viscosity experiments have been performed on some rubber precursors to identify the point in the cure curve which equates to the gelation point. This will assist in the selection of suitable storage conditions for premixed binder precursors.

The following rubber precursors were mixed and divided into 2 subsamples.

- 1 A stoichiometric mixture of Polymer A and Polymer D.
- 2 A stoichiometric mixture of Polymer A and a blend of 1 part Polymer D and 1 part Polymer B by weight.
- 3 A stoichiometric mixture of Polymer A and a blend of Polymer D and Polymer B containing a high proportion of polymer B.

For each precursor, one subsample had its cure curve recorded in the TAM at 80°C, as described earlier. The other subsample was transferred to a glass tube, immersed in a waterbath at 80°C and its viscosity monitored continuously using a Brookfield viscometer.

The time to gelation for each was indicated at the point where a large, rapid increase in viscosity was recorded. When the calorimetric cure curve was complete, the extent of cure at the gel point could then be deduced retrospectively from the fraction of the total heat evolved up to the gelation time. Results are summarised in figure 7.

It can be seen that inclusion of the more slowly reacting Polymer B into the precursor mixture increases the gelation time progressively, as would be expected. However, the fraction of the total reaction which must occur to achieve gelation appears to be fairly constant over the range of conditions studied.

An equation which relates extent of a cure reaction to the functionality of the reactants was described by Stockmayer [5].

$$PaPb = \frac{1}{(Fe-1)(Ge-1)} \quad 9$$

Where    Pa     = Fraction of first functional group reacted  
         Pb     = Fraction of second functional group reacted  
         Fe, Ge = Functionality of each reactant

If the assumption is made that Polymer A has a functionality of exactly 2 and Polymer D has a functionality of exactly 4, then application of this equation to the first mixture (Polymer A + Polymer D) predicts the gel point to occur when 57.7% of the total cure reaction is complete. Considering that these functionalities are only approximately correct, that the two components may have experienced some degradation in storage prior to the experiment and also the contribution of various experimental errors, this predicted value is considered to agree reasonably well with the observed figure of 62%.

Equation 9 cannot be applied easily to multicomponent mixtures where the components have very different reactivities. The observation that the gel point is occurring at about the same extent of reaction in each of the experiments suggests that the nominally difunctional Polymer B component also contributes to the overall crosslinking reaction in some way at 80°C.



## DISCUSSION

The observed relative cure reaction rates of these mixtures can be accounted for by consideration of the chemical structure of their polyol end groups. The slowest reaction occurs with Polymer B. Although this prepolymer only has primary aliphatic end groups, which are expected to be more reactive than secondary ones, these are deactivated by their proximity to fluorinated units in the polymer backbone. The fastest cure is found in mixtures containing polymer C which also has primary alcohol end groups, but these have been separated from the effects of the fluorinated backbone by the insertion of short, non-fluorinated blocks. These were added during manufacture to reduce the acidity of the alcohol end groups and so facilitate its reactivity towards isocyanates. Polymer D does not show the relatively slow reaction rate of polymer B, since the hydroxy groups are also remote from the fluorinated units. However, polymer D does contain some secondary hydroxyl groups resulting in an overall slower cure rate than for mixtures containing polyol C. In principle, polyol D might have been expected to show a clear difference between the faster primary alcohol and the slower secondary alcohol reaction. However, the kinetics of these reactions are not simple, even when there is only one type of hydroxyl group present and a clear distinction between polymer D and polymer C was not apparent.

This work suggests that the time taken for a blended rubber to cure completely and attain its terminal mechanical strength etc will probably be governed by the reaction rate of its slowest reacting constituent (in the case of the 3-component mixture studied here, the reaction between polymers A and B). However, other points of practical significance, such as the point where a pre-mixed blend becomes too viscous for use in the manufacture of filled rubbers, could be reached at a time dictated by the fastest reaction (in this case the reaction between polymer A and polymer D) if this was sufficient to result in gelation by itself. The values for activation energies reported here for polyfluoroether rubbers are similar to that of  $41 \text{ kJ.mole}^{-1}$  reported by Yee and Adicoff [3] for the cure reaction of another polyurethane rubber, polybutadiene, using titration techniques. The fairly low temperature dependence of cure rate will mean that mixtures containing either of the more reactive polyols can be expected to cure extensively within a few hours when mixed at room temperature. Although this may be avoided by immediate rapid cooling, practical heat transfer considerations when processing large samples could make this difficult.

## CONCLUSIONS

A microcalorimetric method to quantify polyurethane cure reactions has been used to record the cure curves of some polyfluoroether/polyurethane rubbers. It has allowed automatic, direct, quantitative monitoring of the entire cure reaction at moderate temperatures. The technique is non-intrusive, non-destructive and does not rely on finding a good extraction solvent.

The influence of the alcohol end group structure on cure reaction rate has been described. The ranking order of reactivity to isocyanate functionalised polymer is Polymer C > Polymer D >> Polymer B.

Fairly low activation energies in the range  $38\text{-}62 \text{ kJ.mole}^{-1}$  were deduced for the cure reaction of these mixtures.

## REFERENCES

- 1 Miller R L and Oebser M A, *Thermochimica Acta*, **36**, 1980, pp121-131.
- 2 Brennan W P, *Thermochimica Acta*, **17**, 1976, pp285-293.
- 3 Yee Y Y and Adicoff A, *Journal of Applied Polymer Science*, **20**, 1976, pp1117-1124
- 4 Van Geel J L C, *Technical Laboratory RVO-TNO* (ass nr 7360-I, Project A68/KL/091).
- 5 Stockmayer W H, *J. Polymer Sci.*, **9**(1), pp69-71, (1952). ERRATA in *J. Polymer Sci.*, **11**(5), page 424, (1953).

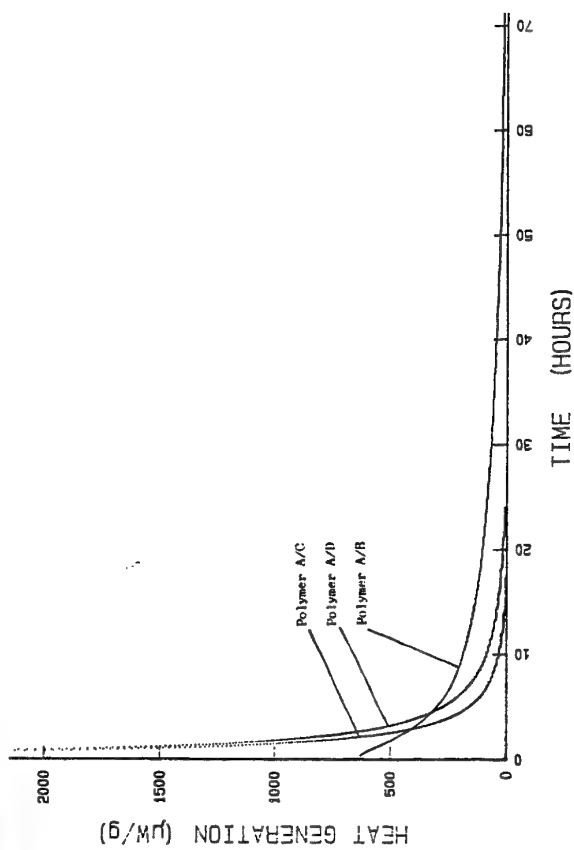


Fig 1 Cure curves of 2-component Polymer mixtures

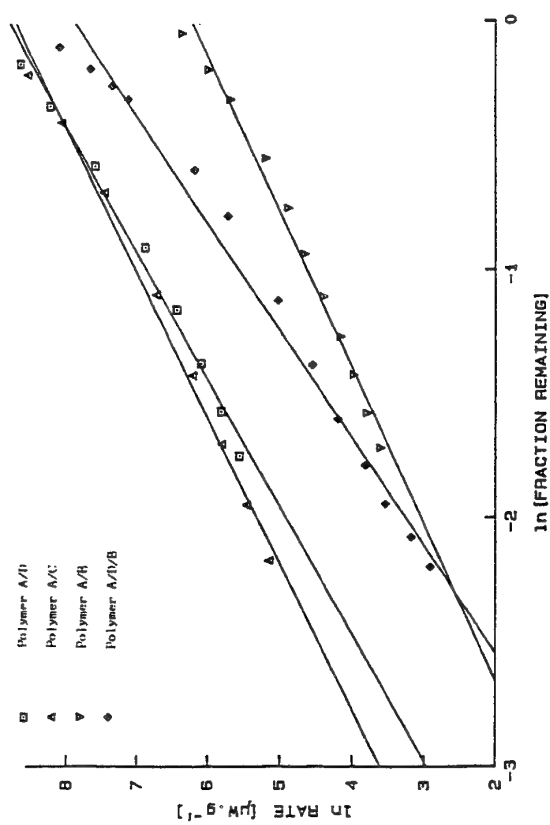


Fig 3 Reaction order plots

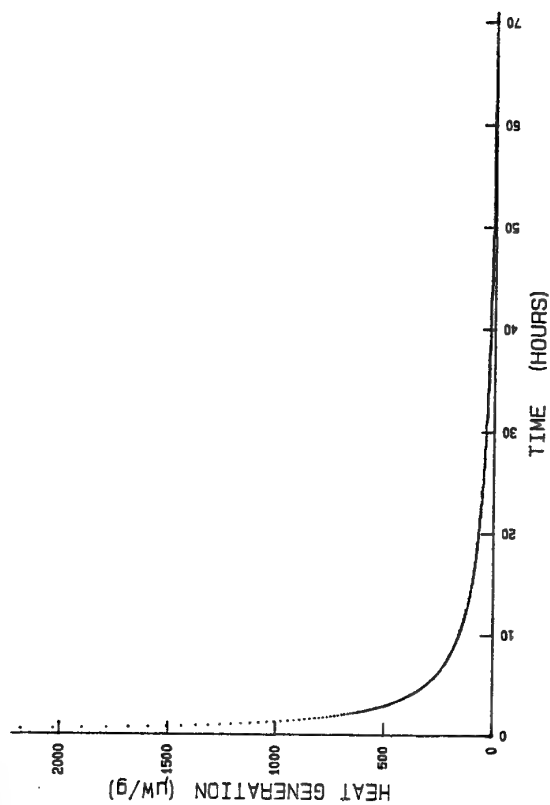


Fig 2 Cure curve of a 3-component Polymer mixture (A/D/B)

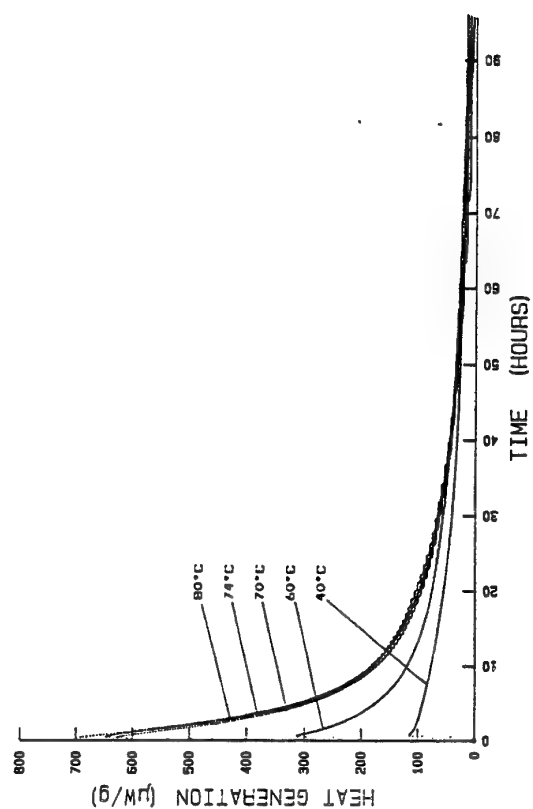


Fig 4 Cure curves for Polymer A/B mixtures at different temperatures

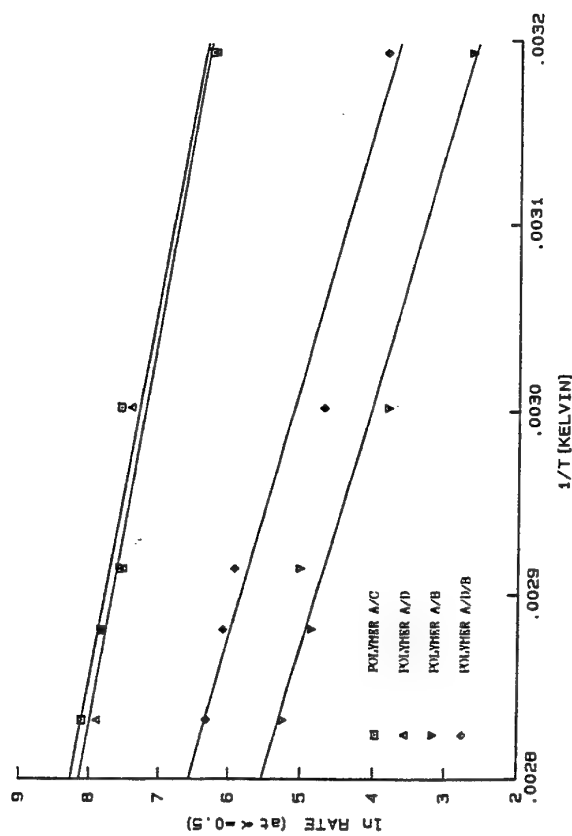


Fig 5 Temperature dependence of cure rate

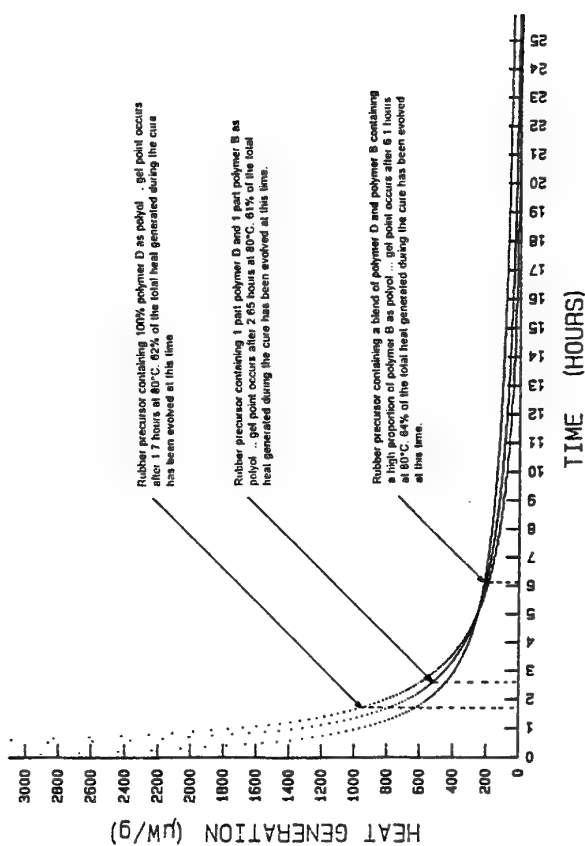


Fig 7 Cure curves of Polymer mixtures - indicating gelation times

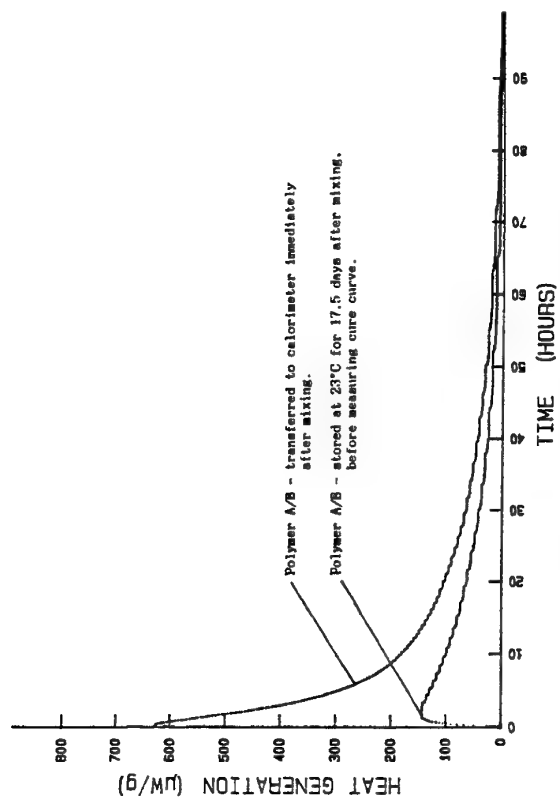


Fig 6 Reduction in area of Polymer A/B cure curve as a result of storage at room temperature

## Use of Isothermal Microcalorimetry in the Early Detection of Potential Drug Formulation Incompatibilities.

Mark A. Phipps and Richard A. Winnike

Glaxo Wellcome Inc, Five Moore Drive, Research Triangle Park, North Carolina 27709, USA.

### Abstract

Drug stability and excipient compatibility are important issues in the pharmaceutical development process. It is well known that environmental factors (*e.g.* temperature, RH *etc.*) can affect the stability, and hence bioavailability, of drug formulations. The choice of formulation components can have a dramatic effect on drug stability and bioavailability. Pharmaceuticals is faced with the challenge of rapidly developing formulations exhibiting long term stability and bioavailability without the benefit of supporting long term data at ambient conditions. Early stability studies are usually carried out at elevated temperatures (typically up to 60 °C) over several weeks to months in order estimate long term stability at ambient conditions by extrapolation. The reliability of extrapolation from stressed conditions and significant time delay are inherent problems with this approach.

A series of microcalorimetric experiments were performed to assess the compatibility of a variety of common pharmaceutical excipients. A method for sample preparation was developed which involved milling/mixing, pre-equilibrating, and calorimetric analysis.

The microcalorimetric method was shown to give good reproducibility for small quantities of material (typically 100 mg). For binary mixtures, a milling/mixing process is important in reducing particle size, inducing intimate contact between mixture components, and providing sample homogeneity. Stress conditions of 50 °C and 75% RH were chosen for initial compatibility screening in order to allow sensitive operation of the calorimeter while providing a more favorable environment for potential reactions to take place.

Excipient mixtures were qualitatively assessed for compatibility (*i.e.* compatible or incompatible) based on observed reaction heat criteria.

### Introduction

Pharmaceuticals has always been faced with the challenge of rapidly developing formulations exhibiting long term stability and bioavailability without the benefit of supporting long term data at ambient conditions. Formulation stability studies (or drug-excipient compatibility assessments) are therefore carried out over shorter time intervals (typically weeks to several months) at elevated temperatures in order to estimate long term stability at ambient conditions by Arrhenius extrapolation. As with

formulations in other industries (e.g. food, cosmetic, pyrotechnic), pharmaceutical formulations (solid and liquid) may contain a variety of excipients other than the active component. These include binders, fillers, lubricants, antimicrobial agents, preservatives, flavorings, stabilizers, *etc.* It is important to assess the compatibility of prospective components of a desired formulation as soon as possible to expedite subsequent formulation development and optimization. Traditionally, analyses of stressed samples are most often performed by HPLC in which the decrease in the parent peak and/or increases in degradation peaks are monitored. Ideally, these analyses should be validated for every excipient and degradant encountered. This is generally time consuming and often not very practical at the early stages of development.

Expeditious excipient compatibility screening is a formidable challenge confronting every major pharmaceutical company. Because of the fast, highly competitive pace of development processes today, more traditional screening techniques are often inadequate in terms of timeliness and reliability. The application of microcalorimetry to excipient compatibility screening will likely provide substantial payback by providing for more timely and reliable data from smaller amounts of drug substance (and in effect minimize resources spent on formulation development and reformulation).

The application of isothermal microcalorimetry in the assessment of solid state stability of pharmaceuticals is not a new concept. Many authors have published data that show the utility of microcalorimetry in the complex field of solid state kinetics and have derived mechanisms, rate constants, and enthalpies for a number of examples<sup>1-9</sup>. To date, however, there has been no record of a standard method to screen for incompatibilities in the solid state at the early stages of formulation development. To maintain a competitive advantage, a screening process is needed which is simple and practical to perform without specialized knowledge in the interpretation of results. It should be rapid and timely where results can be obtained very soon after sample preparation (days) instead of months. The results need to be demonstrated as reproducible so a minimum of false predictions can be attained. Reliability of the technique also needs to be validated using more conventional techniques.

It will be demonstrated here that isothermal microcalorimetry can be used as a preformulation screening technique to identify potential incompatibility issues. A fast, simple and reproducible screening technique has been developed to assess the excipient compatibility in the solid state for a series of pharmaceutically relevant compounds.

## Materials and Method

### Materials

Dibasic calcium phosphate dihydrate, sodium starch glycolate, crospovidone, microcrystalline cellulose, croscarmellose sodium, starch 1500, magnesium stearate and anhydrous lactose were obtained through the Glaxo Wellcome pilot plant inventory. Propyl gallate, propyl paraben, ascorbic acid, salicylic acid, sulfathiazole, benzocaine and malic acid were obtained from Aldrich. Indomethacin was obtained from Sigma.

### High energy mixing

Binary mixtures of excipients and active drug models (*ca* 100 mg of each) were mixed in a vibratory ball mill (Retsch MM2 Vibratory Ball Mill). The mortar was stainless steel with a capacity of 1.5 mL and 2 PTFE 5 mm balls were used. The amplification was set to 50% and the milling time standardized to 10 minutes.

### Low energy mixing

Binary mixtures of excipients and active drug models (*ca.* 100 mg of each) were placed into a small glass vial and shaken for 2 minutes. The mixture was also stirred with a spatula.

### DSC Experiments:

Using binary mixtures of malic acid and propyl paraben, six samples (3-4 mg) from each of the high and low energy mixing techniques were taken and placed in non-hermetic aluminum DSC sample pans. The samples were run on a TA DSC 2920 operating in standard mode at 10 °C·min<sup>-1</sup> from 30 to 150 °C. A continuous nitrogen purge of 40 mL·min<sup>-1</sup> was used.

### Optical Experiments:

All optical photographs were taken using a Nikon OPTI-PHOT-POL microscope under 4 to 40× magnification. Unmilled samples of propyl paraben and malic acid were analyzed as well as the high energy mixture of the two components.

### TAM Experiments:

For all TAM experiments, the samples were mixed using the high energy mixing procedure. Where a single component was analyzed, 200 mg of that component was put through the same mixing regime in the absence of the other component. The sample was transferred to a 3 mL disposable glass TAM ampoule (*ca* 100 mg ± 1 mg) and a hydrostat containing saturated sodium chloride solution (pre-equilibrated at 50 °C and containing a few crystals of sodium chloride in excess), was placed inside the TAM ampoule with the sample. An aluminum crimp seal lid with rubber seal was placed over the ampoule but not crimped. The ampoule was equilibrated in a 50 °C oven for 2

hours prior to crimping. After crimping, the ampoule was replaced in the oven for a further 24 hours to allow equilibration of the crimp seal. The ampoules were then loaded into the calorimeter (Thermometric 2277 Thermal Activity Monitor). The amplification setting in all instances was 300  $\mu\text{W}$  and the collection interval set to 60 seconds. The instrument was calibrated every 7 days using the internal calibration heaters built into the instrument. A minimum of 6 hours but up to 24 hours of data were collected in all instances. In order to assess the true zero location for each experiment, the sample and reference ampoules were switched towards the end of the experiment and lowered back into the measuring position of the calorimeter. By extrapolation of the normal and switched data, the midpoint of the difference between the two is defined as the zero position and all data is adjusted to this true zero value. In addition, for clarity of the results, all example thermal profiles are shown with the initial equilibration and final switching signals removed. Time zero is reported as the time when the sample was first introduced to the stressed conditions. This is, actually, within 10 minutes of the sample mixing. The reference material in all experiments was an ampoule containing 100 mg dried talc with a glass hydrostat containing a stainless steel bar (100 mg). This was chosen to give the closest mass distribution and balance between the sample and reference side.

## Results

Figure 1. DSC thermogram of malic acid/propyl paraben mixture.

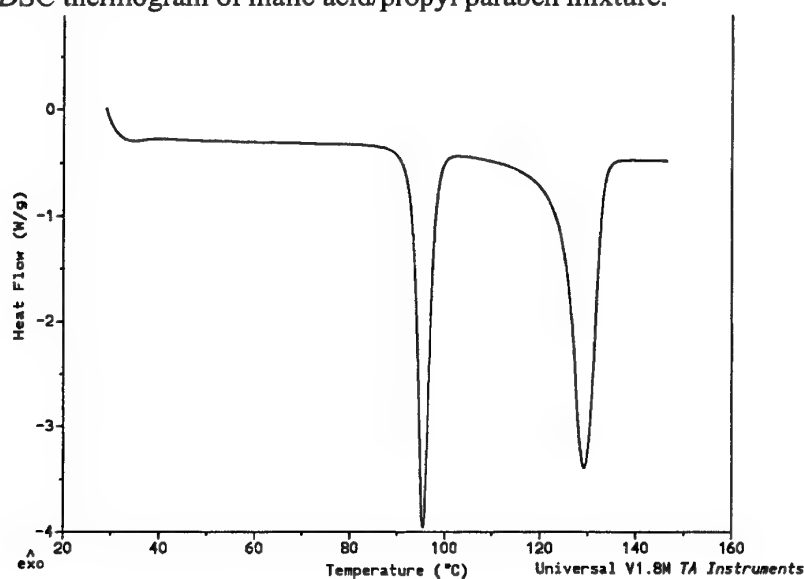


Figure 2. DSC results for malic acid and propyl paraben mixtures.

Low energy mix	mean = 78 $\text{J}\cdot\text{g}^{-1}$	Standard deviation = 26 $\text{J}\cdot\text{g}^{-1}$ (n = 6)
High energy mix	mean = 90.2 $\text{J}\cdot\text{g}^{-1}$	Standard deviation = 1.3 $\text{J}\cdot\text{g}^{-1}$ (n = 6)

Figure 3. Optical photograph of unmilled malic acid.



Figure 4. Optical photograph of unmilled propyl paraben.





Figure 5. Optical photograph of high energy mixed malic acid and propyl paraben.

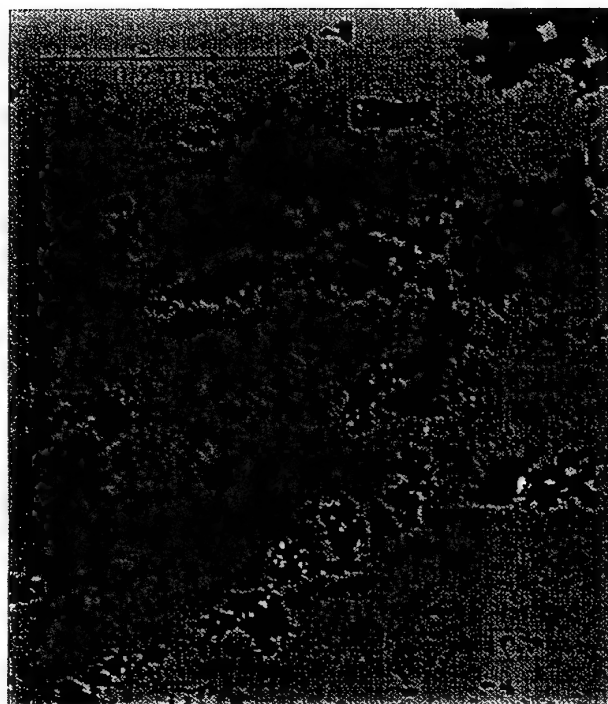


Figure 6. Heat flow vs. time for high energy milled crospovidone samples.

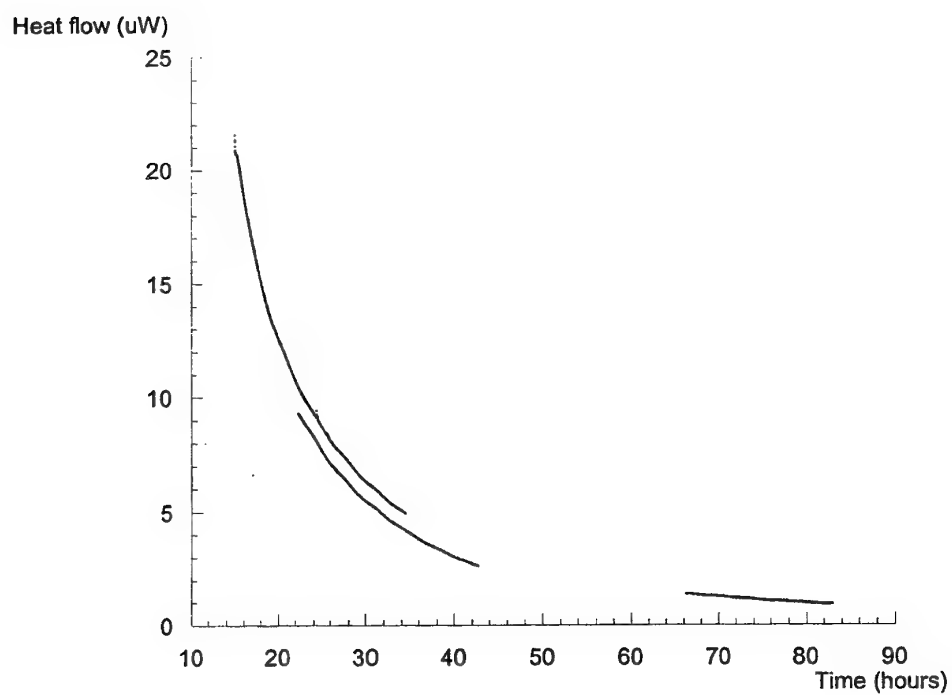


Figure 7. Heat flow vs. time for 4 mixtures of sodium starch glycolate and ascorbic acid.

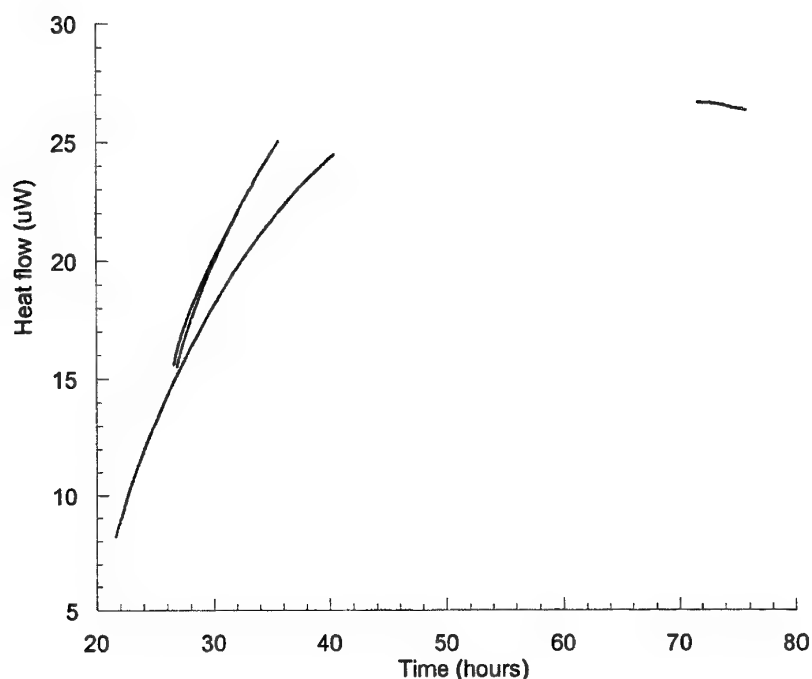


Table 1. List of common excipients and active models.

Common Excipients	Active models
Dibasic calcium phosphate dihydrate	Salicylic acid (phenyl acid)
Sodium starch glycolate	Ascorbic acid (oxidation and hydrolysis)
Crospovidone	Sulfathiazole (primary amine and SO <sub>2</sub> group)
Microcrystalline cellulose	Indomethacin (chloro, acid, aromatic)
Croscarmellose sodium	Benzocaine (primary amine and ester groups)
Starch 1500	
Magnesium stearate	
Anhydrous lactose	
Propyl gallate	
Propyl paraben	

Figure 8. Heat flow vs. time for a mixture of microcrystalline cellulose and salicylic.

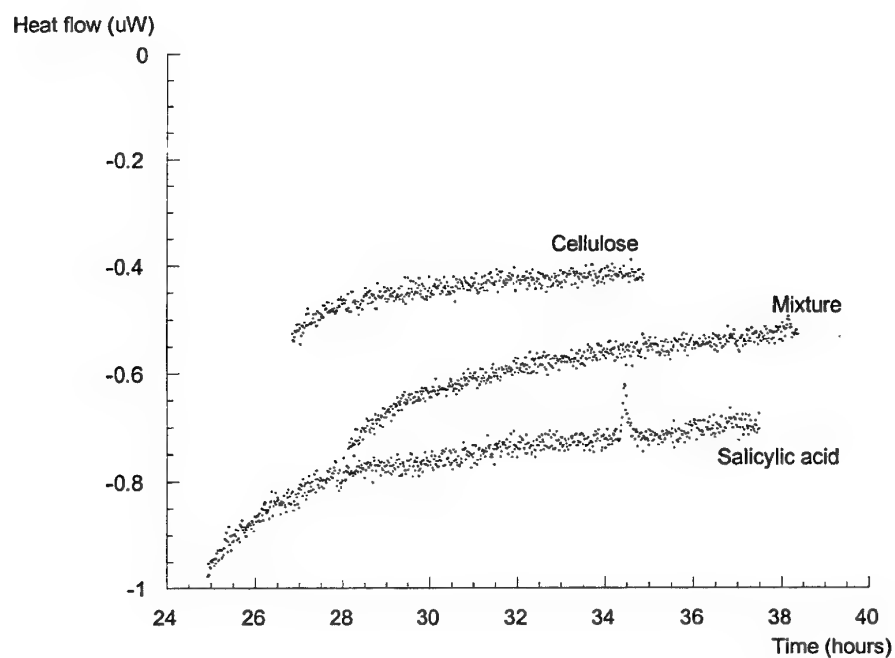


Figure 9. Heat flow vs. time for a mixture of dibasic calcium phosphate dihydrate and indomethacin.

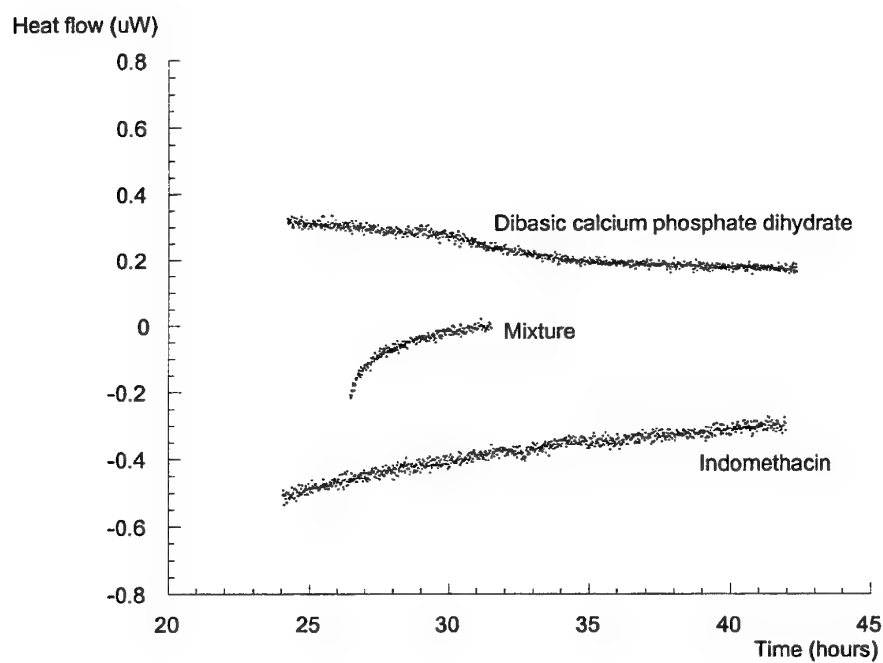


Figure 10. Heat flow vs. time for a mixture of sodium starch glycolate and ascorbic acid.

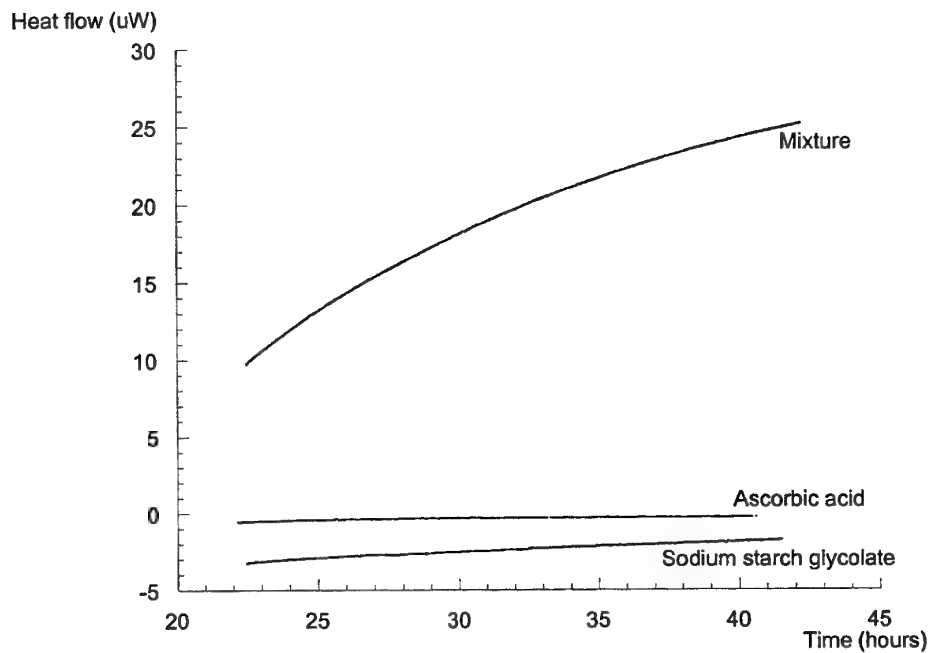


Figure 11. Heat flow vs. time for a mixture of magnesium stearate and salicylic acid.

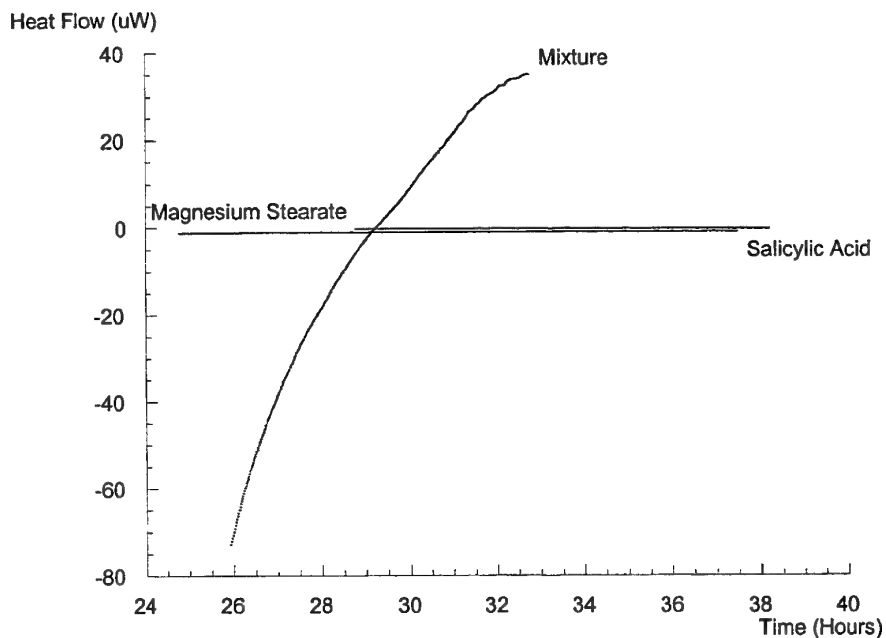


Figure 12. Heat flow vs. time for a mixture of propyl gallate and indomethacin.

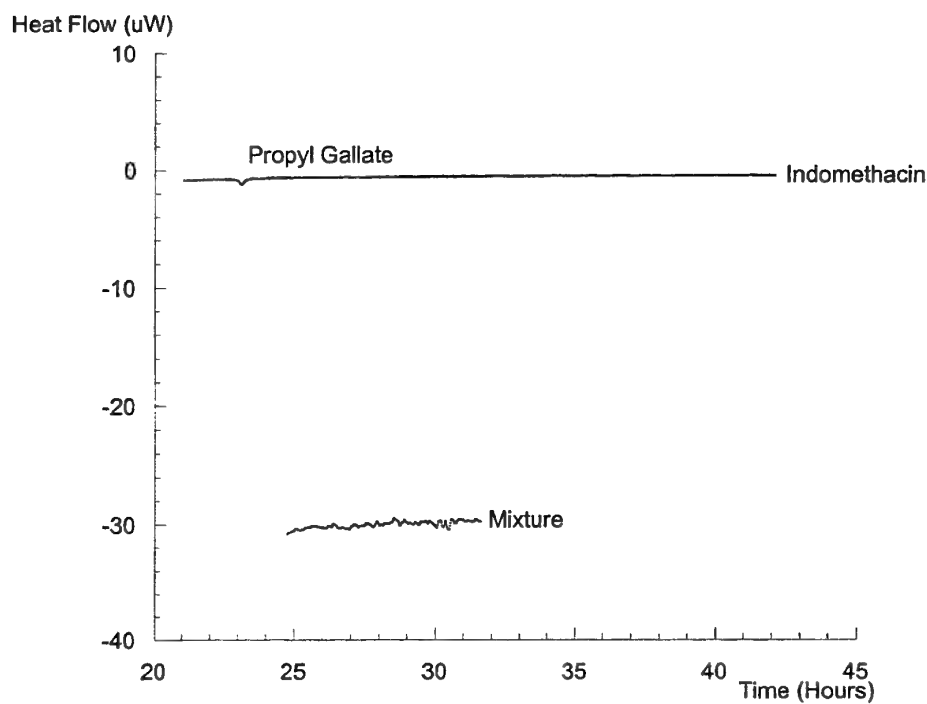


Table 2. Compatibility Screening Results

	(A)	(B)	(C)	(D)	(E)
Dibasic calcium phosphate dihydrate	✓	✗	✓	✓	✓
Sodium starch glycolate	✓	✗	✓	✓	✓
Crospovidone	✓	✓	✓	✓	✓
Microcrystalline cellulose	✓	?	✓	✓	✓
Croscarmellose sodium	✓	✗	✓	✓	✓
Starch 1500	✓	✓	✓	✓	✓
Magnesium stearate	✗	✗	✓	✓	✓
Anhydrous lactose	✓	✓	✓	✓	✓
Propyl gallate	✓	✓	✓	✗	✓
Propyl paraben	✓	✓	✓	✓	✓

Where (A) is salicylic acid, (B) is ascorbic acid, (C) is sulfathiazole, (D) is indomethacin and (E) is benzocaine. ✓ means compatible and ✗ means incompatible.

## Discussion

In any analysis, the reproducibility of the sampling and handling techniques are of vital importance. Reproducible sample handling and homogenous mixing can be particularly difficult with low mass mixtures in the solid state. In order to assess the reproducibility of sample preparation, the DSC experiment described can give a good indication to sample homogeneity and uniformity within the solid preparations. Figure 1 shows the DSC trace for a mixture of malic acid and propyl paraben. These compounds were chosen as they give very well defined and sharp melting endotherms that are easily analyzed. Further, when added together, the melting points are discrete enough to allow analysis of the melting components individually. A direct comparison is possible between the high energy mix and the low energy mixing techniques. The homogeneity of the two mixing techniques was ascertained by taking six samples from each mixing technique and analyzing the enthalpy of fusion for malic acid (lower melting component). [NB The quoted enthalpy of fusion is uncorrected for the mass fraction of malic acid present and does not represent the absolute fusion value. For the purposes of this experiment, the fractional fusion value is sufficient to assess homogeneity of sample.]. For a totally homogeneous mixture this enthalpy of fusion should be consistent for all samples. The low energy mixture gave a standard deviation of  $26 \text{ J}\cdot\text{g}^{-1}$  (Figure 2) which is considerably higher than that observed for the high energy mix ( $1.3 \text{ J}\cdot\text{g}^{-1}$ ). Thus, this indicates that the high energy mix gives very good sample homogeneity compared to the low energy mix and justifies the use for such a high energy mix.

The high energy mix also promotes a decrease in the difference in particle distributions between the two components. Optical photographs of malic acid and propyl paraben are shown in figures 3 and 4, respectively. It is clear that there is a considerable difference in the particle size distribution for each component. This is of concern when dealing with systems in the solid state as, conceptually, any interaction will occur in the first instance on the surface of the solid. High energy mixing while reducing the particle size difference between the two components, increases both the overall surface area and number of contact points thus increasing interaction potential. Using the high energy mix, it is clear that this is achieved by reference to figure 5 which represents an optical photograph of a high energy mixed sample of malic acid and propyl paraben. The same scale is used for figures 3 and 4 and clearly the overall particle size is significantly smaller for the milled samples. The important point though is that the difference in the particle size of the two components is not readily distinguishable under the microscope and is therefore much closer than that of the unmilled samples.

This does, however, raise the issue of crystal disruption and surface energy of the solids before and after milling. Clearly, the 'high energy mixed' samples will have higher surface energy to react<sup>10,11</sup>, higher surface area due to smaller particle size, and enhanced intimate contact between mixture components. This may not be representative of a typical pharmaceutical mixing process but it is not the object of these experiments to reproduce actual mixing regimes. The purpose of choosing a mixing method is to enhance contact between potential reactive sites. Further,  $50^\circ\text{C}$  and 75% relative humidity were chosen as the storage and analysis conditions to enhance and accelerate reaction processes (and ultimately thermal output).

It should be emphasized that the work reported here is towards the goal of developing a screening procedure for solid state compatibility of compounds of pharmaceutical interest. It is not the objective to determine the absolute rate constant, the mechanism of interaction or the enthalpy of reaction. The goal of this screen is to minimize risks and provide focus to the formulation development process by flagging apparently reactive excipients and focusing development processes on more compatible excipients. Currently, this is typically done by storing the mixtures at elevated temperatures and humidities for 1 to 3 months and monitoring (by HPLC) the decrease in the parent peak and/or increases in degradation peaks. Microcalorimetry can potentially cut this storage time (and the time taken to develop appropriate HPLC protocol) and allow a faster assessment of the compatibility of a mixture.

Previously, optical and DSC data have shown that samples prepared using the high energy mixing technique are homogeneous and have a reduced distribution in particle size. The reproducibility of the TAM experiment is paramount in assessing this as a valid technique for the screening of potential incompatibilities. Figure 6 shows three separate samples of crospovidone that have been processed through the high energy mixing protocol. It is clear that there is a very good overlap of the different samples that were run over different time slices of the reaction. The reason for the sloping signal is thought to be due to the slow kinetics to reach equilibrium with the water phase. Even with this complication, good reproducibility is observed. Figure 7 shows the overlap of four different samples of a mixture of sodium starch glycolate and ascorbic acid. These are incompatible mixtures but again a clear reproducibility of results is observed over a 60 hour time interval in the reaction. With these two results, it is demonstrated that the high energy mixing method allows a reproducible way of sample preparation but also increases the reactive potential of the components to react.

The excipients selected for this study were chosen as representative components found in common solid state formulations. In addition, a selection of five active drug models were selected. These were selected because they possess a variety of functional groups which might be susceptible to reaction. The excipients and active models are listed in table 1.

All single components were run as well as all binary combinations of excipients and active models. All mixtures were of a 1:1 composition. For a compound to be defined as compatible, the heat flow observed for the mixture should be approximately the average heat flow of the two single components. This is easily demonstrated in figures 8 and 9. These two combinations clearly show that the heat flow profile for the mixture falls between the heat flow profiles of the two single components. For two compounds to be deemed incompatible, the heat flow of the mixture should deviate significantly from the expected average value of the heat flow of the two single components. Again, this is easily demonstrated by observing the combinations in figures 10 to 12. Figure 10 shows a typical exothermic incompatibility, figure 11 shows a mixed reaction process that starts off endothermic and then proceeds exothermically and figure 12 shows an endothermic incompatibility. These are only examples from the data collected but illustrate the possibility of screening for incompatibilities. The judgment of compatible/incompatible was made graphically by inspection of the three traces on

the same scale. From the data collected, a table of results was formed (table 2). This shows that six combinations were incompatible, one is undefined, and the rest were compatible mixtures. In most cases the assessment of compatibility was straight forward but there were cases where the assessment was difficult because of marginal deviation from the average value of the single components. A method for quantitating (or gauging) the calorimetric output of mixtures compared to the individual components would better facilitate these compatibility assessments.

### Conclusion

It was not the intention of this paper to draw a great deal of attention to the results given here as they are reasonably well defined systems in the pharmaceutical industry and some of the interactions are very predictable. It is the intention however to demonstrate that the method of analysis given here is relatively simple to perform, reproducible, relatively fast, and provides an efficient and effective way to focus formulation development efforts by flagging apparently reactive drug-excipient mixtures early on.

### References

- (1) Koenigbauer, M.J., Brooks, S.H., Rullo, G. and Couch, R.A., Solid-state stability testing of drugs by isothermal calorimetry, *Pharm. Res.* 9 (1992) 939-944.
- (2) Pikal, M.J. and Dellerman, K.M., Stability testing of pharmaceuticals by high-sensitivity isothermal calorimetry at 25 °C: cephalosporins in the solid state and aqueous solution states, *Int. J. Pharm.* 50 (1989) 233-252.
- (3) Tan, X., Meltzer, N. and Lindenbaum, S., Solid-state stability studies of 13-*cis*-retinoic acid and all-*trans*-retinoic acid using microcalorimetry and HPLC, *Pharm. Res.* 9 (1992) 1203-1208.
- (4) Koenigbauer, M.J., Pharmaceutical applications of microcalorimetry, *Pharm. Res.* 11 (1994) 777-783.
- (5) Hansen, L.D., Lewis, E.A., Eatough, D.J., Bergstrom, R.G. and DeGraft-Johnson, D., Kinetics of drug decomposition by heat conduction calorimetry, *Pharm. Res.* 6 (1989) 20-27.
- (6) Buckton, G., Applications of isothermal microcalorimetry in the pharmaceutical sciences, *Thermochim. Acta* 248 (1995) 117-129.
- (7) Wilson, R.J., Beezer, A.E. and Mitchell, J.C., A kinetic study of the oxidation of L-ascorbic acid (vitamin C) in solution using an isothermal microcalorimeter, *Thermochim. Acta* 264 (1995) 27-40.
- (8) Willson, R.J., Beezer, A.E. and Mitchell, J.C., Solid state reactions studied by isothermal microcalorimetry; the solid state oxidation of ascorbic acid, *Int. J. Pharm.* 132 (1996) 45-51.
- (9) Willson, R.J., Beezer, A.E., Mitchell, J.C. and Loh, W., Determination of thermodynamic and kinetic parameters from isothermal heat conduction microcalorimetry: applications to long-term-reaction studies, *J. Phys. Chem.* 99 (1995) 7108-7113.



- (10) Buckton, G., Choularton, A., Beezer, A.E. and Chatham, S.M., The effect of the comminution technique on the surface energy of a powder, *Int. J. Pharm.* 47 (1988) 121-128.
- (11) Buckton, G. and Beezer, A.E., A microcalorimetric study of powder surface energetics, *Int. J. Pharm.* 41 (1988) 139-145.

### Addendum

Concern was highlighted in the paper about the absence of a way of quantitating the calorimetric data to give numeric value which could be used to gauge compatibility or incompatibility. This issue was addressed by Stephan Wilker at this conference. Although it is discussed in detail in his paper entitled "Microcalorimetric investigation of energetic materials - A review of methodic development at BICT", it is worth noting again here. There is one basic equation of note.

$$D = \frac{(P_1 + P_2)M}{(P_1K_1) + (P_2K_2)} \quad \text{Equation 1}$$

Where D is a compatibility index,  $P_1$  and  $P_2$  are the quantities of components 1 and 2 in the mixture respectively, M is the energy release of the mixture,  $K_1$  and  $K_2$  are the energy releases of components 1 and 2 on their own respectively. This equation can easily be adapted to more complex systems than binary mixtures and can also be simplified if the ratio of binary components is 1:1 (Equation 2).

$$D = \frac{2M}{K_1 + K_2} \quad \text{Equation 2}$$

The work presented in this paper does not allow the elucidation of a value for the heat produced by the entire reaction due to the, sometimes, long term nature of the reactions. It is possible, however, to integrate specific time intervals to obtain values for M,  $K_1$  and  $K_2$ .

The compatibility index, D, can then be used in the assessment of the compatibility. Dr. Wilker was interested principally in ballistic propellants and deduced threshold values of D where a mixture would be defined as compatible or incompatible. These threshold values of D may be different for pharmaceutical systems. Nonetheless, this concept should be useful in experimentally designed excipient compatibility studies using response surface modeling to find drug-excipient combinations with low compatibility indices or D values.



# Comparisons of Pyrotechnic Whistle Compositions

by

## Differential Scanning Calorimetry

Joseph A. Domanico  
Gene V. Tracy  
Melvin N. Gerber

Pyrotechnics Team  
SCBRD-ENM-P

Edgewood Research, Development and Engineering Center  
Aberdeen Proving Ground, MD 21010-5423  
Phone: 410-671-2180 FAX: 410-671-4941

### ABSTRACT

Recent efforts on the Advanced Pyrotechnics initiative of the Pyrotechnics Team of the Edgewood Research, Development and Engineering Center located at the Aberdeen Proving Ground, Maryland, have generated several experimental pyrotechnic whistling compositions. Pyrotechnic whistles have been cross-blended with several unusual additives which provide a secondary effect to the high-level acoustic output of the devices. Secondary effects such as large smoke production, long range spark generation, and irritating smoke output are just some of the results of this effort. This paper will show how the various additives affect the performance of the baseline pyrotechnic whistle. The analysis by differential scanning calorimetry will be the center of the presentation. The interpretation of the experimental results will be compared with the actual performance of these peculiar pyrotechnic compositions.

### BACKGROUND

Pyrotechnic whistles and whistle compositions have been studied by the Pyrotechnics Team ERDEC at Aberdeen Proving Grounds since 1993. The team conducted several hundred experiments using different combinations of fuels and oxidizers. Although pyrotechnic whistles have been around for an extremely long time, the goal of the team's efforts was to fully understand the effects between these specific fuels and oxidizers, and the effects caused by the addition of a third component. Table 1 shows the list of fuels which can be used to make a pyrotechnic whistling composition. These fuels can be successfully mixed with either potassium chlorate or potassium perchlorate to make a whistling composition. The preferred oxidizer is the perchlorate as it is safer to handle and provides a more reproducible whistle. Third components varied in their effects on the pyrotechnic whistling compositions. Oxidizers such as those in table 2 were added to the "standard" whistling composition.

In addition to oxidizers, small percentages of powdered metals were also added to the standard whistling composition. The results of adding powdered metals to whistle composition increases the spark production.

The addition of several materials to the baseline pyrotechnic whistling composition raised a concern for safety. Was the addition of a third material increasing the risk of detonation for the composition? Was the resulting composition more sensitive to ignition? Thus a Differential Scanning Calorimeter was used to quickly determine the thermal profiles of the new compositions and study their ignition characteristics. Other devices were used to establish a complete picture of the required ignition stimulus but will not be presented here.

Typical noise levels are shown in table 3. Note the difference in the two basic categories of noise generation; continuous and pulse noise. Pyrotechnic whistles operate continuously in the area where one normally finds pulse noise. The effect of a large amplitude for a duration of several seconds makes the large diameter pyrotechnic whistle suitable as a distraction device.

The typical whistle design is a circular tube containing the pyrotechnic whistle composition. The "standard" whistle composition used as a baseline for the duration of the experiments was chosen as a result of previous experiments. The combination of potassium benzoate and potassium perchlorate was considered to be the safest and most reproducible of all the fuel / oxidizer combinations tested. A general whistle description is defined as a mixture of 27 parts by weight of potassium benzoate and 73 parts by weight of potassium perchlorate is pressed at 7700 pounds per square inch (PSI) into a cylindrical tube from 0.250" diameter up to 3.0" diameter.

## RESULTS

Table 4 shows the ignition point comparison of several pyrotechnic compositions with the 'standard' whistle composition. Notice that there is a large gap in the ignition point between the standard whistle composition and the red smoke composition. The use of potassium perchlorate instead of the potassium chlorate (found in the red smoke composition) helps keep the ignition point as high as practical.

Although the whistle composition ranked third in the ignition point test series, it ranks number one when comparing the energy outputs of the compositions. When compared with a binary mixture of magnesium and potassium perchlorate, the whistle composition releases another 36% in measured energy. Table 5 shows the entire test series.

Previous experiments showed that the addition of a third ingredient could have a significant effect on the pyrotechnic whistle composition. Effects such as coloring the external flame green, red, and even yellow were all possible by the addition of various oxidizers. Spark generation was easily accomplished by the addition of various particle sizes of various metals.

The question arose as to the effect on the ignition point of the various compositions when a third component was introduced to the binary composition. Several scans were completed using the differential scanning calorimeter to observe the changes, if any. Table 6 shows a summary of the ignition points of pyrotechnic whistle compositions when a third component is introduced. The rankings show a definite increase in the ignition point when various nitrates are added. Note the decrease in ignition temperature when sulfur is used as a binder, or when stainless steel or aluminum powder is added to the standard composition.

### CONCLUSIONS

The differential scanning calorimeter is an excellent tool to quickly obtain a thermal "footprint" of a pyrotechnic composition. Although it is often difficult to obtain a homogeneous representative sample due to the very small sample size, conducting several test of the same series can eliminate this drawback. The data generated is the average of the best three out of five runs for a particular test.

The effect of adding a third component to the pyrotechnic whistling composition can both increase and decrease the new composition's thermal ignition temperature. The amount of increase or decrease is not sufficient to either consider that an added safety precaution must be added or can be eliminated. Essentially, three component pyrotechnic whistles can be handled as any other dangerous pyrotechnic composition.

Table 1  
Some Pyrotechnic Whistle Fuels

Name	Chemical Composition
Gallic acid	C7H6O5
Sodium salicylate	C7H5NaO3
Potassium picrate	C6H2KN3O7
Potassium benzoate	C7H5KO2
Sodium benzoate	C7H5NaO2
Potassium dinitrophenate	C6H3N2O5K
Potassium hydrogen phthalate	KC8H5O4

Table 2  
Oxidizers Added to Pyrotechnic Whistle Compositions

Material	Proposed Effect
Barium nitrate	Green color flame
Strontium nitrate	Red color flame
Sodium nitrate	Yellow color flame
Guanidine nitrate	Slow burn rate

Table 3  
Typical Noise Levels

Item	Amplitude (dB)	Noise Type
Whisper	30	Continuous
Conversation	60	Continuous
Alarm clock	80	Continuous
5/4 Ton truck	90	Continuous
Disc sander	100	Continuous
Power saw	110	Continuous
Chain saw	120	Continuous
Pneumatic hammer	130	Continuous
Firecracker	140	Pulse
Cap pistol	150	Pulse
Shotgun	160	Pulse
TOW missile	180	Pulse

Table 4  
Ignition Temperature Comparison

Composition	Ignition Temperature (degrees C)
Bullseye Smokeless Powder	192
Standard Red Smoke Composition	198
Standard Pyrotechnic Whistle Composition	432
A1A Ignition Composition	437
Zirconium / Iron Oxide	507
Magnesium / Potassium Perchlorate	545
Magnesium / Iron Oxide	545
Magnesium / Manganese Dioxide	550

Table 5  
Output Energy Comparison

Composition	Energy (cal per gram)
Standard Pyrotechnic Whistle Composition	3,394
Magnesium / Potassium Perchlorate	2,491
Bullseye Smokeless Powder	1,753
Magnesium / Manganese Dioxide	1,406
A1A Ignition Composition	903
Standard Red Smoke Composition	895
Zirconium / Iron Oxide	581
Magnesium / Iron Oxide	311

Table 6  
Ignition Temperature Comparison

Third Component	Ignition Temperature (degrees C)
Stainless Steel Powder	410
Aluminum Powder	415
Sulfur	427
None (Standard Whistle Composition)	432
Barium Nitrate	446
Strontium Nitrate	452
Sodium Nitrate	453
Guanidine Nitrate	454
Magnesium-Aluminum Alloy Powder	454

**MICROCALORIMETRY : PRELIMINARY INVESTIGATION  
OF DICHROMATED MAGNESIUM AND COMPATIBILITY STUDIES OF  
THE ENERGETIC BINDER POLYNIMMO.**

D Blazer , Dr. T T Griffiths

Defence Evaluation and Research Agency, Fort Halstead, Sevenoaks.

**Abstract**

The paper reports the preliminary results of two investigations which used microcalorimetry. The first involved a study into the effect of chromating magnesium powder to protect it from moisture and atmospheric oxidation.

Magnesium powder, atomised grade 6, was reacted with an aqueous solution of potassium dichromate, concentrated nitric acid and potassium chromium sulphate dodecahydrate.

The treated magnesium was then tested for its chemical resistance to moisture by measuring its thermal activity using sealed ampoules and the flow through cell of a microcalorimeter.

In the second investigation the compatibility of various pyrotechnic ingredients was tested against the energetic binder polyNIMMO.

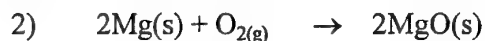
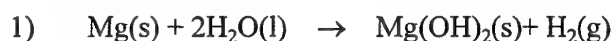
The compatibility between the energetic binder polyNIMMO and a number pyrotechnic ingredients was investigated using microcalorimetry.

Each ingredient was mixed with polyNIMMO and sealed into a glass ampoule. The heat flow was monitored over 60 hours to determine any reaction between the pyrotechnic ingredient and the polyNIMMO.

## Preliminary Investigation of Chromated Magnesium

### Introduction

Magnesium powder is used as a fuel in illuminating and IR emitting pyrotechnic compositions. One major problem with magnesium is that it degrades during storage according to the following two reactions:



Because the heat of reaction for reaction 1 is an order of magnitude higher than reaction 2 then this reaction that is thought to be the primary cause of degradation of magnesium in pyrotechnic compositions<sup>1</sup>.

Pyrotechnic fuels are coated with natural or synthetic binders for a number of reasons, one of which is to protect the fuel from corrosion by moisture. If moisture had been adsorbed onto the surface of the fuel prior to it being coated then there is the possibility that it would be trapped between the fuel and the binder. For safety reasons pyrotechnics are processed at a minimum of 65% relative humidity (RH) in order to reduce the risk of ignition by static electricity. Under these conditions moisture can be adsorbed onto the ingredients and when they are pressed the moisture can be trapped within the compact. In both instances the retained moisture can react with fuels, such as magnesium, during storage.

By chromating magnesium powder before manufacture into pyrotechnic compositions, it was hoped to provide an alternative or better method of protecting the metal from attack by moisture than by coating it with a binder.

### Experimental

#### Material

The magnesium used in this study was atomised grade 6 powder conforming to Defence Standard 134-130.

#### Chromating Procedure

A 50g sample of magnesium powder, atomised grade 6, was added to the aqueous chromating solution at 25°C and stirred in a rotary evaporator. After 30 minutes the magnesium powder was filtered through a Whatman No 3, 18.5cm diameter filter paper and washed three times with 100 cm<sup>3</sup> of distilled water. The powder was dried at 60°C for 24 hours before use.

#### Determination of Chromate Content

The level of chromium content of the treated magnesium was determined by Atomic Absorption Spectroscopy (AAS) using the method of standard additions.



A 10g sample of treated magnesium was dissolved in 50 cm<sup>3</sup> of 1:1 hydrochloric acid containing a few drops of nitric acid ( $d = 1.42\text{gcm}^{-3}$ ). Following dissolution, the sample was made up to 500 cm<sup>3</sup> in a volumetric flask using de-ionised water.

Aliquots of the prepared solution were transferred to three separate 100cm<sup>3</sup> volumetric flasks. To two of the flasks were added known amounts of standard 1000mgcm<sup>-3</sup> chromium solution.

The AAS was set up for the determination of chromium. Standard and sample solutions were aspirated and absorbance readings recorded. A graph was plotted of absorbance against concentration of the added chromium standard and a line was extrapolated through the points to the concentration axis. From this graph the level of chromium present in the treated magnesium sample could then be determined.

### Microcalorimetry

A LKB Thermal Activity Monitor (TAM) model 2277 was used in the study. Treated and untreated magnesium powder (2.5g) were examined in sealed ampoules and in the flow through cell. Experiments were carried out at 55°C.

Sealed ampoule experiments monitor the reactions, if any, taking place in a limited environment. This tends to give decay heat flow curves because reactants are being consumed but not replaced.

The flow through cell provides a continuous stream of reactant over the experimental period. By using this apparatus a better indication of the resistance of chromated magnesium to reaction with moisture can be assessed compared to using sealed ampoules.

A microcalorimetric programme was designed and used in all experiments during which the instrument was calibrated, the base line determined and the heat flow from the ampoule was measured. For the flow through cell, after the sample was lowered into the cell it was left for 24 hours after which the relative humidity was increased from 0-80% over a 50 hour period. The relative humidity was held at 80% for the remainder of the experiment.

### Results and Discussion

The level of chromium on the magnesium powder was 2.5mgg<sup>-1</sup>.

The heat flow obtained for treated and untreated magnesium powder in a sealed ampoule is shown in Fig 1. The treated magnesium showed a higher heat flow than the untreated magnesium. This result was unexpected and the explanation given is that inadequate washing and drying of the treated magnesium resulting in the chromating reaction continuing within the microcalorimeter cell.

The heat flow curves for the untreated and treated magnesium run in the flow through cell are as expected and are shown in Fig 2. The untreated magnesium shows very

little heat flow until the relative humidity is increased when a large heat flow is shown.

The treated magnesium shows no increase in heat flow when the relative humidity is increased. It is therefore concluded that the chromating of magnesium powders will protect them from attack by moisture.

It should be noted that the delayed reaction between the magnesium and dichromate, observed in closed ampoules was still occurring in the flow through cell experiments but is not seen in the heat flow curves due to the difference in scales used for the recordings.

To test the reproducibility of the method used in the flow through cell experiments fixed experimental parameters were used. Results obtained for the heat flow from untreated magnesium powder are very different and show poor reproducibility. The reason for this lack of reproducibility is that at high relative humidities condensation occurs within the cell. This condensation problem requires rectifying before meaningful results will be obtained.

### **Compatibility Studies of the Energetic Binder PolyNIMMO with Pyrotechnic Fuels and Oxidants**

#### **Introduction**

Pyrotechnic compositions can be made less sensitive to accidental ignition by the use of plastic binders. Plastic binders such as Carboxyl-terminated butadiene acrylonitrile co-polymer (CTBN) and Hydroxyl-terminated polybutadiene (HTPB) have been used however, these binders have the disadvantage in that they also decrease the burning rate and energy output. Energetic binders may provide a means of maintaining the burn rate and energy output of pyrotechnic compositions in addition to reducing their sensitivity.

Energetic binders are organic polymers in which the backbone has been chemically substituted by pendant energetic groups such as nitro, nitrate or azide<sup>2</sup>. PolyNIMMO (poly(3-nitratomethyl-3-methyloxetane)) is an energetic binder developed by DERA for use with propellants and high explosives. PolyNIMMO is synthesised by nitration of an oxetane ring then opening of the ring and subsequent polymerisation.

The compatibility of polyNIMMO with various pyrotechnic fuels and oxidants was determined using sealed ampoule microcalorimetry.

#### **Experimental**

##### **Microcalorimetry**

The experimental conditions were the same as those used in the sealed ampoule experiments of the previous work.

## Preparation of Samples

Ampoules and ampoule caps were stored in an oven at 100°C for 24 hours before use. The test materials were dried at approximately 105°C for 24 hours before use and weighed into ampoules. The unstabilised polyNIMMO was then introduced into the ampoule using a syringe. After mixing the binder and test material with a thin stainless steel rod the ampoule was reweighed thus allowing the precise amount of material present in the ampoule to be determined.

## Results and discussion

Table 1 lists the pyrotechnic fuels and oxidants used in this study as well as the proportion of material to binder used.

Unstabilised polyNIMMO was run, to establish a baseline for all other experiments, and the heat flow curve obtained is shown at fig 3. Interpretation of the curve is that the initial exothermic signal is due to a slight cooling of the thermocouples as the sample is introduced into the measuring cylinder. The endothermic peak is due to the decomposition of the nitrate ester group. Bunyan<sup>3</sup> has reported that the decomposition of unstabilised polyNIMMO occurs by the breaking of nitrate ester bonds and that the presence of oxygen influences the reaction.

The slow increase in heat flow signal (from negative to positive) is a combination of the autocatalysis of the energetic binder and the reaction of the polymer with air as previously reported by Bunyan<sup>4</sup>.

Heat flow curves obtained for unstabilised polyNIMMO with the majority of ingredients showed that they were compatible. The only material which was not compatible with unstabilised polyNIMMO was boron.

Initially all the ingredients had been dried prior to testing therefore the boron had had its surface moisture removed. The heat flow curve obtained (fig 4) showed a reaction occurring between the dried boron and the unstabilised polyNIMMO.

In fig 5, boron as received was tested against unstabilised polyNIMMO and the heat flow curve showed an increase in peak heat flow before dropping quickly to a lower value. This suggested that initially two types of reaction sites were present in the as received boron. It was proposed that the reason was that on the surface of the boron as received there was physically bound moisture and chemically bound moisture, both of which had hydroxyl groups capable of reacting with the nitrate ester group in the unstabilised polyNIMMO. On drying only the physically bound moisture would be removed but the hydroxyl groups from the chemically bound moisture is still available for reaction, hence the difference between the curves for as received and dried boron. To test the hypotheses, boric acid which contains hydroxyl groups was mixed with unstabilised polyNIMMO and the test run as before. A large signal was expected but only a weak heat flow was observed which indicated only a small amount of reaction.

Crystals of metaboric acid contains molecules which are linked together by hydrogen bonding, for example, metaboric acid exists in three different crystalline forms one of which contains the cyclic ring shown in fig 6. crystals in which the  $B(OH)_3$  units are linked together by hydrogen bonding<sup>5</sup>.

Similarly orthoboric acid consists of triangular planar  $BO_3$  groups linked through hydrogen bonding to form a layer structure. The layers are held together by weak van der Waals forces.

Therefore the presence of hydrogen bonding in boric acid makes the hydroxyl groups unavailable for reaction with the nitrate ester of the unstabilised polyNIMMO.

Lithium hydroxide and nickel hydroxide were tested against unstabilised polyNIMMO to test the reaction of hydroxyl groups with the nitrate ester group. Both curves (fig 7 and fig 8) obtained were similar in shape to the curve obtained for dried boron and the heat flow signal is below the value for maximum peak flow during the equilibrium phase.

Unstabilised polyNIMMO was mixed in a 10:1 w/w with the aliphatic polyisocyanate cross -linking agent Desmodur N100. This ratio is the approximate amount of Desmodur required to cure the polyNIMMO according to calculation using the OH balance test<sup>6</sup>. The cure reaction curve is shown in fig 9. The curve for the cure reaction is similar to the curves obtained for boron (dried), lithium hydroxide and nickel hydroxide and suggests that a cure reaction is involved in all these instances.

## Conclusions

Chromating magnesium appears to protect the metal from degradation due to its reaction with moisture.

Microcalorimetry proved to be a good, quick method for testing the compatibility of pyrotechnic ingredients.

The results of this preliminary investigation showed that boron should not be used with the energetic binder.

This has been attributed to the reaction between hydroxyl groups present on the surface of boron and the nitrate ester group in polyNIMMO.

## References

1. "Microcalorimetric Study of the Ageing Reactions of Atomized Magnesium Powder", Shortridge R G, Chin A, Hubble W R, Naval Surface Warfare Center, Ordnance Engineering Directorate, Crane Division, Indiana 47522 - 5050, 1992.
2. "The Synthesis of Poly(3-nitratomethyl-3-methyloxetane) From Commercially Available Starting Materials", P. Golding, R.W. Millar, N.C. Paul, M.J. Stewart, MEMO 27/88, R.A.R.D.E., Waltham Abbey, January 1989.

3. "*Report on the Development of New Test Methods to Investigate the Degradation and Stabilisation of New Energetic Binders*", P.F. Bunyan, A.V. Cunliffe, DRA Report DRA/DWS/WX4/CR9459/1.0, May 1994.

4. "*Calorimetric Studies of the Thermal Decomposition of Poly(3-nitratomethyl-3-methyloxetane)* ", P.F. Bunyan, MEMO 52/91, R.A.R.D.E., Fort Halstead, November 1991.

5. "*Introduction to Inorganic Chemistry*", K.M. Mackay, R.A. Mackay, International Textbook Company London, 3rd Edition, 1981.

6. Personal communication with Miss S. E. Gaultier, DERA.

Tables.

Material under test	Mass g	Mass polyNIMMO g	% of test material in the sample	Source
polyNIMMO	0.8226	-	-	ICI BXPP370
Desmodur	0.0702	0.7171	8.1	Bayer
Aluminium	0.4545	0.5099	47.1	Aluminium Powder Co, 5 $\mu$ m, PNo. WSSLV0576
Barium Nitrate	0.4675	0.4201	55.1	V2006 R72
Barium Peroxide	0.4132	0.7512	35.5	Hopkin & Williams AnalaR
Bismuth (III) Oxide	0.3515	0.4175	45.7	Merck Ltd
Boric Acid	0.430	0.4565	48.5	BDH AnalaR
Boron (dried 140°C)	0.4704	0.6260	42.9	LN49 R73
Boron (as supplied)	0.4147	0.4552	47.7	LN49 R73
Magnesium	0.4428	0.5091	46.5	Active Metals Grade 6 Blown
Magnesium Oxide	0.3126	0.7743	28.7	Hopkin & Williams GPR
Potassium Nitrate	0.4281	0.2713	61.2	V3605 R72
Potassium Oxalate	0.4467	0.7414	37.6	BDH AnalaR
Potassium Perchlorate	0.4088	0.7875	34.2	Barium & Chemicals inc, Ohio, USA
Silica	0.4332	0.3507	55.3	Sigma General Grade
Silicon	0.4862	0.5725	46.0	LN8 R73
Sodium Nitrate	0.4818	0.6349	39.1	1/9 R72
Strontium Nitrate	0.4458	0.4615	49.1	1/10 R72

Table 1 : Materials used in the Practical Work.

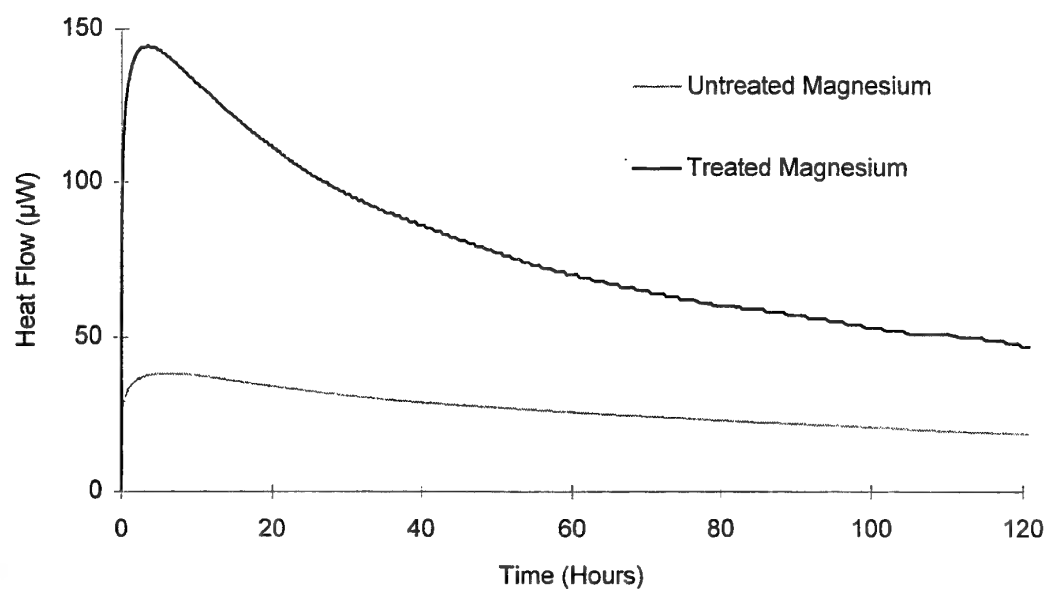


Figure 1: Heat flow curves for treated and untreated magnesium in sealed ampoules

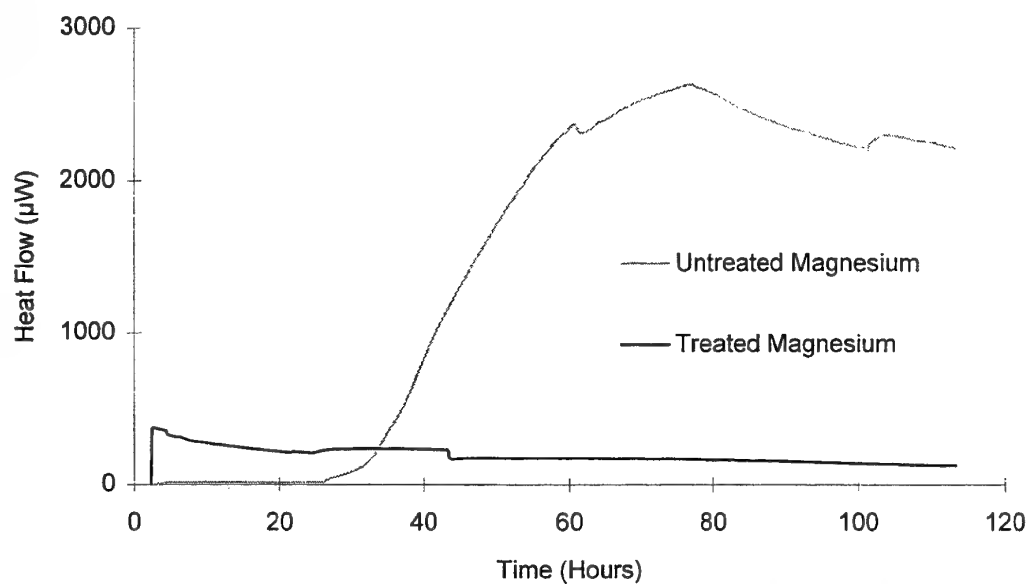


Figure 2: Heat flow curves for treated and untreated magnesium in the Flow Through Cell of the Microcalorimeter.

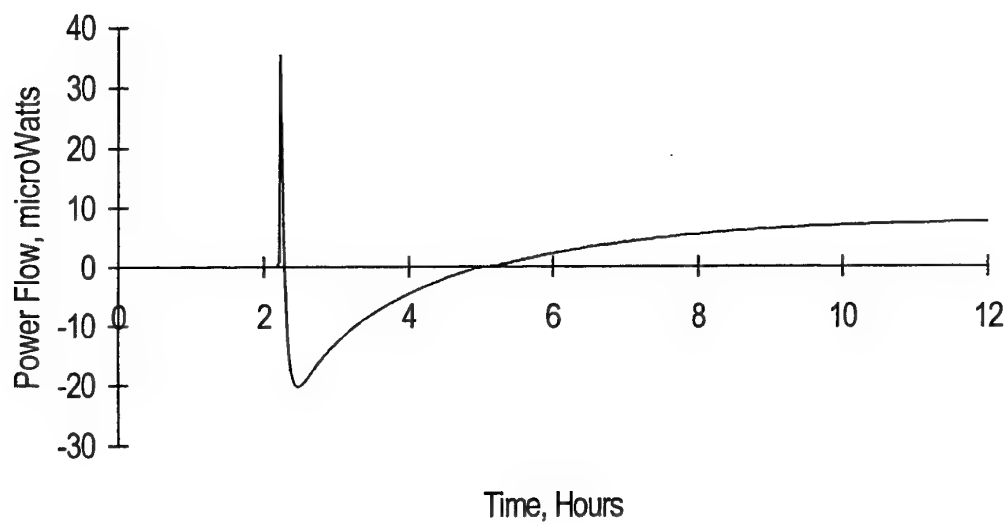


Figure 3 : Heat flow curve for unstabilised polyNIMMO.

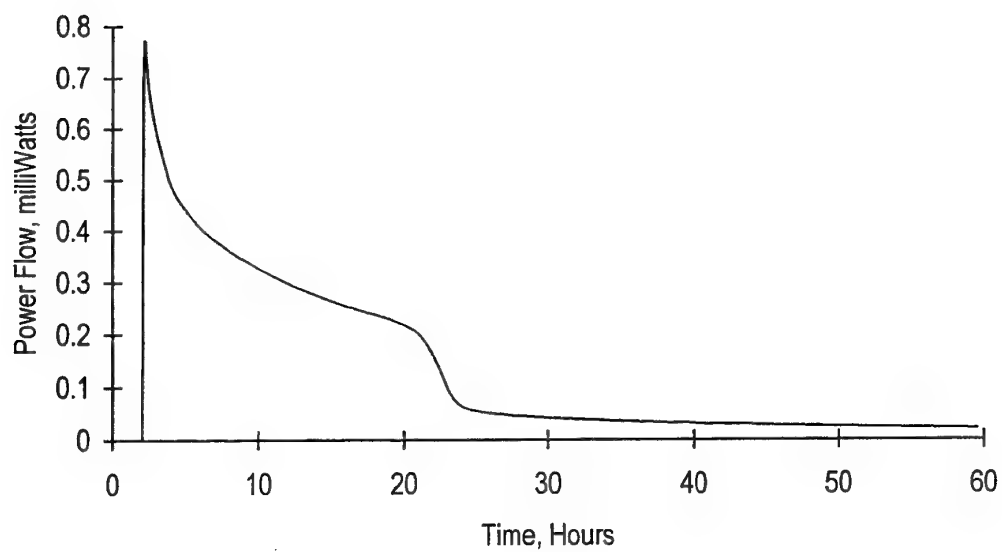


Figure 4 : Heat flow curve for unstabilised polyNIMMO  
with dried boron.



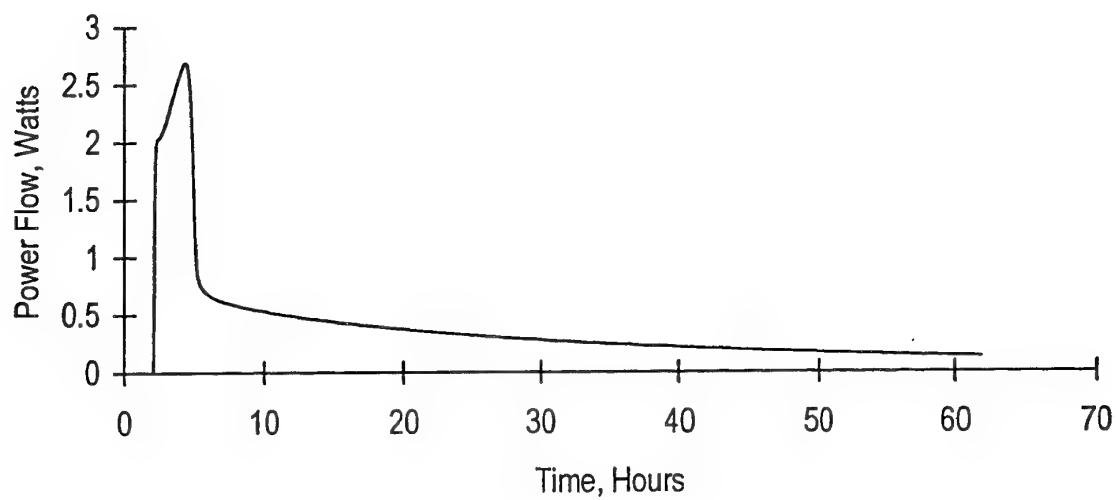


Figure 5 : Heat flow curve for unstabilised polyNIMMO with boron as received.

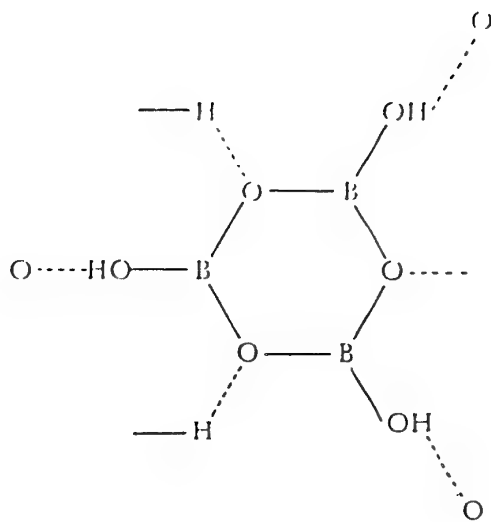


Figure 6 : Structure of metaboric acid.

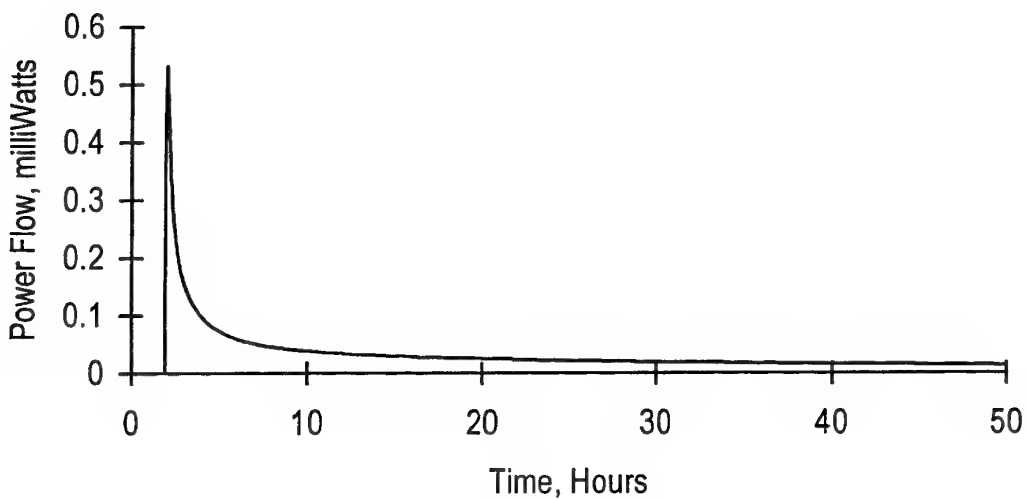


Figure 7 : Heat flow curve for unstabilised polyNIMMO with lithium hydroxide.

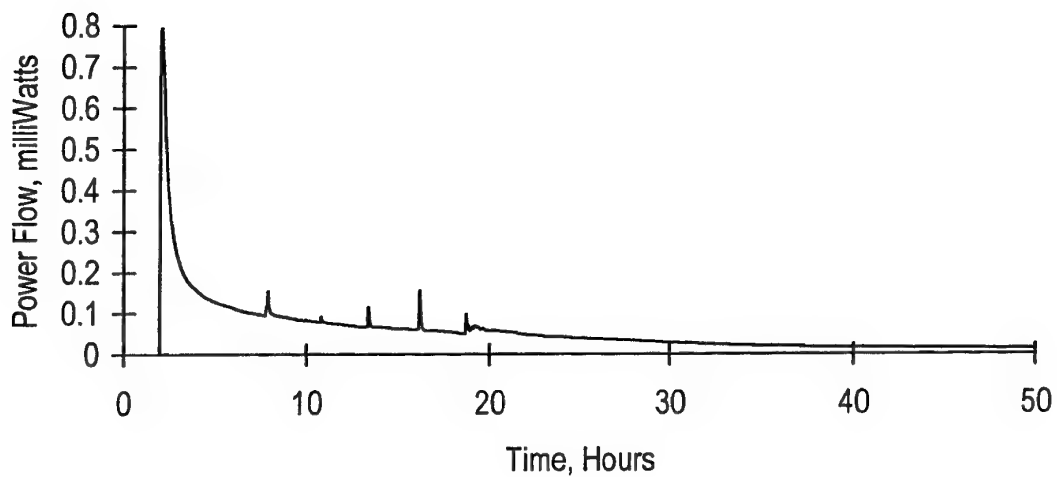
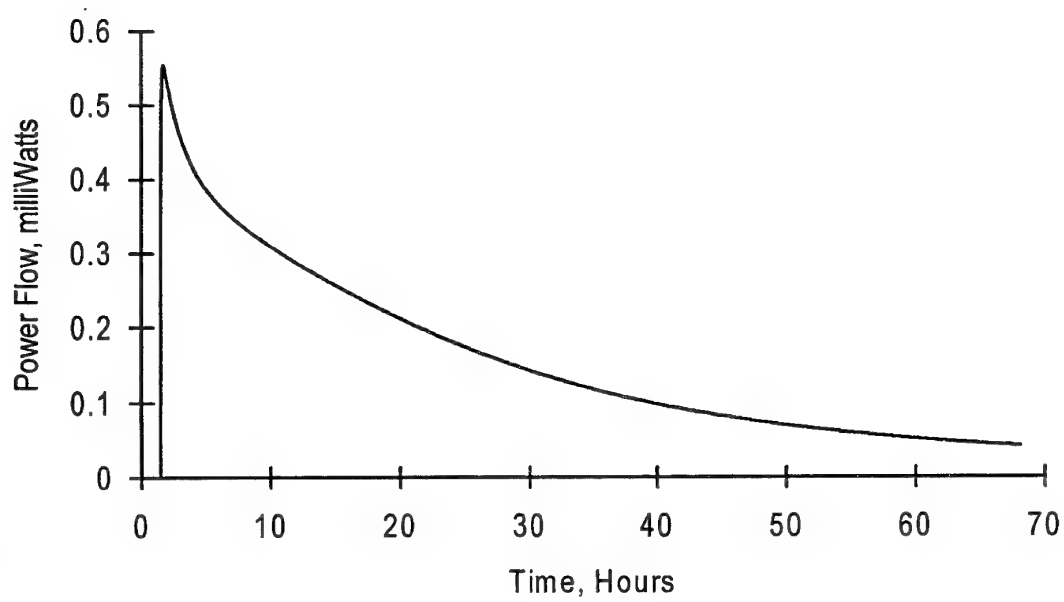


Figure 8 : Heat flow curve for unstabilised polyNIMMO with nickel hydroxide.



*Figure 9 : Heat flow curve for unstabilised polyNIMMO mixed in a ratio of 10:1 with Desmodur N100.*

## AGEING STUDIES ON THE BORON-POTASSIUM DICHROMATE SYSTEM

E.L.Charsley<sup>1</sup>, H.S.Fieldhouse<sup>1</sup>, T.T.Griffiths<sup>2</sup>, J.J.Rooney<sup>1</sup> &  
S.B.Warrington<sup>1</sup>

1. Thermal Analysis Consultancy Service, Leeds Metropolitan University,  
Calverley Street, Leeds, LS1 3HE, U.K.
2. Defence Evaluation and Research Agency, Fort Halstead, Sevenoaks,  
Kent TN14 7BP, U.K.

### SUMMARY

This paper describes a preliminary study on the ageing of boron-potassium dichromate compositions using isothermal microcalorimetry and thermal analysis techniques. Compositions containing 7% and 50% by weight of Trona boron were aged in a humidity cabinet at 50°C and 69%RH together with the components and a sample of washed boron. After ageing the samples were studied in the relative humidity perfusion cell of a microcalorimeter. The experiments were performed at 50°C and 69%RH in flowing air. Modifications to the relative humidity cell are described which have enabled problems experienced due to condensation to be reduced. Sealed ampoule microcalorimetry experiments were also carried out on aged samples in ambient air and dry argon.

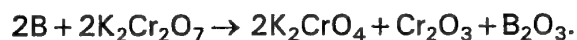
The samples were also characterised by a number of thermal analysis techniques. These included studies under ignition conditions by DSC, time to ignition measurements and the use of thermogravimetry to monitor the uptake of water. In addition, DSC under non-ignition conditions was used to study the influence of ageing on the first stage of the boron-potassium dichromate reaction.

The measurements to date show that the composition containing 7% boron aged rapidly under the chosen conditions. It was found that the initial pyrotechnic reaction, in the region of 400°C, was modified after exposure times as short as 24 hours.

## INTRODUCTION

Pyrotechnic compositions containing boron have long been recognised as suffering from ageing problems attributed to reaction of the boron with moisture and atmospheric oxygen. In the present work a preliminary study is described where isothermal microcalorimetry and thermal analysis techniques have been used to study the ageing of boron-potassium dichromate compositions and their components.

This system was chosen since earlier thermal analysis studies had shown significant changes on storage in relatively short periods of time [1]. In addition, the reaction mechanism of the system had already been characterised by thermal analysis techniques in conjunction with temperature profile analysis [2]. These latter studies showed that the reaction takes place in two stages (Figure 1). The first reaction stage, in the region of 400°C, corresponded to the reduction of the potassium dichromate to form potassium chromate. This reaction may be represented schematically by the equation:-



The second reaction stage corresponds to the reaction of the potassium chromate formed in the first stage with excess boron. This reaction was shown to be necessary for the propagation of the combustion reaction. Measurements by adiabatic combustion calorimetry showed that maximum exothermicity was achieved in the region of 20% boron content.

## EXPERIMENTAL

### Materials

For the present study boron-potassium dichromate compositions containing 7% and 50% by weight of Trona boron were used. The boron used was to specification Def. Stan. 13-128/1 with a mean particle size of  $0.6\mu\text{m}$ , as measured by a Fisher sub-sieve sizer. The potassium dichromate was to specification Def. Stan. 13-67/2. The compositions were prepared by dry blending in a Turbula mixer in the required proportions by weight.

The washed boron was prepared by washing in hot water using the method described in Def Stan 07-61/1.

### Sample conditioning

Samples were stored at  $50^{\circ}\text{C}$  and 69%RH in a non-injection humidity cabinet, the required relative humidity (RH) was achieved using a saturated solution of sodium nitrate. The RH value is taken from Reference 3. Compositions and their components were stored in Petri dishes. 90mm diameter dishes were used for 10g samples and 35mm diameter dishes for 2-3g samples to obtain approximately similar bed depths.

### Thermal Analysis Measurements

Measurement of water content of samples was carried out by heating samples in a thermobalance (Du Pont Model 951) at  $10^{\circ}\text{C min}^{-1}$  to temperatures of  $105^{\circ}\text{C}$  and  $300^{\circ}\text{C}$  and maintaining the temperature until constant weight was obtained. The former temperature corresponds to the drying temperature normally used to dry boron and the latter temperature

provides a measure of the more firmly bound water. The experiments were carried out in an argon atmosphere to avoid complications due to oxidation of the boron.

Time to ignition studies were carried out in an argon atmosphere using the apparatus described previously [4]. For this test, a furnace pre-heated to a temperature of 900°C was lowered over a 50mg sample, compressed under a 1kg dead-load, in a quartz crucible.

DSC measurements were made under ignition conditions using a heat flux DSC apparatus specially developed for pyrotechnic systems [4]. The experiments were performed in argon by heating samples, compressed under a 1kg dead-load, in quartz crucibles at 50°C min<sup>-1</sup>. A sample weight of 50mg was used for the compositions containing 7% boron and 20mg for the 50% boron compositions.

The influence of ageing on the initial pyrotechnic reaction stage, obtained under non-ignition conditions, was investigated by DSC (TA Instruments Model 2920) using the 7% boron composition. The experiments were carried out by heating 5mg samples in platinum crucibles at 5°C min<sup>-1</sup> in an argon atmosphere.

#### Isothermal Microcalorimetry Experiments

Isothermal microcalorimetry experiments were carried out using an isothermal microcalorimeter (Thermometric Thermal Activity Monitor Model 2270). In view of the uncertainty of measurements in sealed ampoules due to possible oxidation depletion effects, the main emphasis of the work has been on using the relative humidity perfusion cell (RHP), where the measurements can be carried out in a flowing atmosphere at the required humidity.

Preliminary experiments at 50°C with a humidity setting of 69% RH and an air flow rate of 100 cm<sup>3</sup> hour<sup>-1</sup>, showed very noisy heat flow traces with the presence of large spikes (Figure 2). This was attributed to condensation within the perfusion cell and indeed droplets of moisture could be seen in the gas flow outlet.

In order to address this problem, a number of modifications to the RHP system were carried out and these are shown schematically in Figure 3. The standard plastic outlet tube was replaced by a stainless steel capillary heated to a temperature in the region of 100°C by the passage of a direct current. Since it was considered likely that condensation could also take place in the top region of the perfusion cell, the temperature of the flow switch heater was increased from its recommended operating value of 60°C to 80°C and aluminium foil was wrapped around the perfusion unit to increase the heating in this region. In addition the normal gas flow path was reversed as shown, so that the outlet gas stream was shielded from any cold spots by the dry inlet gas.

In the standard apparatus, the gas is supplied to the RHP unit using a peristaltic pump this has been shown to have several disadvantages. For work in inert atmospheres it is necessary to extract the inert gas from a reservoir or from a gas stream. Additionally, there is the possibility of diffusion of air through the flexible tubing used in the pump. To avoid these problems the peristaltic pump has been replaced by an electronic mass flow controller (MKS Type 1179A). This enables stable gas flow to be achieved and allows the direct switching between air and an inert gas (normally argon). The gas supply system is shown in Figure 3 and uses molecular sieves to dry the gases and a scrubber to remove oxygen impurities from the inert gas stream. It is intended to replace the plastic tubing connecting the mass flow



controller to the RHP attachment, with metal tubing to reduce further the oxygen impurities in the gas stream.

The improvement in the heat flow signal from the RHP following the above modifications is shown in Figure 4, where it can be seen that the condensation spikes have been eliminated. It is possible to carry out experiments up to 3 days in length at 69% RH without condensation problems (this is the time taken to exhaust the water level in the upper humidifier). Recent experiments have shown that the system can be successfully operated up to a humidity setting of 100%.

Calibration of the apparatus was carried out using 200 $\mu$ l of a saturated solution of sodium nitrate and the heat flow signal has been measured as a function of humidity content. A calibration experiment is shown in Figure 5 where the RH setting has been increased in steps of 0.5%. The results are plotted in Figure 6 and it can be seen that there is an excellent linear correlation between the heat flow signal and the RH value. The calculated zero heat flow value then gives the setting required to give the desired RH, which in the experiment shown corresponded to 67.8%.

## RESULTS AND DISCUSSION

### TG Studies

The results of the TG measurements on the 50% B-50%  $K_2Cr_2O_7$  composition after storage are plotted in Figure 7, for both temperature ranges an increase in moisture levels was observed. The overall gains in weight on ageing as measured by the TG experiments were smaller than those observed by direct weighing. This indicates that not all of the water taken up by the composition was removed on heating to 300°C. Thus after 32 days the TG

measurements showed a water content of 1.3% compared with 1.7% by direct weighing.

Comparison of the measurements for the washed and unwashed boron samples show the efficiency of the washing process in reducing the moisture content of the unaged sample from 4.7% to 0.8%. Comparison of the results of ageing these samples with those of the 50% boron composition, showed a higher increase in the level of formation of firmly bound water in the latter case.

#### TTI Measurements

Measurements on the unaged composition containing 7% boron showed that ignition took place after 13.5 seconds at a temperature of about 390°C. The heating rate in the ignition region was about 1100°C min<sup>-1</sup>. The influence of ageing on the time to ignition is shown in Figure 8 and indicate that the time to ignition increases markedly with storage time up to 10 days. Further storage did not produce a significant change.

The experiments on the composition containing 50% boron gave results that fell into two groups with ignition taking place at around 8 seconds or 11 seconds. These times corresponded to temperatures of about 280°C and 360°C, respectively. The first temperature is in the region of the solid-solid transition of potassium dichromate. No significant changes in the times to ignition were observed on storage.

#### DSC Studies Under Ignition Conditions

The ignition DSC studies on the composition containing 7% boron also showed that a significant change occurred in the initial period of storage. The

ignition temperatures are plotted in Figure 9, they show an increase from 387°C to 419°C after 10 days storage. The ignition temperature would not appear to change greatly after this time, although due to the apparently low value measured at 20 days further work would be required to define accurately the curve.

Measurements on the composition containing 50% boron showed that the ignition temperature appeared to increase by some 6°C after 32 days storage. The effect of ageing was therefore much less marked than that observed with the 7% boron composition and was not concentrated in the initial period of up to 10 days.

#### DSC Studies under Non-ignition Conditions

The influence of storage on the first exothermic reaction stage is shown in Figure 10 where DSC curves are given for compositions stored for different times. It can be seen that storage for as short a period as 3.2 days has resulted in a marked change in the appearance of the DSC curve. In the unaged composition a very sharp exothermic reaction was given, with no evidence for an endothermic peak at 398°C due to fusion of the potassium dichromate. In the sample aged for 3.2 days a small dichromate fusion peak was observed and a much broader exothermic reaction was given. Increasing the storage period up to 10.6 days resulted in well defined dichromate fusion peak followed by a broad exothermic reaction with a significantly higher peak temperature. In agreement with the measurements carried out under ignition conditions the reaction was not changed markedly on further storage.

## Microcalorimetry Studies

In the Introduction it was noted that it was desirable to use the RHP cell due to uncertainties in the measurements due to oxygen depletion that could occur in sealed ampoules. This is illustrated in Figure 11 where an experiment has been carried out on sample of boron in a sealed ampoule in air at 50°C and 69% RH. It can be seen that the signal had dropped to zero after 30 days. It was shown the reduction in the signal was due to oxygen depletion, since after the ampoule had been uncapped to replenish the air and then resealed a large heat flow signal was given.

The difference between experiments carried out in the RHP cell and in sealed ampoules is shown in Figure 12 for experiments on 500mg samples of washed boron in air at 69%RH. The signal for the sample in the sealed ampoule can be seen to decrease much more rapidly than that in the RHP cell and after 80 hours was  $17\mu\text{W g}^{-1}$  compared with  $324\mu\text{W g}^{-1}$  for the sample in the RHP cell.

An RHP experiment on the 7% B-93%  $\text{K}_2\text{Cr}_2\text{O}_7$  composition, carried out over a three day period, is shown in Figure 13. It can be seen that the signal has dropped rapidly to give a slowly decreasing signal in the 10-20 hour region with a value of about  $150\mu\text{W g}^{-1}$ . The results of RHP experiments on samples aged for different periods in the humidity cabinet is shown in Figure 14. The heat flow signal has been measured after 15 hours in the RHP cell. The plot shows that, in agreement with the thermal analysis experiments, the majority of the ageing effect took place in the period up to 10 days.

In view of the small sample size needed in the DSC experiments carried out under non-ignition conditions, it is possible to make measurements

on samples that have been aged in the TAM. This is illustrated in Figure 15 which shows a DSC experiment carried out on a 5mg sample of the 7% B-93%  $K_2Cr_2O_7$  composition aged for 24 hours in the RHP cell. Comparison with the unaged sample shows the marked change that has taken place in this short time period. The technique also offers the possibility of investigating the uniformity of reaction within the RHP cell.

The influence of ageing on the composition containing 50% boron was investigated by RHP experiments on samples that had been aged for 0 and 18 days. It can be seen from Figure 16 that there appears to be little ageing effect, since the curves converged after a period of 10 hours. This is in agreement with the observations from the thermal analysis experiments.

Some experiments were also carried out on the 50% B-50%  $K_2Cr_2O_7$  composition in sealed ampoules to investigate the potential for ageing of samples in laboratory air in the absence of an external source of moisture. It can be seen from Figure 17 that both unaged and aged samples gave signals in the region of  $30\mu W g^{-1}$ , indicating that ageing could take place in samples that were sealed from external moisture. The higher signal given by the aged composition requires confirmation by further experiments, but would be consistent with the higher moisture content introduced in the ageing process.

An experiment carried out on an unaged 50% B-50%  $K_2Cr_2O_7$  composition, sealed in a dry argon atmosphere using a dry bag, is also shown in Figure 17. It can be seen that the exclusion of air from the system has markedly reduced the rate of reaction. It might however be expected that the curves would converge as oxygen depletion took place.

## CONCLUSIONS

It has been shown that it is possible to follow ageing in the boron-potassium dichromate pyrotechnic compositions, stored in air in a humidity cabinet at 50°C and 69%RH, using isothermal microcalorimetry in conjunction with a range of other thermal analysis techniques. The microcalorimetry experiments were carried out using an RH perfusion cell modified to eliminate condensation problems to enable experiments to be carried out at 50°C and 69%RH.

Experiments on a 7% B-93%  $K_2Cr_2O_7$  composition have shown that significant ageing took place on storage for periods as short as 3 days. The changes observed by the measurements in the RHP cell and the thermal analysis studies under ignition conditions show good agreement. Measurements on the fuel-rich 50% B-50%  $K_2Cr_2O_7$  composition showed that the ageing effects were much less significant than those observed with the lower boron content composition.

DSC studies under non-ignition conditions have confirmed that the ageing process influences directly the pyrotechnic reaction between boron and potassium dichromate in the region of 400°C which has been attributed to the reaction:-  $2B + 2K_2Cr_2O_7 \rightarrow 2K_2CrO_4 + Cr_2O_3 + B_2O_3$ . The sensitivity of the DSC technique also means that it is possible to make measurements on samples that have been aged directly in the RHP cell. In view of the small sample sizes used in the DSC technique, it would also be possible to use the method to investigate the uniformity of reaction within a sample in the RHP cell.

## REFERENCES

1. E.L.Charsley, T.T.Griffiths et al; unpublished work.
2. Charsley, T. Boddington, J.R. Gentle and P.G. Laye; *Thermochim. Acta*, 22 (1978) 175.
3. L.Greenspan; *J.Res. Nat. Bur. Stan. -A. Phys. and Chem.*, 81A (1977), (1), 89.
4. E.L.Charsley, S.B.Warrington & T.T.Griffiths; Development of Thermal Analysis Techniques for the Study of Pyrotechnic Systems, *Pyrotechnics*, 26th International ICT Conference, Fraunhofer-Institut Chemische Technologie, 1995, 23-1.

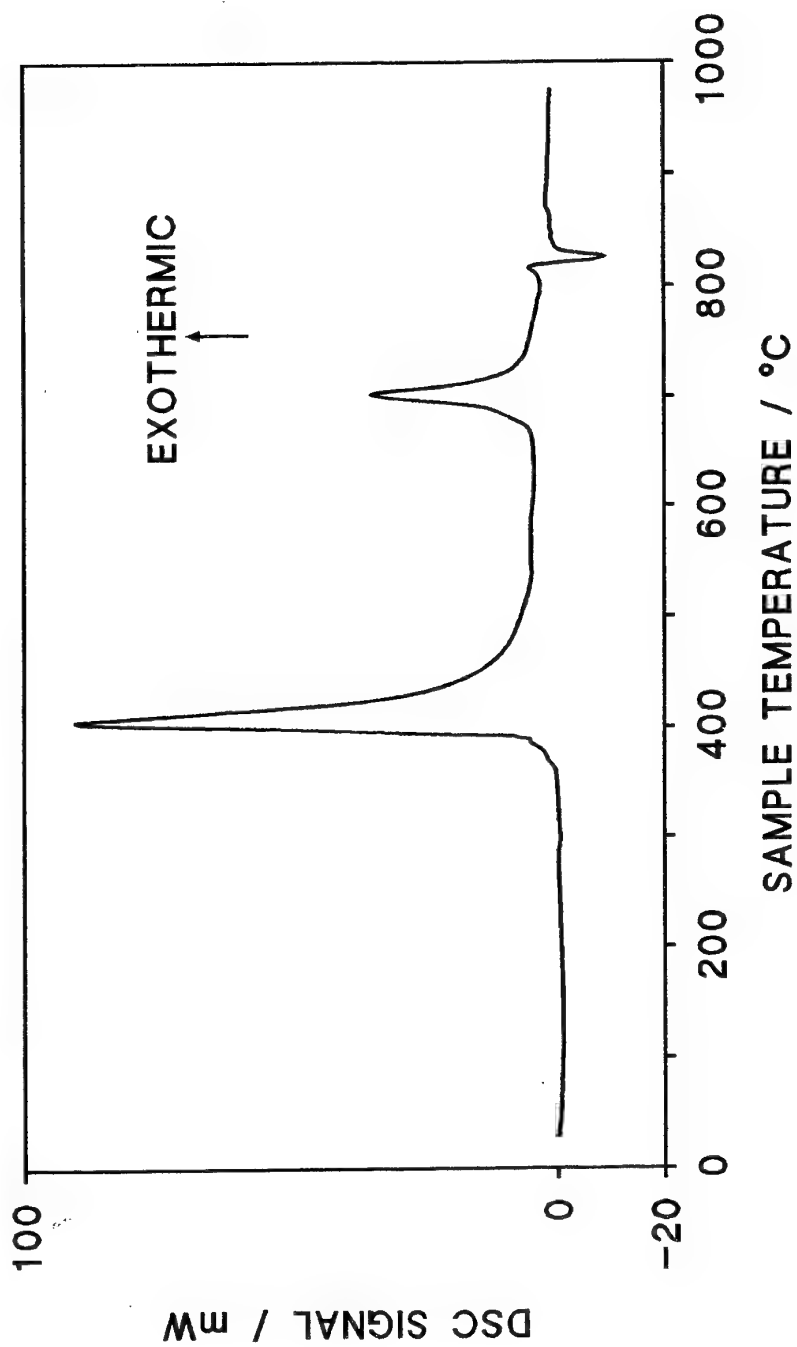


FIG. 1 HIGH TEMPERATURE DSC CURVE FOR A 7% B-93%  $\text{K}_2\text{Cr}_2\text{O}_7$  COMPOSITION  
(Sample weight, 9.9mg; heating rate,  $10^\circ\text{C min}^{-1}$ ; atmosphere, argon)



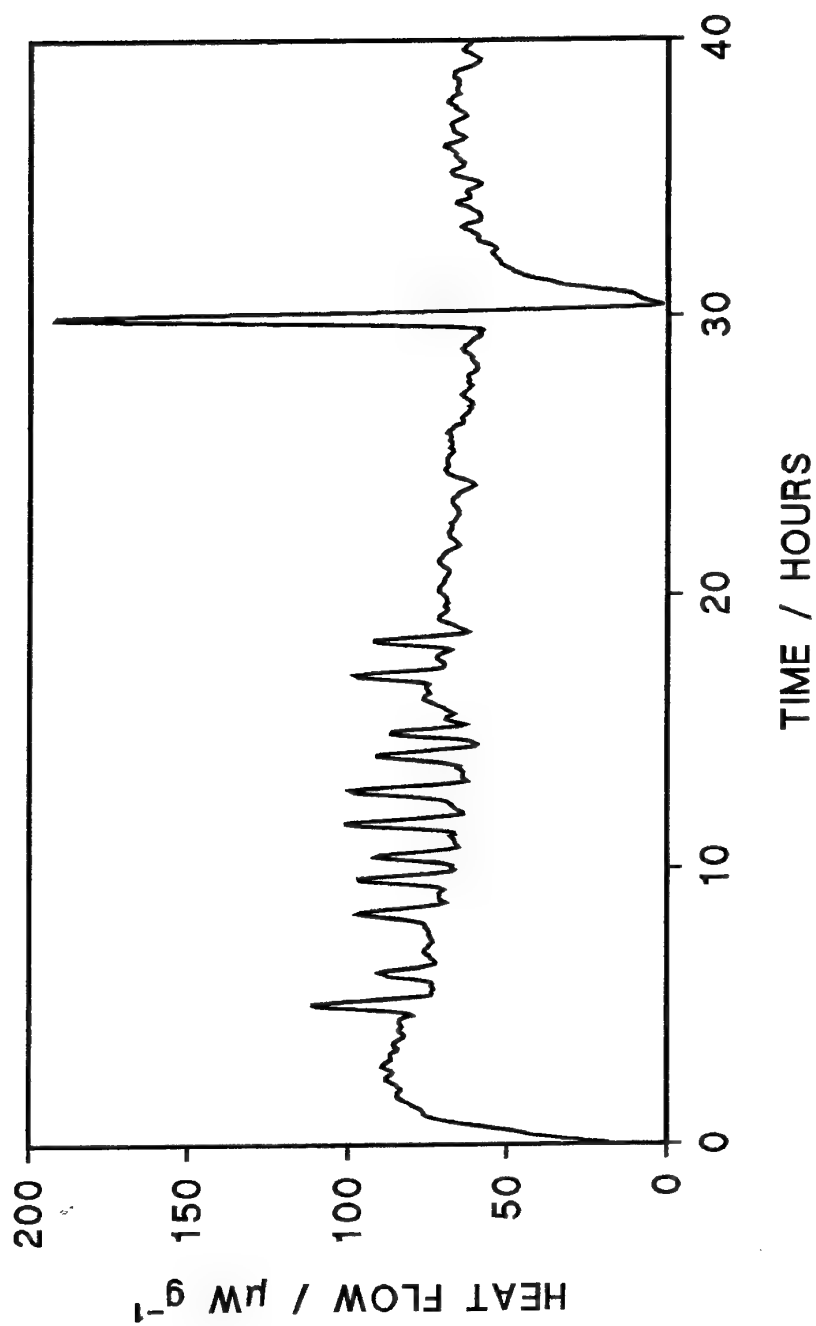


FIG. 2 MICROCALORIMETRY CURVE OBTAINED USING UNMODIFIED RHP CELL  
FOR A 50% B-50% K<sub>2</sub>Cr<sub>2</sub>O<sub>7</sub> COMPOSITION  
(Sample weight, 500mg; temperature, 50°C; 69%RH; atmosphere, air)

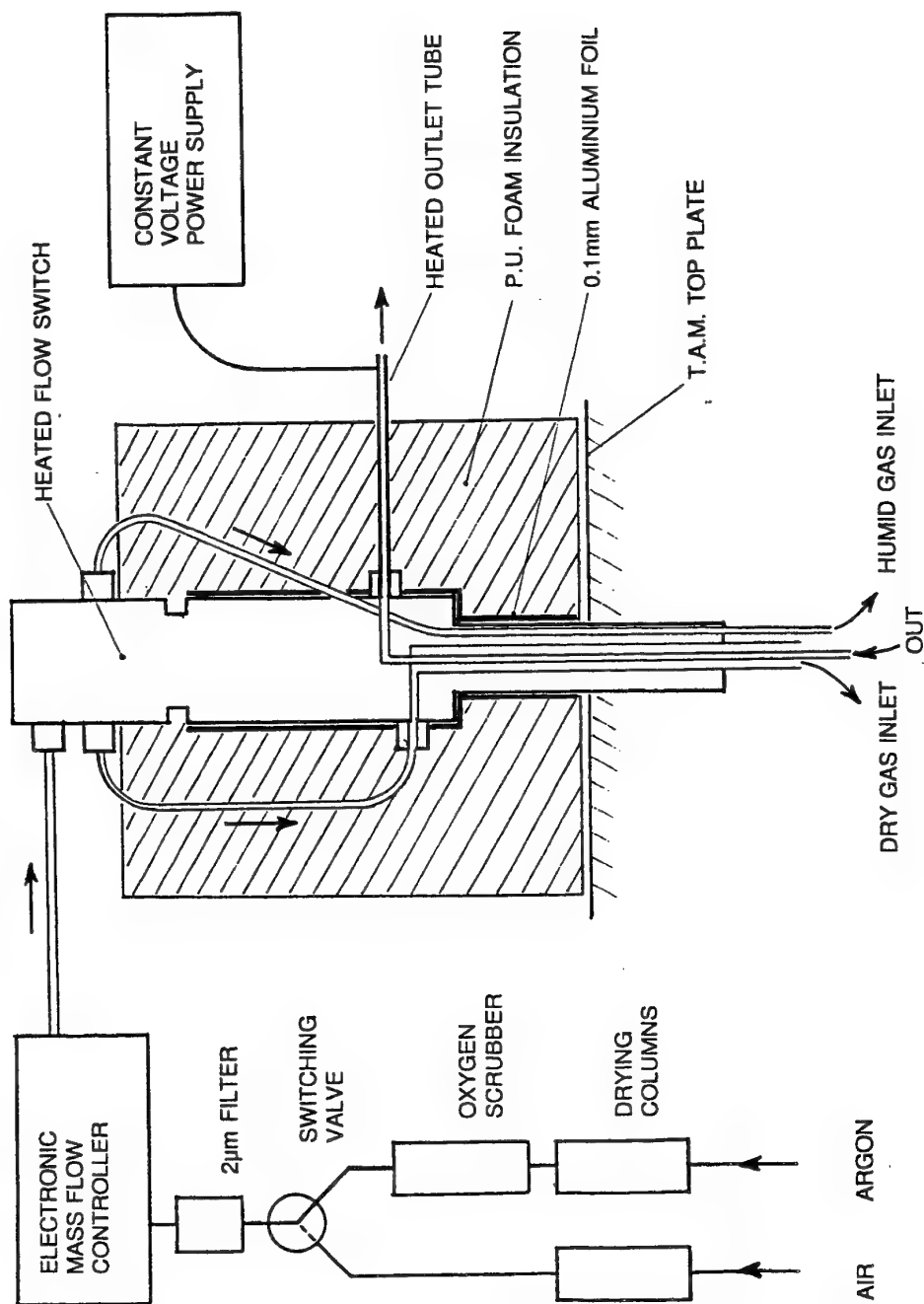


FIG. 3 MODIFICATIONS TO THE R.H.P CELL

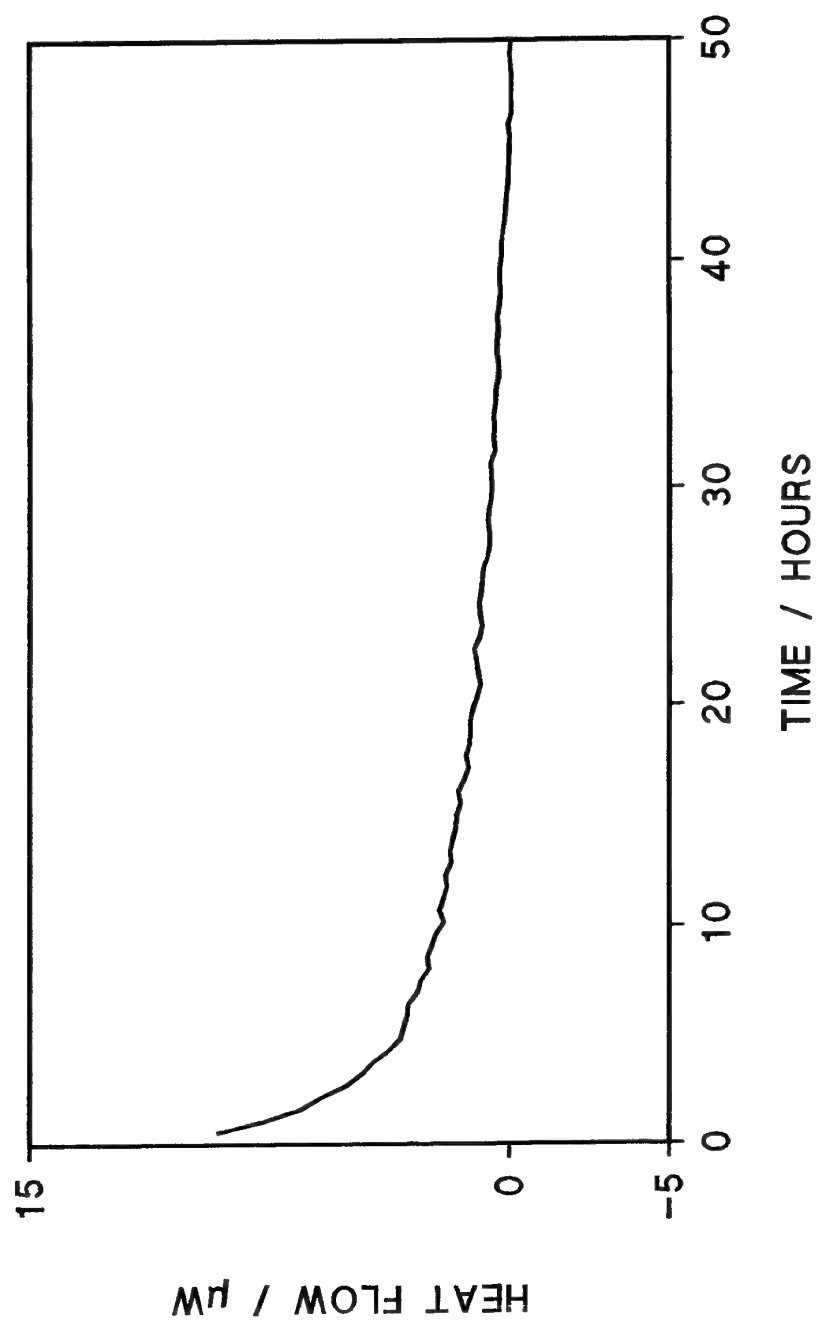


FIG. 4 SIGNAL FOR AN EMPTY STEEL AMPOULE OBTAINED USING THE MODIFIED RHP CELL  
(Temperature, 50°C; 69%RH; atmosphere, air)

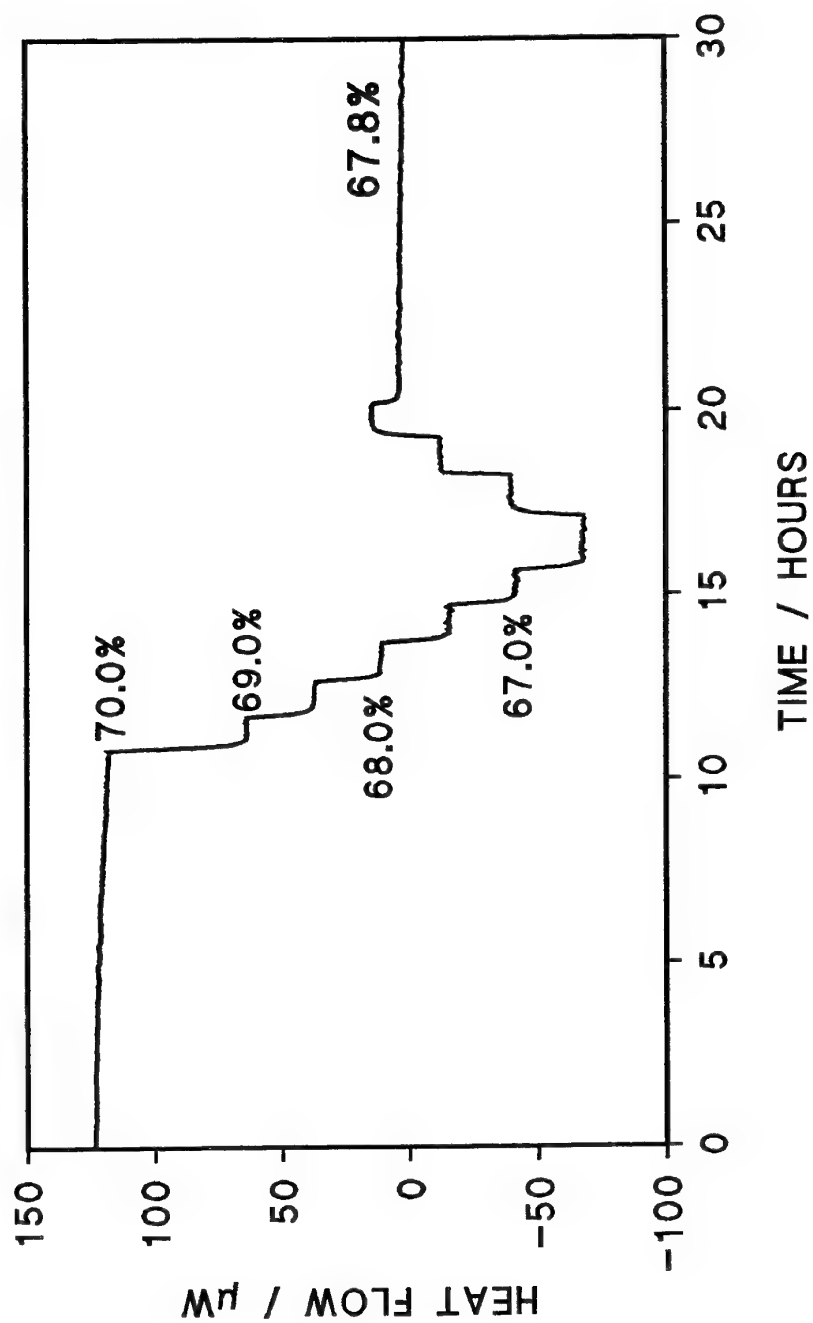


FIG. 5 CALIBRATION EXPERIMENT FOR RHP CELL USING A SATURATED  
SODIUM NITRATE SOLUTION  
(Sample volume, 200 $\mu\text{l}$ ; temperature, 50°C; atmosphere, air)

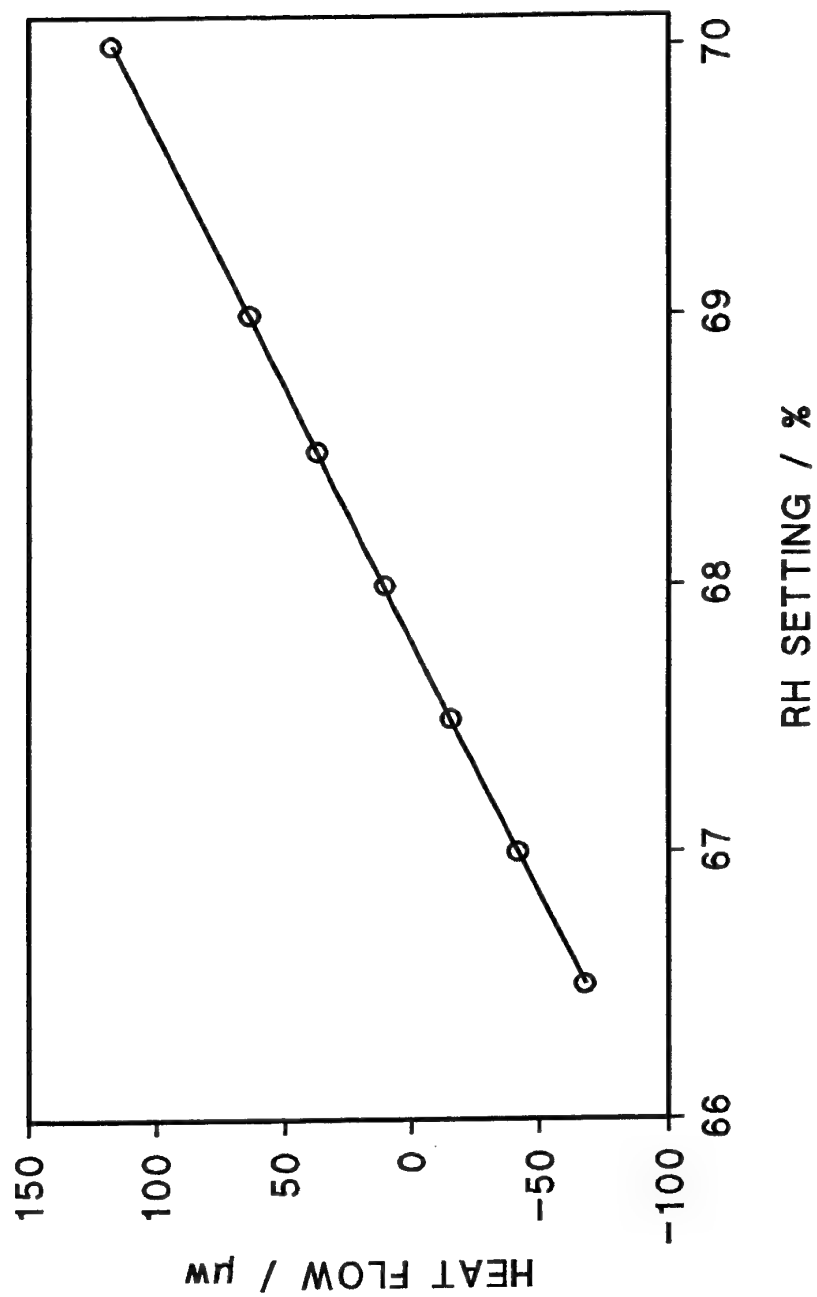


FIG. 6 PLOT OF HEAT FLOW V RH SETTING OBTAINED IN CALIBRATION  
EXPERIMENT FOR RHP CELL USING A  
SATURATED SODIUM NITRATE SOLUTION  
(Sample volume, 200 $\mu$ l; temperature, 50°C; atmosphere, air)

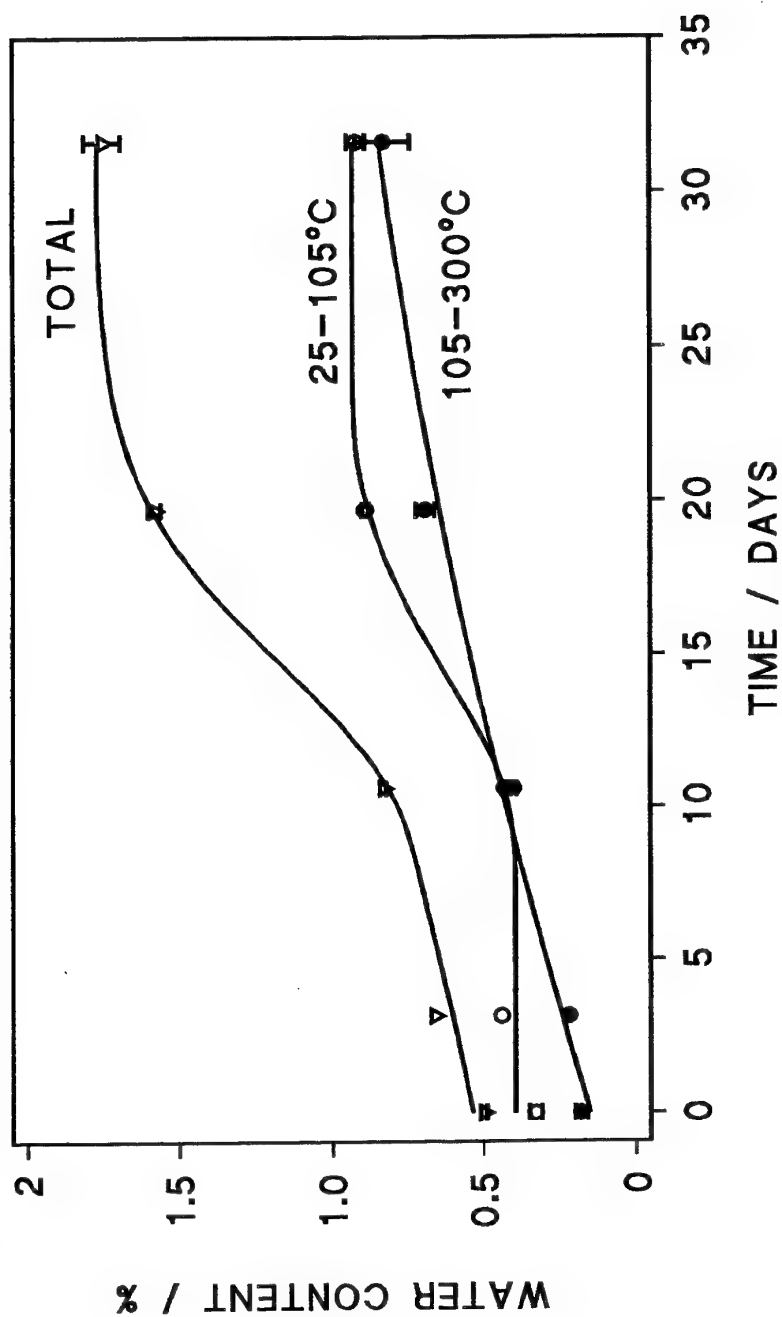


FIG. 7 TG RESULTS FOR A 50% B-50%  $K_2Cr_2O_7$  COMPOSITION  
AGED IN AIR AT 50°C AND 69%RH  
(Sample weight, 30mg; atmosphere, argon)

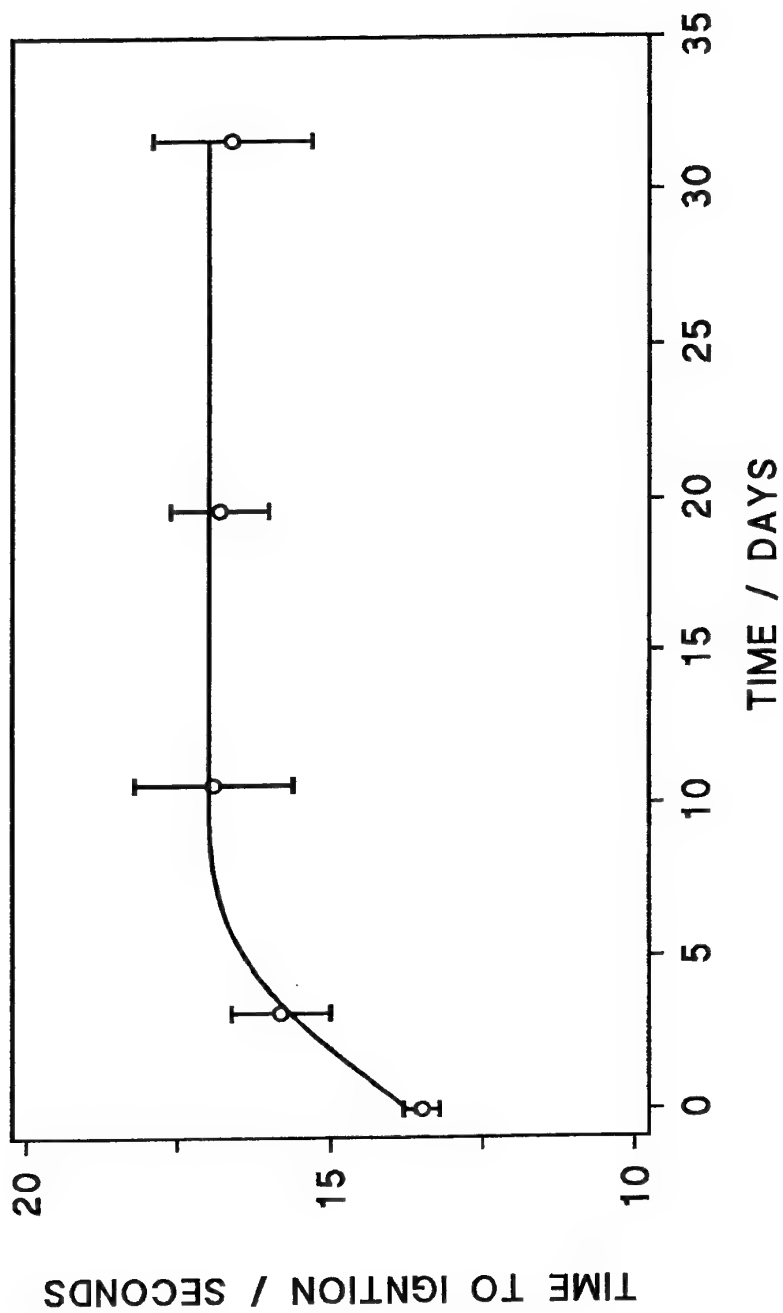


FIG. 8 TIME TO IGNITION MEASUREMENTS FOR A 7% B-93%  $K_2Cr_2O_7$  COMPOSITION  
AGED IN AIR AT 50°C AND 69%RH  
(Sample weight, 50mg; isothermal temperature, 900°C atmosphere, argon)

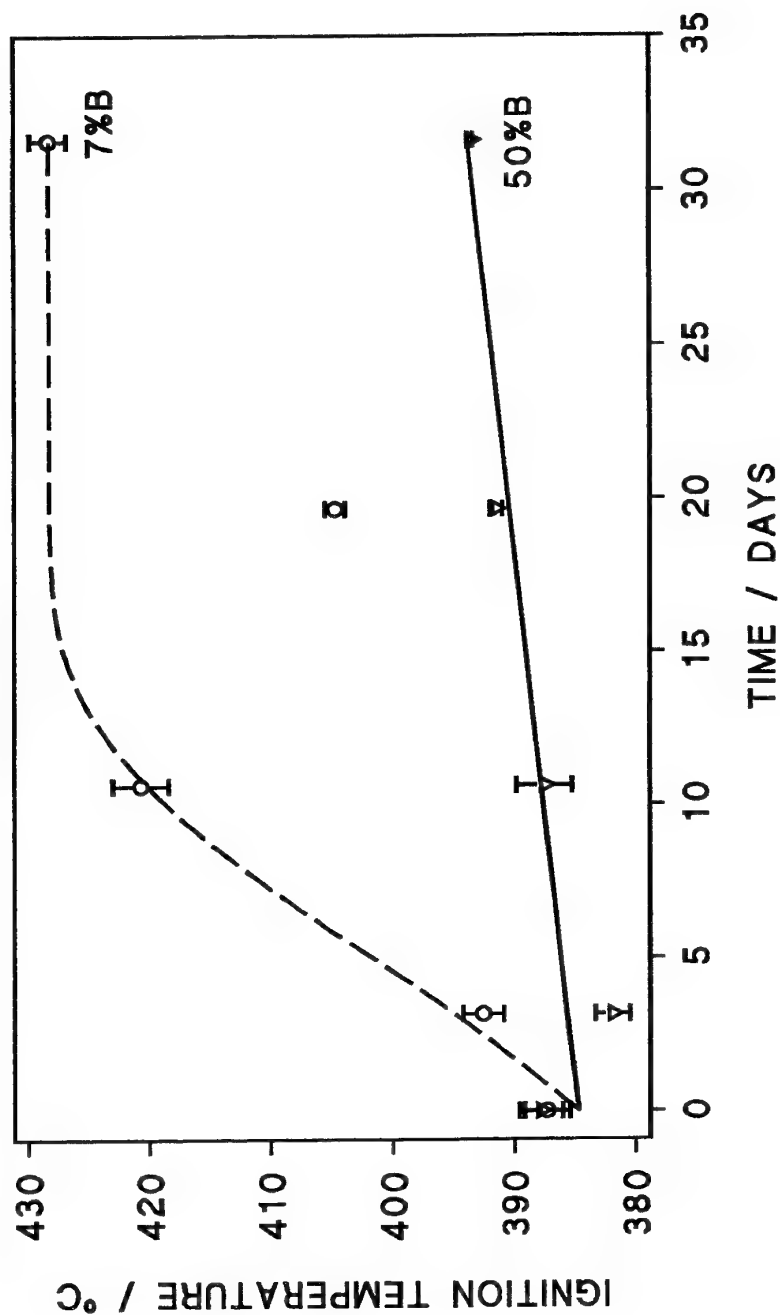


FIG. 9 DSC IGNITION TEMPERATURES FOR B-K<sub>2</sub>Cr<sub>2</sub>O<sub>7</sub> COMPOSITIONS  
AGED IN AIR AT 50°C and 69%RH  
(Heating rate, 50°C min<sup>-1</sup>; atmosphere, argon)



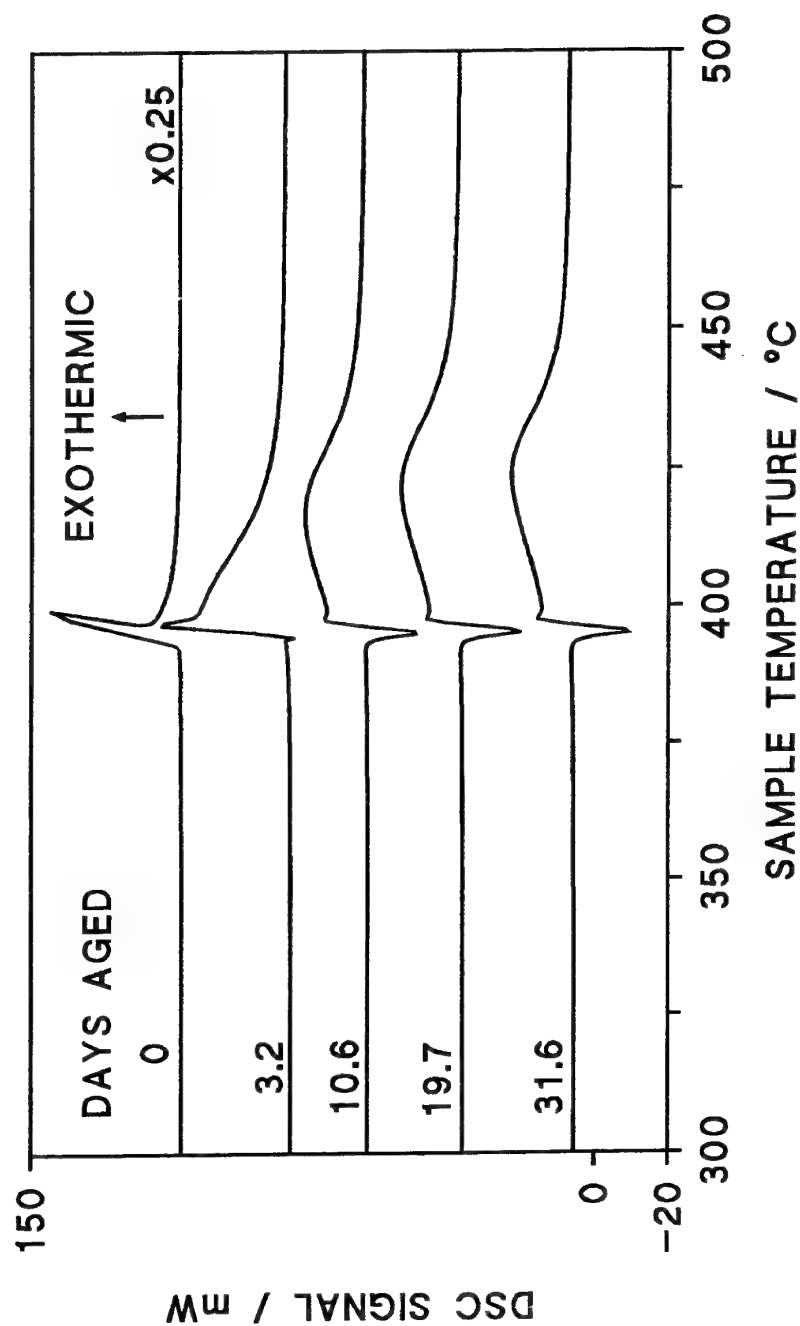


FIG. 10 DSC CURVES FOR A 7% B-93%  $K_2Cr_2O_7$  COMPOSITION AGED IN AIR AT 50°C & 69%RH FOR DIFFERENT TIMES  
(Sample weight, 5mg; heating rate, 5°C min<sup>-1</sup>; atmosphere, argon)

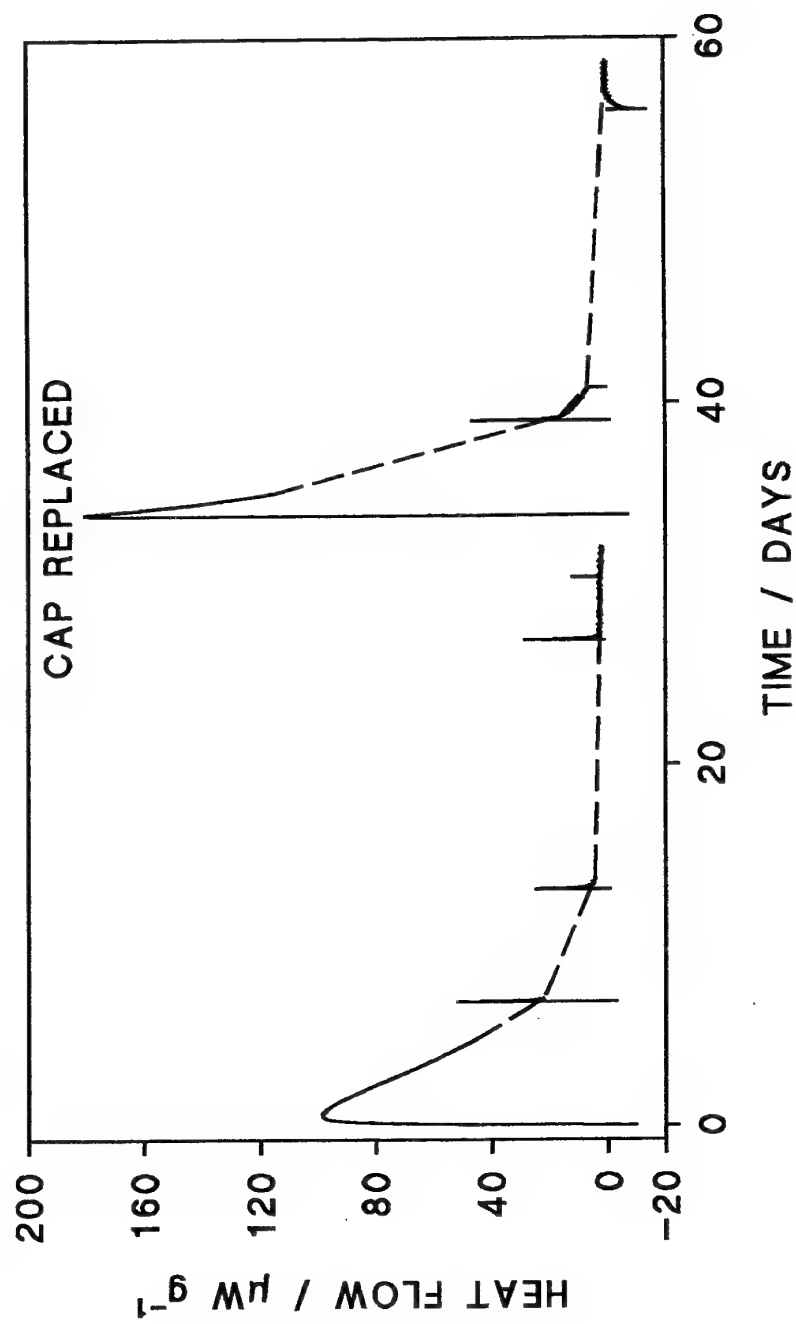


FIG. 11 MICROCALORIMETRY PLOT FOR MEASUREMENTS ON A TRONA BORON  
SAMPLE IN A SEALED AMPOULE  
(Sample weight, 500mg; temperature, 50°C; 69%RH; atmosphere, air)

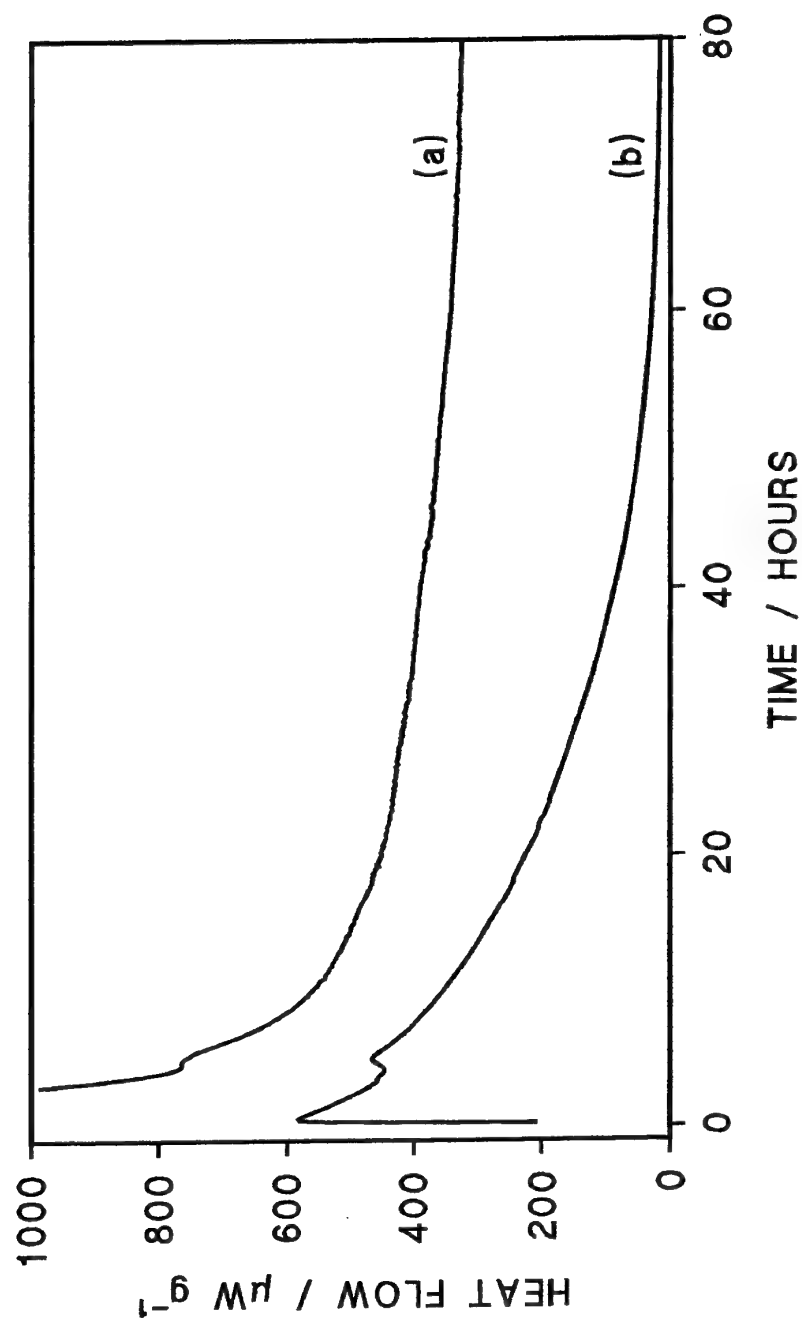


FIG. 12 COMPARISON OF MICROCALORIMETRY CURVES IN (a) RHP CELL AND (b) SEALED AMPOULE FOR WASHED SAMPLES OF TRONA BORON IN AIR AT 50°C, 69%RH

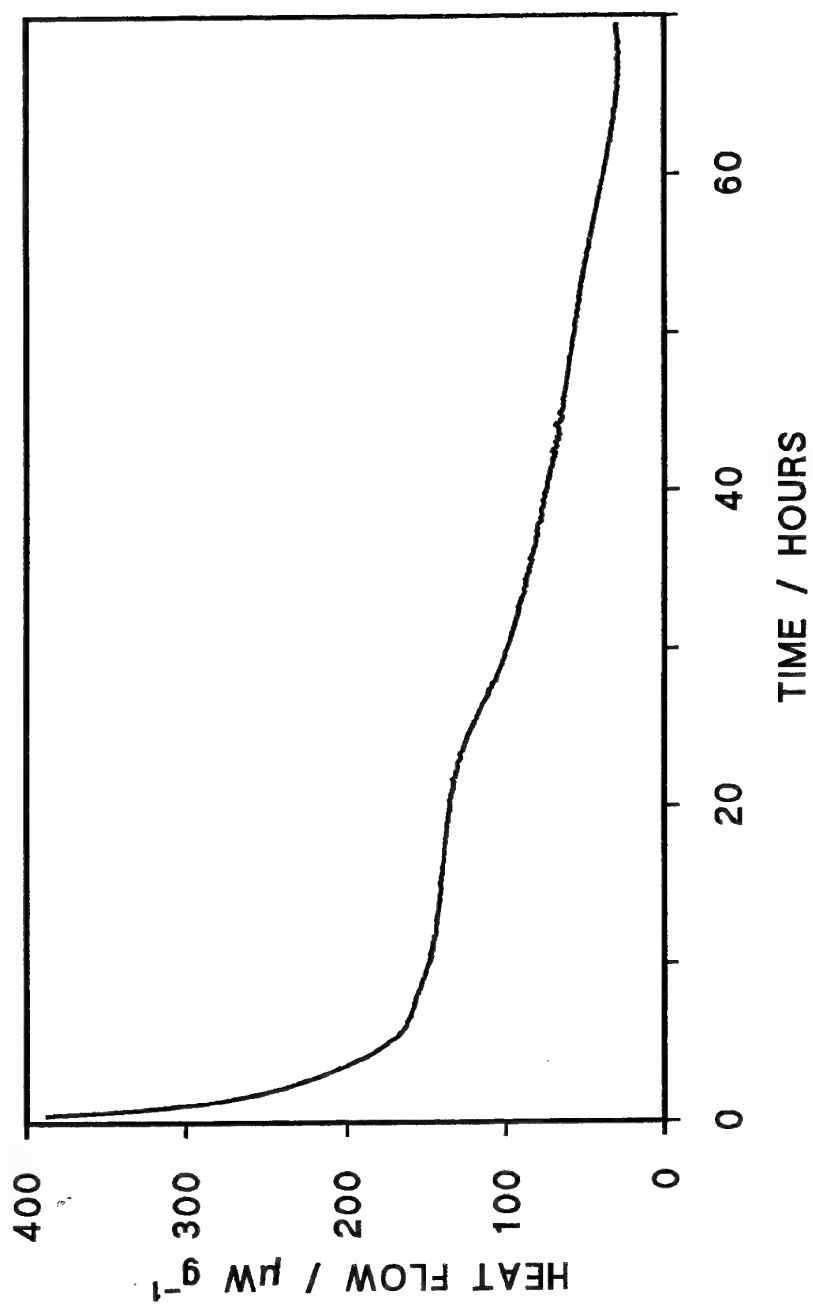


FIG. 13 MICROCALORIMETRY CURVE FOR A 7% B-93%  $K_2Cr_2O_7$  COMPOSITION  
OBTAINED USING THE RHP CELL  
(Sample weight, 557mg; temperature, 50°C; 69%RH; atmosphere, air)

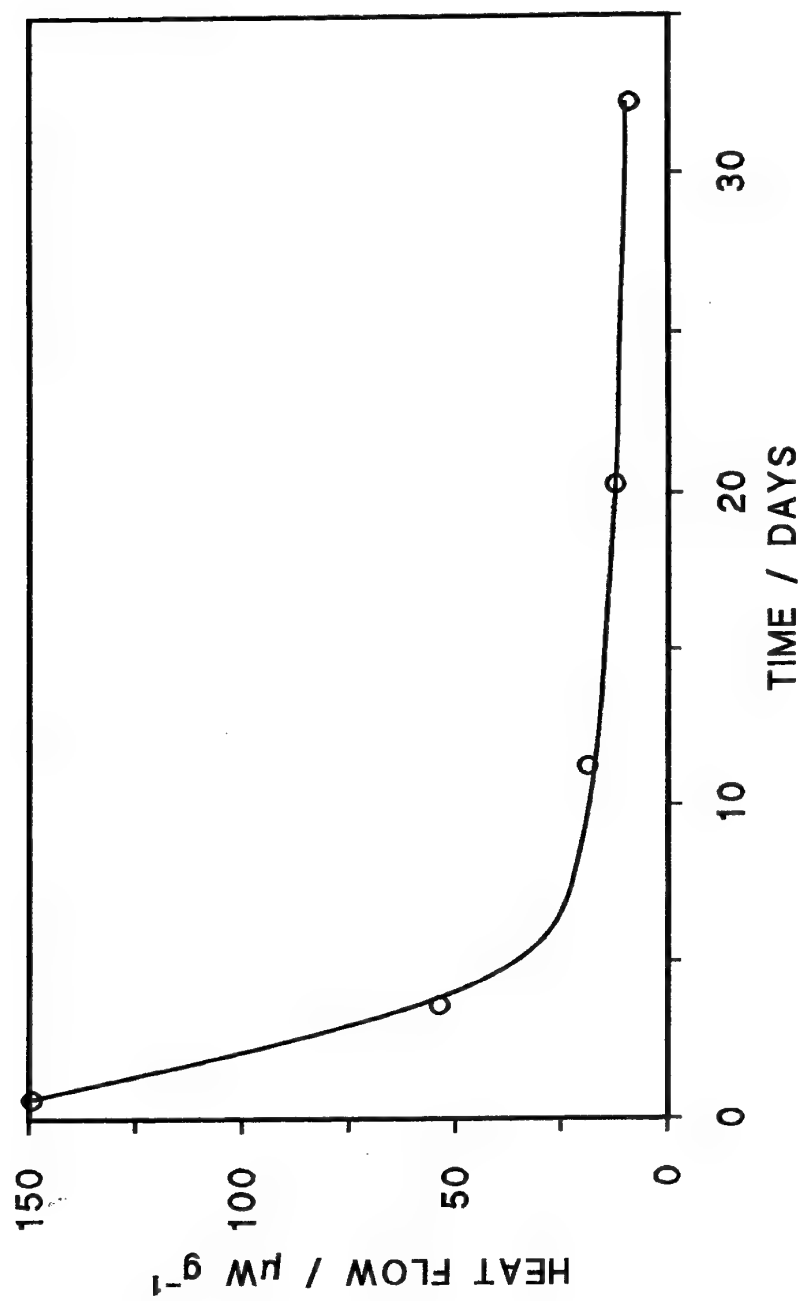


FIG. 14 MICROCALORIMETRY PLOT FOR RHP MEASUREMENTS ON A 7% B-93%  $\text{K}_2\text{Cr}_2\text{O}_7$  COMPOSITION AGED FOR DIFFERENT TIMES (Sample weight, 500mg; temperature,  $50^\circ\text{C}$ ; 69%RH; atmosphere, air)

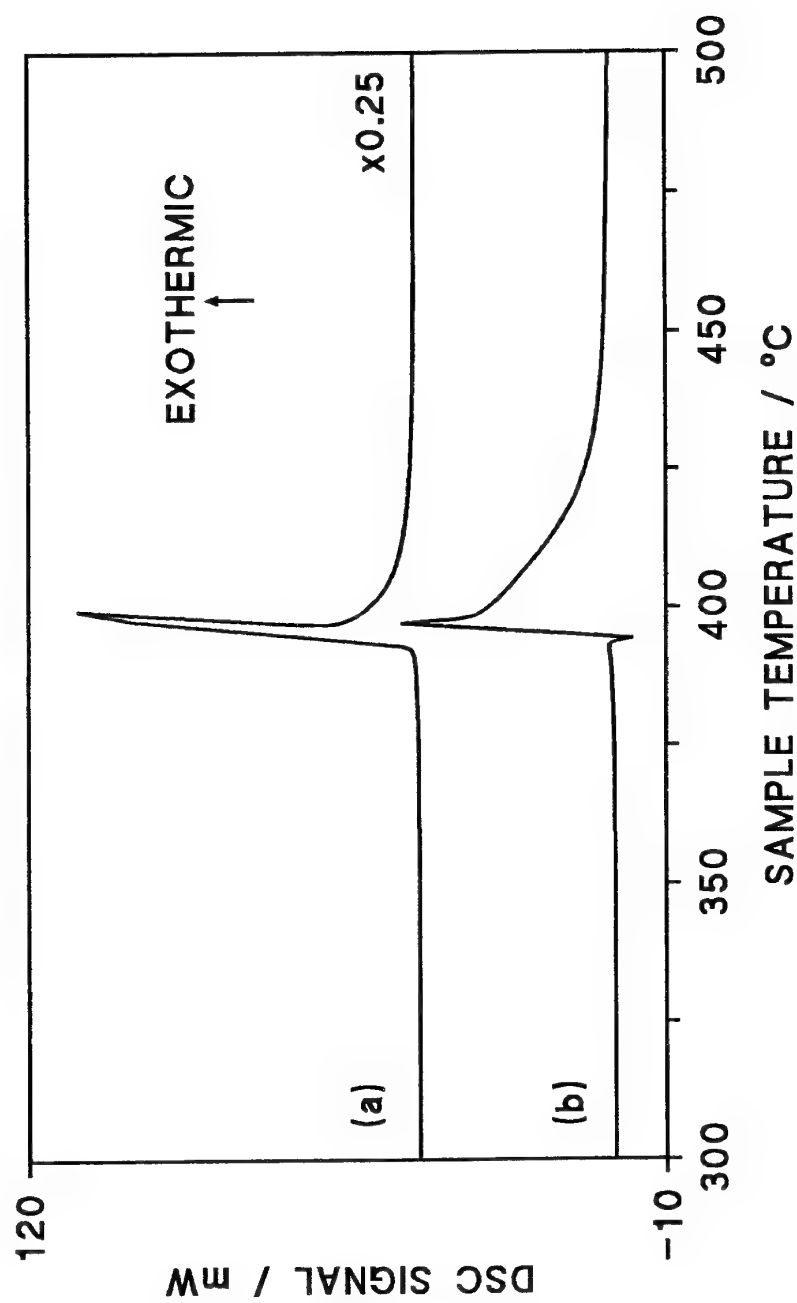


FIG. 15 DSC CURVES FOR A 7% B-93%  $K_2Cr_2O_7$  COMPOSITION (a) UNAGED AND (b) AFTER 24 HOURS IN RHP CELL IN AIR AT 50°C, 69%RH (Sample weight, 5mg; heating rate, 5°C min<sup>-1</sup>; atmosphere, argon)

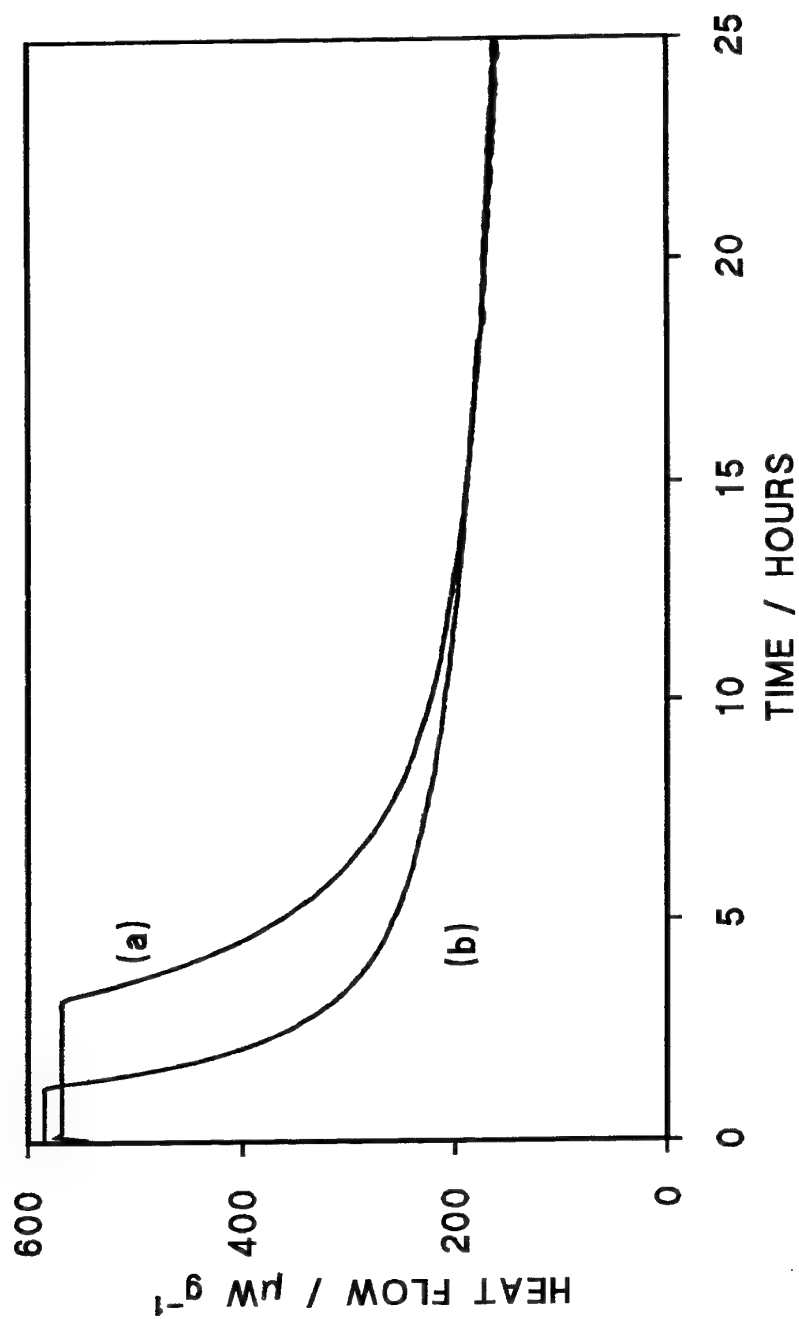


FIG. 16 MICROCALORIMETRY CURVES FOR A 50% B-50%  $\text{K}_2\text{Cr}_2\text{O}_7$  COMPOSITION  
 (a) UNAGED AND (b) AGED 18 DAYS IN AT  $50^\circ\text{C}$ , 69%RH  
 OBTAINED USING THE RHP CELL  
 (Sample weight, 500mg; temperature,  $50^\circ\text{C}$ ; 69%RH; atmosphere, air)

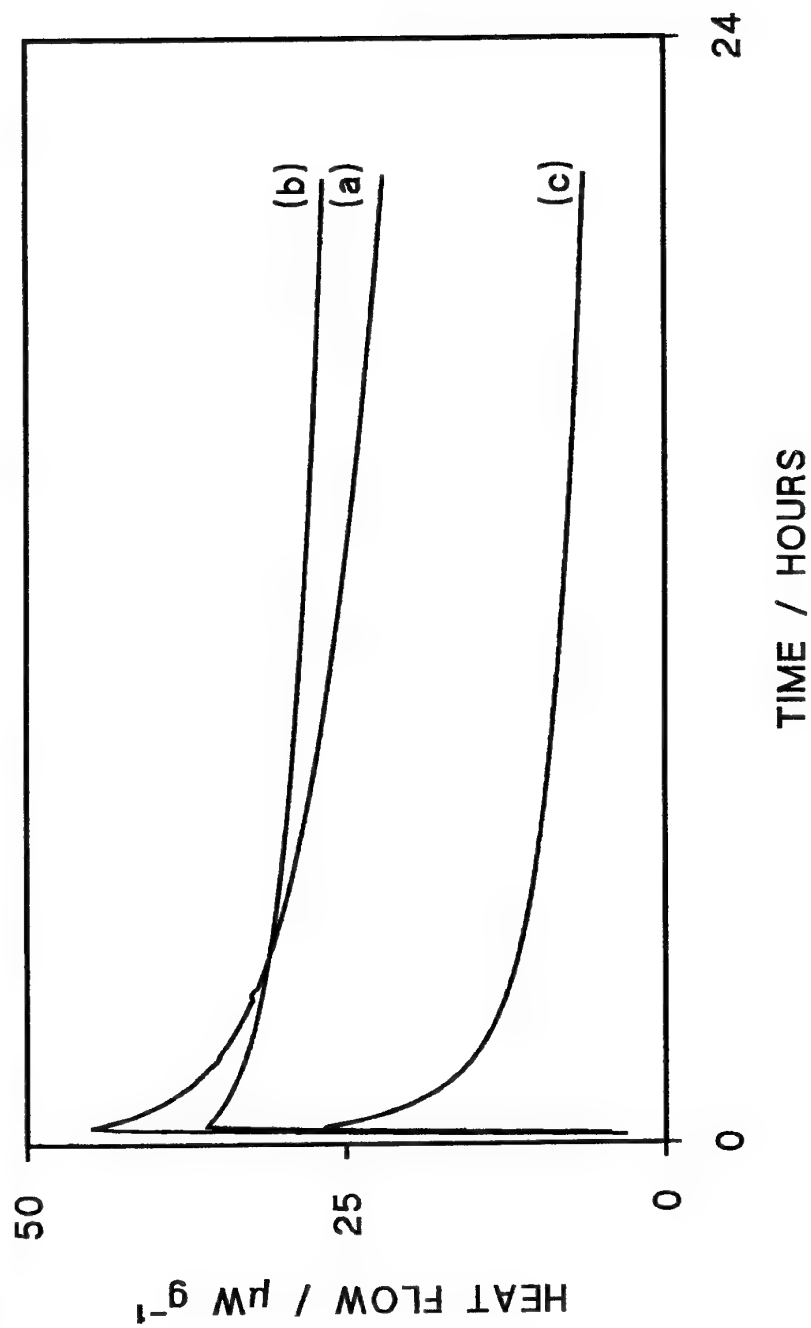


FIG. 17 MICROCALORIMETRY CURVES FOR 50% B-50%  $\text{K}_2\text{Cr}_2\text{O}_7$  COMPOSITIONS IN SEALED AMPOULES. AMBIENT AIR (a) UNAGED (b) AGED IN AIR FOR 32 DAYS AT  $50^\circ\text{C}$ , 69%RH. DRY ARGON (c) UNAGED



## PHENOMENON OF AUTOCATALYSIS IN DECOMPOSITION OF ENERGETIC CHEMICALS

Sima Chervin and Glenn T. Bodman

Health, Safety and Environment, Eastman Kodak Company,  
Rochester, NY 14652-6270

Kinetic equations of decomposition of several nitrobenzene (NB) derivatives were developed from isothermal DSC data. The mechanism of decomposition of all chemicals appeared to be autocatalytic with a slow first-order initiation reaction. Reaction orders, activation energies, and frequency factors of both (autocatalytic and initiation) reactions were determined for all chemicals. It was demonstrated that:

- utilization of a kinetic model with two parallel reactions (1st order initiation reaction and autocatalytic reaction) that have different activation energies accounts for the change in chemical behavior sometimes observed at low temperatures,
- reaction orders of the autocatalytic reaction are directly associated with the isothermal DSC curve shapes,
- elevated temperature ageing of chemicals that decompose autocatalytically results in small to very significant reductions in their subsequent thermal stability.

### INTRODUCTION

Characterization of decomposition reactions of energetic chemicals is vital for developing safe chemical manufacturing processes and assessing the stability of chemicals under various conditions, e.g., storage and transportation. Differential scanning calorimetry (DSC) is widely used for studying thermal decomposition of chemicals. Relating the experimentally obtained decomposition characteristics to safety recommendations for specific situations is a challenging process. However, when kinetic equations of decomposition developed from experimental data are available, they can be used for quantitative prediction of decomposition under a variety of conditions. This significantly increases the accuracy of thermal hazard assessment and supports the development of a safe but not overly conservative process. The kinetics of decomposition are also important in assessing the potential of materials for thermal explosion during drying, storing, shipping and handling operations.

Chemicals that decompose autocatalytically are considered more hazardous because these reactions can accelerate even under isothermal conditions during prolonged storage. Therefore, for assessing thermal hazards and determining the necessary precautionary measures, it is important to identify the decomposition mechanism. All tetrazoles studied earlier [1] appeared to have an autocatalytic decomposition mechanism with various autocatalytic reaction orders (0.7-2.2). The current study is targeted at investigating the decomposition of nitrobenzenes, and drawing generic conclusions about the phenomenon of autocatalysis.

The detailed objectives of this study were:

- determining the decomposition mechanism of the nitrobenzene chemical class,
- deriving kinetic equations for four representatives of this class that demonstrated significantly different decomposition curves in scanning DSC experiments,
- using the derived kinetic equations for predicting chemical behavior under various conditions
- establishing a relationship between the derived kinetic equations and the DSC curve shapes to provide a foundation for estimating certain kinetic parameters from DSC curve shapes,
- studying and predicting the effects of ageing of chemicals on their subsequent thermal stability.

## EXPERIMENTAL

DSC experiments were conducted using the TA Instruments Model 2910 differential scanning calorimeter. The sample size was approximately 1 mg. The sample was inserted into a glass capillary [2], after which the capillary was centrifuged and sealed under nitrogen. The DSC experiments were conducted isothermally (for at least three different temperatures) and in a scanning mode at 10°C/min heating rate. The instrument was calibrated using a dedicated 1 mg indium standard in a glass capillary at 1°C/min for the isothermal experiments and at 10°C/min heating rate for the scanning experiments. The cell constant, onset slope and temperature correction factors are automatically updated by the TA2200 DSC computer.

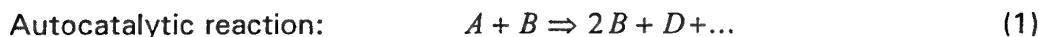
## RESULTS AND DISCUSSION

The method [1] that was used to derive kinetic equations of decomposition of nitrobenzenes is based on utilization of the results of at least three isothermal DSC experiments. Use of the isothermal technique is strongly recommended, especially for the investigation of new reactions where the reaction mechanism is not known. The advantage of an isothermal approach is greater simplicity of data interpretation, generation of more reliable kinetic data, and broader applicability. This is because the isothermal method eliminates temperature as a variable in each measurement so that the level of ambiguity in the interpretation of data is reduced. The method utilized consists of the following steps [1]:

1. Collecting experimental data in the form of heat flow versus time from isothermal DSC experiments at three or four different temperatures
2. Converting the experimental DSC data into conversion versus time data using DSC Isothermal Kinetics Data Analysis Program Part 1
3. Fitting a specific kinetic equation to the concentration versus time data using Batch CAD Rate Program
4. Calculating rate constants at the experimental temperatures using Batch CAD Rate Program
5. Determining activation energy and frequency factor from the temperature dependence of the rate constant
6. Verifying the kinetic equation by simulating decomposition of the chemical under different conditions using the derived kinetic equation and BatchCAD Reaction Program and comparing the simulation results to experimental curves.

Decomposition of four nitrobenzene derivatives was studied at several isothermal temperatures to develop kinetic equations. The overlays of the isothermal DSC curves are presented in Figures 1-4. It can be seen that all four nitrobenzenes exhibited acceleration of the heat flow rate under isothermal conditions, which indicates the reactions are autocatalytic in nature. The main characteristic feature of an autocatalytic reaction is that one of the reaction products catalyzes the reaction, hence the rate of the reaction is proportional not only to the reactant concentration, but also to the product concentration. Another feature of autocatalytic decomposition is that it requires a certain initial concentration of the catalyst present to trigger the autocatalytic reaction. The catalyst can be either introduced into the reaction zone (which is not typical for decompositions), or a parallel slow  $n$ th order reaction can generate the necessary catalyst to trigger the autocatalytic reaction. The following kinetic model will represent the described reaction mechanism.

### Reaction Scheme



### Kinetic Model

Autocatalytic reaction:  $r_1 = k_1 C_A^m C_B^n$   $k_1 = A_1 \exp(-E_1 / RT)$  (3)

Initiation reaction:  $r_2 = k_2 C_A$   $k_2 = A_2 \exp(-E_2 / RT)$  (4)

where

$C_A, C_B$  are concentrations of the reactant and the product/catalyst,  
 $r_1, r_2$  are rates of the autocatalytic and initiation reactions,  
 $k_1, k_2$  are rate constants of the autocatalytic and initiation reactions,  
 $m, n$  are reaction orders with respect to the reactant and the catalyst,  
 $E_1, E_2$  are activation energies of the autocatalytic and initiation reactions,  
 $A_1, A_2$  are frequency factors of autocatalytic and initiation reactions.

In order to derive decomposition kinetics, the following parameters of the model have to be determined for each chemical:  $n, m, E_1, A_1, E_2, A_2$ . The calculations were performed using the isothermal DSC experiments for each chemical (Figures 1-4) according to the method previously reported for tetrazoles [1]. The derived kinetic equations were verified by predicting decomposition in a scanning DSC experiment (for all chemicals), isoageing and subsequent decomposition of the residues (for three chemicals), and decomposition in accelerating rate calorimeter (for one chemical). All parameters of the derived kinetic models for the four chemicals are summarized in Table 1.

Table 1. Kinetics of Decomposition of Nitrobenzene Derivatives

Chem #	Mol Wt	Autocatalytic Reaction				Initiation Reaction	
		$m$	$n$	$E_1, \text{ kJ/mol}$	$A_1, \text{ s}^{-1}$	$E_2, \text{ kJ/mol}$	$A_2, \text{ s}^{-1}$
1	279	2.3	1.5	118	$1.38\text{e}+10$	172	$9.84\text{e}+11$
2	202	0.5	1.8	113	$5.28\text{e}+6$	157	$3.23\text{e}+10$
3	141	0.6	0.8	149	$1.67\text{e}+9$	294	$2.58\text{e}+19$
4	202	0.6	0.6	128	$6.80\text{e}+8$	155	$3.20\text{e}+4$

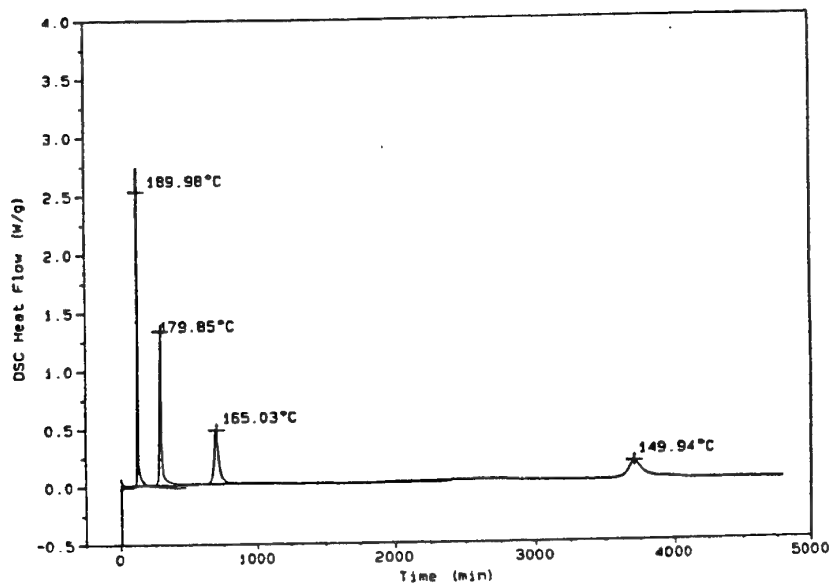


Fig. 1 Isothermal DSC curves of 2-benzyloxy-5-chloro-4-nitroaniline (Chemical 1) decomposition at four temperatures.

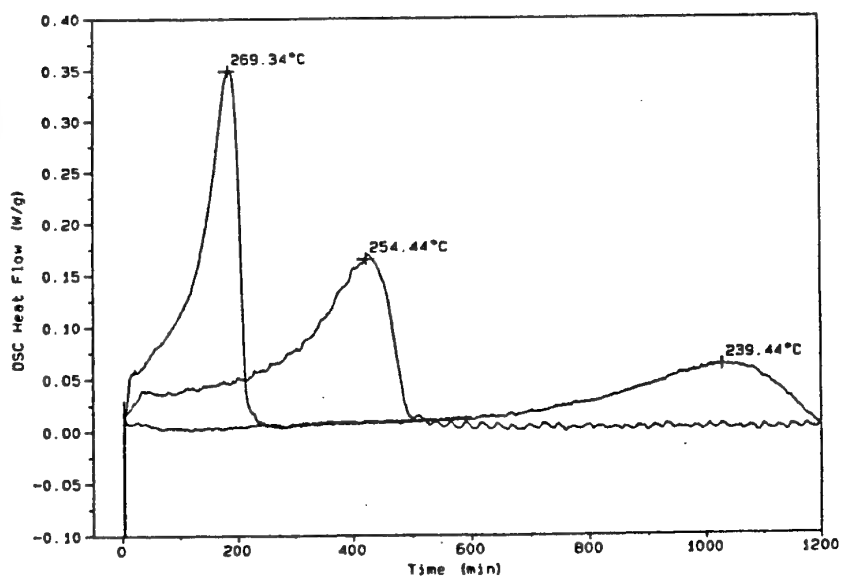


Fig. 2 Isothermal DSC curves of 3-chloro-4-nitrobenzoic acid (Chemical 2) decomposition at three temperatures.

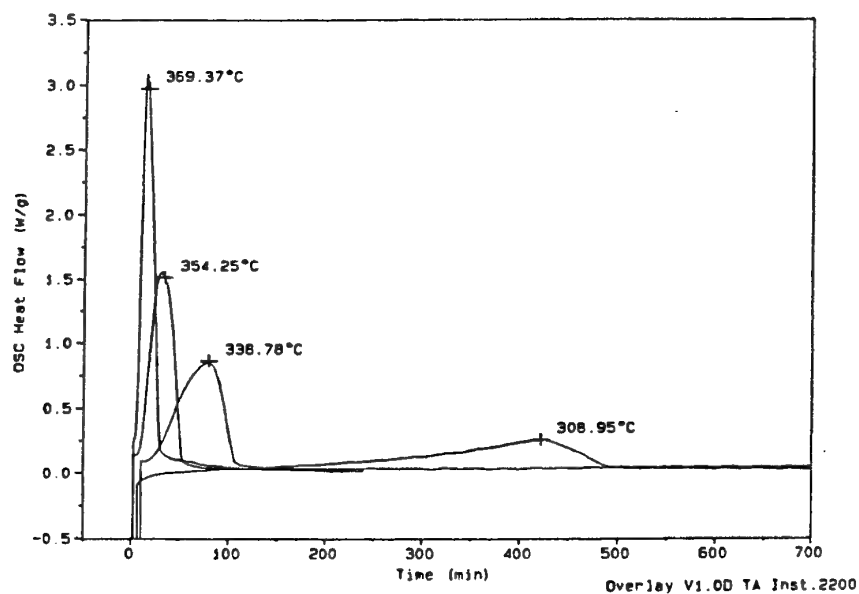


Fig. 3 Isothermal DSC curves of p-fluoronitrobenzene (Chemical 3) decomposition at four temperatures.

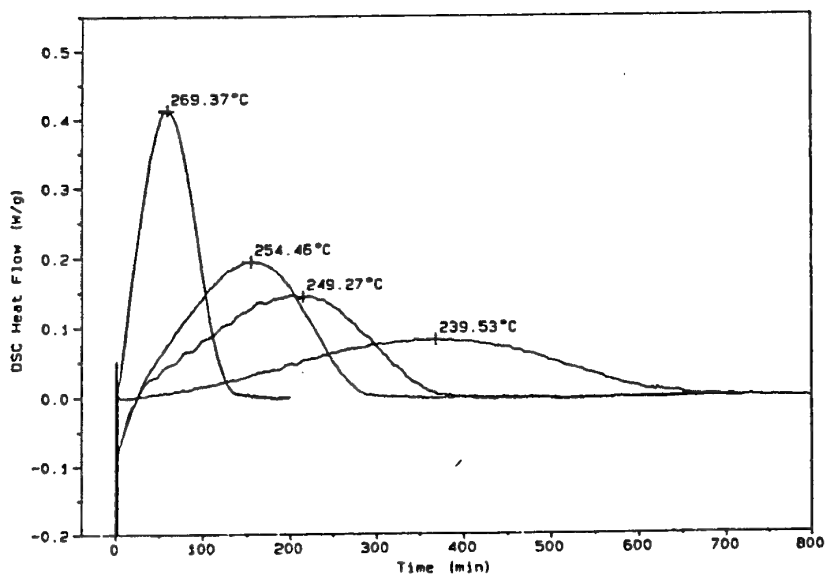


Fig. 4 Isothermal DSC curves of 5-chloro-2-nitrobenzoic acid (Chemical 4) decomposition at four temperatures.

### *Relationship Between the Decomposition Kinetics and DSC Curve Shape*

Kinetic models allow prediction of thermal response under widely different conditions. Isothermal DSC curve shape is indicative of decomposition kinetics. Understanding the relationship between the kinetics and isothermal curve shape may allow screening level prediction of plant hazards from isothermal DSC curves. Following are some examples of the relationship between isothermal DSC curve shape and the associated kinetic models.

For instructional purposes an overlay plot (Figure 5) was prepared showing a single isothermal DSC curve for each of the four nitrobenzenes. For decompositions with high reaction orders ( $m, n > 1$ ) the isothermal heat flow curve will yield a narrow and sharp peak, which will have a concave curvature of its onset and return to baseline regions (Figure 1, 5-curve 1). These decomposition reactions usually have a distinct, long induction period with no measurable heat flow, after which the decomposition starts to accelerate and goes to completion in a relatively short period of time. For autocatalytic decompositions with reactant ( $m$ ) and catalyst ( $n$ ) reaction orders less than one, the isothermal heat flow curve will yield a broader shallow (dome-shaped) peak, which will have a convex curvature of its onset and return to baseline regions (Figure 4, 5-curve 4). These decomposition reactions usually start to occur as soon as the chemical is exposed to an elevated temperature without any significant induction period.

A symmetrical isothermal heat flow curve (Figure 4) is an indication of autocatalytic decomposition with equivalent reaction orders with respect to the catalyst and the reactant ( $m = n$ ). Asymmetric curves result from autocatalytic decompositions for which there are significantly different reactant ( $m$ ) and catalyst ( $n$ ) reaction orders. As an example, curve 2 (Figure 5) illustrates the case when  $n \gg m$ , which results in a long, gradual leading edge of the decomposition exotherm followed by a sharp return to baseline. The mirror image of curve 2 (Figure 5) is possible when  $m \gg n$ .

A measurable positive heat flow at the very beginning of isothermal DSC experiments indicates that the initiation reaction ( $r_2$ ) has a relatively high rate under experimental conditions and occurs simultaneously with the autocatalytic decomposition throughout the experiments (Figures 2, 3, 5, curves 2, 3). This means that the heat flow curve recorded during isothermal or regular DSC experiments is a combination of rates of two competing reactions: initiation and autocatalytic, whose ratio can change depending upon their activation energies and experimental conditions. The

exact rate of the initiation reaction throughout the isothermal and scanning DSC experiments of Chemical 2 can be seen on its simulated decomposition curves (Figures 6, 7). It is clear from the scanning DSC reaction rate plot that the autocatalytic reaction became measurable only at temperatures higher than 330°C, when the overall reaction rate curve began to deviate from the initiation reaction rate curve. It was predicted that a large part of the chemical decomposed by the initiation reaction during the scanning DSC experiment (40%), as well as the isothermal DSC runs (19-24%). At reduced isooage temperatures the predicted amount of chemical decomposed by the initiation reaction would decrease. This would occur because the higher activation energy of the initiation reaction would cause a more rapid decrease in the reaction rate with temperature. Theoretically at a low enough temperature the entire reaction would occur according to the autocatalytic mechanism, and at a high enough temperature the initiation reaction could be dominant. This would dramatically alter the decomposition heat flow curve, which could be wrongly interpreted as a change in reaction mechanism. In DSC runs at higher scanning rates, the percentage of the chemical decomposed by the initiation reaction would be higher.

By analyzing the overlay of scanning DSC curves of the four nitrobenzenes (Figure 8), we can see that similar information about autocatalytic reaction orders could be obtained from the scanning DSC curves (assuming we know that decomposition mechanism is autocatalytic). Curve 1 would represent high reaction orders, curve 4 would represent low and equal reaction orders, curve 2 would represent a low reactant and a high catalyst reaction order. However, to distinguish between the relative rates of the initiation and autocatalytic reactions and to determine the effect of the initiation reaction on the overall reaction rate does not appear to be possible from the scanning DSC curves.

The existing opinion is that the scanning DSC curve shapes are related to the activation energies of decomposition reactions, i.e., high activation energy reactions yield a narrow, sharp peak of significant heat flow in a scanning DSC test and low activation energy reactions yield a broad, shallow peak in the same test. For autocatalytic decompositions, it appears that the reaction orders of the autocatalytic reaction have an even greater effect on the DSC curve shape.



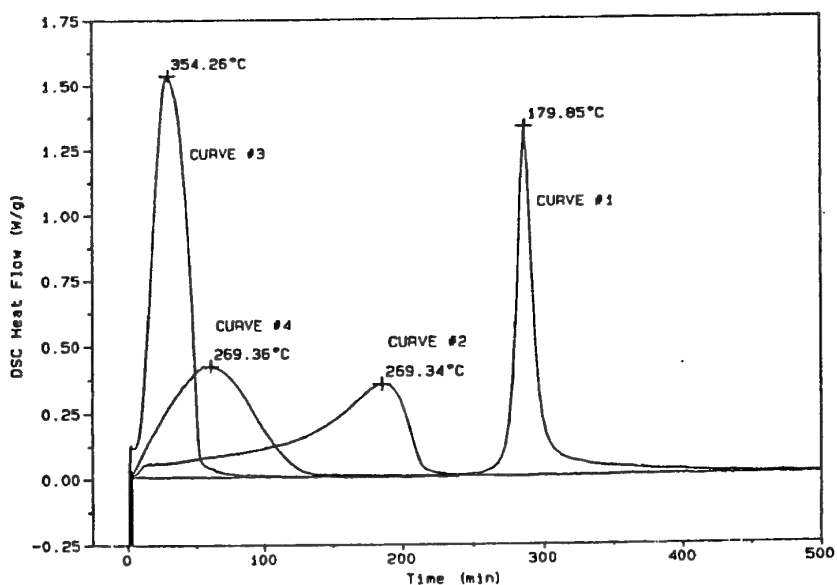


Fig. 5 Overlay of isothermal DSC curves of four nitrobenzenes: curve 1 - 2-benzyloxy-5-chloro-4-nitroaniline, curve 2 - 3-chloro-4-nitrobenzoic acid, curve 3 - p-fluoronitrobenzene, curve 4 - 5-chloro-2-nitrobenzoic acid (isothermal test temperatures are printed with each curve).

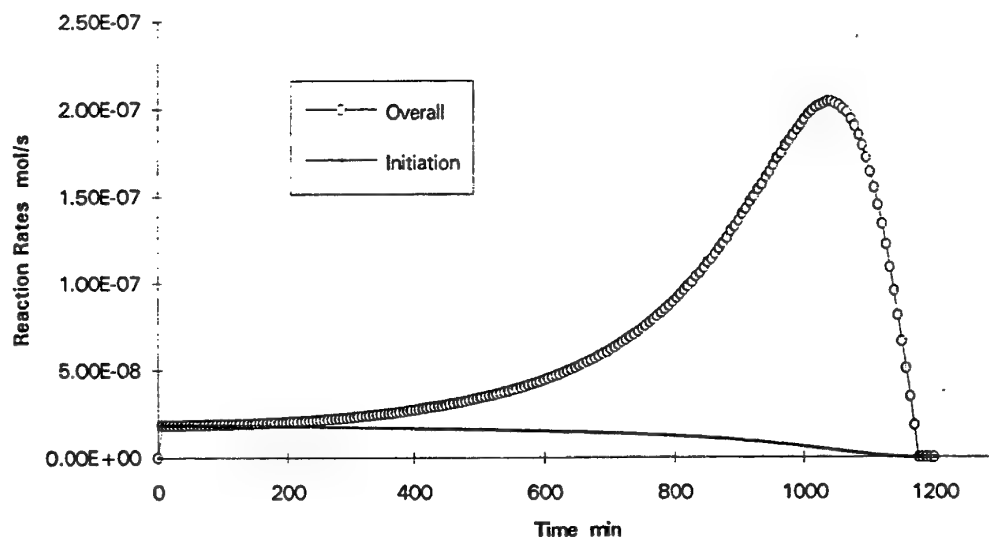


Fig. 6 Simulated rates of the initiation and overall reactions during isothermal DSC test at 241°C of 3-chloro-4-nitrobenzoic acid (Chemical 2).

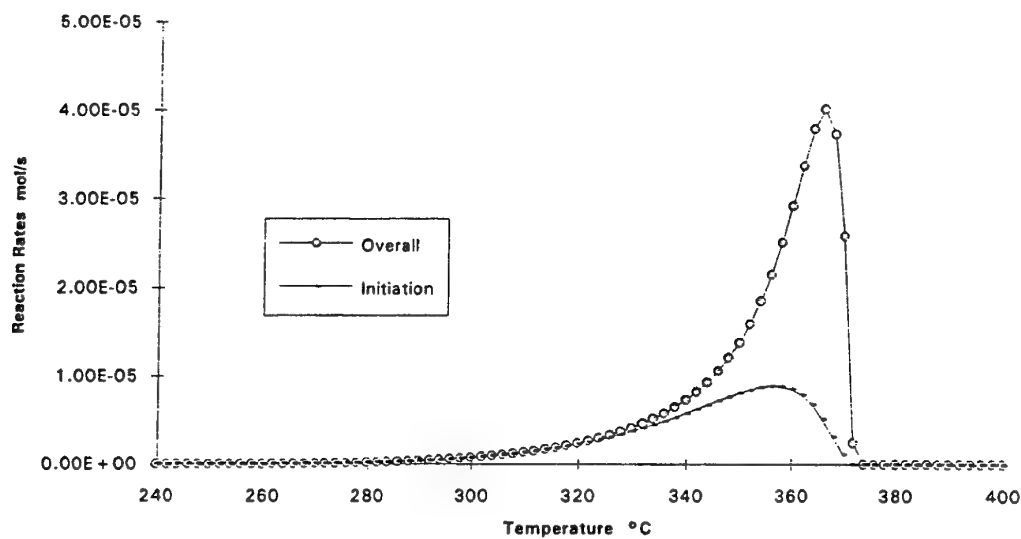


Fig. 7 Simulated rates of the initiation and overall reactions during a scanning DSC test of 3-chloro-4-nitrobenzoic acid (Chemical 2).

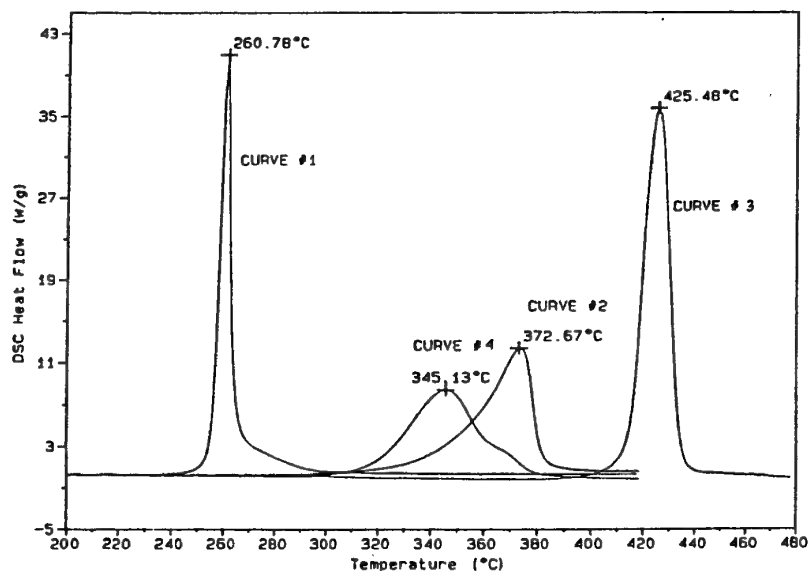


Fig. 8 Overlay of scanning DSC curves of four nitrobenzenes: curve 1 - 2-benzyloxy-5-chloro-4-nitroaniline, curve 2 - 3-chloro-4-nitrobenzoic acid, curve 3 - p-fluoronitrobenzene, curve 4 - 5-chloro-2-nitrobenzoic acid (decomposition peak temperatures are printed with each curve).

### *Effect of Low-Temperature Ageing of Chemicals on Their Subsequent Thermal Stability*

Chemicals that decompose autocatalytically are susceptible to thermal ageing effects to varying degrees. Understanding these effects in detail becomes increasingly important as longer and more adiabatic operations are considered, or when the thermal history of a raw material is not well defined.

An interesting phenomenon was observed from the testing of the residues obtained from isothermal experiments of Chemicals 1 and 2. The scanning DSC on the residues showed lower decomposition onset and peak temperatures (Figures 9, 10). This demonstrates that, although there was no measurable reaction during the low-temperature isothermal runs, a slow decomposition was occurring and a certain amount of the catalyst was produced. Hence, when the samples were subjected to elevated temperatures during the scanning DSC experiments on the residues, the catalyst accelerated the decomposition and shifted its onset to lower temperature.

Both isoages were simulated using the derived kinetic equations of decomposition and the amount of the catalyst that could have been formed during the isoages was determined. These catalyst concentrations (3% for Chemical 1 and 30% for Chemical 2) were assumed to be present prior to the scanning DSC measurements of the respective isoage residues. Simulated scanning DSC curves assuming different concentrations of the catalyst at the beginning of the experiments (from 0 to 30%) were overlaid with the original (unaged sample) curve in Figures 11, 12 to study the effect of the initial catalyst concentration on the thermal stability of these chemicals. In Figure 11, the original curve and the 3% catalyst concentration curve should be compared to the curves presented in Figure 9. In Figure 12, the original curve and the 30% catalyst concentration curve should be compared to the curves presented in Figure 10. Both simulations predict the experimental results quite accurately.

The predicted changes in scanning DSC decomposition parameters of the nitrobenzenes as a function of the concentration of the catalyst present at the beginning of the simulated scanning DSC experiment are summarized in Table 2.

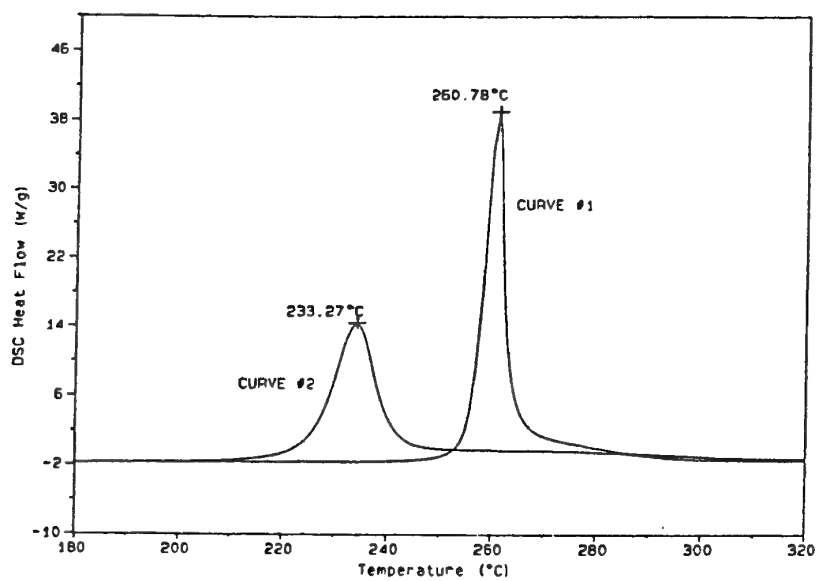


Fig. 9 Overlay of scanning DSC curves of the original (curve 1) and isoaged at 155°C for 48 hours (curve 2) samples of 2-benzyloxy-5-chloro-4-nitroaniline (Chemical 1).

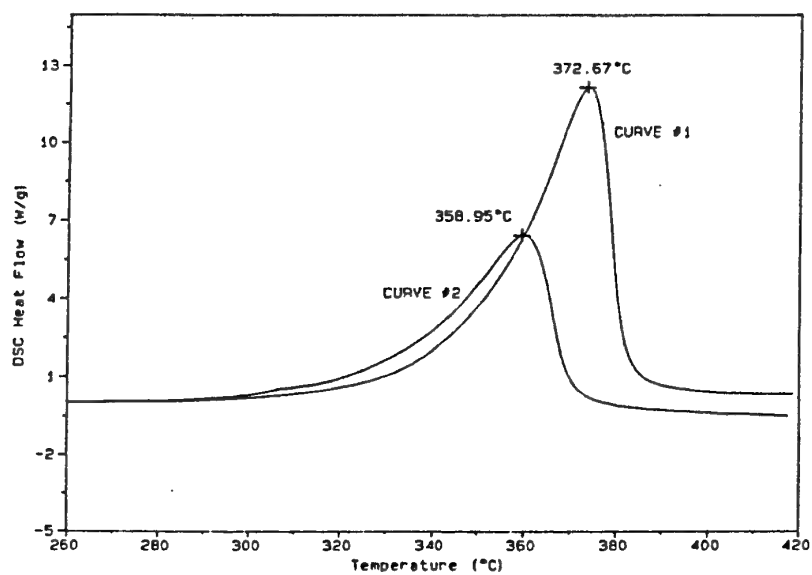


Fig. 10 Overlay of scanning DSC curves of the original (curve 1) and isoaged at 271°C for 2 hours (curve 2) samples of 3-chloro-4-nitrobenzoic acid (Chemical 2).

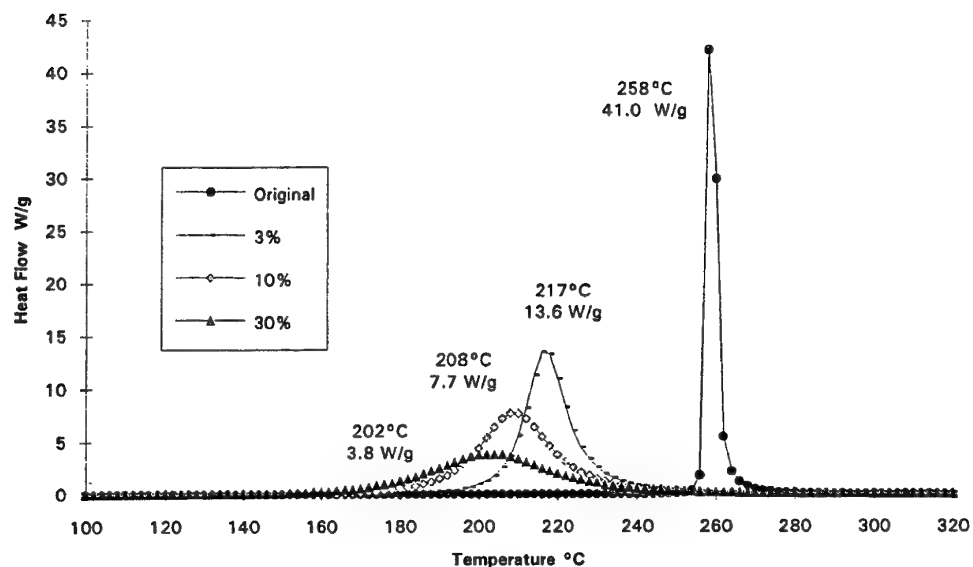


Fig. 11 Overlay of simulated scanning DSC of 2-benzyloxy-5-chloro-4-nitroaniline (Chemical 1) original sample and hypothetical samples containing 3%, 10%, 30% of the catalyst/product.

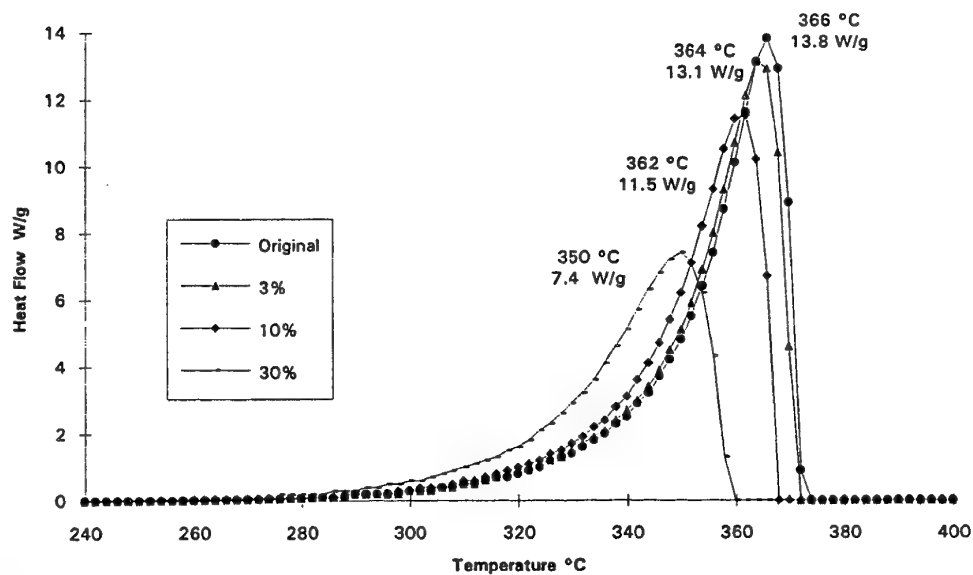


Fig. 12 Overlay of simulated scanning DSC curves of 3-chloro-4-nitrobenzoic acid (Chemical 2) original sample and hypothetical samples containing 3%, 10%, 30% of the catalyst/product.

Table 2. Effect of the Initial Catalyst Concentration on the Change in Decomposition Onset and Peak Temperatures

Chemical #	Conversion by initiation reaction in scanning DSC, %	$\Delta T_o^{1)}$ , °C			$\Delta T_p^{1)}$ , °C		
		3%	10%	30%	3%	10%	30%
1	0.22	47	90	102	41	50	56
2	40	0	3	16	2	4	16
3	10	40	53	66	8	12	20
4	0.0003	36	47	56	7	10	18

<sup>1)</sup> Difference in decomposition onset/peak temperature between the original sample and the sample containing an assumed concentration of the catalyst.

Analyzing the simulation results summarized in Table 2 and the DSC curves overlaid in Figures 9-12, it can be seen that the largest decrease in both the decomposition onset and peak temperatures were observed for Chemical 1, which has the highest reaction orders and an insignificant contribution from the initiation reaction in the overall reaction rate. Moreover, a very small amount of the catalyst (< 3%) caused a significant change in the decomposition curve. The influence of the catalyst concentration on the decomposition characteristics decreases with increase in the catalyst concentration. The significant impact of the small amount of catalytic impurity on the chemical decomposition is caused by high reactant and catalyst reaction orders ( $m, n$ ), which increase the influence of the concentration change on reaction rate.

When analyzing the effect of catalyst concentration (ageing) on decomposition with low reactant and catalyst reaction orders (Chemicals 3, 4), it can be seen that the presence of the product/catalyst results in a smaller, but still significant drop in the decomposition onset temperature, while the peak temperature is much less influenced. The decomposition curves are broadened with an increase in the amount of catalyst present. The less substantial change in the decomposition peak temperatures of the isoaged samples is predicted because of the low ( $m, n < 1$ ) reaction orders of the autocatalytic reaction, which decreased the influence of the change in catalyst concentration on reaction rate.

The effect of ageing is almost completely eliminated when the initiation reaction has a significant rate under the experimental conditions and competes with the autocatalytic reaction (Chemical 2, 40% conversion by initiation reaction in a scanning DSC run). Presence of 3-10% of the catalyst had practically no effect on the DSC curves. Even 30% of the catalyst concentration triggered only a 16°C drop in both the onset and the peak temperatures. Apparently, a substantial change in the decomposition temperature of the isoaged sample does not occur because the initiation reaction (which is not influenced by the presence of the catalyst and would result in a higher decomposition onset temperature when performed on partially decomposed sample) dominates at low temperatures (Figure 7) and has a relatively significant rate throughout the entire decomposition (40% of the chemical decomposes by the initiation reaction).

Summarizing the discussion, it can be concluded that the chemicals most influenced by thermal ageing are those that have high reactant and catalyst reaction orders and a very low rate of initiation reaction under ageing conditions. Lower reaction orders, as well as increased initiation reaction rates will minimize the impact of chemical ageing on subsequent thermal stability.

### CONCLUSIONS

Kinetic equations of decomposition have been derived for four representatives of the nitrobenzene class of chemicals. All chemicals demonstrated an autocatalytic reaction mechanism with a range of reaction orders (0.5-2.3) and activation energies of the initiation and autocatalytic reactions.

Utilization of a kinetic model with two parallel reactions (1st order initiation reaction and autocatalytic reaction) can account for the change in chemical behavior sometimes observed at low temperatures without the need to assume a change in reaction mechanism. Different activation energies of the competing initiation and autocatalytic reactions will result in a temperature dependent change in the relative contributions of each reaction into the overall heat flow rate. This change in chemical behavior has sometimes been interpreted incorrectly as a change in reaction mechanism.

It was demonstrated that the shape of isothermal and, to a lesser extent, scanning DSC curves appear to be a good indicator of the reaction orders of autocatalytic reaction. It was also shown that the initiation reaction can have a significant rate under experimental conditions and can be competing with the autocatalytic reaction.

It was determined that the ageing of autocatalytically decomposing chemicals can lead to a significant decrease in the subsequent decomposition onset and peak temperatures. This is most predominant for chemicals with high reactant and catalyst autocatalytic reaction orders and very low rates of initiation reaction under experimental ageing conditions.

Autocatalytically decomposing chemicals present additional thermal hazard due to their varying susceptibility to ageing effects. Prolonged storage of these types of chemicals under elevated temperatures, even if much lower than the measured decomposition onset temperature, can decrease the thermal stability of the chemical and lead to a hazardous situation during storage or subsequent use.

#### **ACKNOWLEDGMENTS**

The authors would like to thank Paul R. Kingsley for carrying out the experimental work necessary to complete this project.

#### **REFERENCES**

1. S. Chervin and G. T. Bodman, *Process Safety Progress*, 1997.
2. L. F. Whiting, M. S. Labean and S. S. Eadie, *Thermochim. Acta*, 136 (1988) 231.



# THE DECOMPOSITION OF BRANCHED GAP

## BY THERMOANALYTICAL TECHNIQUES

D. E. G. Jones\*, R. A. Augsten, Hongtu Feng and K. J. Mintz

Canadian Explosives Research Laboratory, 555 Booth St, Ottawa K1A 0G1, Canada

### Abstract

This paper will outline the results of a dynamic and isothermal study of Branched GAP (B - GAP), where GAP is glycidyl azide polymer, using various thermoanalytic techniques, including DSC, TGA, ARC and HFC(Heat Flux Calorimetry). These results have been used to determine kinetic parameters for the decomposition of B - GAP and the parameters will be compared with those obtained for GAPTRIOL in an earlier study. Both materials undergo a two-stage decomposition process in an inert medium. Agreement of kinetic parameters obtained from various techniques is good, thereby allowing discussion of the mechanism for the decomposition process with some confidence. Results will be reported for ARC experiments on B - GAP using the step heat-wait-search technique, with a variety of start-up conditions. Some of the start-up conditions used led to thermal runaway, however analysis of the data to obtain an estimate of kinetic parameters will be presented.

### 1. Introduction

Earlier studies in our laboratory on GAPTRIOL[1] have been carried out using DSC, TGA and ARC. The DSC data showed a large exotherm followed by a smaller, shallow exotherm,

\*Corresponding author

corresponding to a two stage mass loss observed in the TGA in an inert medium. The second stage was relatively slow compared to the first stage, apparently a result of the first order loss of nitrogen from the azide group. The kinetic parameters obtained by all three techniques were in reasonable agreement but did suggest that the overall reaction is not first order. In this work, dynamic and isothermal studies were done on B - GAP and the results were compared with those obtained for GAPTRIOL.

## 2. Experimental

A TA 2100 Thermal Analyst System with 2910 DSC and 2950 TGA modules was used with a carrier gas flow of  $50 \text{ cm}^3 \text{ min}^{-1}$ . Dry oxygen-free nitrogen was used for both DSC and TGA experiments, and dry air was used for TGA experiments only. Heating rates from  $2 - 10 \text{ }^\circ\text{C min}^{-1}$  were used for DSC and TGA measurements. Isothermal experiments were carried out from  $190 \text{ }^\circ\text{C}$  to  $230 \text{ }^\circ\text{C}$  and the data were interpreted using the TA Isothermal Kinetics Software.

The DSC was calibrated for heat flow and temperature. B - GAP was sealed in glass microampoules[2]. Sample mass was about 0.7 mg.

The TGA was calibrated for mass and temperature. The standard reference weight was used for mass calibration and the reference weight was checked against a Mettler M3 electrical microbalance with a reproducibility of  $\pm 1 \text{ } \mu\text{g}$ . The temperature was calibrated using the Curie Point magnetic method[3]. Calibration was done at each heating rate. A platinum sample pan was used for all TGA measurements. Sample size was about 3 - 4 mg.

The ARC is a commercial automated adiabatic calorimeter developed by Dow and licensed to CSI (Columbia Scientific Industries), Austin, Texas, for the purpose of assessing the thermal hazard potential of chemicals[4]. Samples of 100 - 500 mg of B - GAP were placed in lightweight, spherical

titanium bombs, which were closed off so as to maintain any pressure resulting from vapourization and decomposition of the sample. Most of the tests were carried out in an inert atmosphere (Ar), but three used air. The standard ARC procedure of "heat-wait-search" was used with a heat step of 5°C.

The heat flux calorimeter (HFC) used was a Setaram C 80, twin cell Tian-Calvet instrument. It has a massive aluminum block with two identical cylindrical cavities for sample and reference cells located symmetrically about the center. A heating rate of 0.3 °C min<sup>-1</sup> was used. A specially designed high pressure vessel was used and the working pressure was 5.5 MPa. Sample mass was about 45 mg and experiments were carried out in both Ar and air.

### 3. Results and Discussion

#### DSC and TGA

The DSC and TGA curves of B-GAP at 10°C min<sup>-1</sup> are compared in Figure 1. An exotherm with an onset temperature of 170 ± 4 °C and  $\Delta H = 2.59 \pm 0.15$  kJ g<sup>-1</sup> was observed, compared with the onset temperature of 180 ± 4 °C and  $\Delta H = 2.58 \pm 0.05$  kJ g<sup>-1</sup> for GAPTRIOL. The exotherm corresponds with the initial mass loss observed in the TGA experiments carried out in nitrogen.

The following description of the kinetic results is based on the nth order rate law:

$$d\alpha/dt = k (1-\alpha)^n$$

and the Arrhenius equation

$$k = Ze^{(-E/RT)}$$

where  $\alpha$  is the fraction of sample reacted ( $0 \leq \alpha \leq 1$ ),  $k$  is the rate constant of the reaction,  $n$  is the order of the reaction,  $E$  is the activation energy and  $Z$  is the pre-exponential factor in the Arrhenius equation.

For the DSC dynamic measurements, the various heating rate results were analysed by plotting  $\ln(\beta/T_m^2)$  against  $1/T_m$  where  $\beta$  is the heating rate and  $T_m$  is the peak temperature, corrected for thermal lag [5]. Figure 2 shows these results.

The software package obtained from TA Instruments was used to determine  $n$  and  $k$  from a plot of  $\ln(d\alpha/dt)$  against  $\ln(1-\alpha)$ . Figure 3 shows the plot of  $\ln(k/\text{min}^{-1})$  against inverse isothermal temperature in the isothermal DSC experiments, where  $k$  is the rate constant for the  $n$ th order model.

From Figure 1 it is found that about 40 % mass loss took place in the first stage which likely corresponds to loss of  $N_2 + H_2$  from the repeating units in B - GAP, similar to GAPTRIOL. Higher mass loss than expected (30 % based on conversion of azide to cyano group and  $N_2 + H_2$ ) suggests that significant decomposition arising from the second stage reaction has occurred. The first reaction is much faster than the second stage reaction. The first stage reaction was assumed to be first order, hence the second stage reaction is believed to be of higher order.

Figure 4 shows a plot of  $\ln(\beta/^\circ\text{C min}^{-1})$  against reciprocal temperature at 10 % conversion in the TGA experiments, for the purpose of determining the kinetic parameters [6].

An isothermal study for B - GAP was also performed by TGA. The plots of  $\ln(1-\alpha)$  against time gives a straight line with a  $R^2$  values  $\geq 0.996$ . Figure 5 shows a plot of  $\ln(k)$  against inverse isothermal temperature, where  $k$  is the slope of the first order plots. The slope of the line in Figure 5 gives  $E$  and the intercept is  $\ln Z$ .

After the isothermal DSC experiments, the samples were re-run from room temperature to 500  $^\circ\text{C}$  at  $\beta = 10^\circ\text{C min}^{-1}$ . The residual  $\Delta H$  values appear to decrease with isothermal temperature increase in a linear fashion, but the peak temperature of the reaction did not change significantly. The  $\Delta H$  for the second, smaller exotherm(see Figure 1) showed no significant change. The second

reaction is likely due to oxidation of the polymer chain and is similar to the ARC results discussed below. The peak temperature obtained from the DTGA curve is about 350 °C compared with 370 °C obtained from the DSC curve, both at  $\beta = 10\text{ }^{\circ}\text{C min}^{-1}$ .

## ARC and HFC

Figure 6 shows the results for tests carried out on B-GAP in Ar and in air using ARC. At the end of the “staircase”, the ARC detects the exotherm (self heating rate,  $\text{SHR} > 0.02\text{ }^{\circ}\text{C min}^{-1}$ ) and does not apply any more heat steps until the SHR drops below  $0.02\text{ }^{\circ}\text{C min}^{-1}$ , i.e. at the end of the exotherm. Figure 7 shows clearly that the onset temperature is significantly lower in air than in Ar. However, the temperature and pressure in the air test did not rise as rapidly initially, but eventually these increases were so great that the test had to be terminated, because of the likelihood of an explosion.

The ARC results for B- GAP in air produced a weak exotherm with an onset temperature of about 115 °C, followed by a large exotherm. The early exotherm is a result of the oxidation of B - GAP in the air environment. Figure 7 also shows these results. The magnitude of the second exotherm was found to be sample mass dependant and, also, a critical mass for explosion was suggested by the data. These results are shown in Figure 8 .

additionally, experiments were also carried out using HFC to confirm the results from ARC. Under the high pressure of air (5.5 MPa) a large exotherm,  $\Delta H = 8.26 \pm 0.26\text{ kJ g}^{-1}$  with an onset temperature  $125 \pm 3\text{ }^{\circ}\text{C}$  was observed. The HFC results for B - GAP at ambient and high pressure of air are compared with the results under 5.5 MPa of Ar in Figure 9. The HFC results show clearly the effect of oxidation promoting early onset and an increased magnitude of the exotherm energy.

The HFC and ARC results are compared in Figure 10.

#### 4. Summary

The activation energy and the pre-exponential factor of B - GAP were obtained from four different types of experiments. These results are shown in Table 1. It is found that the values of the activation energy and the pre-exponential factor obtained by the different methods agree within the estimate of uncertainty. Similar results for the activation energy and the pre-exponential factor were obtained for GAPTRIOL[7]. From Table 1, it can be seen that the activation energy of B- GAP is lower than that of GAPTRIOL, indicating that B - GAP is more reactive.

#### References

- 1 D. E. G. Jones, L. Malechaux and R. A. Augsten, *Thermochimica Acta*, 242 (1994) 187
- 2 D. E. G. Jones and R. A. Augsten, *Thermochimica Acta*, 286 (1996) 355
- 3 ASTM E1582 *American Society for Testing and Materials*, Philadelphia, PA. USA
- 4 J. C. Tou and L. F. Whiting, *Thermochimica Acta*, 48(1981) 21
- 5 ASTM E698 *American Society for Testing and Materials*, Philadelphia, PA. USA
- 6 J. H. Flynn and L. A. Wall, *Polymer Letter*, 19(1966)323

**Table 1**

**Comparison of Kinetics Parameters of B - GAP and GAPTRIOL by Various Methods**

Methods	E/kJ mol <sup>-1</sup>		ln(Z/min <sup>-1</sup> )		n
	B - GAP	GAPTRIOL	B - GAP	GAPTRIOL	
DSC(dynamic)	138 ± 4	160	30.74 ± 0.05 <sup>a</sup>	25.04 <sup>a</sup>	[1]
DSC(isothermal)	145 ± 9	178	33.0 ± 2.2	41.0	0.66 <sub>B-GAP</sub>
TGA(dynamic)	136 ± 8*	155	28.57 ± 0.08 <sup>a</sup>	34.92 <sup>a</sup>	[1]
TGA(isothermal)	134 ± 4	----	28.1 ± 1.0	-----	[1] <sup>b</sup>
ARC	132 <sup>c</sup> (air)	182(nitrogen)	29.03	42.15	0.88 <sub>GAPTRIOL</sub>

<sup>a</sup> The reaction was assumed to be first order.

<sup>b</sup> The reaction was assumed to be first order based on the linearity of the plot in Figure 6b.

<sup>c</sup> The experimental value is mass dependant. This value derived from an experiment using 0.33 g of B- GAP.

\*The uncertainty is derived from the average between 4% - 15% mass loss.

Figure 1

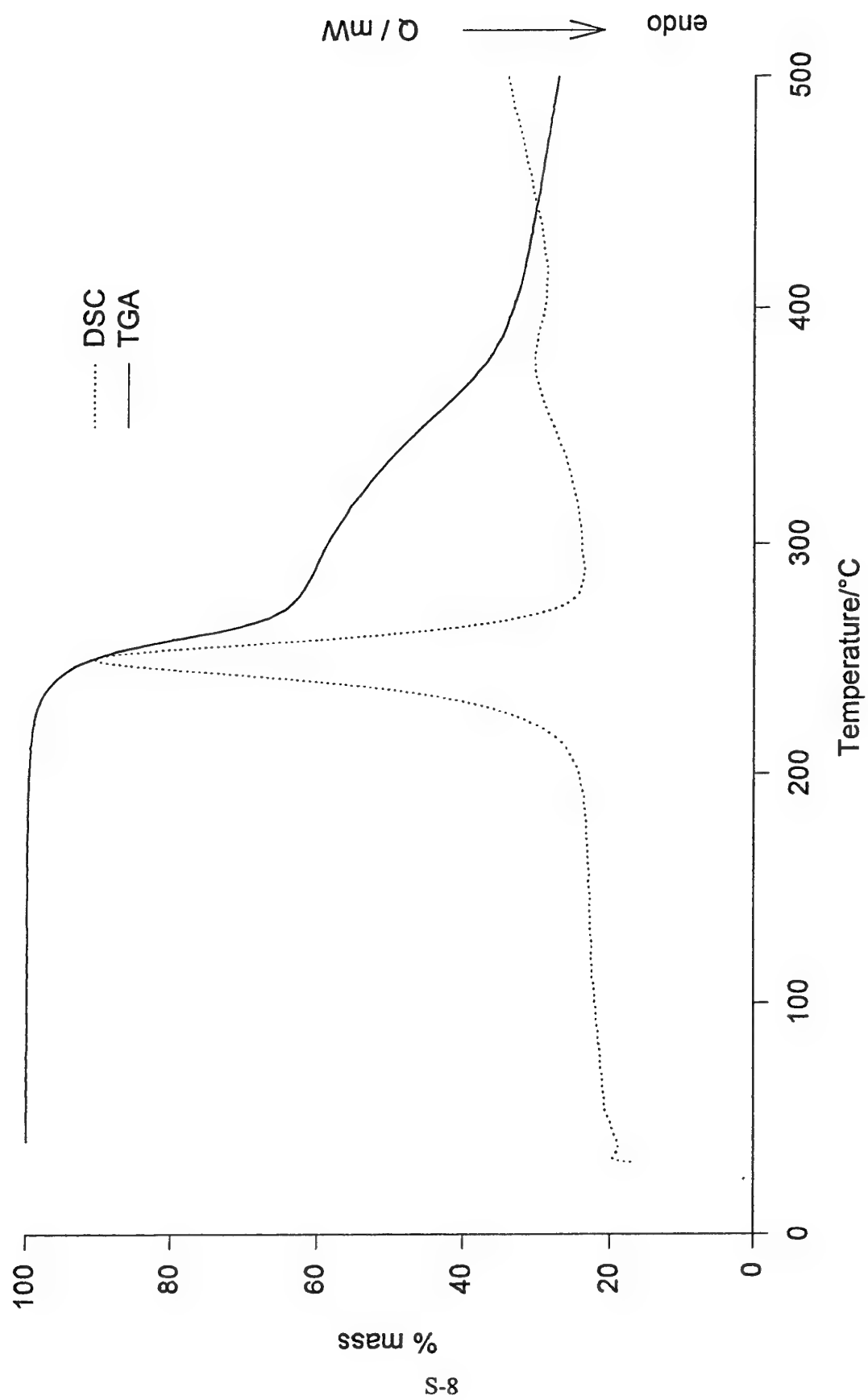




Figure 2

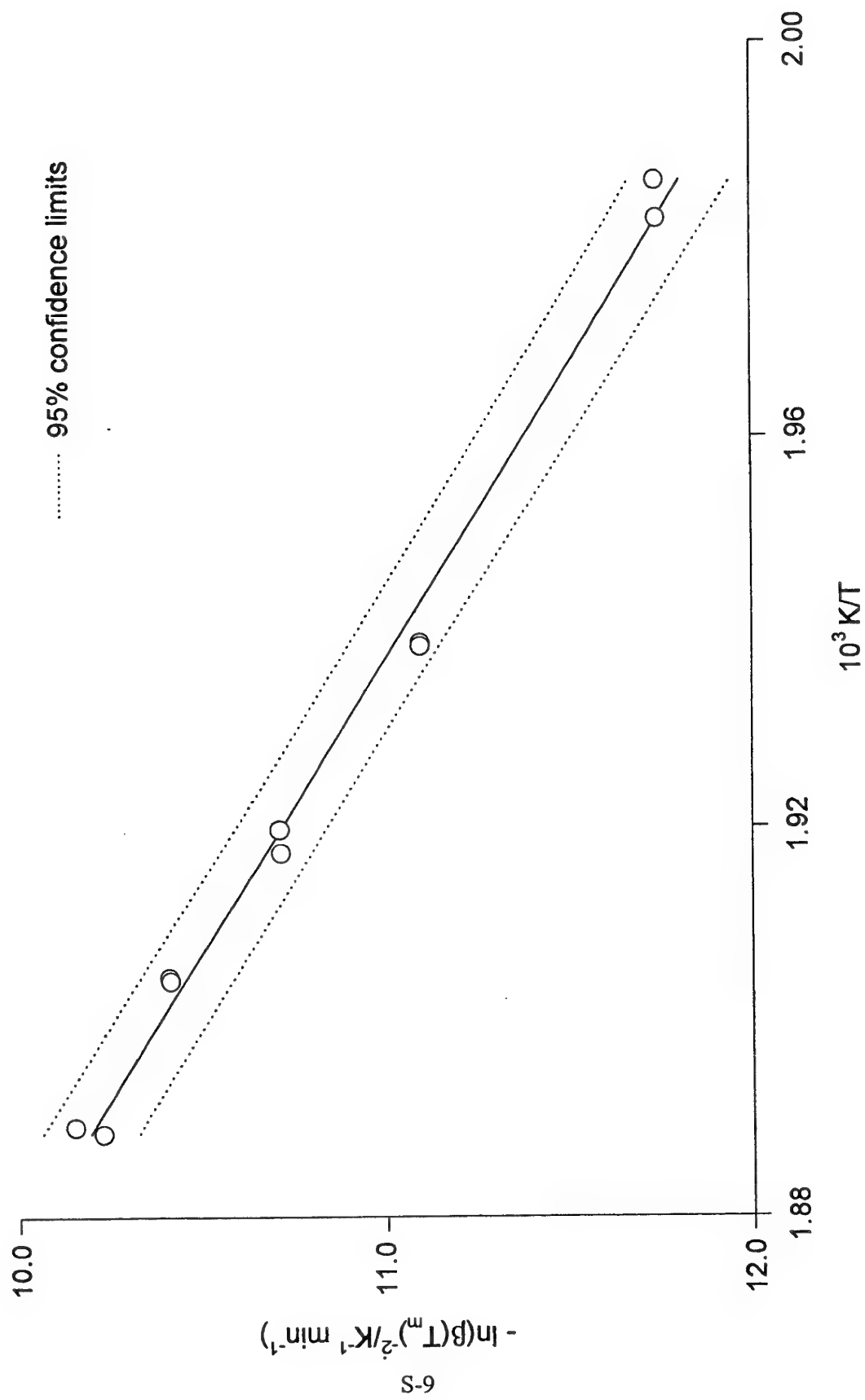


Figure 3

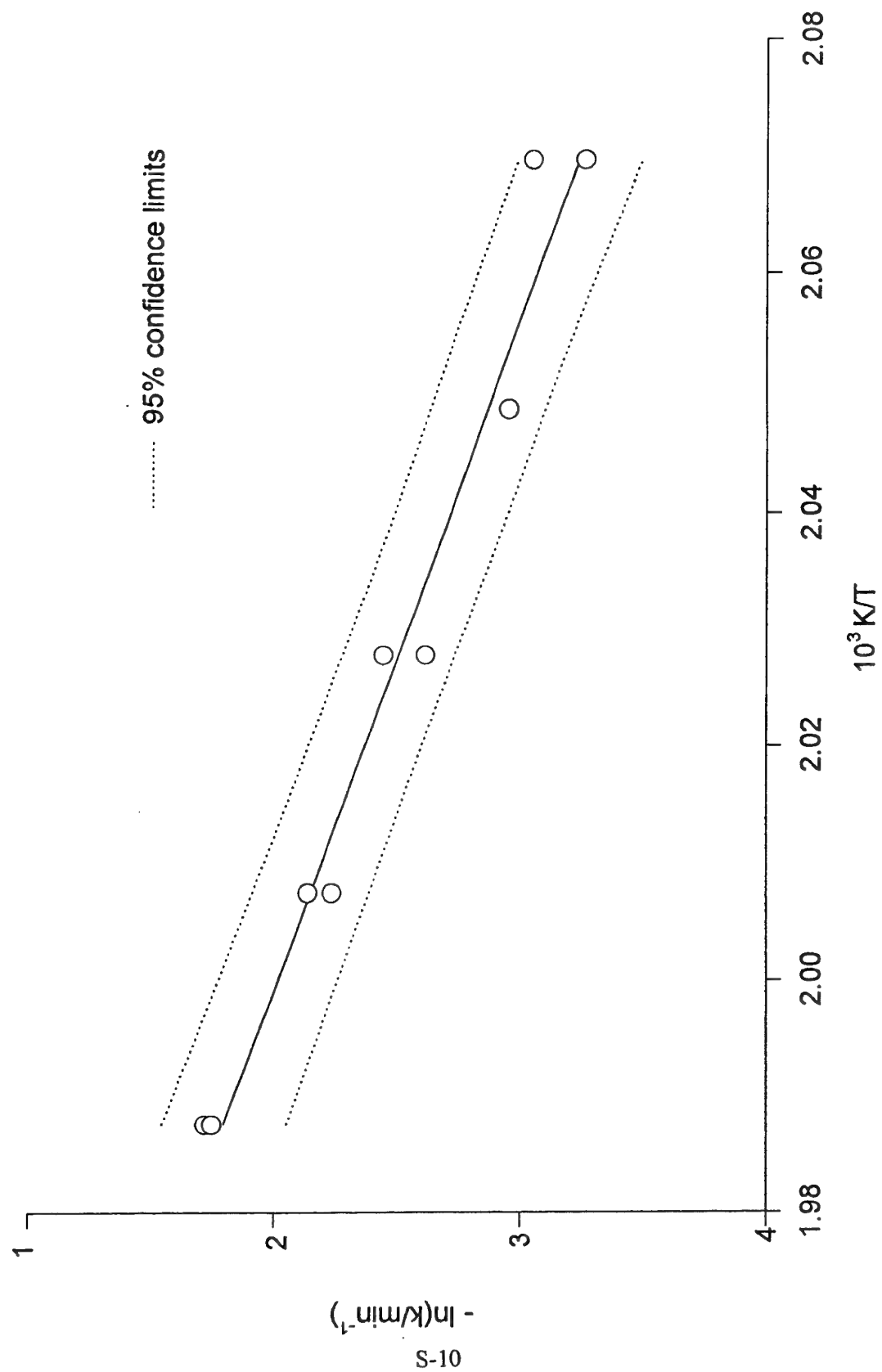


Figure 4

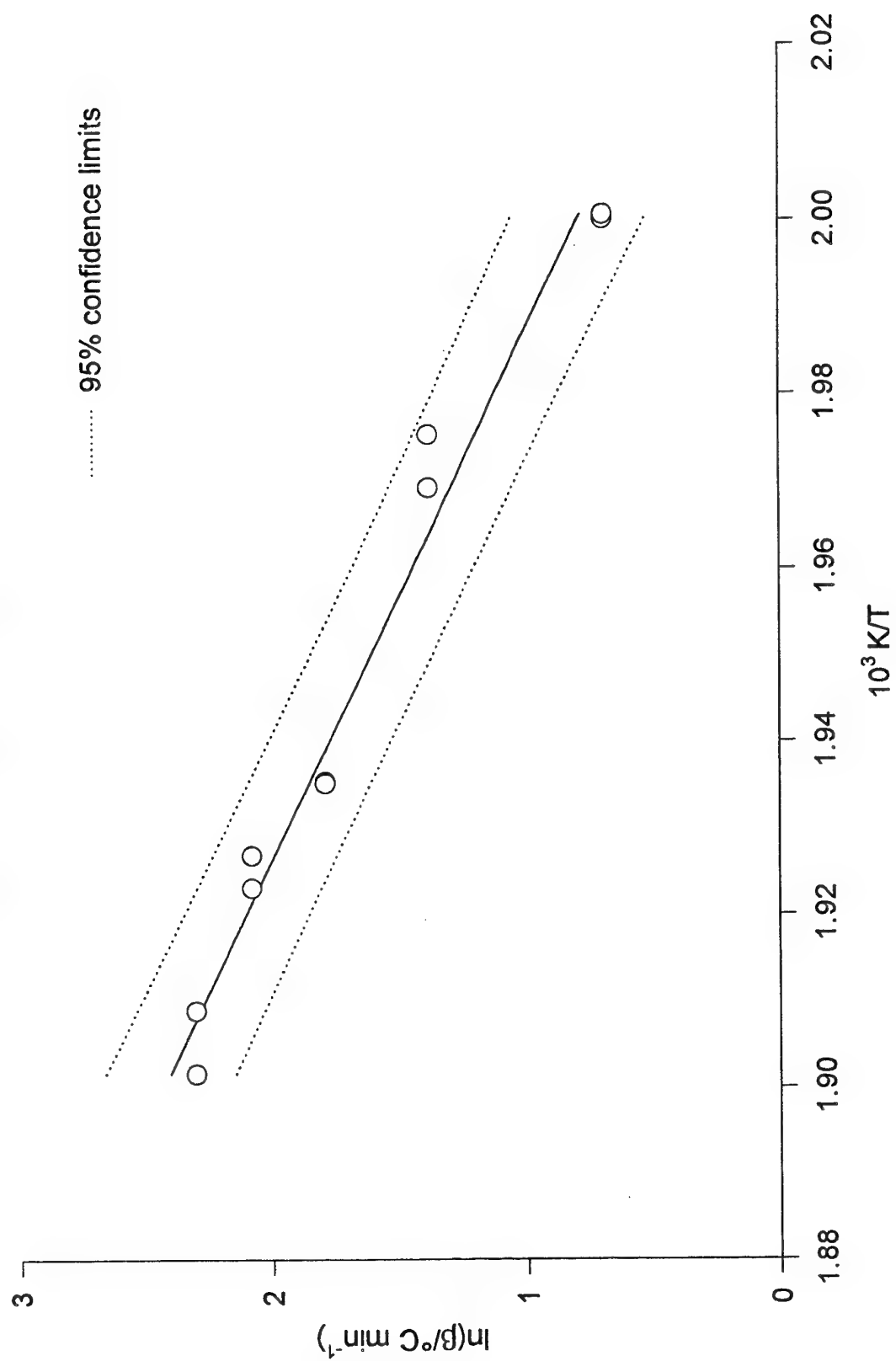


Figure 5

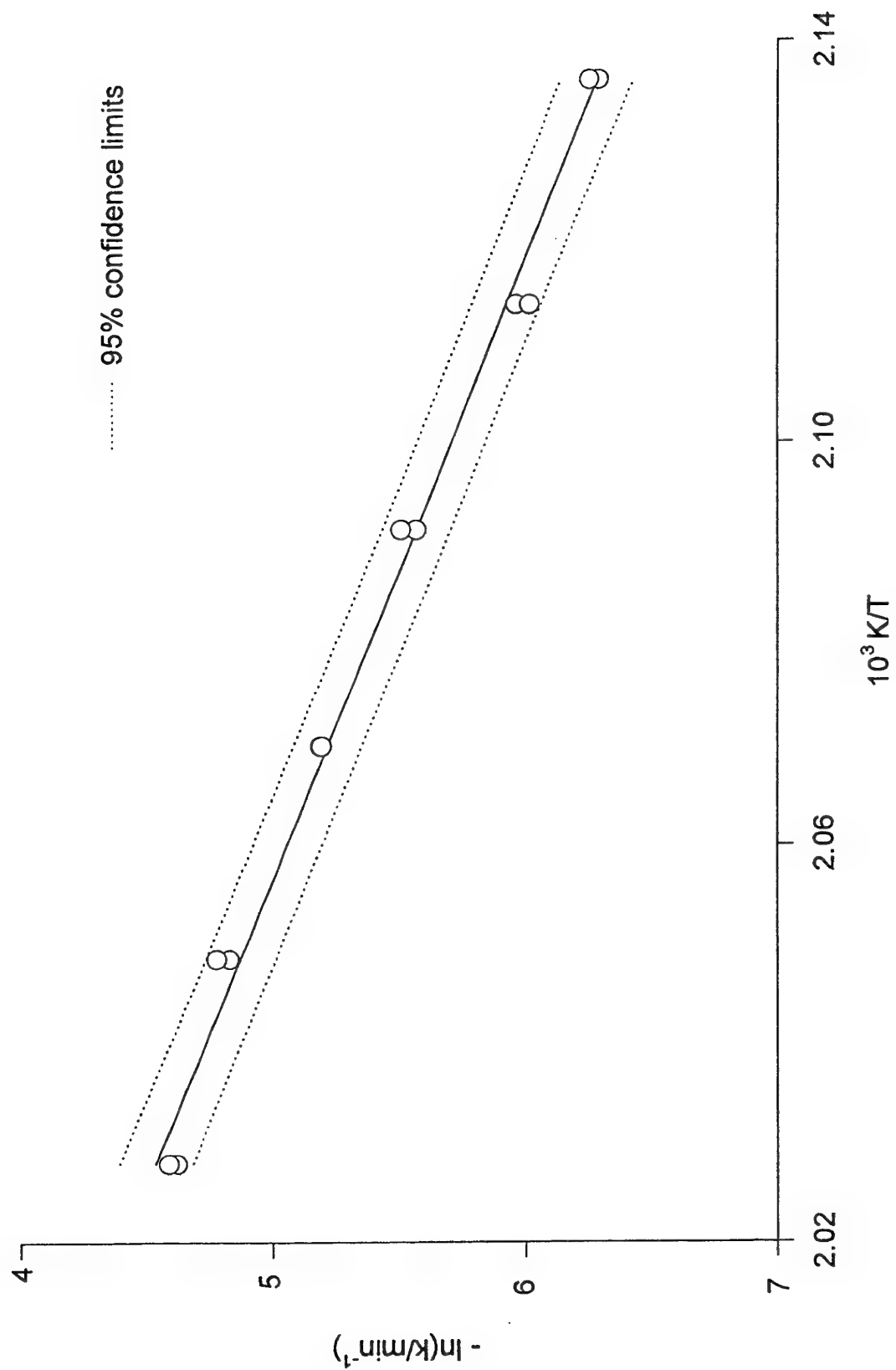


Figure 6

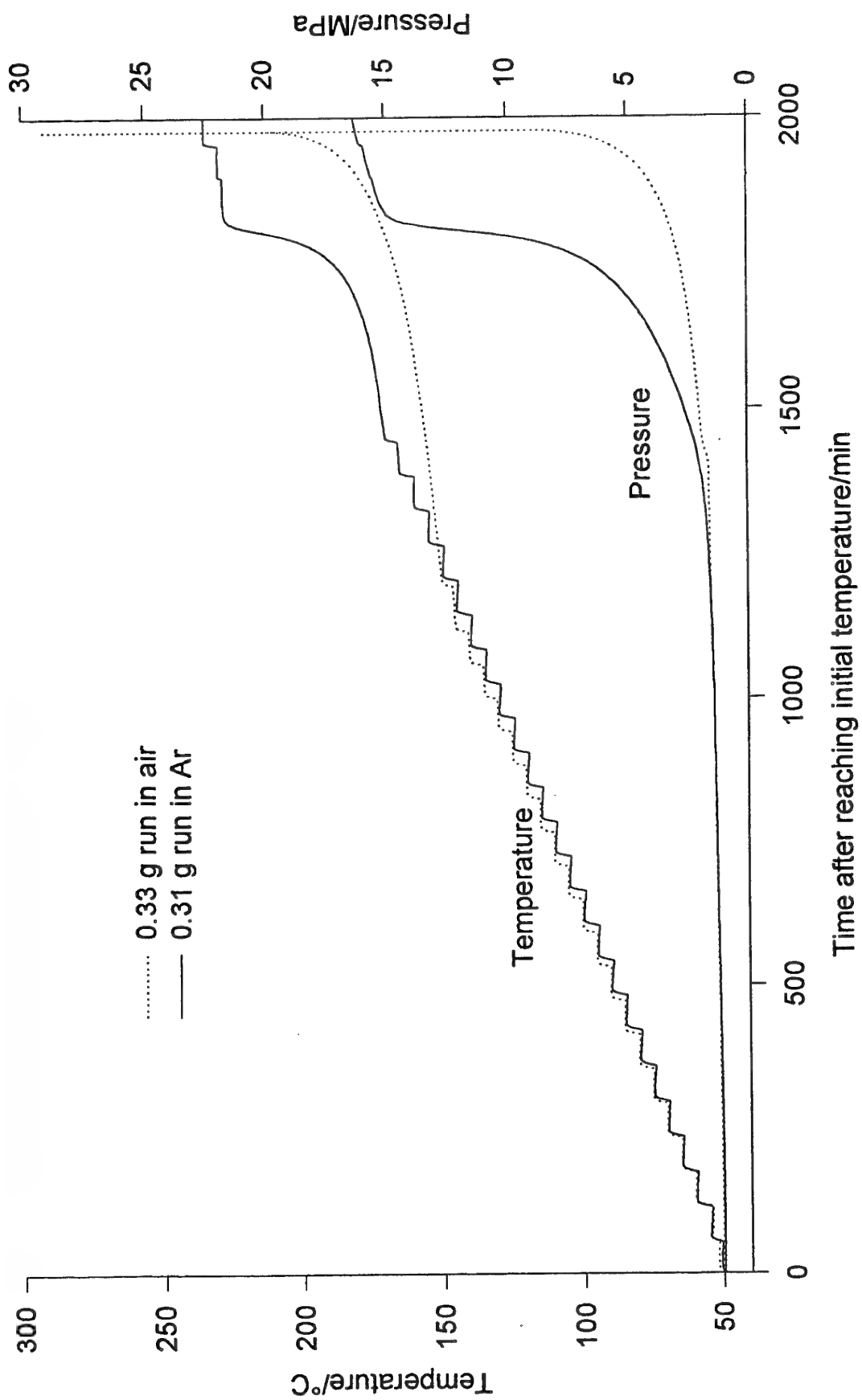


Figure 7

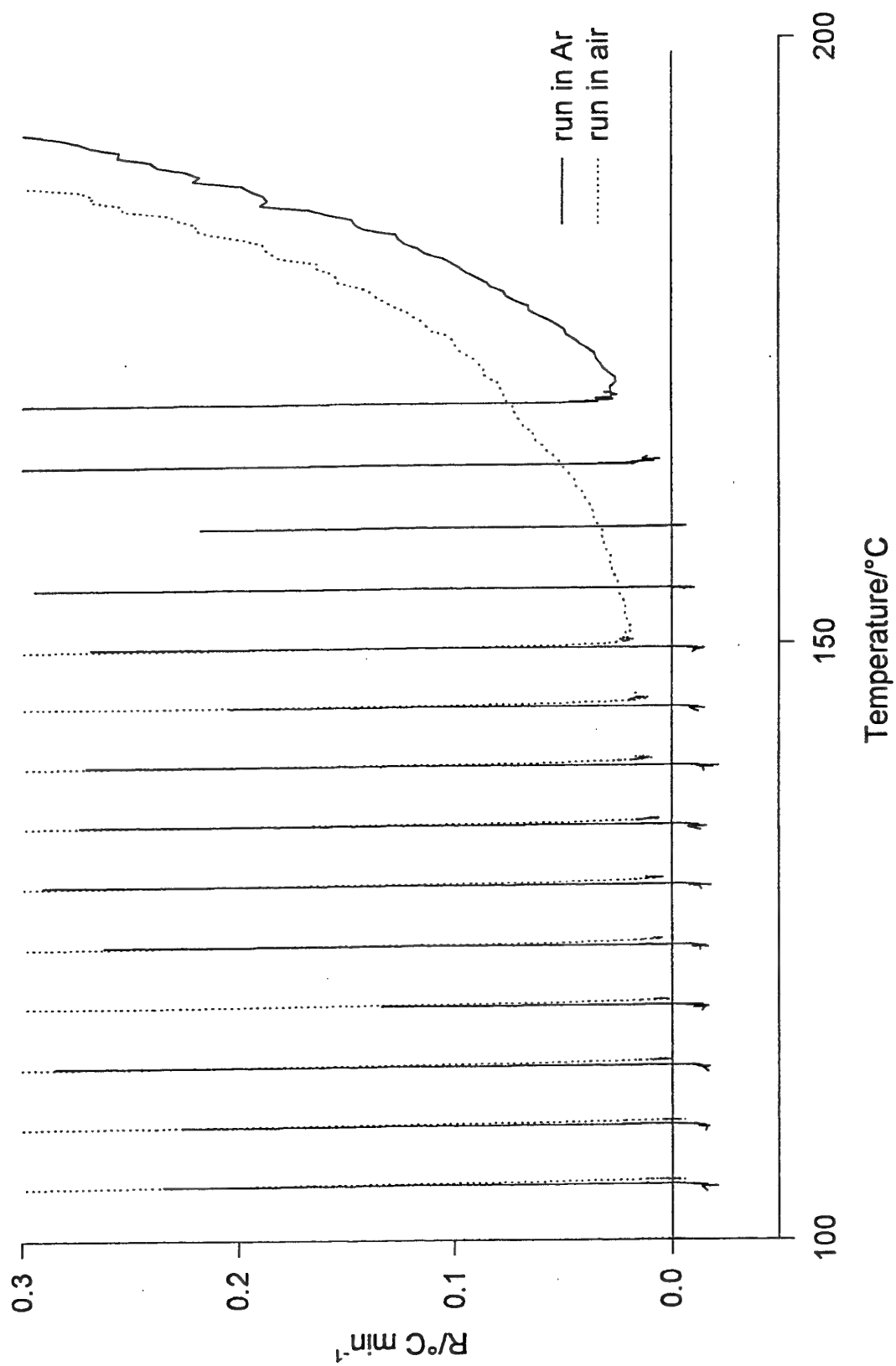


Figure 8

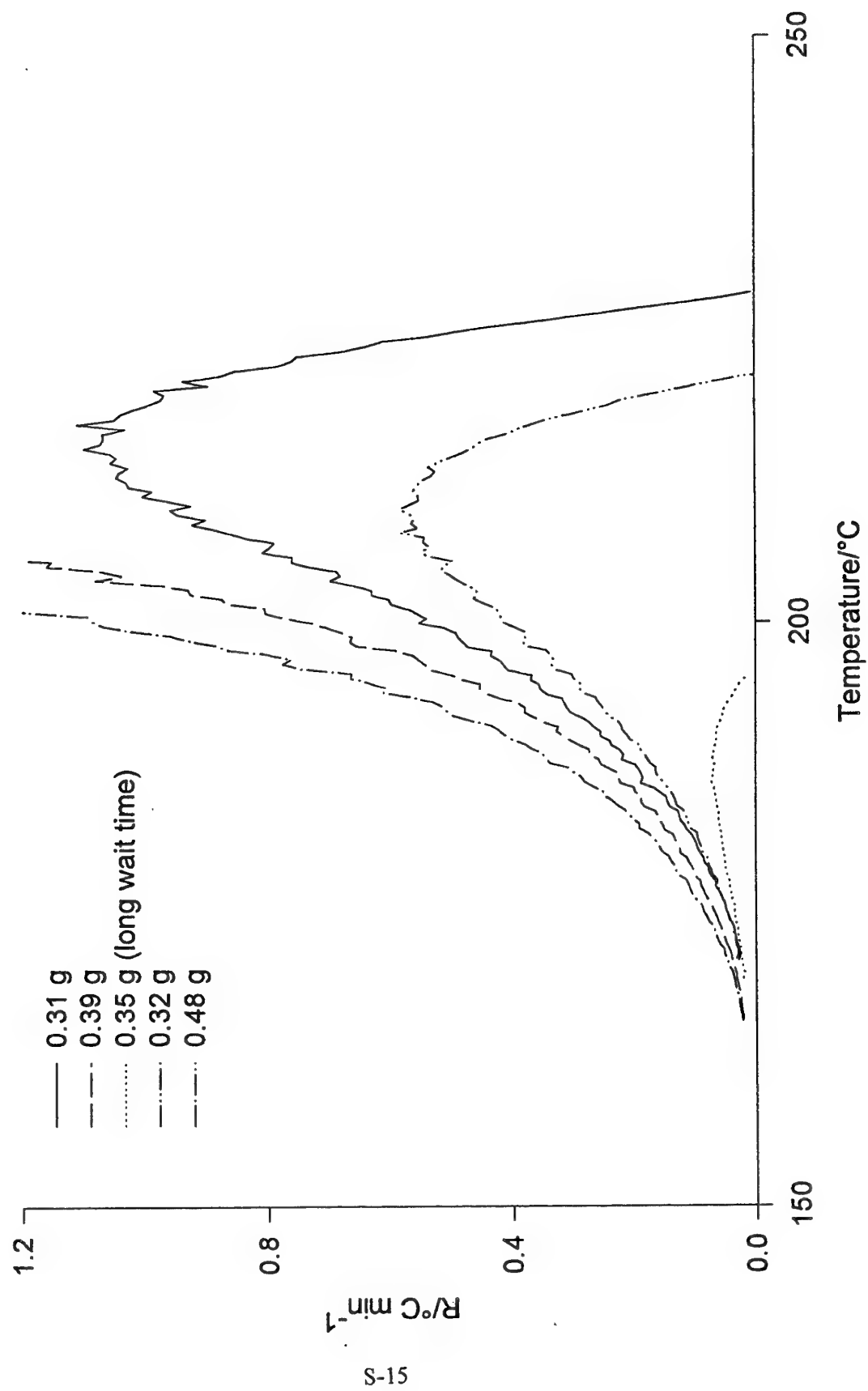


Figure 10

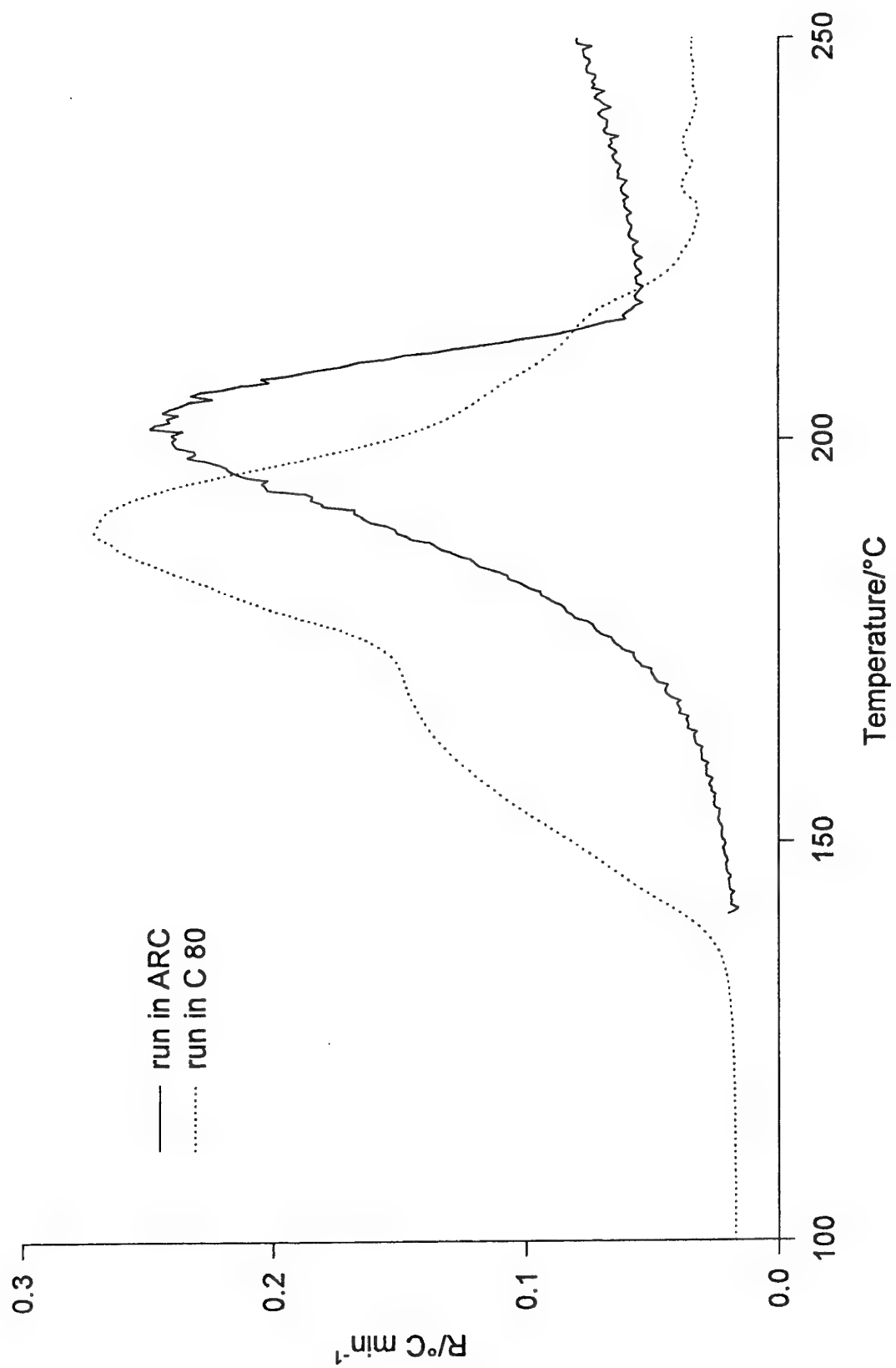
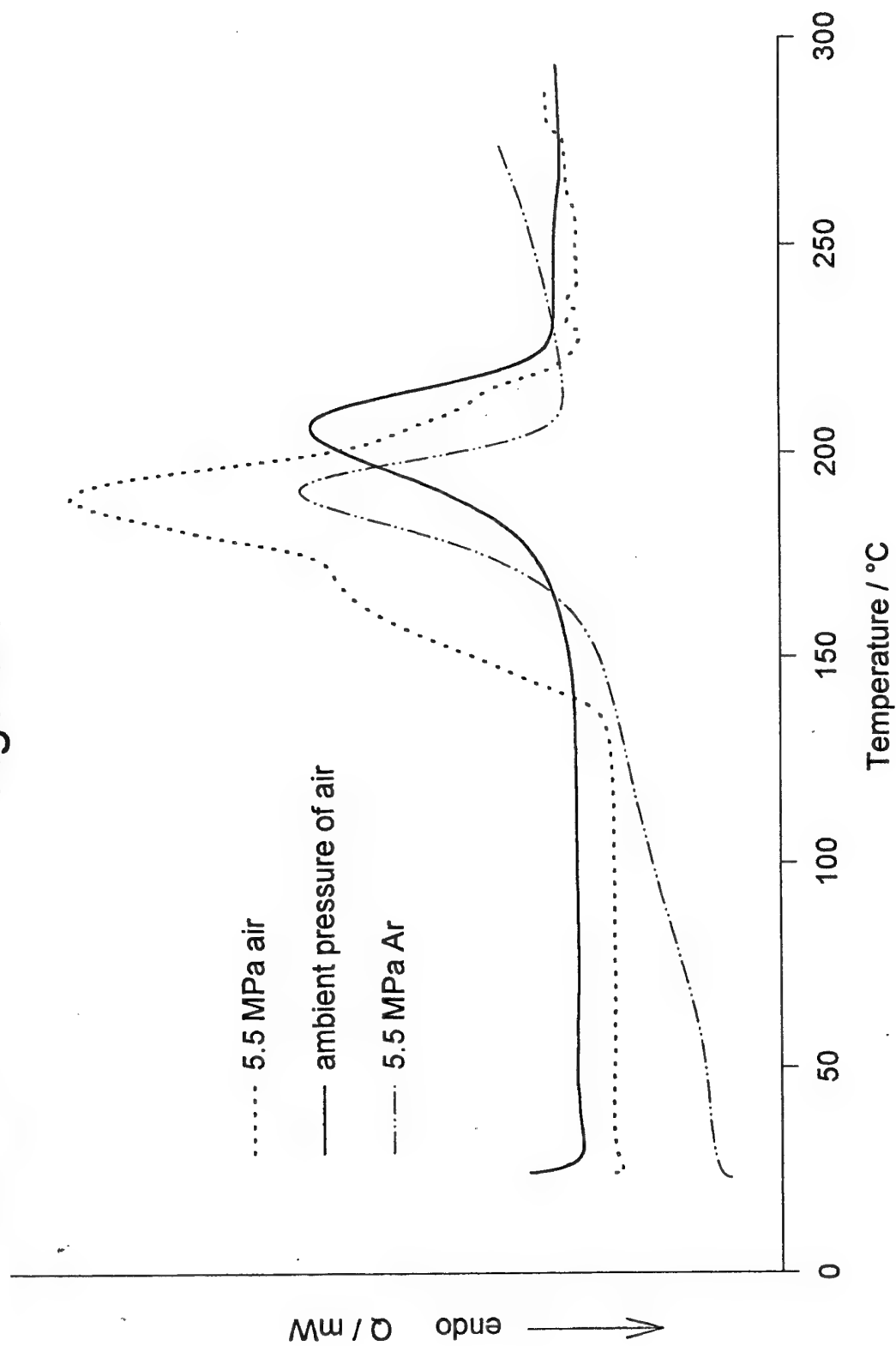




Figure 9



# THERMAL STABILITY OF AMMONIUM DINITRAMIDE (ADN) AND ADN CONTAINING VARIOUS STABILIZERS

Robert F. Boswell and Dr. Albert S. Tompa  
Indian Head Division, Naval Surface Warfare Center  
101 Strauss Ave., Indian Head, MD 20640-5035

## ABSTRACT

Since the first synthesis of ADN by SRI, there have been continuing unresolved questions about its thermal stability and decomposition kinetics. In addition a great deal of interest has been focused on ADN compatibility with various ingredients in propellant and explosive formulations. In this study an effort has been made to increase the thermal stability of ADN by the addition of stabilizers. Russell<sup>(1)</sup> at NRL showed how ADN decomposes into the dinitramic acid ( $\text{NH}_4\text{N}(\text{NO}_2)_2 \rightarrow \text{NH}_3 + \text{HN}(\text{NO}_2)_2$ ). Therefore by adding stabilizers which are basic in nature, such as urea, hexamethylenetetramine, cyanoquanidine and TEPAN the dissociation reaction should be inhibited. Isothermal heating method was employed to obtain kinetic data by microcalorimetry and differential scanning calorimetry (DSC).

## INTRODUCTION

Isothermal kinetic temperatures ranged from 80 to 96°C for microcalorimetry and 115 to 140°C for DSC. A plot of  $\ln t$  (min) at the exothermic decomposition peak maximum versus the reciprocal of the absolute temperature will have a slope of  $E/R$ , where  $E$  is the activation energy and  $R$  is the gas constant. The equation used to analyze the data is  $\ln k = \ln A - E/RT$ , where  $k$  is the rate constant,  $A$  is the Arrhenius frequency factor. Once  $E$  and  $A$  are known and assuming a first order equation  $k$  may be calculated. The activation energies and rate constants were used to compare stabilized and unstabilized ADN. If an additive shows an increase in activation energy and a decrease in the rate constant this would show a stabilizing affect on the thermal stability of ADN.

## EXPERIMENTAL

The crystalline (neat) ADN was prepared at NSWC/IH using the pilot plant batch process. The particle sizes ranged from 5 - 50 microns. These crystals are slightly elongated and no attempt was made to round these crystals. The prilled ADN containing hexamine, cyanoquanidine and tetraethylenepentamine/acrylonitrile (TEPAN) were prepared by United Technologies at their Chemical Systems Division using their melt/stir prilling process. The average particle size ranged from 300 to 350 microns. The prilled ADN containing urea was prepared by Thiokol by using their gas flow prilling process. Their average particle size was around 100 microns. In each prilling process the stabilizers are physically mixed with the ADN before the prilling process.

## DISCUSSION

An example of a microcalorimeter thermograph is shown in Figure 1. The sample starts to exotherm after one day and reaches its peak maximum in approximately three days. The activation energy of 35.8 kcal/mol from microcalorimetry data is shown in Figure 2. Our value for the liquid phase was found to be 32.8 kcal/mol (Figure 3). Manelis reports that their value for the liquid phase activation energy is close to their solid phase value of 35 kcal/mol. Figure 4 is a isothermal DSC curve at 120°C of neat ADN. Its time to exothermic peak maximum is 255 min. The sample starts to exotherm at approximately 58 min and returns to baseline approximately 600 min. Figure 5 is of ADN prilled which contains urea. At 120°C the sample starts to exotherm approximately in

400 min with a peak maximum at 542 min and returning to baseline around 980 min. Urea shows a large affect on increasing the thermal stability of ADN. A comparison of thermal data of neat ADN with prilled ADN stabilized with urea is shown in Table 1. At every isothermal temperature the sample containing urea showed an increase in time of decomposition compared to neat ADN. This is also evident by the increase in the activation energy and decrease in its rate constant. Arrhenius plot of ADN which contains urea is shown in Figure 6. Table 2 is the comparison of activation energies and rate constants of the stabilized ADN with neat ADN. Not all additives showed an increase in stabilizing effect. The rate constant i.e. 100°C shows only an increase in stability using urea. The sample containing hexamine and cyanoquanidine shows an increase in activation energy, but the rate constant for practical reasons are the same. The ADN containing TEPAN showed an decrease in its thermal stability.

### CONCLUSION

When comparing crystalline ADN with prilled stabilized ADN there appears to be some improvement in its thermal stability. Prilled ADN containing urea showed an increase in its thermal stability. Comparing rate constants and activation energies the urea ADN rate constant decreased from  $4.22 \times 10^{-4} \text{ (min}^{-1}\text{)}$  for neat to  $1.5 \times 10^{-4} \text{ (min}^{-1}\text{)}$  for the urea stabilized and its activation energy increased from 33 to 37 kcal/mol. Though all stabilized ADN sample showed an increase of their activation energies compared to the neat crystalline ADN they did not show an increase in thermal stability as measured by the rate of reaction at 100°C. Its been reported that ADN containing hexamine showed an increase thermal stability at lower temperatures. This was not evident by DSC at temperatures ranging from 115 to 140°C. The samples containing hexamine and cyanoquanidine had little or no affect on ADN stability. The sample containing TEPAN shows a decrease in thermal stability when comparing rate constant.

### ACKNOWLEDGMENTS

I would like to thank Dr. Anton Chin and Dr. Dan Ellison for their microcalorimetry work. I would also like to thank J. Guimont at CSD for his support.

### REFERENCES

1. T. P. Russell and A. G. Stern et al. "Thermal Decomposition and Stabilization of Ammonium Dinitramide", JANNAF Combustion Proceeding, Langley Research Center, Hampton, VA. Oct 1992.
2. G. B. Manelis, "Thermal Decomposition of Dinitramide Ammonium Salt", 26th International Annual Conference of I.C.T., July 1995, p 15-1.

TABLE 1  
THERMAL STABILITY OF NEAT ADN AND PRILLED ADN CONTAINING UREA BY DSC

TEMP °C	ADN/IH PEAK MAX (min)	ADN + UREA PEAK MAX (min)
115	399.4	959.9
120	255	541.8
125	150.8	308.7
130	113.5	184.8
140	30.2	58.7
Ea kcal/mol	32.8	36.6
Rate Constant 100° (min <sup>-1</sup> )	$4.22 \times 10^{-4}$	$1.51 \times 10^{-4}$
A (min <sup>-1</sup> )	$7.44 \times 10^{15}$	$4.44 \times 10^{17}$
Rate Reduced	1	0.35

TABLE 2  
COMPARISON OF ACTIVATION ENERGIES AND ADN RATE CONSTANTS  
BY ISOTHERMAL DSC

SAMPLE	Ea Kcal/mol	100°C RATE CONSTANT (10 <sup>-4</sup> min <sup>-1</sup> )
Crystalline ADN	33	4.2
Prilled ADN w/Urea	37	1.5
Prilled ADN w/0.5% Hexamine	37	3.8
Prilled ADN w/0.5% cyanoquanidine	36	4.2
Prilled ADN w/0.5% TEPAN	35	6.8

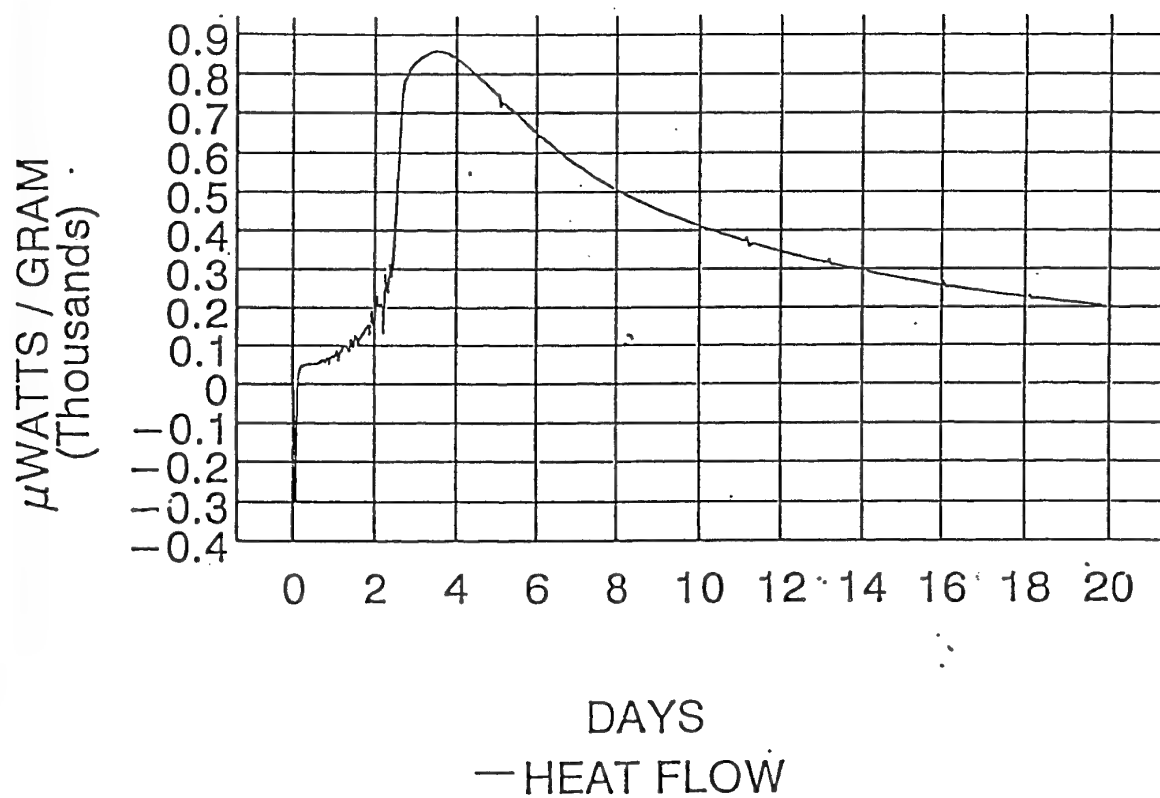


FIGURE 1. ISOTHERMAL MICROCALORIMETRY CURVE OF NEAT ADN AT 85°C

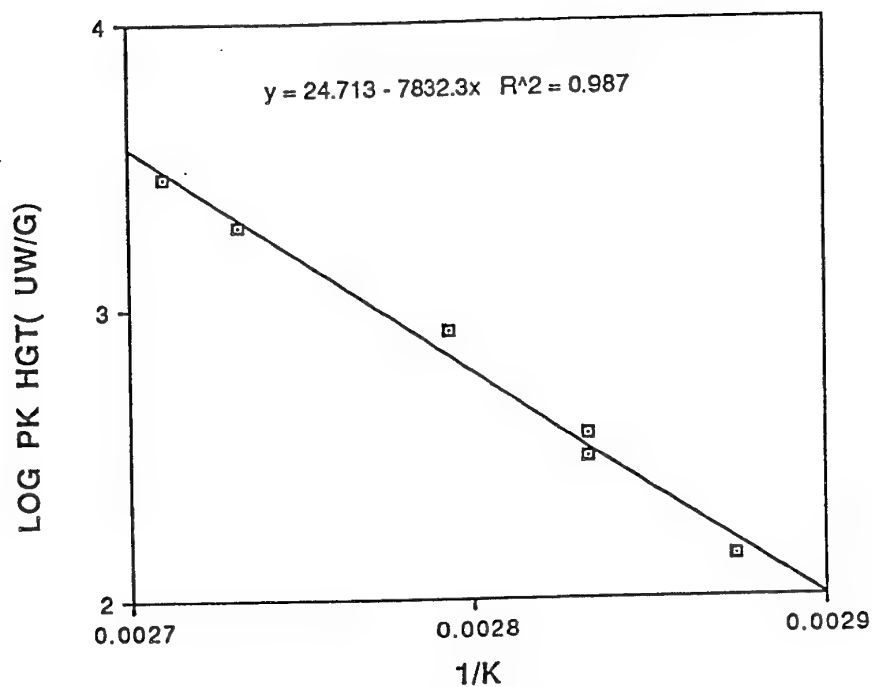


FIGURE 2. ARRHENIUS PLOT OF CRYSTALLINE ADN FROM MICROCALORIMETRY DATA;  $E_a = 35.8$  KCAL/MOL

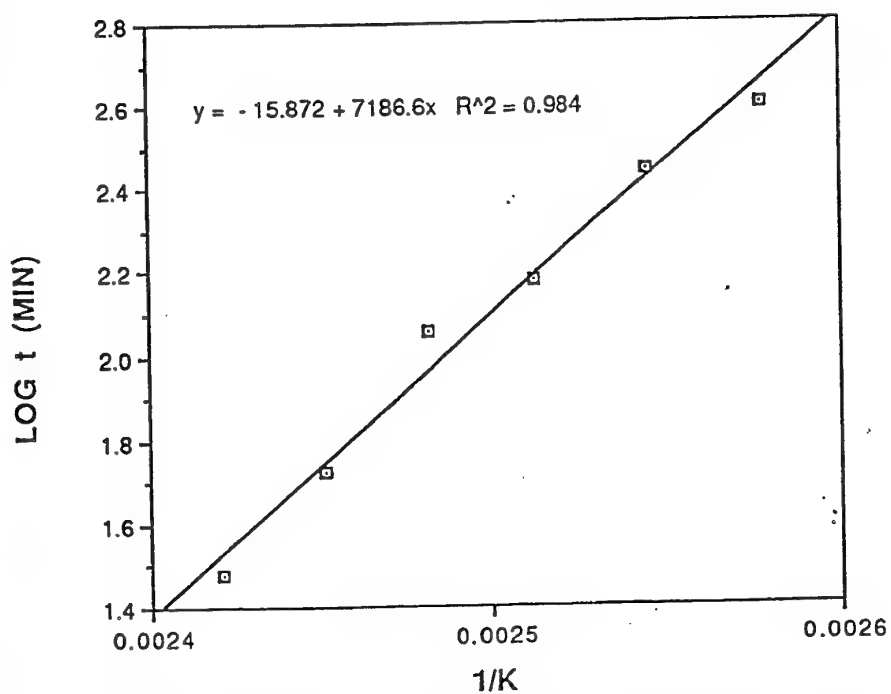


FIGURE 3. ARRHENIUS PLOT OF CRYSTALLINE ADN FROM ISOTHERMAL DSC DATA;  $E_a = 32.8$  KCAL/MOL

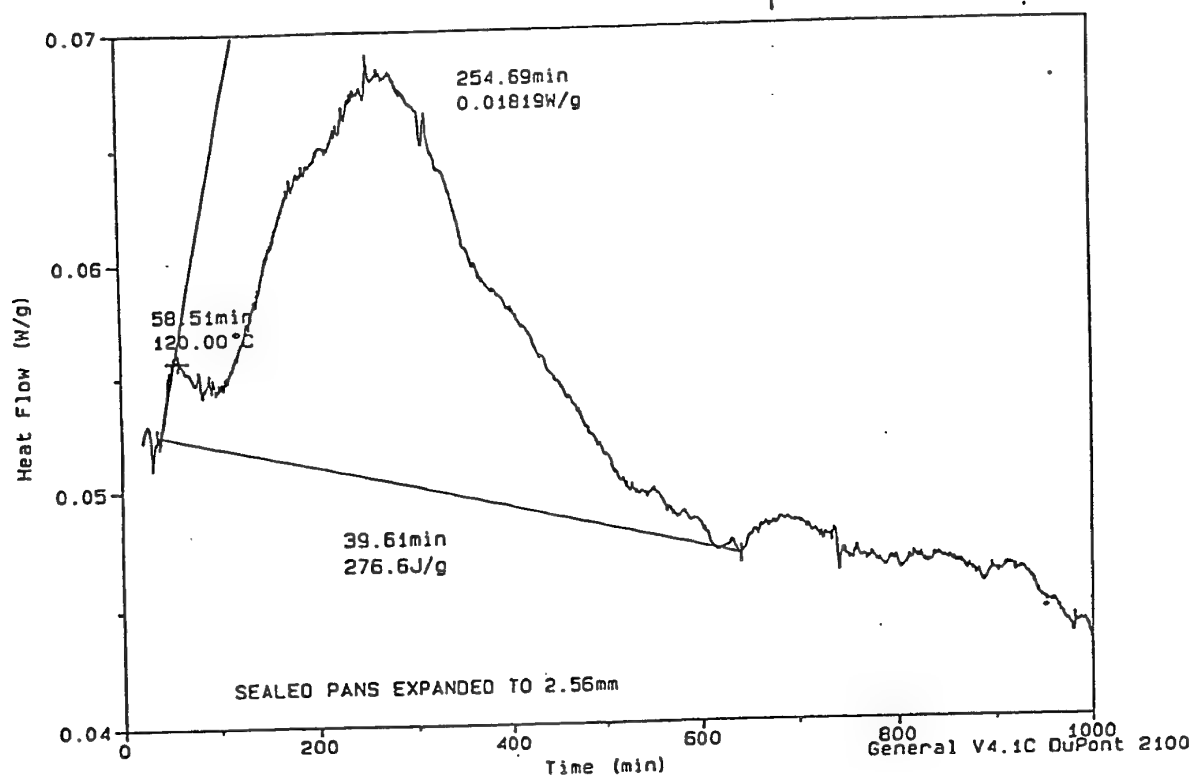


FIGURE 4. ISOTHERMAL DSC OF NEAT ADN AT 120°C

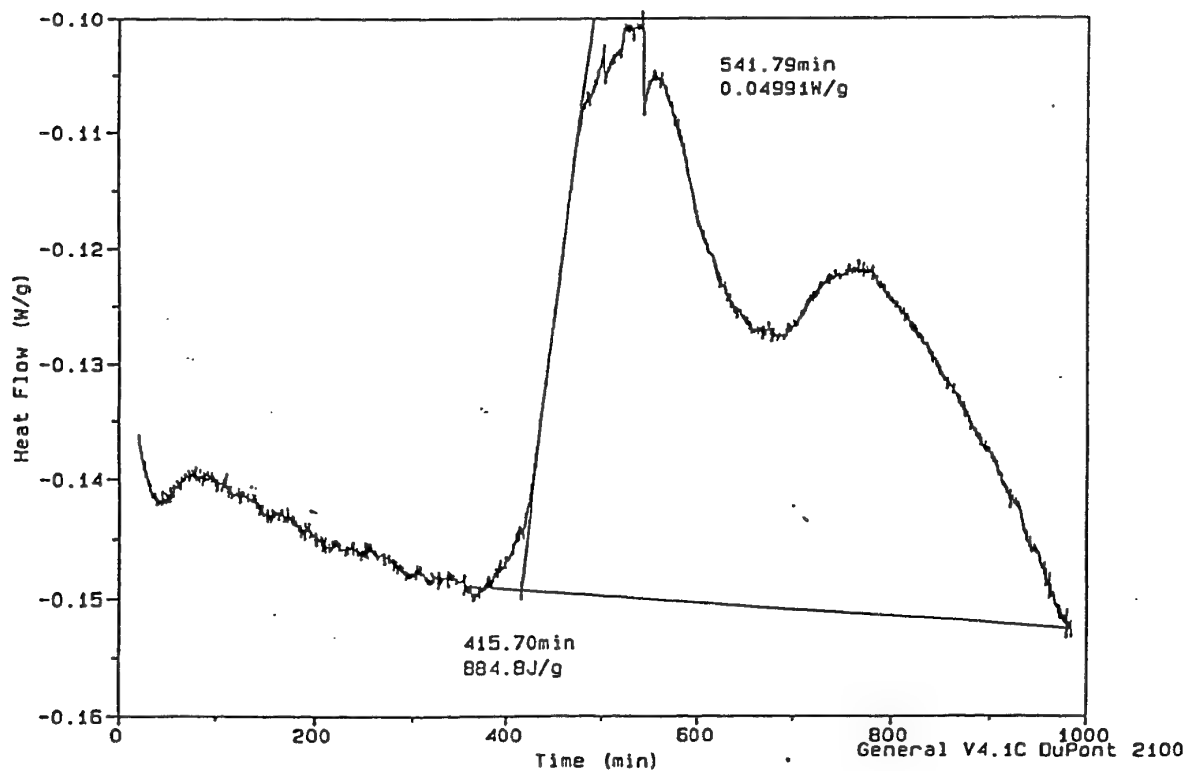


FIGURE 5. ISOTHERMAL DSC CURVE OF ADN WITH UREA AT 120°C

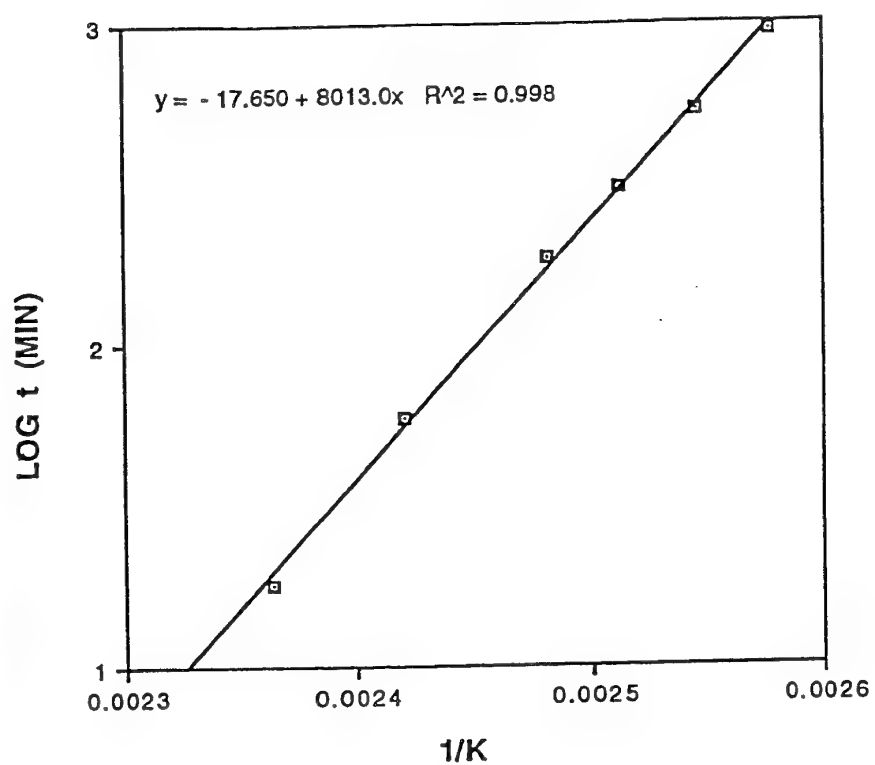


FIGURE 6. ARRHENIUS PLOT OF ADN PRILLED WITH UREA  
FROM ISOTHERMAL DSC DATA;  $E_a = 36.6$  KCAL/MOL



# THE FACTORS THAT MAY AFFECT THE ACCURACY OF MICROCALORIMETRIC DATA

Daniel S. Ellison and Anton Chin

Test & Evaluation Department  
Ordnance Engineering Directorate  
Crane Division, Naval Surface Warfare Center  
Crane, Indiana 47522-5001 USA

## ABSTRACT

There are many factors which may affect the experimental results of microcalorimetric analysis of energetic material, especially the double based propellants. The most common factors are 1) precondition temperature and time, 2) sample size to sample cell volume ratio (available space in the container after the sample is loaded), 3) amount of moisture/ air trapped in the sample cell, 4), leaky sample cell, 5) pressure effect to heat flow, and 6) heat flow selection for activation energy ( $E_a$ ) calculation. Each of the factors will or may affect the accuracy and reproducibility of the microcalorimetric data to some extent.

In this paper, the authors will introduce the fundamental principles and procedures of experimental microcalorimetry to reduce the error and deviation to a minimum. In addition, technique of high pressure microcalorimetry and its effects on the results of testing double-base propellants are also introduced.

## I. INTRODUCTION

Microcalorimetry of energetic materials presents a new look at materials that vary over a wide range in heat flow characteristics. Propellants are excellent for the analysis of aging trends because they generate significant heat flow even at low temperatures (45 to 80°C). The interesting fact is that the calorimeter does not know what it is measuring it just gives the user the results of heat generation, chemical adsorption/desorption, physical reactions or combinations of all previous. Its up to the user to separate the various processes into their individual components. In many cases it is just a matter using other data to compare the heat curves. It also possible to analyze each component and sum up to get the original heat flow curve. The user's knowledge of the chemistry is important in unlocking what the calorimeter curves mean.

## II. COMMON FACTORS THAT AFFECT THE TEST DATA

**A: Preconditioning before measurement:** Many users ignore the first few days to weeks of data obtained from propellant samples because of the strange initial effects that have been observed [1]. Figure 1 shows what would be lost by preconditioning the test.

A series of samples were aged for a period of sixty days and samples analyzed by HPLC for the stabilizers formed. The chemical reactions that are occurring during the first few days are significant. Figure 2 shows that diphenylamine (DPA) is being depleted and that the daughter intermediate products are forming. All these changes are occurring within the first ten days at 80°C. Of course monitoring at lower temperatures will allow more time to precondition with less affect. But still eliminates useful information about chemical reactions going on at lower temperatures that can be seen as heat flow reactions in the microcalorimetric signal.

**B. Sample Size to Sample Cell Volume Ratio:** A microcalorimeter is unique in its ability to measure small heats generated from relatively large samples when compared to a differential scanning calorimeter (DSC) [2]. Most DSC's use from 1 to 50 milligrams (mg) and restricted to low pressure aluminum pans and high temperatures in order to detect any signal at all. The microcalorimeter can hold very large sample. For propellants this can be from 1 to 25 grams typically, and more for custom designed microcalorimeters. Since propellants come in a variety of grain sizes, they will not fill the calorimeter test ampule in at the same bulk density. As part of the initial evaluation of 20 mm propellant temperatures in the 45°C 50°C as well as 65.5, 75, and 80°C were used.

The results of a partially filled ampule, about 3.5 grams, show shown in figure 3. This seemed about right, but more signal was desired to increase confidence in the data, something in the range of 10 to 25  $\mu$ watt level instead of 5  $\mu$ watts. A 7.3 gram sample was loaded into a 20 cc internal volume ampule. Figure 4 revealed a dramatic difference in output. The signal level did not double, but rather it stayed endothermic for days. A close examination of the figure 4 shows a oscillating pattern in the heat flow curve. The curve was mathematically duplicated by summing an exponential curve with a low frequency sinusoidal curve. It was reasoned the propellant behaves as if a gas phase reaction is happening. If the free space is playing a part in this system, then changing the free space should have some affect.

Figure 5 is the result of filling the 20 cc ampule up to minimize the free space. It is clearly evident that the response time is increased and the effect of the gas phase is not observable. At 65.5 °C there is indications of sample size and free space affects. Figure 6 illustrates the microcal response as the available space in the ampule is reduced. Since propellant aging is affected by the free space in the ordnance item, this would indicate that testing propellants in the microcalorimeter show take into consideration duplicating the same bulk loading density.

**C. Amount of moisture/air trapped in the sample cell:** One of the most perplexing problems

with interpreting microcalorimetric data and other tests such the 65.5°C fume stability test is the uncontrolled nature of some of the large scale test. It is known that moisture will result in the break down of propellants and cause acid catalysis. A test like the fume test always results in excess air and moisture being allowed randomly into the 8 oz. glass jar with glass stopper. This is usually caused by the pumping action of the observed gas phase reactions. In the summer when the humidity is high the number of propellant samples fuming is higher than during the dry months. This will only result in unreliable results.

The microcalorimeter test ampules used for propellant experiments are made from 316 stainless steel and are capable of standing at least 200 psi. When a propellant is loaded in the item, there will always be some short term reactions which will consume the available oxygen and moisture that was trapped in the item when sealed. Bulk propellant tested in the fume test are subjected to the same conditions and should not be expected to age the same way as propellant as in the 20 mm cartridges..

These initial reactions with moisture and air can easily be minimized by purging the ampules with dry nitrogen for 5 minutes to remove the air atmosphere and surface moisture. This is only done to take away factors which are not present after loading. The goal is to measure what natural aging has done to the propellant, and not what handling and loading will do to the propellant.

**D. Leaky sample cells and pressure effects:** This is really a question about what the data means from the evaluation 20 mm propellant over a period of 120 days. Three propellant produced in 1979, 83, and 1987 were running in the microcalorimeter at 80°C. At approximately 105 days the heat flow curves began exhibiting a oscillation which repeated itself every 1.5 days. The results from the samples are shown in figure 7a and 7b. The first question that came mind in that this is just the venting of the ampule as the pressure is exceeded the limits of the ampule. The ampules were weighed and loss in mass was found, but still there was no unstable behavior to the cycling one would expect from venting. It seemed to be to consistent with just a pressure leak. Figure 7a shows that the oscillation started and then stopped.

This oscillation was seen in another 20 mm propellant in 105 days just like those in figure 7a and except it more unstable in its build up and had two peaks in stead of one.

It was decided to use a Setaram Microcalorimeter equipped with a high pressure cell that was capable of measuring pressure up to 300 bars. The Setaram pressure vessel is made from hastaloy C and can hold about 3.5 grams of propellant. It is believed that for a stable oscillation to occur an equal volume of free space is needed to provide a clean separate heat flow spikes. The pressure ampule was loaded with 1.68 gram of the propellant placed in a small glass tube to keep it from direct contact with the steel ampule. Figure 8 compares the heat flow curve and the pressure curve for the same propellant as in figure 7c. The temperature was 80.7°C and oscillation occurred started at 95 days. Clearly the pressure trace is sigmoidal and step pressure rises are observable when the spikes in the heat flow curve start. If the vessel were leaking one would expect a change in the rate of pressure rise at 90 days.

#### **E. Heat flow and selection points for Energy of Activation Calculation:**

Microcalorimeter heat flow curves are usually plotted as  $\mu\text{watts/gram}$  versus time. When trying obtain kinetic data the user is not always presented with a clear way to use the heat flow data. If the reactions are steady state, then the heat rate at the level point can be used for different temperatures. If the curves are constantly changing such as Figure 9, then the area of the curve should be used to the point for heat rate data. The heat rate data should be used at the same point of conversion. One cannot run the sample long enough to go to completion in most cases. If the mechanism is consistent then the heats taken at the point of conversion will give an accurate measure of the  $E_a$ .

### **III. SUMMARY**

To obtain accurate and reproducible data from a microcalorimeter it is necessary to measure the propellant under the same sample loading density used in the ordnance item. This will minimize gas phase reactions. You should measure the whole range of the aging from start to finish without preconditioning your sample. Aging can be done in ovens and the sample transferred to the calorimeter for measurement as long as the data does not ignore critical points during aging. The user must know the limits of the closed system ampules so that pressure effects can be understood. The calculation of  $E_a$  values depends upon the data being taken at equal points of conversion for each temperature.

### **IV. REFERENCES**

1. L. G. Svensson, L. E. Paulson and T. Lindblom, "A Microcalorimetric Study of Temperature and Stabilizer Effects on the Heat Generation in Gun Propellants", 4<sup>th</sup> Gun Propellant Conference, Mulwala, Australia. (1990).
2. A. Chin, D. S. Ellison, B. R. Hubble, and R. G. Shortridge, "Microcalorimetric Analysis of Mg and MTV Compositions Using Adsorption/Desorption Technique", Proceedings of 22<sup>nd</sup> International Pyrotechnics Seminar, Fort Collins, Colorado, p-93 (1996).

20 MM PROPELLANT  
80°C, 4.0 GRAMS, 4 CC AMPULE

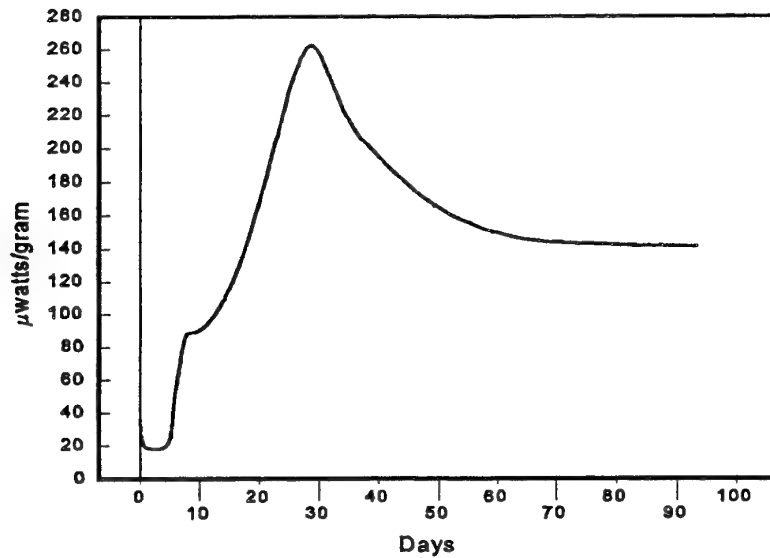


Figure 1. Typical microcalorimetric heat flow curve at 80°C

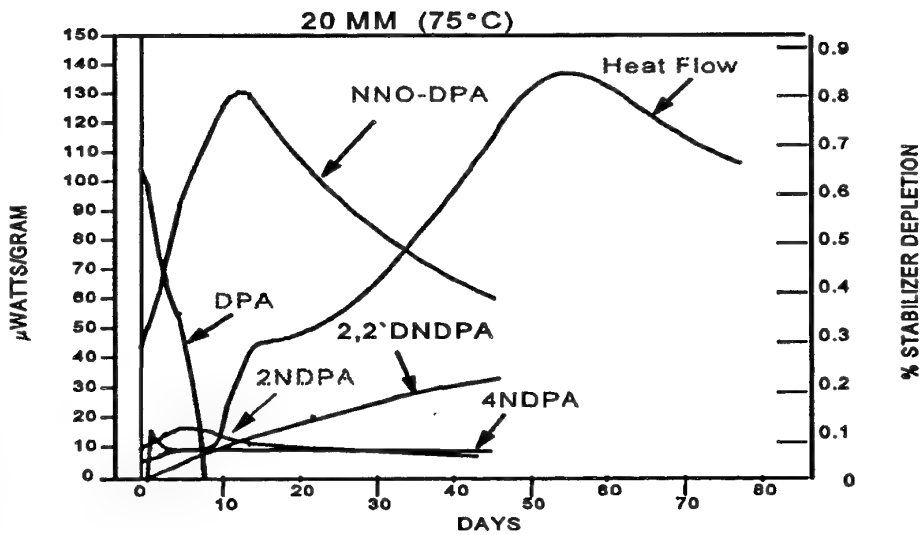


Figure 2. Stabilizers formed during a 45 day aging period overlaid on the microcalorimetric heat flow curve at 75°C.

20 MM PROPELLANT, MANUFACTURED 1984  
50°C, 3.5 GMS, 4 CC AMPOULE

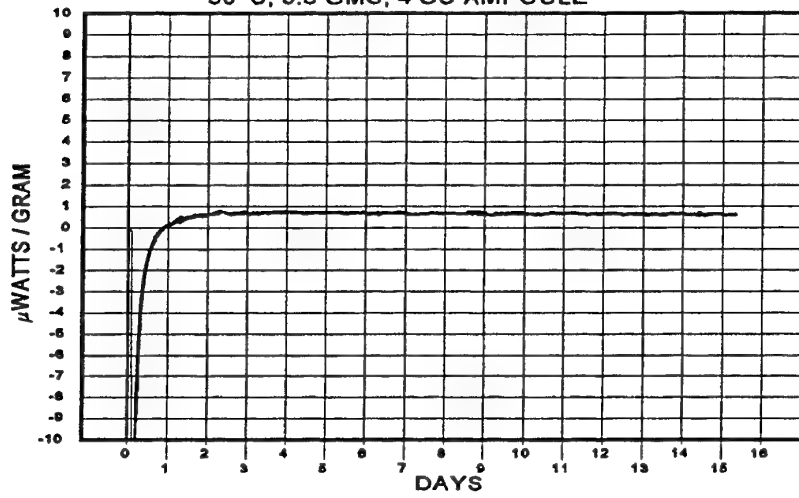


Figure 3. Response to a 3/4 full 4 cc ampule.

20 MM PROPELLANT, MANUFACTURED 1984  
50°C, 7.3 GMS, 20 CC ampule

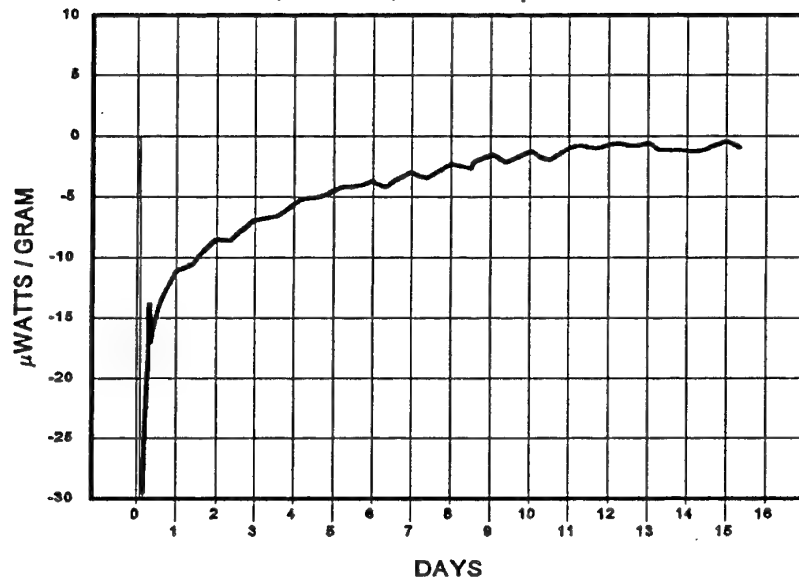


Figure 4. Effect of larger freespace on heat flow curve.

20 MM BALL PROPELLANT  
MICROCAL HEAT FLOW DATA, 50°C, 25.5 GMS, 20 CC AMPULE

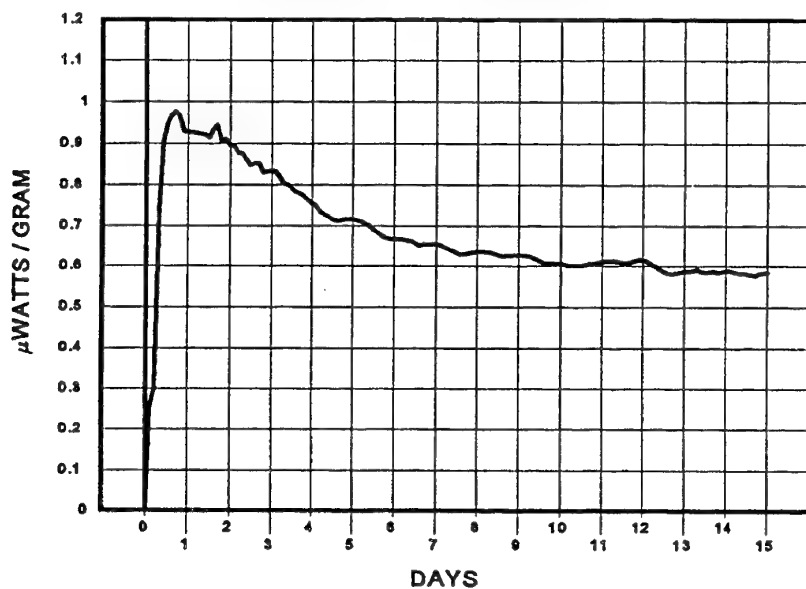


Figure 5. Effect of reducing free space in 20 cc ampule

20 MM PROPELLANT, MANUFACTURE 1992  
65.5°C, 1 TO 4.45 GMS SIZES

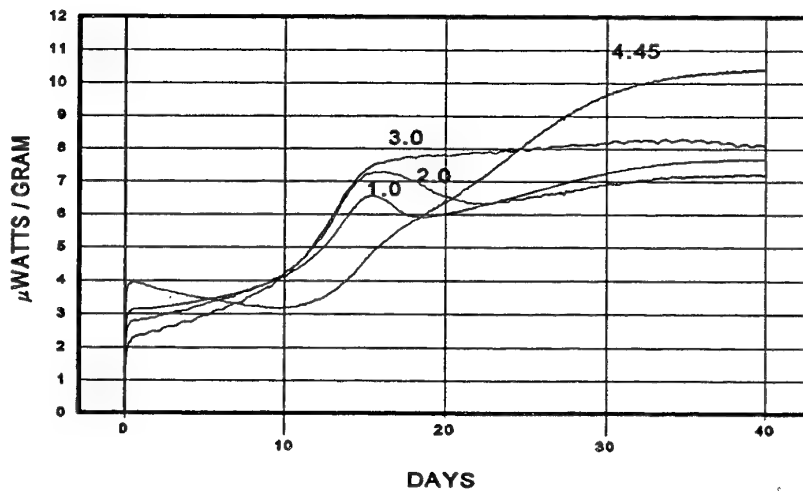


Figure 6. Effect of changing sample to free space ratio.

**20 MM PROPELLANT, MANUFACTURED 1979**  
**80C, 2.5 GMS, 4 CC AMPULE**

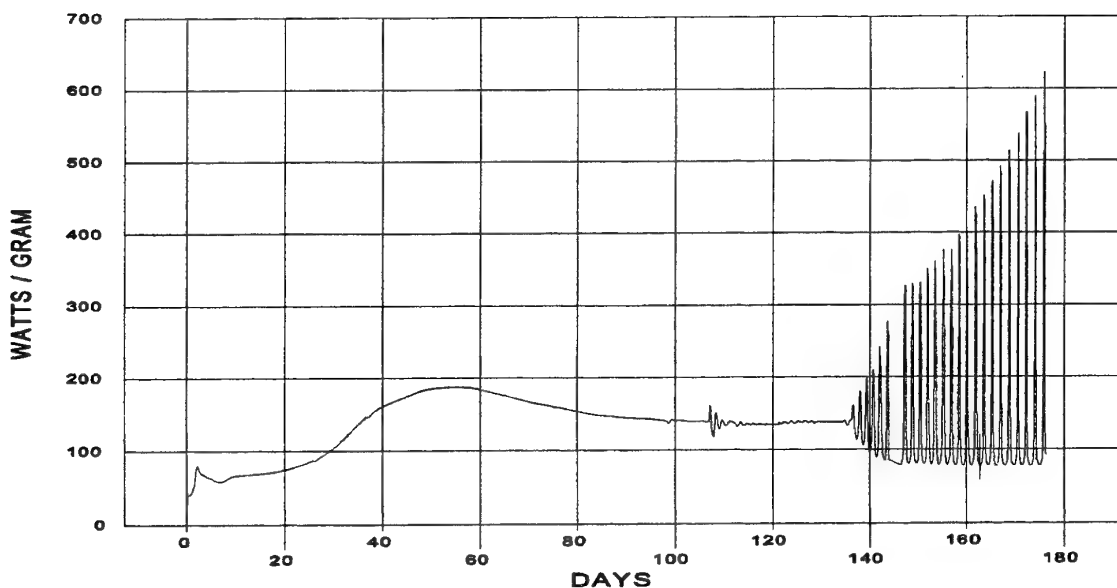


Figure 7a. Oscillation starting after 105 days

**20 MM PROPELLANT, MANUFACTURED 1987**  
**80C, 2.0 GMS, 4 CC AMPULE**

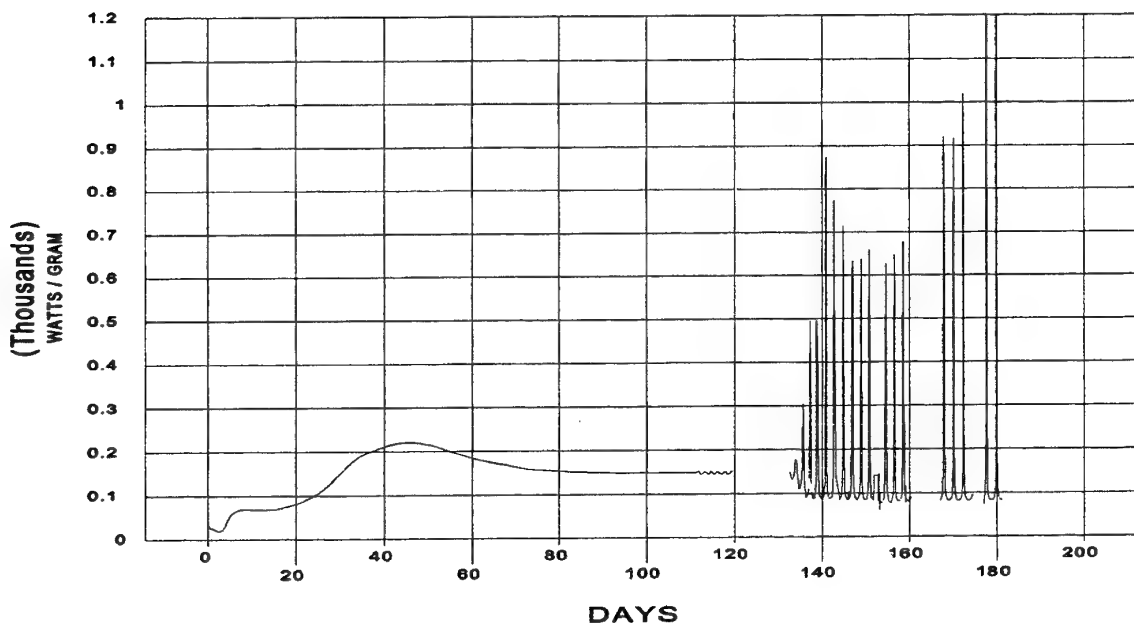


Figure 7b. Oscillation starting after 105 days



20 MM PROPELLANT, MANUFACTURED 1993  
80°C, 4.3 GMS, 4 CC AMPULE

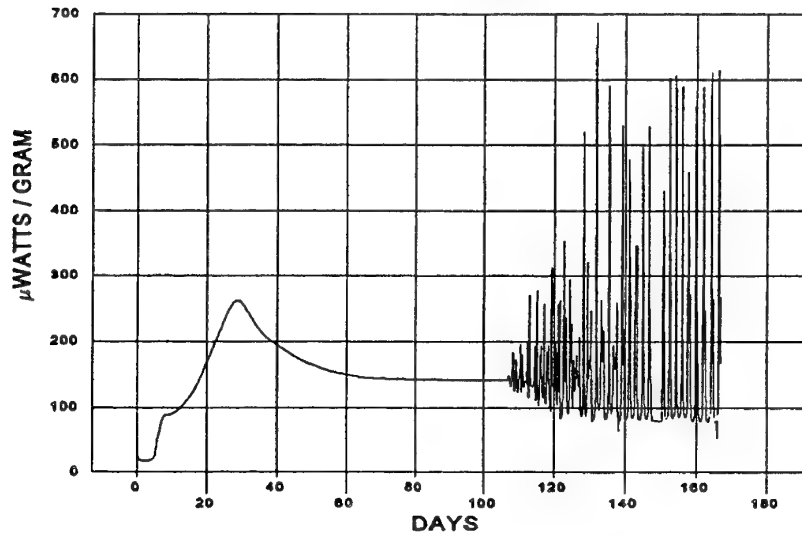


FIGURE 7c. Oscillations in a full 4 cc ampule

20 MM PROPELLANT, MANUFACTURED 1993  
PRESSURE EFFECTS (1.684 gms, 80.7°C)

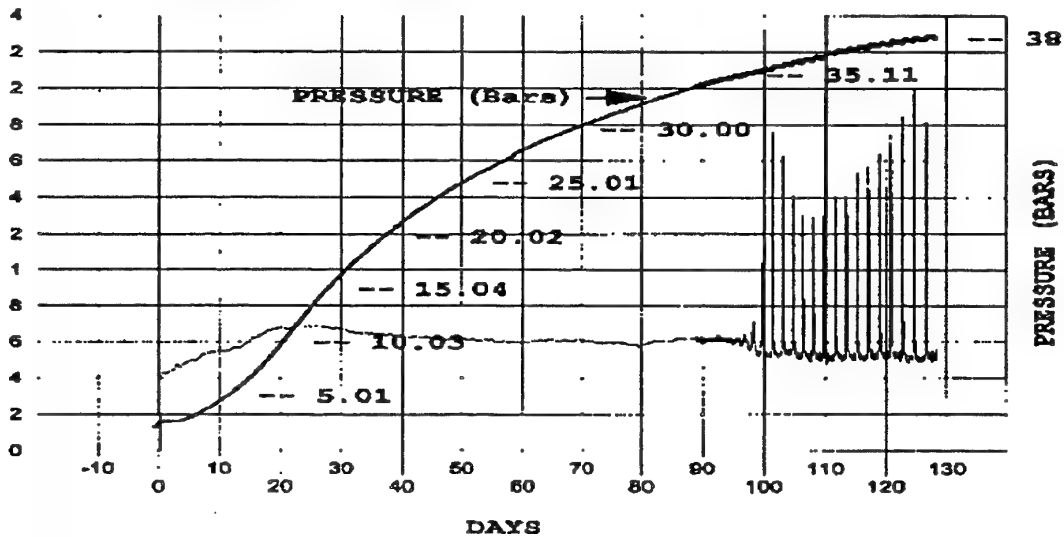


Figure 8. Pressure monitoring of oscillations

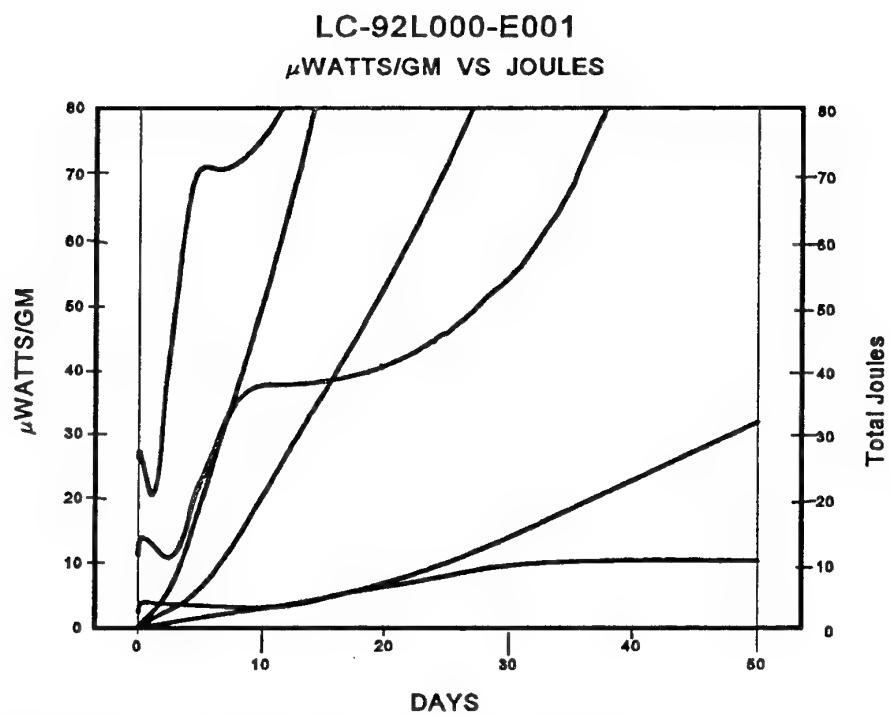


Figure 9. Calculating  $E_a$  from points of constant conversion

## PRACTICAL APPLICATION OF MICROCALORIMETRY TO THE STABILITY STUDIES OF PROPELLANTS

M.RAT<sup>1</sup>, P.GUILLAUME<sup>2</sup>, S.WILKER<sup>3</sup>, G.PANTEL<sup>3</sup>

1. SNPE, Centre de Recherche du Bouchet, Rue Lavoisier, Le Bouchet - BP N°2, F-91710 Vert-Le-Petit, France
2. P.B.CLERMONT s.a., Rue de Clermont 176, B-4480 Engis, Belgium
3. Bundesinstitut für chemisch-technische Untersuchungen beim BWB (BICT), Großes Cent, D-53913 Swisttal, Germany

### ABSTRACT

The heat flow calorimetry (HFC) is one of the most useful technique for assessing a service lifetime of nitro-cellulose based propellant.

The measurements are conducted at temperatures between 80°C and 30°C. The values of constant heat production rates are taken for the calculation of the activation energy and the preexponential factor according to a zero order Arrhenius kinetics. The HFC results can be correlated with stabiliser consumption results. Moreover, assuming a maximum loss of energy of the propellant that still delivers an acceptable ballistic behaviour, it is possible to evaluate a service lifetime of the propellant. However, the error in lifetime calculation depends on the correctness of the measurements of the specific heat production rates.

In order to standardise a test procedure and to minimise the errors, a detailed study of various factors affecting the HFC results has been undertaken. The factors considered are:

1. the moisture content of the propellant,
2. the loading density of the cell,
3. the quality of the sealing of the cell,
4. the apparatus used ( TAM or CALVET).

Spherical propellants were used for this study. The results obtained in the three laboratories are compared and discussed. An excellent agreement is obtained between the different laboratories when those parameters are fixed.

In addition correlations between stabiliser consumption and heat production rates have been worked out for the moisture content of the propellant and the loading density of the HFC cell.

## **1. INTRODUCTION**

The Heat Flow Calorimetry (HFC) is one of the most useful technique for assessing a service lifetime of nitrocellulose based propellant [1].

The fundamental principle of HFC is that all chemical or physical reactions which produce heat are recorded during the whole measuring time.

The measurements are conducted at different temperatures between 80 and 30°C. The values of constant heat production rates are taken for the calculation of the activation energy and the preexponential factor according to Arrhenius kinetics.

The HFC results can be correlated with stabiliser consumption results [2].

Moreover, assuming a maximum loss of energy of the propellant that still delivers an acceptable ballistic behaviour [3], it is possible to evaluate a service lifetime of the propellant.

However, the error in lifetime calculation depends on the correctness of the measurements of the heat production rates.

In order to minimise the errors, a detailed study of various factors affecting the HFC results [4] has been undertaken.

Spherical propellants were used for this study.

We have considered the following factors.

- I. the moisture of the propellant
- II. the loading density of the cell.

Those 2 parameters are encountered in the real life of the propellant in the cartridges and can affect the rate of decomposition of the propellant.

Beside those two parameters we have to consider the reproducibility of the measurements.

Measurement in three different laboratories were carried out in order to check the reproducibility of the results, to standardise the test procedure and hence to minimise the errors in service life calculations.

## **2. EXPERIMENTAL PROCEDURE**

For the purpose of this study, double base spherical propellants were used. Most of the work has been done with the K6210 propellant.

The experiments were runned in a TAM calorimeter with glass ampoules. Three different working ampoules were used :

3 cm<sup>3</sup> (BICT and PB Clermont)  
4 cm<sup>3</sup> (SNPE)  
20 cm<sup>3</sup> (SNPE)

At least double measurements were recorded on each samples. The measurements were started as soon as the samples were introduced into the microcalorimeter.

The measurements were started with a fresh sample at 80°C for at least 8 days. Then the samples are measured at lower temperatures until they reach a constant HFC signal that is used for the evaluation of the kinetic parameters. The measuring temperatures lie in the range between 80 and 30°C.

The influence of the following parameters was investigated :

- the moisture content of the propellant
- the mass of the propellant in the cell

Some measurements have been made with fresh samples at temperature below 80°C in the range between 70 and 50°C.

A few measurements have also recorded been in a CALVET calorimeter with a sample vessel of 92 cm<sup>3</sup>.

In parallel we have analysed the stabiliser products at different time of samples that had been aged under the same conditions.

### **3. RESULTS AND DISCUSSIONS**

#### **3.1. Analysis of the shape of the HFC curves**

In the case of double base propellants (see FIG 1), we have a certain and reproducible structure of the curves of freshly introduced samples which can be described by

- a first maximum
- a minimum
- a second maximum
- a final nearly constant value

Combining HFC measurements with stabiliser analysis we can better understand what chemically happens during HFC measurements.

As it can be seen on FIG 2, the DPA concentration decreases while the measurement goes on. In the minimum only a few percent of the original of DPA remains while N-NO-DPA is increasing rapidly reaching a maximum value at the second maximum of HFC (all DPA has disappeared at that point). Finally the heat generation being more or less constant implies a constant stabiliser consumption.

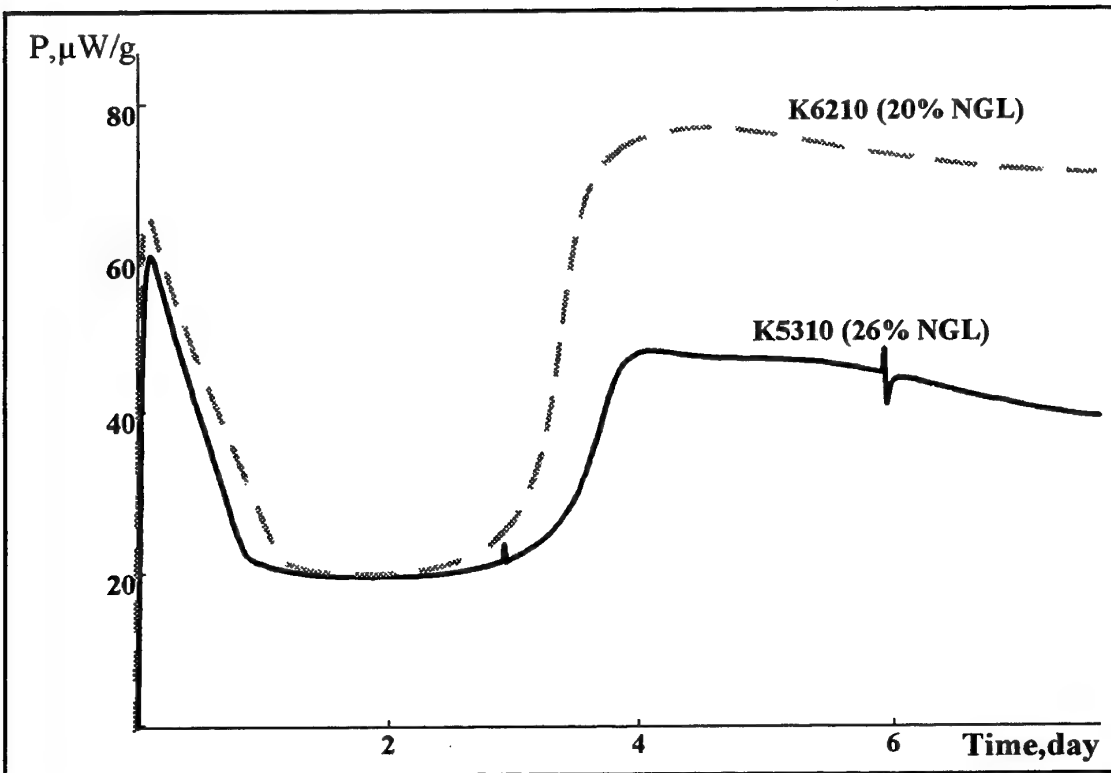


**FIG 1:** Heat flow calorimetry of different spherical propellants at 80°C

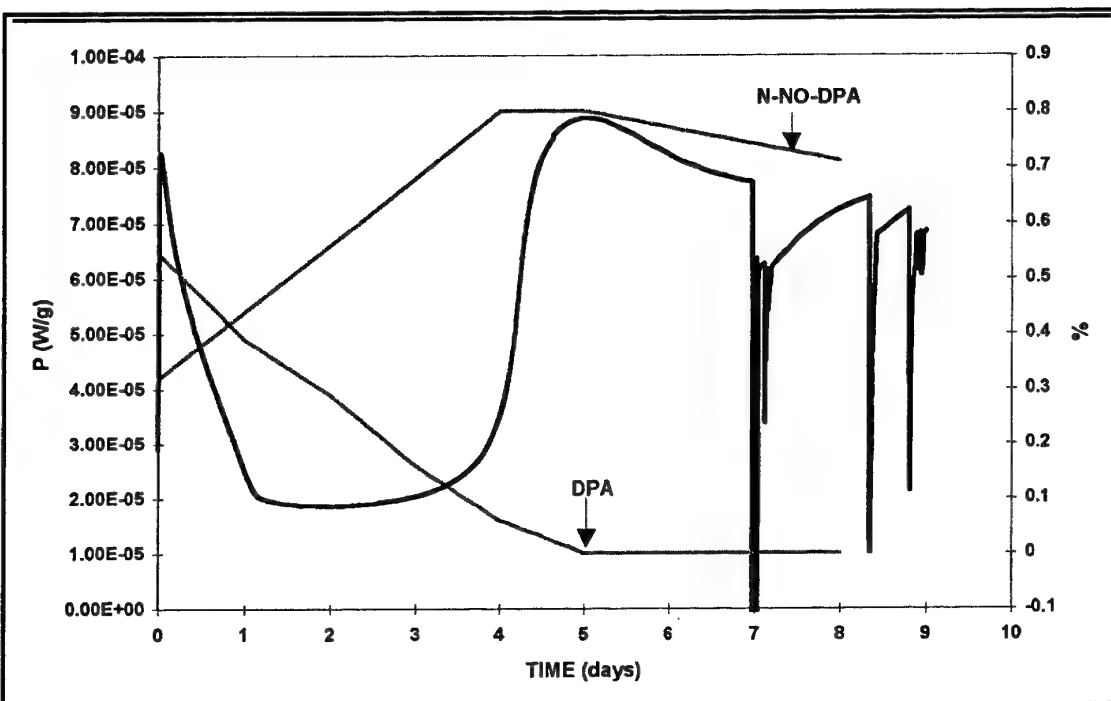


**FIG 2:** Heat flow calorimetry at 80°C of propellant K6210 (lot 215) combined with stabiliser loss.

The same shape is recorded at lower temperature (e.g. 70, 60 or 50°C) when a fresh sample is introduced (FIG 3). However as expected, the time to reach the different stages is much longer and the heat flux much lower, but the energy release is comparable (FIG 4). That means that the decomposition mechanism is unchanged for all these temperatures.

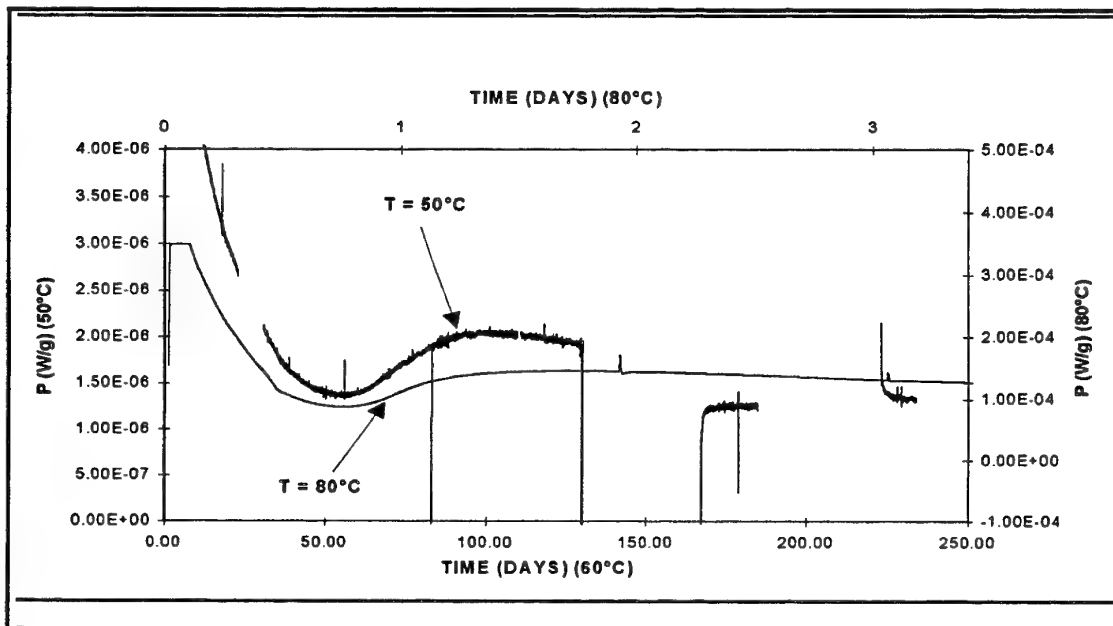


FIG 3: Heat flow calorimetry of propellant K6210 at different temperatures

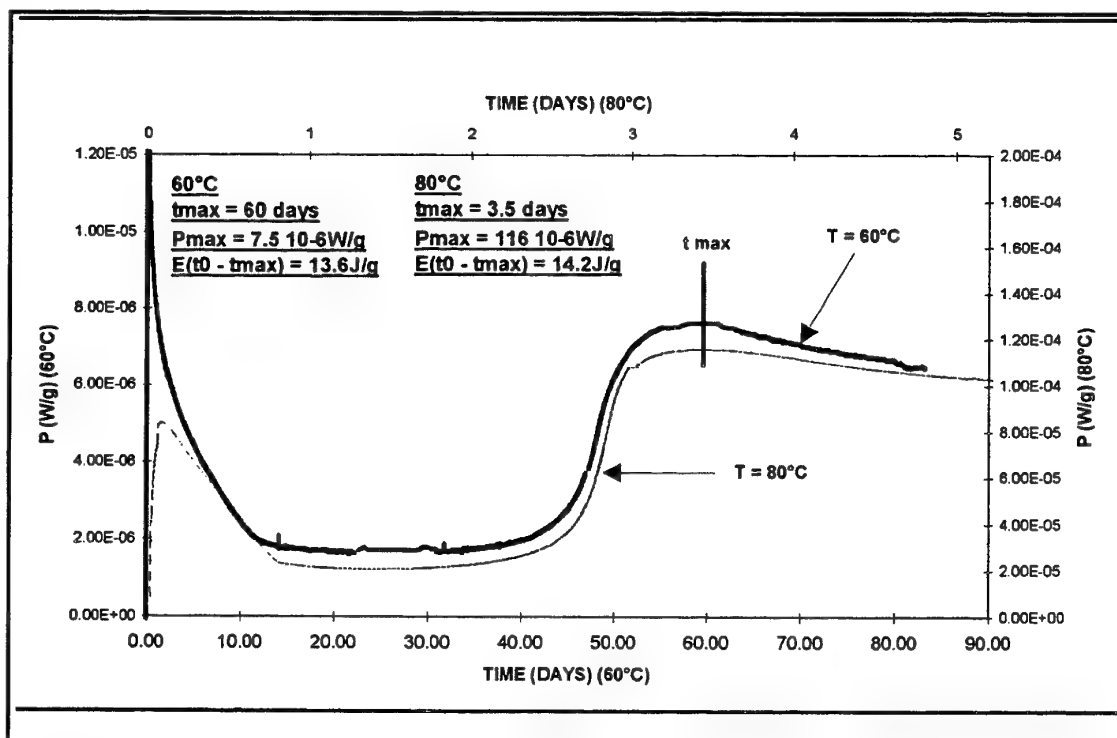


FIG 4: Comparison of freshly introduced samples of propellant K6210 (lot 218) at different temperatures

Using a zero order reaction the heat production rate can be described by the following equation [5]

$$q = A \cdot e^{-E/RT} \quad (1)$$

At the same stage of decomposition of the reaction (same energy release) at 2 different temperatures  $T_1$  and  $T_2$  we have

$$t_1 \cdot e^{-E/RT_1} = t_2 \cdot e^{-E/RT_2} \quad (2)$$

and hence combining (1) and (2)

$$q_1 t_1 = q_2 t_2 = \text{constant}$$

$$\text{or } \ln q = -\ln t + \text{constant}$$

On a graph we can draw the curves  $\ln q$  as a function of  $\ln t$  for the different temperatures. The intersection of the various curves with a straight line of slope -1 corresponds to a same stage of the reaction.

On FIG 5 you can see the results of the plot for the HFC measurement presented in FIG 3. This shows that when you reach the same part of the HFC curve at different temperatures you reach the same degradation point.

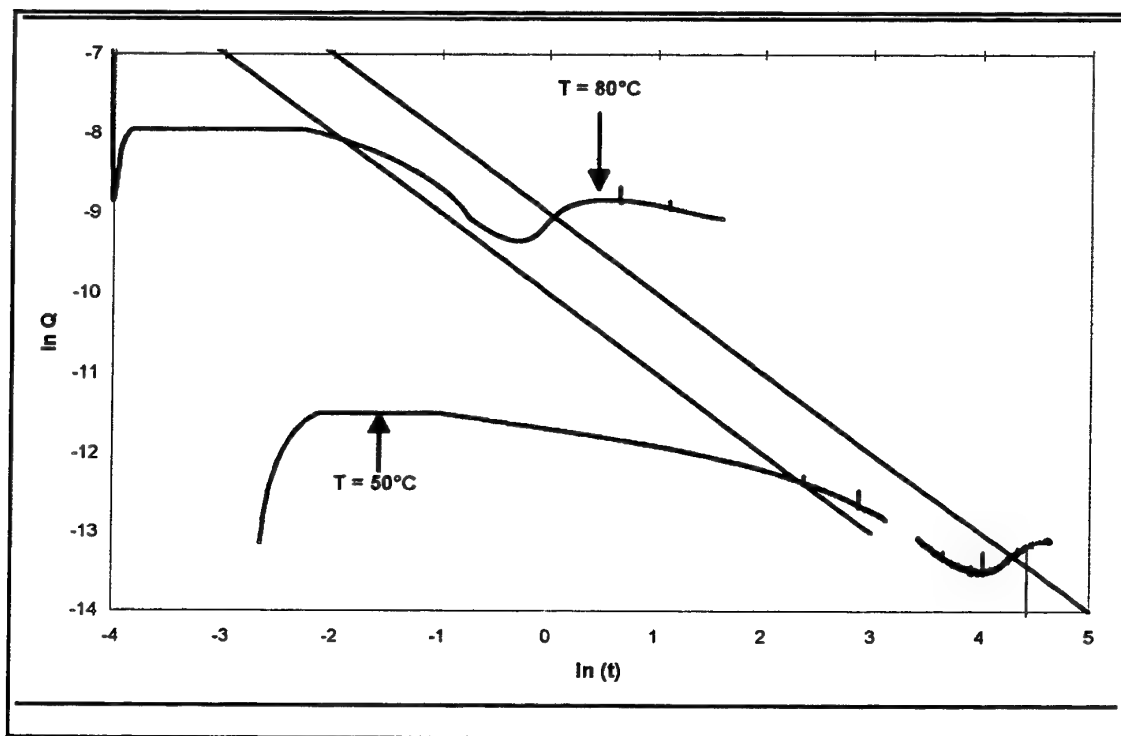


FIG 5: Iso-stages of decomposition during HFC experiments with fresh samples at different temperatures



### 3.2. Influence of the moisture content

The propellant K6210 has been conditioned for several days at different relative humidity before measurements.

1. drying on  $P_2O_5$  or  $CaCl_2$  : RH = 0 % ( KF = 0.02%)
2. conditioning at 65 % RH ( KF = 0.65%)
3. conditioning at 80 % RH ( KF = 0.85%)

The HFC results are presented on FIG 6 and the values reached at different stages of the HFC reactions in TABLE I.

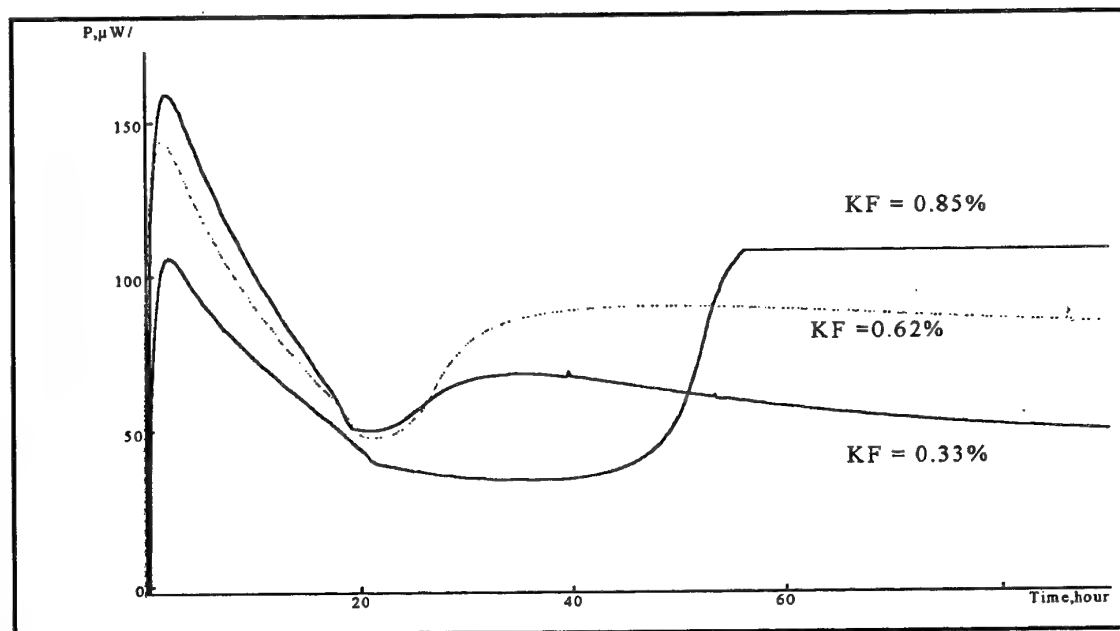
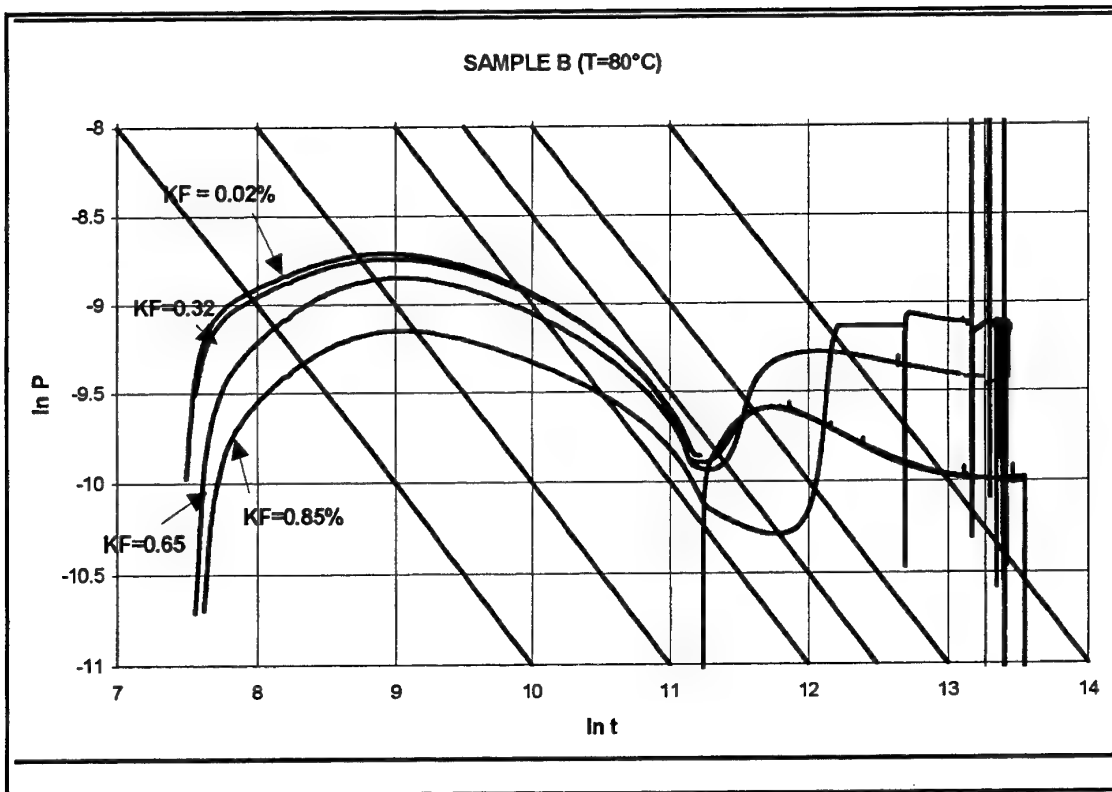


FIG 6: Heat flow calorimetry at 80°C of propellant K6210 at different moisture content

Table I: Important values of HFC measurements of fig 6 for propellant K6210

MOISTURE (%)	1. Max [ $\mu W/g$ ]	1. Min [ $\mu W/g$ ]	2. Max [ $\mu W/g$ ]
0.05	164 [2.0h]	52 [20.3h]	67.8 [1.4d]
0.33	158 [2.1h]	50 [19.5h]	68.3 [1.5d]
0.62	145 [2.3h]	49 [22.2h]	91 [2.04d]
0.85	106 [2.6h]	34 [37.7h]	[3.12d]

On FIG 7 we have drawn the  $\ln q$ .  $\ln t$  plot for the mentioned samples. One can remark that the different stage corresponds to the same degradation point of the propellant.



**FIG 7:** Iso-stage of decomposition for HFC experiments at 80°C with samples having different moisture contents.

This is also confirmed by the measurement of stabiliser consumption where the same trend is recorded ( see FIG 8 and 9). That is to say :

1. the rate of consumption of DPA decreases when the moisture content of the propellant increases (unusual behaviour).
2. the maximum of N-NO-DPA increases with moisture.
3. the steady state reached after the second maximum increases with the moisture. This is also true for the constant values measured at lower temperatures

When one calculates the activation energy and the preexponential factor (TABLE II), it appears that the activation energy remains nearly constant but the preexponential factor differs significantly leading to different service life

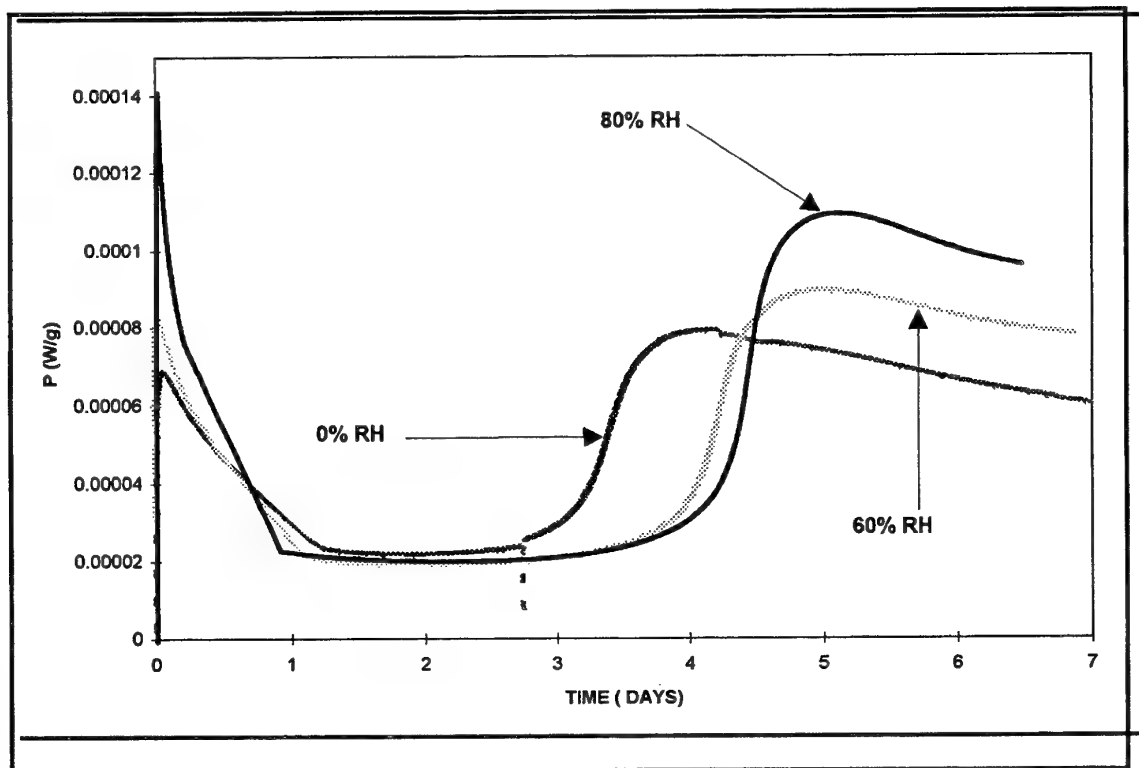


**FIG 8:** Heat flow calorimetry at 80°C of K 6210 (lot 215) after various conditionnings

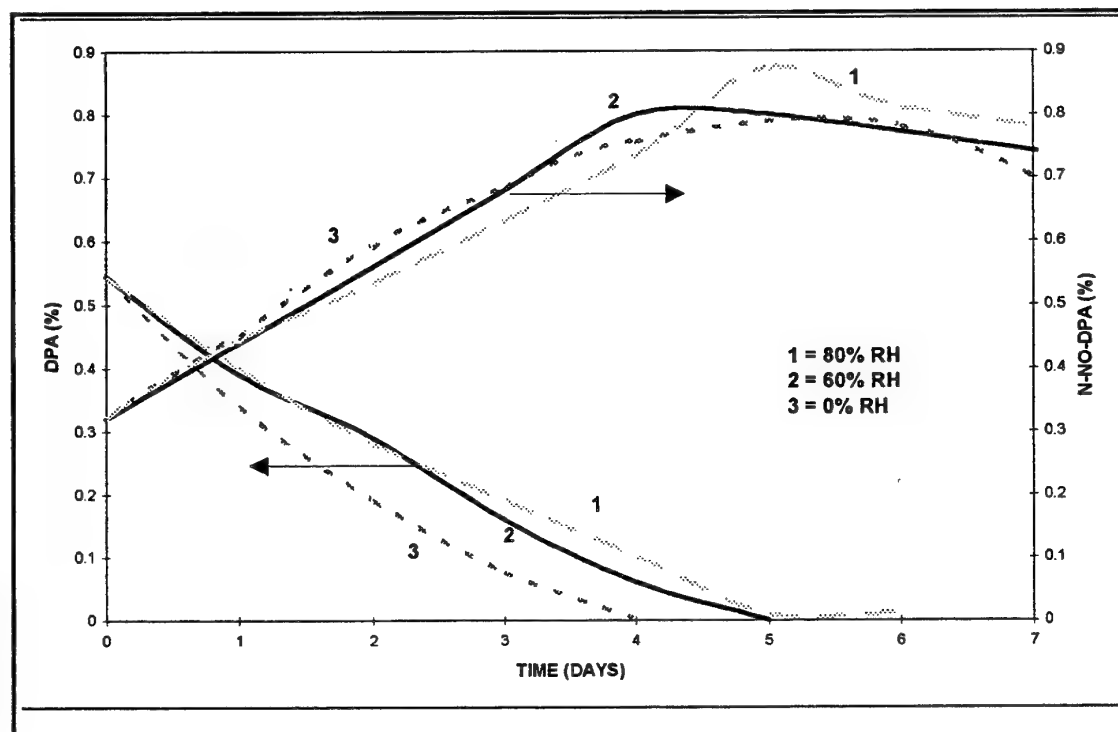


**FIG 9:** Stabiliser consumption of K 6210 ( lot 215) at 80°C

**Table II:** kinetic parameters for the fig 6

moisture content (KF)		activation energy (60-40)	pre-exp. factor (60-40)	correlation coefficient	SERVICE LIFE AT 40°C	SERVICE LIFE AT 30°C
(%)	(%)	(kJ/mol)	(W/kg)		(Years)	(Years)
start	end					
0.05	0.20	98.3	$1.1 \cdot 10^{13}$	0.977	9.3	32
0.33	0.24	88.1	$2.5 \cdot 10^{11}$	0.996	7.7	23
0.62	0.61	101.0	$4.4 \cdot 10^{13}$	0.993	6.2	22
0.85	0.86	106.1	$4.5 \cdot 10^{14}$	0.996	4.2	16
		activation energy (80-60)	pre-exp. factor (80-60)	correlation coefficient		
		(kJ/mol)	(W/kg)			
0.05	0.20	124.7	$1.2 \cdot 10^{17}$	0.999		
0.33	0.24	118	$1.3 \cdot 10^{16}$	0.999		
0.62	0.61	121	$5.8 \cdot 10^{16}$	0.998		

### 3.3. Influence of the loading density

In order to see the ability of HFC measurements to show reproducible values within different laboratories having different cells, we have undertaken a study of the loading density of the cells.

Indeed if one is using a larger cell, with an unknown propellant, it is interesting to know the evolution of HFC curves in order to avoid any damages to the apparatus that may arise from a large build up of pressure inside the cell. To reduce this risk one way is to reduce the amount of propellant in the cell, the other way is to start at lower temperature but then the time to reach a constant heat flow will be much longer.

An other point is to see if a different filling of the ampoule can lead to different results for the sample studied.

On FIG 10 one can see the evolution of the HFC curves for different filling of the ampoule. When the loading density of the ampoule is decreasing, the shapes of the HFC curves vary from the shape described earlier to the following shape :

1. first maximum
2. first minimum
3. second sharp maximum
4. second minimum
5. increase to a nearly constant value

This last increase leads to a higher heat flux value when the loading density decreases.

The time to reach a nearly constant value increases also when the loading density decreases. On TABLE III, the value recorded for lot 222 with an half filled cell is given in comparison with the values recorded for a full filled cell.

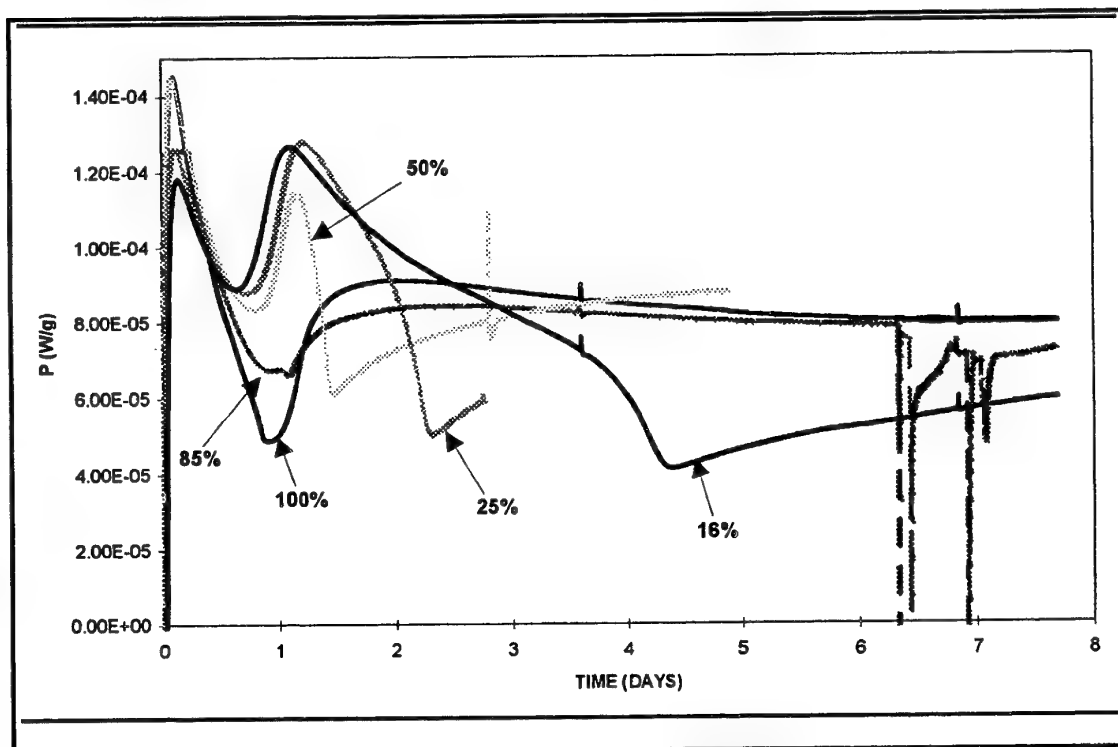


FIG 10: Influence of the loading density on the HFC signal at 80°C.

Table III : HFC results for propellant K 6210 lot 222

T (°C)	P (full cell) (μW/g)		P (Half cell) (μW/g)	
	A	B	C	D
80	66.8	66.8		
60	5.8	6.3	7.75	8.4
50	1.9	1.97	2.55	2.67
40	0.63	0.65	0.9	0.94

The change of the shape of the HFC curves may be due to the fact that all DPA is transformed before oxygen has been consumed.

In order to verify this hypothesis, some experiments have been run with an full filled ampoule where the air has been replaced by pure oxygen .

As it can be seen from FIG 11, the same shape of curve arises with an oxygen atmosphere.

When the kinetic parameters are calculated, the main difference is due to the preexponential factor (see TABLE IV). We can suppose that additional reactions with oxygen occur increasing the consumption rate of the stabiliser leading to a diminution of the service life of the propellant.

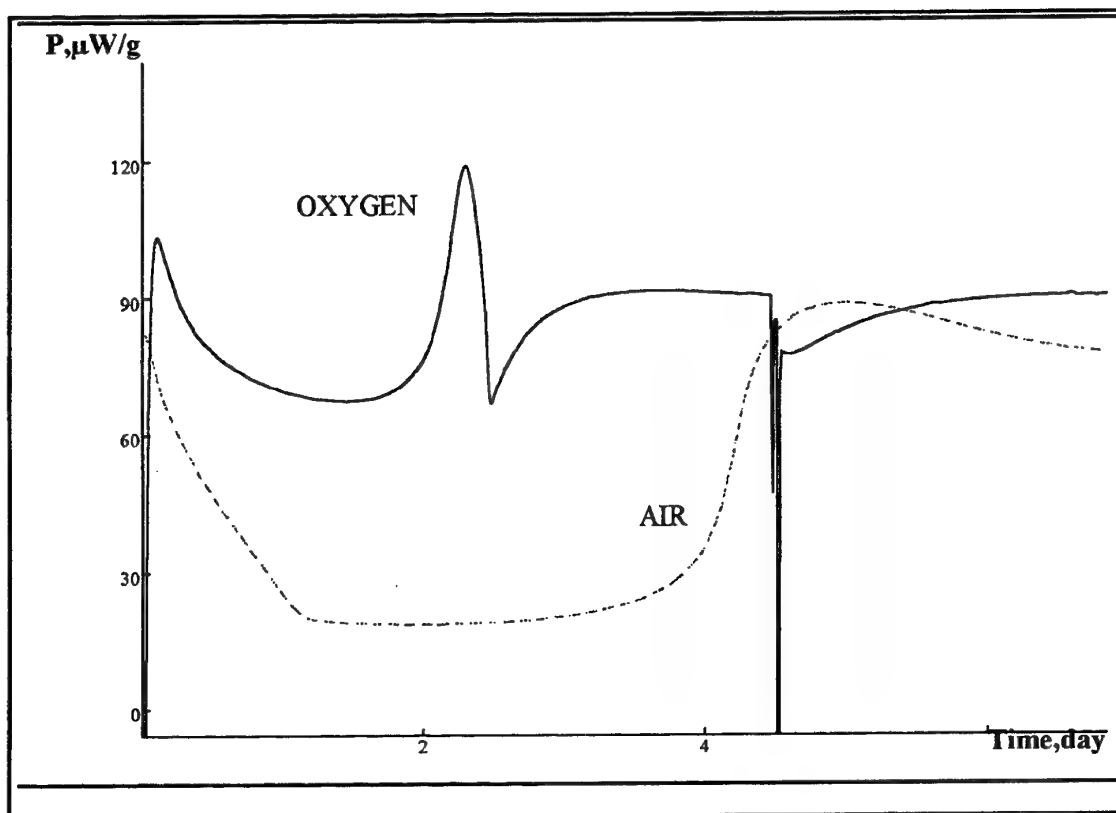


**FIG 11:** Heat flow calorimetry of propellant K6210 ( lot 215) under different atmospheres at 80°C

**Table IV:** Kinetic parameters for propellant K6210 lot222

CELL	Activation energy (kJ/mol)	pre-exp. factor W/Kg	TIME AT 40°C (Years)
FULL	97.1	$9.99 \cdot 10^{12}$	6.1
HALF	94.1	$4.41 \cdot 10^{12}$	4.3

### 3.4. Influence of the sealing of the ampoule

In some experiments an "abnormal" shape of the HFC curve is recorded (FIG 12) or some endothermic peaks are observed (e.g. fig 2 or 10).

The "abnormal" shapes are much like the shapes observed at low loading density or when air is replaced by oxygen. It can be concluded that those "abnormal" shape arises when the ampoule is not firmly sealed or not closed and then air can enter.

The endothermic peaks arise only after a few days at high temperatures. During the measurement a build up of the pressure occurs due to the degradation process of the propellant. According to the quality of the sealing of the glass ampoule, the ampoule will

hold different pressure (a few bars) before it leaks. The appearance of those endothermic peaks is thus the results of the leaks.

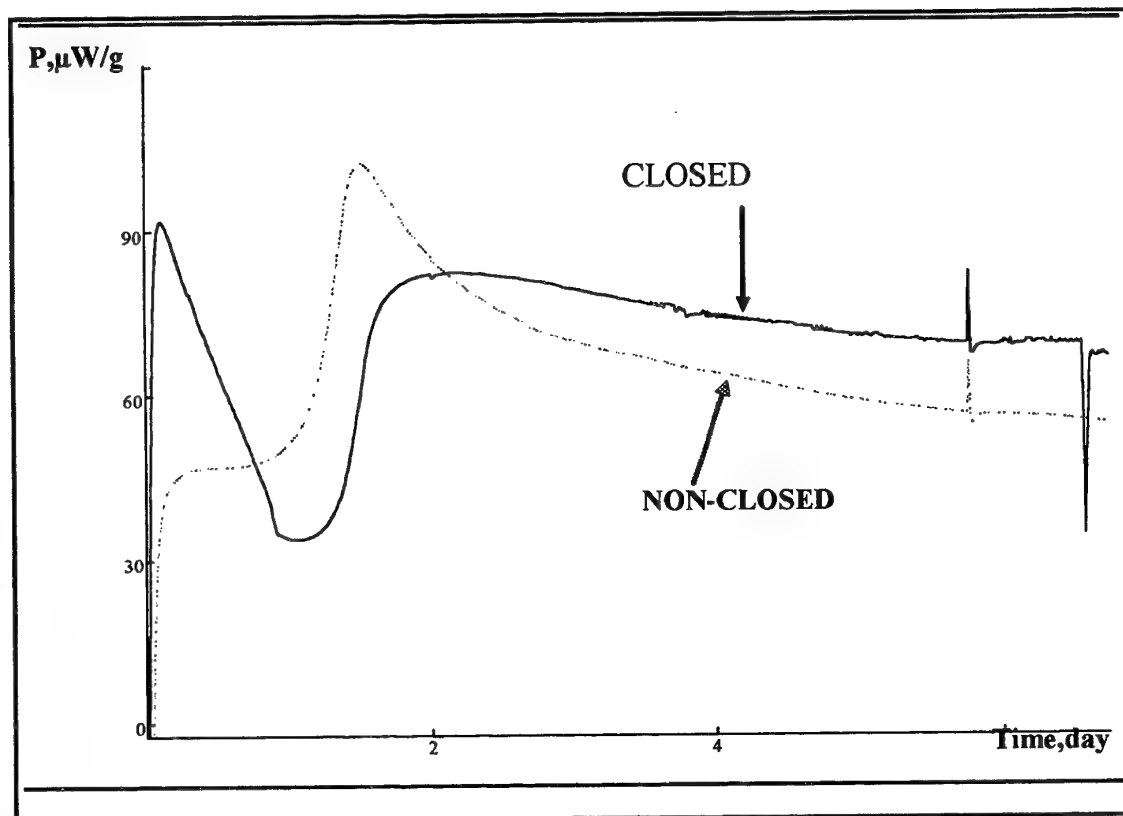


**FIG 12:** Heat flow calorimetry at 80°C of propellant K6210 (lot 219) with a closed and a non-closed ampoule

### 3.5. Comparison between two types of calorimeters

A few experiments have been run in 2 different calorimeters : TAM and CALVET (Setaram). The comparison of the results is given on FIG 13 for lot 215.

The results obtained in the CALVET are for 46 g. of propellant in a 92 cm<sup>3</sup> cell and for the TAM in a 4 cm<sup>3</sup> cell with 2 g. of propellant. The results obtained show a good agreement especially if one takes into account the differences in sample size. The loading density is comparable (see chapter 3.3).

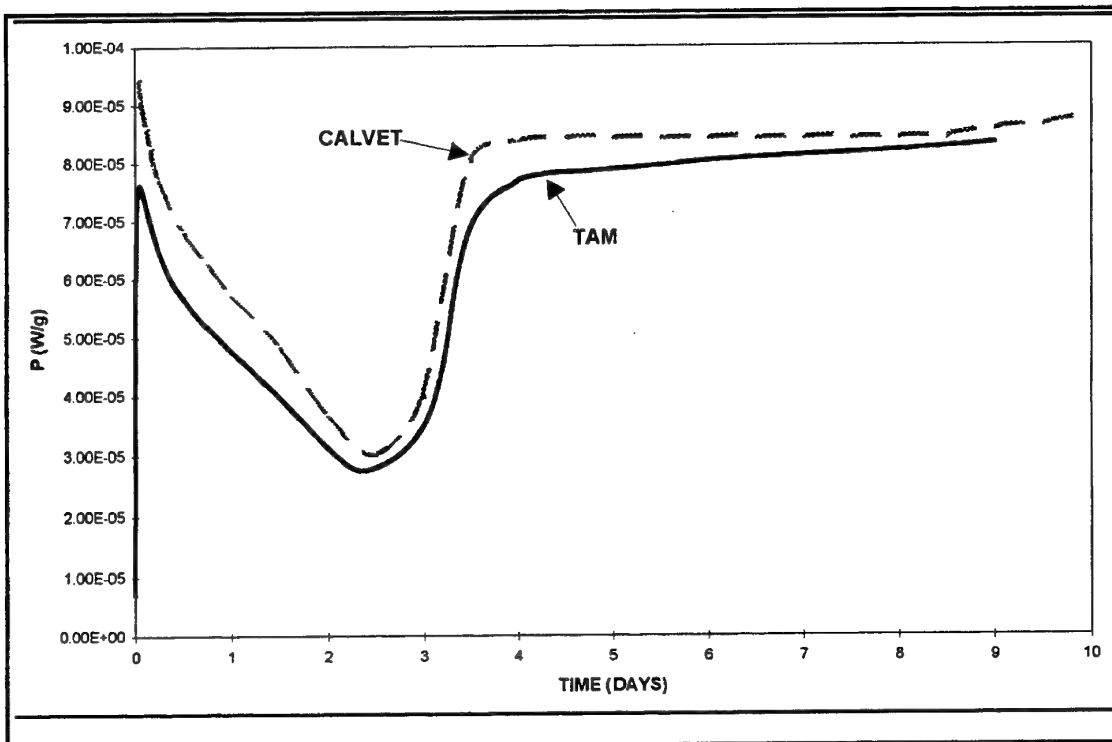


**FIG 13:** Heat flow calorimetry at 80°C of propellant K 6210 (lot 215) in different apparatus.

### 3.6. Comparison between different laboratories

Taking into account the above influences, HFC experiments have been run in three laboratories on common samples.

The results (FIG 14) show an excellent agreement between the three laboratories not only for the final value but also for the values and the time to reach the different significant points of the HFC curves ( table V). An excellent agreement is also recorded when the loading density is lowered to the same value (see FIG 15).

An other sample (lot 220) has been measured in BICT and PBC at the different temperatures between 80°C and 40°C (TABLE VI). Those experiments were conducted on non conditioned samples at different seasons. As it appears from the table, little differences (max. 10%) arise in each group of duplicate experiments. If the experiments are repeated without taking into account the conditioning of the samples, much larger differences appear (up to 30%), leading to an error of 40% for the service lifetime.

From the results obtained during the study of the influence of the moisture one can suspect that experiment 1 was performed with a sample having a high moisture content and experiment 2 and 3 with near the same moisture content, lower than for experiment 1.



As soon as the moisture conditions are the same, the results are in excellent agreement with a dispersion of the results less than 10% for the calculated service lifetime. It has been confirmed with lot 223 (table VIII and IX).

Moreover special care has to be paid to measurements at low temperatures for the calibration of the apparatus. In addition, the use of the « Switch technique » allows to verify the true level of the zero line and hence to reduce the error on the HFC values at low temperature.

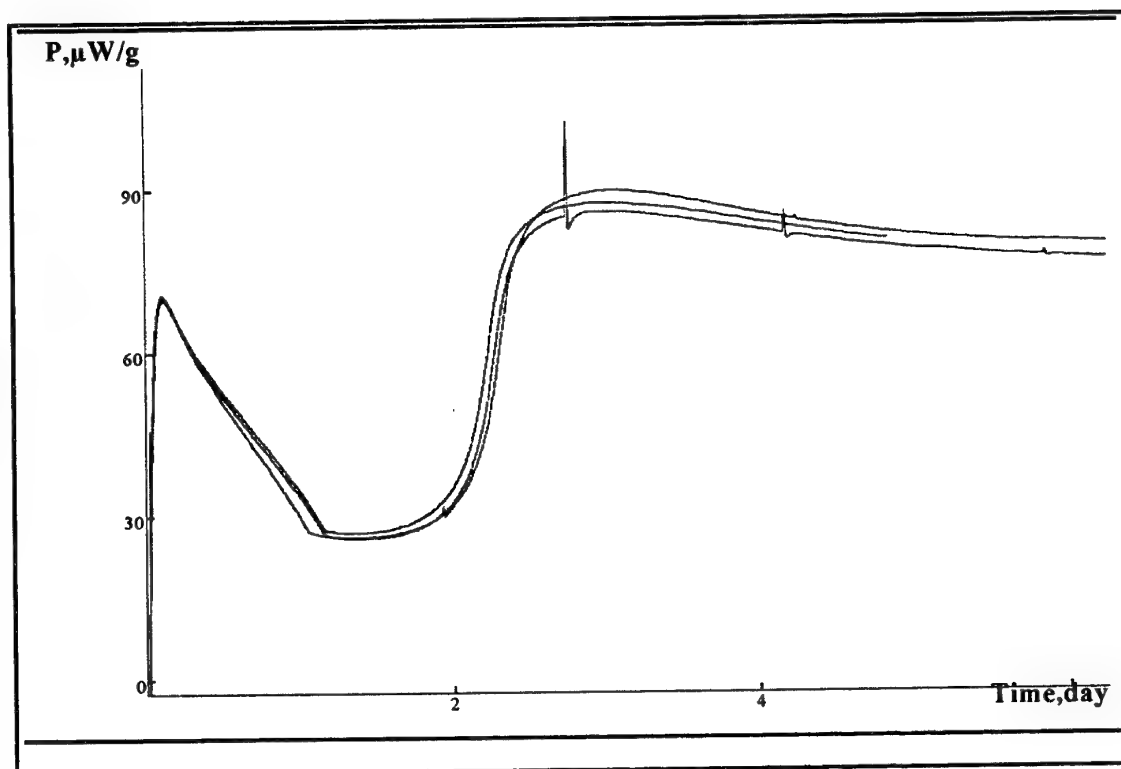


**FIG 14:** Heat flow microcalorimetry at 80°C of propellant K 6210 (lot223) in three different laboratories

**Table V:** Important values of HFC measurements of propellant K6210 in the 3 laboratories

LABORATORY	1. Max [ $\mu\text{W/g}$ ]	1. Min [ $\mu\text{W/g}$ ]	2. Max [ $\mu\text{W/g}$ ]
BICT	70.3 [3.2h]	25.8 [1.41d]	85.8 [3.03d]
BICT	69.4 [2.9h]	25.1 [1.39d]	86.7 [3.02d]
CRB	69.7 [3.2h]	26.9 [1.35d]	87.3 [3.01d]
PBC	70.8 [3.1h]	26.1 [1.36d]	89.7 [3.06d]
PBC	71.5 [3.1h]	26.0 [1.36d]	89.6 [3.06d]

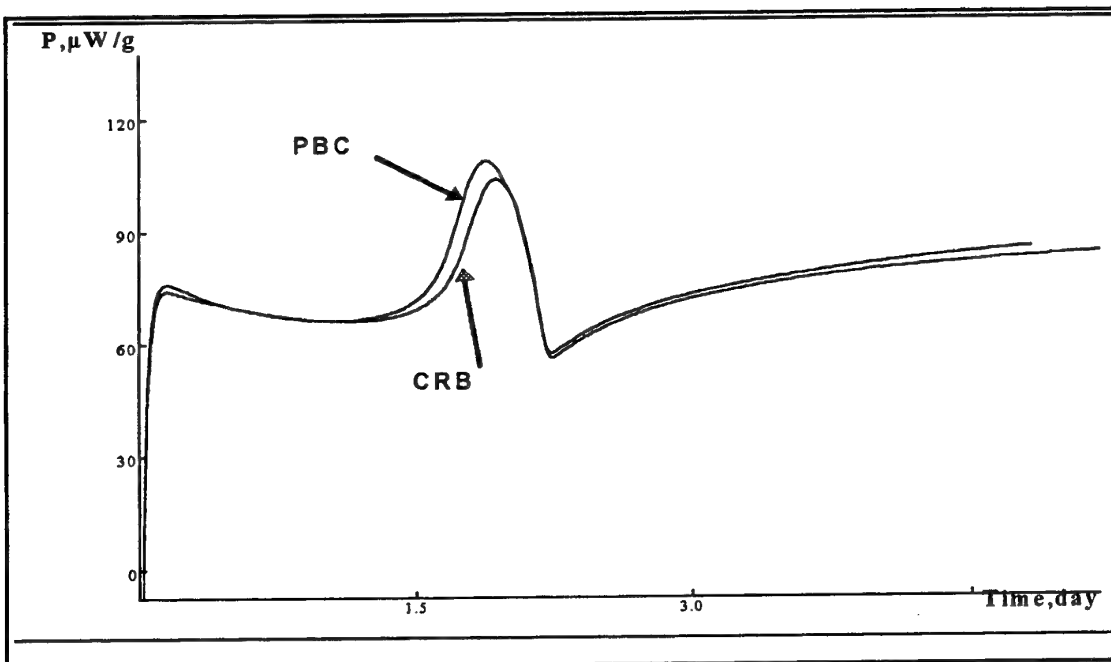


**FIG 15:** Heat flow calorimetry at 80°C of propellant K 6210 (lot 223) at a loading density of .38 g/cm<sup>3</sup> in 2 different laboratories

**Table VI:** HFC results for propellant K 6210 (lot 220)

	EXPERIMENT 1		EXPERIMENT 2		EXPERIMENT 3		AVER. VALUE	STAND. DEV.
T	A	B	C	D	E	F		
(°C)	(μW/g)	(μW/g)	(μW/g)	(μW/g)	(μW/g)	(μW/g)	(μW/g)	(%)
80	81.1	79.7	- <sup>a)</sup>	67.5	76.8	75	75.8	6.4
60	7.2	6.9	6.06	6.0	7.5	7.0	6.7	8.8
50	3.24	2.88	1.83	1.72	2.05	1.96	2.2	26.7
40	0.77	0.77	0.60	0.56	0.55	0.56	0.6	19.6

a) value not constant because of endothermic peaks due to gas evolution

**Table VII:** Kinetic parameters for propellant K 6210 (lot 220)

		ALL VALUES	EXP. 1	EXP. 2	EXP. 3	EXP 2+3
activation energy	(KJ/mol)	103	94.3	101.7	111.5	106.6
pre-exp. factor	(W/kg)	$9.7 * 10^{14}$	$4.6 * 10^{12}$	$5.1 * 10^{13}$	$2.2 * 10^{15}$	$3.3 * 10^{14}$
service life	(year)	$6.2^a) / 23^b)$	$4.5^a) / 14^b)$	$6.9^a) / 24^b)$	$7.0^a) / 29^b)$	$6.9^a) / 27^b)$

a) service life at 40°C

b) service life at 30°C

**Table VIII:** HFC results for propellant K 6210 (lot 223)

T	PBC		BICT		AVER. VALUE	STAND. DEV.
(°C)	(μW/g)	(μW/g)	(μW/g)	(μW/g)	(μW/g)	(%)
80	80	81	75.8	75.3	78.3	3.3
60	6.6	7	6.9	6.6	6.7	6.7
50	2.1	2.0	2.0	2.0	2.0	3.0
40	0.62	0.60	0.56	0.66	0.62	6.8

**Table IX:** kinetic parameters for propellant K 6210 (lot 223)

		ALL VALUES	PBC	BICT
activation energy	(KJ/mol)	103	104.2	103
pre-exp. factor	(W/KG)	$9.4 * 10^{13}$	$1.5 * 10^{14}$	$9.1 * 10^{13}$
service life	(year)	$6.4^a / 23^b$	$6.2^a / 23^b$	$6.4^a / 24^b$

a) service life at 40°C

b) service life at 30°C

#### **4. CONCLUSIONS**

In this paper we have discussed different parameters that have an incidence for the reliability and reproducibility of the results.

At the start, HFC test which gives you the rate at which the reaction is going forward has to be combined with stabiliser consumption experiments or molar mass degradation that give the actual stage of the decomposition reaction. Then it is possible to calculate the service life of the propellant.

It is still unknown what the service life would be if a not preaged sample is used for HFC experiments for all the temperature lower than 80°C.

But it is impossible to do HFC measurements within an acceptable time frame with unaged samples.

In order to standardise a test procedure one has to take into account all the different parameters.

This means that

1. the propellant has to be conditioned before measurement or the moisture content of the propellant has to be fixed.
2. the filling of the ampoule has to be kept constant in the ampoules for all measurements of the different samples. A completely filled ampoule is to be preferably used because it is more close to the situation encountered in the cartridges.

3. great care must be devoted to the sealing of the measuring ampoule. To be sure of the quality of the measurements at least duplicate experiment have to be made.
4. special care must be paid for HFC measurements at low temperature and the « switch technique » is a good way to reduce the error.

As a conclusion it can be said that HFC measurements can be run with an excellent reproducibility in different laboratories and/or vessels if the parameters like loading density and moisture content are fixed.

## **5 REFERENCES**

- [1] C.J. Elmqvist, P.E. Lagervist, L.G. Svenson, « Stability and Compatibility Testing Using a Microcalorimetric Method » J. Haz. Mat 7, 281-285 (1983); L.G. Svenson, C.K. Forsgren, P.O. Backman, « Microcalorimetric Methods in Shelf Life Technology », Proc. ADPA Symp. on Compatibility of Plastics and Other Materials with Explosives, Propellants and Pyrotechnics, New Orleans 1988, p. 132-137; M. Rat « Application de la microcalorimétrie à l'étude de la stabilité des poudres pour armes », Symp. Chem. Probl. Conn. Stabil. Explos. 361-380 (1979); S. Wilker, G. Pantel, U. Ticmanis, « Wärme flußkalorimetrische Untersuchungen an Anzündhüchtem », Proc. Int. Conf. ICT 26,84 (1995); G. Holl, S. Wilker, G. Pantel, P. Guillaume, « Former and modern methods of the determination of the service life of propellants », Proc. 87th AGARD Conference on Service Life of Solid Propellant Systems, Athens 1996, p.18-1 - 18-13
- [2] P. Guillaume, A. Fantin, M. Rat, S. Wilker, G. Pantel, « Stability Studies of Spherical Propellants », Proc. Int. Conf. ICT 27, 16-1 - 16-14 (1996)
- [3] H.P.J. Jongeneelen, « Investigation into the ballistic stability of nitrate ester propellants », TNO Report Ass. TL 7980-II (1971)
- [4] W. Verbeek, « Investigation into the cause of the initial heat effect » TNO Report TL1974-19 part II (1974)
- [5] I.L.C. van Geel, « Self-Ignition Hazard on Nitrate Ester Propellant » Dissertation TH Delft (1969)

# THE APPLICABILITY OF MICROCALORIMETRY AND GAS FLOW AMPOULE SYSTEM TO STUDY THE SHELF LIFE OF PYROTECHNICS

Anton Chin, Daniel S. Ellison, Bill R. Hubble and Robert G. Shortridge

Test & Evaluation Department  
Ordnance Engineering Directorate  
Crane Division, Naval Surface Warfare Center  
Crane, Indiana 47522-5001 USA

## ABSTRACT

Before the first generation of Gas Flow Ampoule System (GFAS) was introduced by AB Bofors, Sweden in 1985, the method to study the compatibility and aging trend of pyrotechnics was limited to measurements in closed sample ampoules. Without the capability to accurately control the atmosphere and humidity level, the application of this method using sealed ampoule was very limited. The early model of BoMic 2277-900 GFAS had extended the application field to include also long term stability of pyrotechnics under various environmental conditions. Although the improvement is noticeable, the Model 2277-900 GFAS has still suffered from the very basic design problems such as unstable baseline, inaccurate humidity control, irreversible adsorption/desorption cycling capability, and condensation of water into the sample cell, just to name a few.

The new improved Model 2255-010 digital and computer control GFAS has improved some of the earlier problems to some extent. Extreme care is still needed to operate this equipment so the optimum results can be obtained.

## I. INTRODUCTION.

The chemical stability of most energetic compositions is highly dependent on the external environmental parameters such as oxygen, moisture and reactive air pollutants. For most cases, water is the major cause for the degradation of pyrotechnic compositions containing powdered metals such as magnesium, aluminum, zirconium, and silicon, etc. just to name a few. The composition attracts the moisture usually by surface adsorption, capillary condensation, chemical reaction or complexation. Therefore, the knowledge of interactions between moisture and pyrotechnics is extremely critical for improving our understanding of the aging process and degradation mechanism.

Based upon the results of a number of microcalorimetric investigations of the aging characteristic of various pyrotechnic fuels and compositions, including some from our laboratory, it was felt that there are some serious problems existed in the experimental microcalorimetry.

The old microcalorimetric method using conventional one direction external gas flow cell system [1, 2, 3, 4] for studying the moisture degradation mechanism, have suffered from inconsistency and inaccuracy of test results. These problems are mainly due to the absence of suitable equipment which can precisely controls the adsorption/desorption process during the reaction between moisture and any material involved. In this paper, we will report the development of the new adsorption/desorption technique and the application of this technique to study the thermal parameters involved in the degradation of magnesium in a pyrotechnic composition (i.e. MTV). The service limits and application criteria to operate the ThermoMetric microcalorimeter and Model 2255-010 GFAS will also be discussed.

## II. PRINCIPLE OF ADSORPTION/DESORPTION TECHNIQUE

The adsorption of a gas or moisture on a solid surface may be a purely physical process (reversible), or may involve chemical reaction (irreversible). Both types of adsorption are exothermic. In a microcalorimetric experiment where a sample is in contact with a stream of moisture, the observed heat flow is the summation of a number of individual and independent physical and/or chemical processes. For example for magnesium, moisture adsorption on a number of materials (i.e. (i) magnesium, (ii) magnesium hydroxide, and (iii) sample cell walls) will occur and each process will have its own unique heat flow associated with it. In addition, once moisture has adsorbed on the magnesium surface, a chemical reaction will occur to form new magnesium hydroxide. If the above adsorption experiment is at some stage stopped and the moisture flow replaced with dry or lower relative humidity inert gas, the direction of the heat flow will be reversed (desorption). The desorption is endothermic and will continue until all the heat flow associated with the adsorption process steps is release. That is, the physical adsorption steps are reversible whereas the chemical reaction steps are not. The above thermodynamic analysis of the described microcalorimetric experiment provide the basis for the Adsorption/Desorption Technique developed. Figure 1 and the equations followed illustrate this basic technique [5].

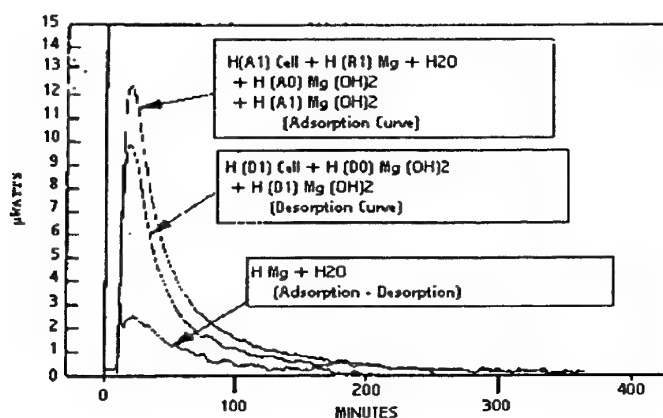


Figure 1. Example of Adsorption/Desorption Heat Flow Curves From Microcalorimeter/GFAS Tests. Desorption Curve is Purposely Turned Over to the Top for Easier Comparison.

$$H_{(A \text{ total})} = H_{(A1) \text{ cell}} + H_{(R1) \text{ Mg} + \text{H}_2\text{O}} + H_{(AO) \text{ Mg(OH)}_2} + H_{(A1) \text{ Mg(OH)}_2}$$

$$H_{(D \text{ total})} = H_{(D1) \text{ cell}} + H_{(DO) \text{ Mg(OH)}_2} + H_{(D1) \text{ Mg(OH)}_2}$$

$H_{(A)}$  = Heat of Adsorption       $H_{(D)}$  = Heat of Desorption       $H_{(R)}$  = Heat of Reaction.

$H_{(AO)}/H_{(DO)}$  = Heat of Adsorption/Desorption of original  $\text{Mg(OH)}_2$  coating before humidity test.

$H_{(A1)}/H_{(D1)}$  = Heat of Adsorption/Desorption of newly formed  $\text{Mg(OH)}_2$  after humidity test.

Base on the law of conservation of energy,  $\Delta H_{(A)} = \Delta H_{(D)}$  for a reversible physical reaction (i.e. adsorption/desorption). Thus

$$H_{(A1) \text{ cell}} = H_{(D1) \text{ cell}}, \quad H_{(AO) \text{ Mg(OH)}_2} = H_{(DO) \text{ Mg(OH)}_2}, \quad \text{and}$$

$$H_{(A1) \text{ Mg(OH)}_2} = H_{(D1) \text{ Mg(OH)}_2}.$$

$$H_{(A \text{ total})} - H_{(D \text{ total})} = H_{(R1) \text{ Mg} + \text{H}_2\text{O}} \quad (\text{the lower curve in Figure 1})$$

From the above equations, it is clear that the heat of adsorption/desorption of sample cell and heat of reaction of Mg and  $\text{H}_2\text{O}$  can be calculated. As for the  $H_{(AO) \text{ Mg(OH)}_2}$  and  $H_{(A1) \text{ Mg(OH)}_2}$ , it will require a little more complex microcalorimetric and GFAS work to resolve. To achieve this goal, we must first quantitatively correlate the heat of adsorption of  $\text{Mg(OH)}_2$  to its weight on the surface of magnesium. This can be accomplished by applying a sequential adsorption/desorption technique in which a series of adsorption and desorption cycles are run for various increasing lengths of time. In other words, in the first cycle the adsorption is stopped while only a part (<30%) of the magnesium is reacted, then quickly turn to desorption until dry. Repeat the second cycle till more magnesium is reacted (<60%), and if needed the third cycle should follow. If the experiment is carried out properly, no more than two cycles is needed. By algebraically subtracting the heat flow expressions for subsequent steps, it is possible to isolate values for each individual adsorption and desorption step associated with the entire cycle. Figure 2 shows the flow chart of the basic sequential adsorption and desorption technique:

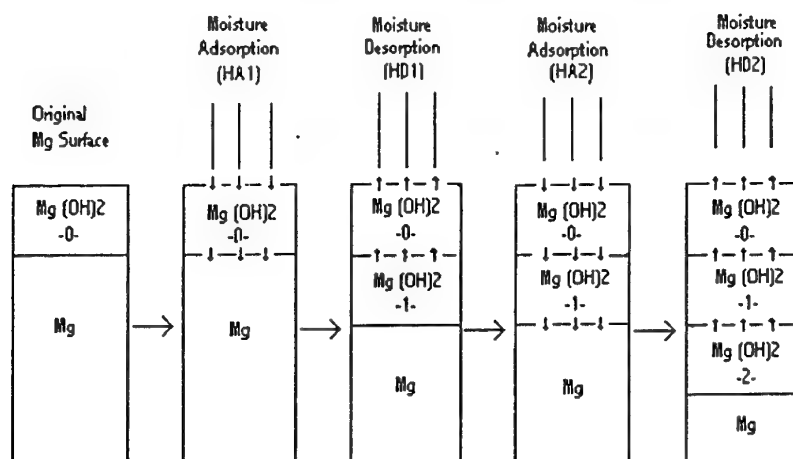


Figure 2. Theoretical Adsorption/Desorption Flow Chart of Magnesium Powder With Moisture. More Magnesium Hydroxide is Formed at Each Sequential Adsorption/Desorption Step at the Expense of Pure Magnesium in Deeper layers.

Based on the same principle described in the previous section:

$$H_{(A1 \text{ total})} = H_{(A1) \text{ cell}} + H_{(R1) \text{ Mg} + \text{H}_2\text{O}} + H_{(AO) \text{ Mg(OH)}_2} + H_{(A1) \text{ Mg(OH)}_2}$$

$$H_{(D1 \text{ total})} = H_{(D1) \text{ cell}} + H_{(DO) \text{ Mg(OH)}_2} + H_{(D1) \text{ Mg(OH)}_2}$$

$$H_{(A2 \text{ total})} = H_{(A2) \text{ cell}} + H_{(R2) \text{ Mg} + \text{H}_2\text{O}} + H_{(AO) \text{ Mg(OH)}_2} + H_{(A1) \text{ Mg(OH)}_2} + H_{(A2) \text{ Mg(OH)}_2}$$

$$H_{(D2 \text{ total})} = H_{(D2) \text{ cell}} + H_{(DO) \text{ Mg(OH)}_2} + H_{(D1) \text{ Mg(OH)}_2} + H_{(D2) \text{ Mg(OH)}_2}$$

Where

$H_{(R1) \text{ Mg} + \text{H}_2\text{O}}$  = heat of reaction of first stage adsorption cycle

$H_{(R2) \text{ Mg} + \text{H}_2\text{O}}$  = heat of reaction of second stage adsorption cycle

$H_{(A1) \text{ Mg(OH)}_2}$  = heat of adsorption of  $\text{Mg(OH)}_2$  of first stage cycle

$H_{(A2) \text{ Mg(OH)}_2}$  = heat of adsorption of  $\text{Mg(OH)}_2$  of second stage adsorption cycle

$H_{(A1) \text{ cell}}$  = heat of adsorption of inner surface of sample cell for time length  $t_1$

$H_{(A2) \text{ cell}}$  = heat of adsorption of inner surface of sample cell for time length  $t_2$



All other symbols with D means desorption. Based on the same thermodynamic principle again,

$$H_{(A2 \text{ total})} - H_{(D2 \text{ total})} = H_{(R2) \text{ Mg} + \text{H}_2\text{O}} = (\text{heat of reaction of 2}^{\text{nd}} \text{ stage adsorption cycle})$$

$$H_{(D2 \text{ total})} - H_{(D1 \text{ total})} = H_{(D2) \text{ Mg(OH)}_2} = H_{(A2) \text{ Mg(OH)}_2} = (\text{heat of adsorption of 2}^{\text{nd}} \text{ stage adsorption cycle})$$

If the time length of the first stage and second stage adsorption cycle is different, then

$$H_{(A1) \text{ cell}} \neq H_{(A2) \text{ cell}}, \quad H_{(D1) \text{ cell}} \neq H_{(D2) \text{ cell}}.$$

In the actual calculation, the difference can be easily resolved by a separate controlled experiment.

### III. MICROCALORIMETRIC TEST WITHOUT GFAS

Test of the pyrotechnic samples at this condition usually means that only test data such as compatibility and degradation trend under normal storage condition is needed. Under this condition the composition is well sealed and is not exposed to the environment. Since we began the microcalorimetry work in 1988, we have never experienced any significant problem by running dry samples at this condition. In order to obtain true and accurate results, the following two criteria should be observed:

1. Precondition the sample before test - This is a very important procedure and many people are actually neglecting that. The sample should be preconditioned for at least one day (Dry under vacuum at low temperature, i.e. 50 - 70°C depending on types of samples) before testing. This will help eliminating the possibility of unstable baseline cause by the trace impurities and volatile trapped in the closed sample cell, especially when elevated temperature is used (i.e. 60-80°C). When the fluctuation of room temperature is small ( $< \pm 8^\circ\text{F}$ ), the effect on the stability of the heat flow is minimal.
2. Switch the sample/reference sample cells - if the heat flow is too small and begin drifting near the detecting limit of the detector ( $< 0.2 \mu\text{W}$ ), a "Switch" technique shall be used to suppress baseline variation. The heat flows of the sample taken from both the sample and reference side detectors are taken into account. The average result is the true heat flow.

### IV. MICROCALORIMETRIC TEST WITH GFAS

Most problems associated with microcalorimetry is coming from using the GFAS. The problems

commonly encountered are:

1. Condensation - cause negative and drifting baseline. This is a design problem. When the exhaust outlet pipe of GFAS is exposed to a relatively cooler room temperature, the outgoing water vapor will condense. The longer the exhaust pipe, the more condensation will occur. The Model 2255-010 GFAS has a 2" over-length exhaust pipe exposed outside of the microcalorimeter, this is the major cause for the condensation. A heating element, a faster flow rate, or a shorter sample cell will help, but will not solve the entire problems. The GFAS needed to be redesigned with shorter exhaust pipe and more effective exhaust mechanism.
2. Over-pressure (vapor pressure) in the two humidity chambers - cause water overflow into the sample cell resulted in negative baseline. This is a problem usually occurs when the bath temperature is higher than 50°C (another design problem !). At higher than this temperature, the vapor pressure inside the two humidity chambers is high enough to overcome the back pressure (pressure by capillary) of the capillary tube. This over-pressure (>92 mm/Hg) will therefore force the moisture inside the humidity chamber flow into the sample cell without the help of flow pump. From this point on, the vicious cycle of drifting baseline and negative heat flow will begin. This problem shall be checked by using an empty sample cell before the sample (Mg) is loaded. Otherwise, you may not notice that there was a negative baseline because the heat flow generated by Mg and moisture will compensate that. As we mentioned before, this is a manufacturing design problem. A gas control valve is suggested to be put at the inlet of the capillary tube inside the humidity chamber to eliminate the problem.
3. Fluctuation of room temperature ( $\pm 4^\circ\text{F}$ ) - cause heat flow fluctuation with changing room temperature. Fluctuation of room temperature more than  $\pm 4^\circ\text{F}$  will begin to affect the stability of the true heat flow. Controlling the room temperature is the user's responsibility. This become more important when low heat flow from sample is expected.
4. Unstable flow rate control - cause condensation and inaccurate results. Please keep it in mind that the lowest possible flow rate should be used for the test, preferably below 80 c.c./hr. If the flow rate is too high it will cause condensation problem, especially when high bath temperature is used. If too low, it will have moisture deficiency problem. This means that the rate of moisture supply is less than the rate of reaction between moisture and sample (Mg). Therefore, the best is to use the least amount of sample at lowest possible gas flow rate without compromising the integrity and accuracy of the result.
5. Sample quantity - cause incomplete reaction and false test results. What is the optimum quantity of sample shall be used for test ? Well, it will depend on several factors:

A. Type of sample:

- a. unconfined - powder (i.e. Mg)
- b. confined - press samples (i.e. MTV)

The unconfined sample will have more reactive and adsorption surface which will generate

enough heat flow for accurate measurement. In this case, for example for the magnesium powder or similar type of sample, the least possible quantity of sample used is best for the accuracy of the test. Another benefit is the moisture flow rate can be limited so the possibility of condensation is reduced. The physical factors such as geometric configuration, loading method, and consistency of physical location and the configuration of how the sample staggered each time in the sample cell will affect the reactive surface area. If the amount of sample is too much, a thicker layer will stack up in a small sample cell. Because of this, the moisture can not penetrate into the lower layer of the sample and will therefore result in incomplete reaction. In addition, the adsorption reaction on the sample cell wall will become inconsistent every time. Therefore, the only way to reduce this problem is to reduce the sample amount to the extent that maximum reactive surface area and full reaction can be obtained.

It is obvious that the confined samples have less problem than the unconfined one. The users have to carry out some control experiments, or by experience, to select the optimal test parameters.

#### B. Sample loading technique:

a. Unconfined sample - As mentioned above, the quantity of sample must be minimum, and the method of loading must be as consistent as possible. If the sample has leaned over to one side in the sample cell, then it will affect the reactive surface area. Tapping the sample cell slightly on a flat surface may help the sample inside spread more evenly.

b. Confined sample - To avoid the reactive surface of the sample cell being inconsistent every time, a thumb tag is suggested to be used to hold the sample pellet up so there will be no connection between the sample and sample cell.

### V. CONCLUSION

There is no doubt that there are real problems existed in the operation of the microcalorimeter. Before all the problems can be solved, there is still room for improvement, simply by carefully handling the experiment based on the guidelines mentioned above.

### VI. REFERENCES

1. L. G. Svensson, P. E. Lagerkvist, and N. G. Gellerstedt, Proceedings of the ADPA Symposium on Compatibility of Plastics and Other Materials with Explosives, Propellants and Pyrotechnics, Hilton Head Island, South Carolina, p-19 (1985).
2. R. G. Shortridge, A. Chin, and B. R. Hubble, "Microcalorimetric Study of the Aging Reactions of Atomized Magnesium Powder", and references therein. NWSCC/RDTR-92/003, Naval Surface Warfare Center, Crane Division, Crane, IN 47522-5001, (1992).

3. R. G. Shortridge and B. R. Hubble, "Microcalorimetric Study of the Aging Characteristics of Silicon Fuel in Pyrotechnic Ignition Compositions", Proceedings of the 18<sup>th</sup> International Pyrotechnics Seminar, Breckenridge, Colorado, p-847 (1992).
4. C. V. Driel, J. Leenders, and J. Meulenbrugge, "Ageing of MTV", and references therein. Presented and Published at the 26th International ICT-Conference, Karlsruhe, Federal Republic of Germany, 4-7 July, (1995).
5. A. Chin, D. S. Ellison, B. R. Hubble, and R. G. Shortridge, "Microcalorimetric Analysis of Mg and MTV Compositions Using Adsorption/Desorption Technique", Proceedings of 22<sup>nd</sup> International Pyrotechnics Seminar, Fort Collins, Colorado, p-93 (1996).

## ADVANCES IN MICROCALORIMETRY

Edwin A. Lewis<sup>1,2</sup>, Laura J. Lewis<sup>1</sup>, Donald J. Russell<sup>1</sup>, and Craig R. Johnson<sup>1</sup>

1. Calorimetry Sciences Corporation, PO Box 799, Provo, Utah 84603-0799, USA

2. Department of Chemistry and Biochemistry, Brigham Young University,  
Provo, Utah 84602, USA

During the last 20 years or so there has been increased interest in the use of calorimeters to study the kinetics of slow reactions. This has been driven by the availability of commercially produced instruments of reasonable quality and high sensitivity [1]. As the use of calorimeters in stability and compatibility studies has expanded, new experimental and data analysis techniques have been developed that extend the calorimetric method to study of systems that are very stable or which degrade by complex processes [2-5].

Continuing challenges to the use of microcalorimetry in materials stability and compatibility studies include: the absence of generally accepted calibration procedures required for reliability and intercomparison purposes, the need for improved experimental protocols to speed up these measurements in particular for screening applications, and the development of instruments with improved sensitivity needed for the study of more stable materials and for smaller samples.

This paper describes:

- (1) our experience with several calibration procedures including: the use of internal electrical calibration heaters, slow discharge battery systems, and the imidazole catalyzed hydrolysis of triacetin, a chemical calibrant system first proposed by Wadso [6] and more recently reported on in depth by Beezer [5].
- (2) an incremental method we use to improve sample throughput in long experiments.
- (3) the design and performance of a new heat conduction calorimeter with nanowatt sensitivity.

- 1. L.D. Hansen, Pharmaceutical Technology, April (1996)
- 2. L.D. Hansen, E.A. Lewis, D.J. Eatough, R.G. Bergstrom, D.Degraft-Johnson, Pharmaceutical Research, 6 (1989) 20
- 3. L.D. Hansen, D.J. Eatough, E.A. Lewis, R.G. Bergstrom, D.Degraft-Johnson, K. C. Thompson, Can. J. Chem., 68 (1990) 2111
- 4. R.J. Wilson, A.E. Beezer, J.C. Mitchell, L. Watson, J. Phys. Chem, 99 (1995) 7108
- 5. R.J. Wilson, A.E. Beezer, J.C. Mitchell, Preprint (personal communication from A.E. Beezer), August (1996)
- 6. A. Chen, I. Wadso, J. Biochem. and Biophys. Meth., 6 (1982) 297, 20

# **VARIOUS CALORIMETRIC TECHNIQUES APPLIED TO THE CHARACTERISATION OF ENERGETIC MATERIALS.**

S. Moreau , P. Le Parlouer

SETARAM, 7 rue de l'Oratoire, 69300 Caluire, FRANCE.

Energetic materials are expected to detonate on heating. Temperature, pressure, heating rate, are parameters to be strictly controlled at different stages of the processing and storage of explosives, propellants and pyrotechnics.

Differential scanning calorimetry (DSC) is especially adapted to the investigation of small amounts of sample according to various heating rates. Most of the thermodynamic data related to the energetic materials are measured : temperature and heat of melting, specific heat, thermal conductivity, temperature and heat of decomposition, ...

The influence of the atmosphere, especially oxygen, on the detonation of pyrotechnics is also easily investigated by DSC. Tight high pressure crucibles are necessary for the determination of temperature and heat of decomposition of black powders, explosives. In some investigations (RDX decomposition) the pressure in the crucible is controlled in order to study its influence on the decomposition rate.

But calorimetry provides a complementary way to DSC with the investigation of larger amounts. Heat of reaction and pressure evolved during the reaction can be measured in the same time. Also, with special mixing vessels, the reactivity of materials entering the composition of propellants is evaluated.

Furthermore, high sensitivity calorimetry proves to be a powerful tool to obtain the degradation kinetics of very slow reactions (e.g. in storage condition) and to study the compatibility between energetic materials.

## **INTRODUCTION**

The production, manufacturing and storage of explosives and energetic materials present very often a risk of potential hazards. The thermal stability, the explosion potential and the material reactivity have to be precisely known to prevent serious problems associated with thermal explosions.

Thermal analysis techniques and in particular differential scanning calorimetry (DSC) have long been considered to be very helpful in the qualitative and quantitative characterization of the thermal behaviour of energetic materials(1, 2, 3, 4, 5). However only small amounts of materials can be investigated by DSC and the reproducibility of the sampling is a real problem, especially when heterogeneous compounds have to be considered. In this case combining DSC to thermogravimetry can provide complementary data (mass variation, thermal transformation) for a better understanding of the reaction.

If larger amounts of energetic material are to be investigated, calorimetry provide a complimentary way of analysis. Various types of studies are possible : long term stability of materials, compatibility test, reactions between solid or liquid compounds.

### **1. Differential scanning calorimetry**

Most of the investigation are run on decomposition or detonation of materials including kinetics studies. But a lot of information is also provided to quality control or reliability testing by measuring melting, purity, specific heat and thermal conductivity.

The Setaram DSC111 is very well suited to all these experimentations. It is especially designed to work with tight crucibles resisting to very high pressures e.g. 100 bars at 800°C (Figure 1), which is an absolute necessity in the investigation of energetic materials decomposition. Indeed if the test is ran in an open crucible, sample vaporization may occur and no exothermic effect of decomposition will be detected.

Depending on the type of crucibles used the internal pressure will be fixed either by the pressure of evolved gases of decomposition or by a special pressurization device. The pressure can also be controlled during the whole experiment, by connecting a tubular link between the crucible and an external pressure supply.

The above mentionned crucibles are widely used in the investigation of energetic materials for measuring their thermal properties (7).

#### **1.1. Melting**

The determination of temperature of melting is one of the easiest way to characterize an organic material. By DSC the corresponding heat of melting and the shape of the DSC peak give a rapid indication of the degree of purity of the material.

For example the melting process of tolite (Figure 2) must be precisely known as tolite has to be melted when manufacturing munitions or when mixed with hexogene for the formation of hexolites.

## 1.2. Purity

The DSC method used for purity determination is essentially based on the Van't Hoff relation:

$$T_s = T_o - (RT_o^2 X^* / \Delta H_m) \cdot (1/F)$$

where

$X^*$	: molar fraction of impurity in the sample
$F$	: molten fraction of sample
$T_s$	: melting temperature at equilibrium of the sample (K)
$T_o$	: melting temperature at the equilibrium of the pure substance
$R$	: 1.987 cal.mol <sup>-1</sup> .K <sup>-1</sup>
$\Delta H_m$	: melting enthalpy of the pure substance (cal.mol <sup>-1</sup> )

From the DSC melting peak the variation of  $T_s$  versus  $1/F$  is obtained. The molar fraction of impurity is calculated from the slope of the curve (Figure 3). The method is very rapid and can be used as a quality control in the production of explosives.

## 1.3. Specific heat

It is one of the most important thermal parameters to be known for different reasons :

- knowledge of the amount of heat to be produced for the transformations of raw materials in reactors, furnaces,...
- characterization of materials, especially for quality control.
- determination of thermal diffusivity, when combined with thermal conductivity measurements.

In the field of energetic materials, specific heat data are used to calculate the amount of heat produced in order to reach the temperature of detonation or explosion for an explosive or pyrotechnics composition.

Specific heat is easily measured using the DSC technique. With the DSC111, two different methods (continuous heating and step heating) are used and give both precise and reproducible data (8). Examples are given in figures 4 and 5.

## 1.4. Thermal conductivity

The knowledge of thermal conductivity is needed to calculate the thermal diffusivity when the specific heat of a sample is known. All these different parameters are very important especially to understand the thermal behavior of explosives when they are used in cartridges, rockets...

Thermal conductivity can be obtained with the DSC 111 (9).



## **1.5. Decomposition - Detonation**

DSC is especially suitable for the hazards and special problems occurring with energetic materials. With the DSC 111 different types of experimentations are possible :

- heat the sample in confined conditions (tight high pressure crucible).
- heat the sample in various gas atmospheres (open crucible)
- heat the sample with variable heating rates (kinetics calculation, autoignition)
- heat the sample under variable gas pressure (controlled high pressure crucible)
- investigate the sample with isothermal conditions (kinetics calculation).

### **1.5.1. Confined conditions**

Octogene (HMX) is considered as thermally stable explosive because its decomposition starts only above 200°C (3). In confined conditions, octogene detonates when it is heated (Figure 6).

### **1.5.2. Influence of the nature of gas**

The nature of gas around the sample should be carefully controlled in investigating pseudo stable materials. It is illustrated by the analysis of a pyrotechnic composition including boron, resin and potassium nitrate, in an open crucible. Under nitrogen the detonation of the mixture occurs at 533°C liberating 665 calories per gramm of sample (Figure 7). If the same experiment is run under oxygen the detonation occurs at higher temperature (594°C) and is much more exothermic (980 cal.g<sup>-1</sup>).

### **1.5.3. Influence of the heating rate**

The heating rate fixed for the DSC analysis has a very strong influence on the decomposition or autoignition phenomenon as shown in figure 8.

The temperature at the maximum of the decomposition peak increases with the value of the heating rate. Furthermore with a heating rate higher than 3°C/min, the explosive powder starts to decompose around 180°C then detonates violently. The autoignition of the powder occurs only if the heating rate is high enough.

The variation of the temperature of decomposition or autoignition is used to calculate the activation energy of the reaction according to the OZAWA equation (10).

### **1.5.4. Influence of gas pressure**

The controlled high pressure crucibles used with the DSC 111 enables to simulate what occurs when a pressure of gas is applied on an explosive sample during heating. The thermal behavior of hexogene (RDX) has been characterized

under different pressures of nitrogen : 2 and 20 bars (figure 9). It is shown that under 2 bars only a small part of the melting peak is detected before the decomposition. Under 20 bars, the beginning of the decomposition is shifted to higher temperature that allows to detect more clearly the melting of hexogene.

It is also noted that the rate of decomposition increases with the value of nitrogen pressure.

#### **1.5.5. Isothermal conditions.**

When kinetic determinations have to be carried out , the isothermal test is the most suitable to obtain a good precision in the calculated data.

The use of this method is illustrated by the investigation of the isothermal decomposition of a black powder at various temperatures (Figure 10). The corresponding exothermic effects enable to determinate the variation of the rate of decomposition versus time. Using an appropriated kinetic determination, the activation energy is calculated with an Arrhenius plot.

#### **1.6. Thermogravimetry and differential scanning calorimetry (TG-DSC)**

Combining TGA and DSC techniques is very interesting to obtain complimentary data on the mass evolution associated with thermal effects occurring in the sample. Simultaneous TG-DSC can therefore be applied to the characterization of energetic materials (11).

The use of only one sample is especially important when the sampling of small amounts of materials is a problem. That is mostly the case with explosives which are very complex mixtures. By combining TG and DSC on the same sample a good correlation can be obtained between TG and DSC data, as illustrated by the thermal decomposition of nitrocellulose (Figure 11). The calculation of the TG derivative curve shows that the DSC and DTG peaks are very similar that is to say that the kinetic parameters of the decomposition can be obtained from both curves.

### **2. Calorimetry**

Calorimeters, which used to be ran mainly isothermally with an isolated sample, , are now becoming more flexible and provide for various modes of operation :

- scanning temperature (DSC mode).
- step scanning temperature.
- constant temperature (Isothermal calorimetry mode).
- mixing (Reaction calorimetry).

Furthermore depending on the type of calorimeter (12), it is possible to measure simultaneously the pressure evolved during a reaction or a decomposition and the heat dissipated (Figure 12).

### **2.1. Scanning temperature**

A relatively short response time allows for some calorimeters to be used in a scanning mode. Moreover calorimeters vessels are rather large (approximately from 1 up to 100 milliliters for Setaram's calorimeters). Therefore calorimetry can be considered as a complimentary way of investigation to DSC with larger an amount of sample, which is very convenient for heterogeneous materials.

### **2.2. Step scanning temperature**

This method is very suitable for the investigation of the long term stability of energetic materials especially on storage conditions (13). Relevant equations have recently been developed (14), which provides kinetic and thermodynamic parametres for such very slow decompositions.

The method is illustrated by the stability study of propulsive powders (Figure 14). The heat flow associated to each isothermal step have been plotted on the same graph and activation energy has been calculated using an Arrhenius plot. This experiment has been carried out with Setaram's Micro-DSC. It is very interested to note the short lost time between two steps (about 1000 seconds only).

It is also possible to conceive step scanning experiments to investigate the compatibility between raw materials entering into the composition of energetic mixtures. Such type of experiments is succesfully used in the pharmaceutical industry to study the compatibility between drug and excipient.

### **2.3. Constant temperature**

Standard procedures have been designed to monitor the ageing of propulsive powders (11), one of wich using isothermal calorimetry : The measurements are carried out in vessels filled with powder during 48 hours at 50°C. The result is the maximum value of the heat flow. If it is above a "critical" value selected at 100 mW/kg the powder is thought to be too extensively decomposed for further use.

### **2.4. Mixing**

Setaram 's calorimeters are equipped with various types of mixing cells (Figure13) which can be used to apply microcalorimetry in the compatibility test for pyrotechnics (16). Microcalorimetry proved to be more reliable than traditional VST (vaccuum stability test) methods.

Also during the preparation of explosives, different operations of mixture have to be done between liquids and solids. Calorimetry, when using mixing vessels, gives a way to measure the heat evolved during the mixing operation (for

example nitration) to check the reactivity of raw materials entering the composition of propellants, like boron in oxidising medium.

## **CONCLUSION**

DSC techniques have been widely used so far to investigate energetic materials in a traditional way. Now calorimeters are becoming more flexible and will provide for a wider range of experimentations.

## REFERENCES

1. L.W. COLLINS, L.D. HAWS, *Thermochimica Acta*, 21 (1977) 1-38
2. J.N. MAYCOCK, L.L. ROUCH, V.R. PAIVERNEKER, *Inorg. Nucl. Chem. Lett.*, 4 (1968).19.
3. J.E. SINCLAIR, W. HONDEE, *Jahrestagung 1971, Institute fur Chemie der Treib und Explosivstoffe*, p.57.
4. J.N. MAYCOCK, *Thermochimica Acta*, 1 (1970) 389
5. R.N. ROGERS, *Thermochimica Acta*, 11 (1975) 131.
6. V.R. PAIVERNEKER, J.N. MAYCOCK, *Anal. Chem.* 40 (1968) 1325.
7. SETARAM applications file 3 "Thermic hazards evaluation", 1981
8. J. MERCIER, *Journée d'étude sur les capacités calorifiques des systèmes condensés, CADARACHE (France) Sept 1986*.
9. J.N. MAYCOCK, V.R. PAIVERNEKER, *Explosivstoffe*, 17 (1969) 5.
10. P. LE PARLOUER, J. MERCIER, B. JALON, *Thermochimica Acta* 103 (1986) 21-26
11. M. DREYFUS, M. LEVEQUE, O. RUALT, 17th ICT Meeting, Karlsruhe, June 1986
12. File 6 "C80 : Experimental vessels", SETARAM.
13. P. LEPARLOUER, *Thermal analysis, proc. 7th ICTA, Kingston (Canada) 1982*, p.190
14. R.J. WILSON, A. BEEZER, *The Journal of Physical Chemistry*, 1995, 99.
15. Y. OHTSUKA, M. MATSUO, S. KANEKO, *Evaluation of thermal stability of energetic materials. Setaram. ref: B 0977*

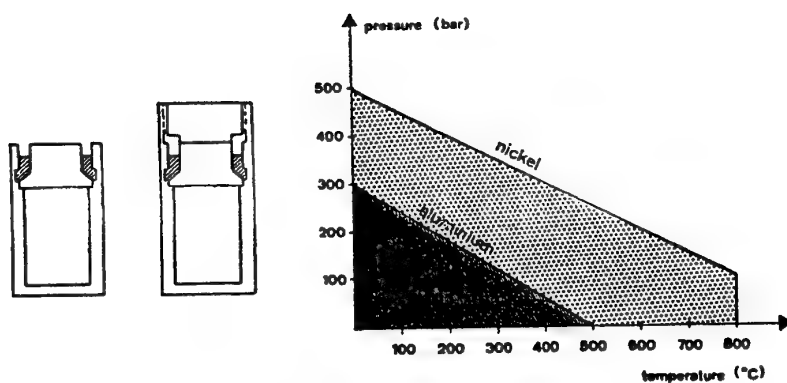


Figure 1 - Stainless steel crucibles.  
Limit of use in pressure.

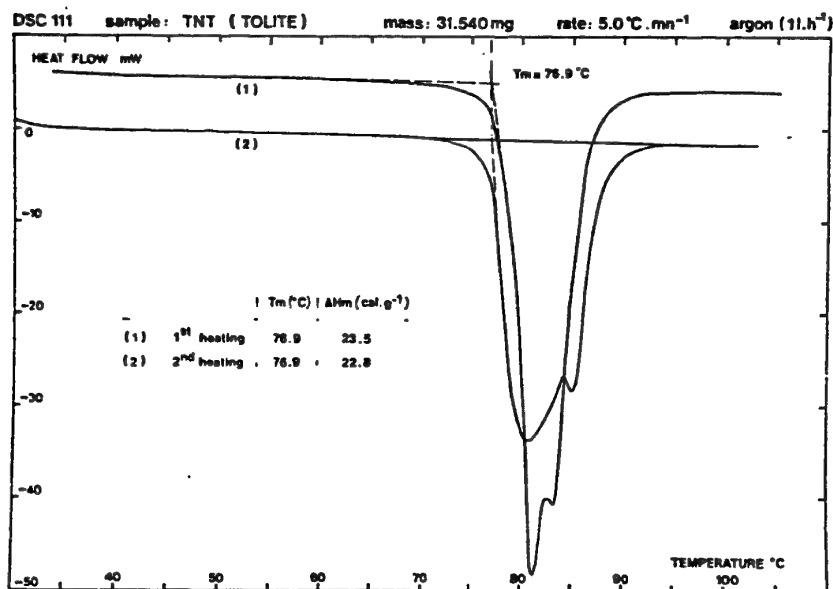


Figure 2 - Melting of tolite

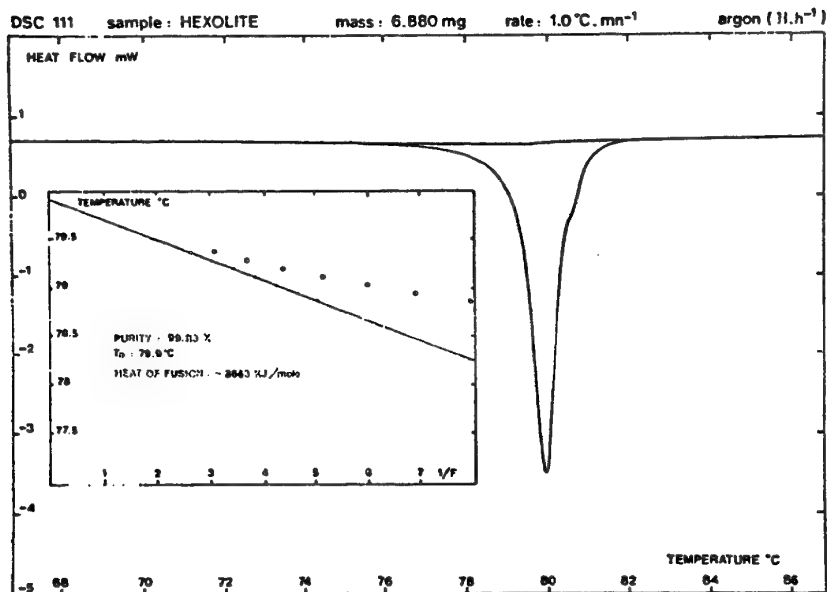


Figure 3 - Determination of hexolite purity.

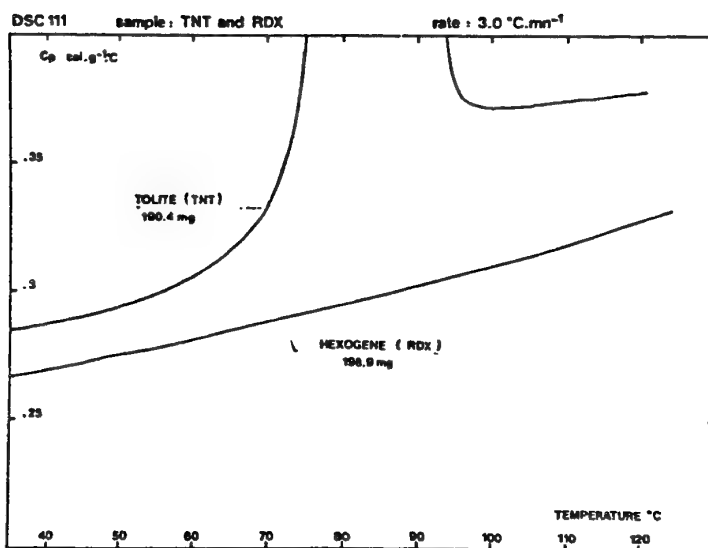


Figure 4 - Determination of TNT and RDX specific heat.

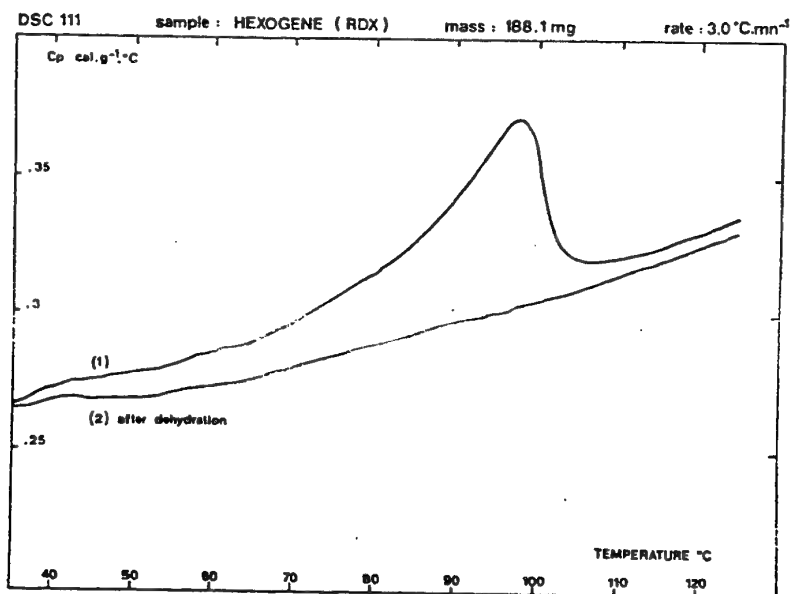


Figure 5 - Determination of dry and humid RDX specific heat

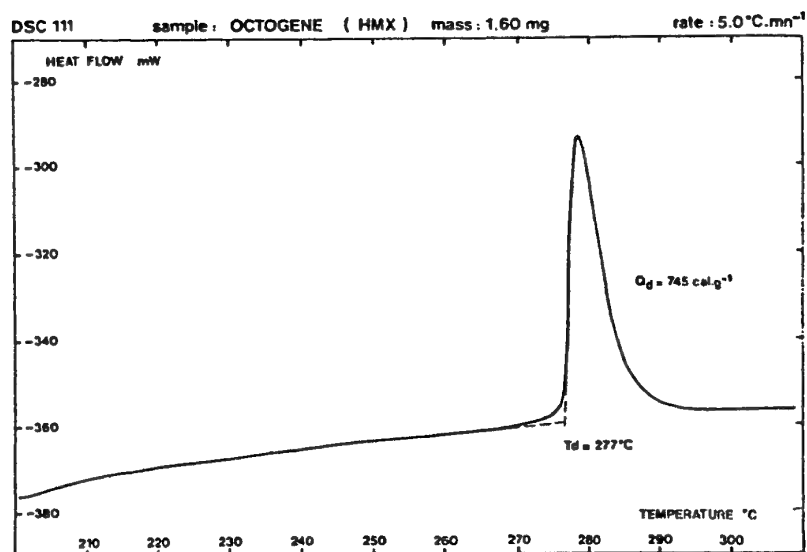


Figure 6 - Decomposition of octogene.



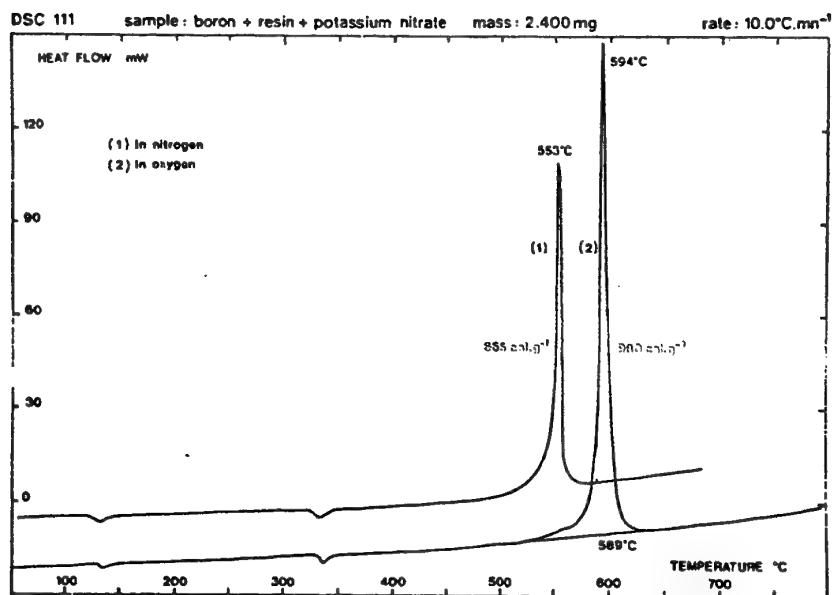


Figure 7 - Decomposition of a pyrotechnic composition under N<sub>2</sub> and O<sub>2</sub>.

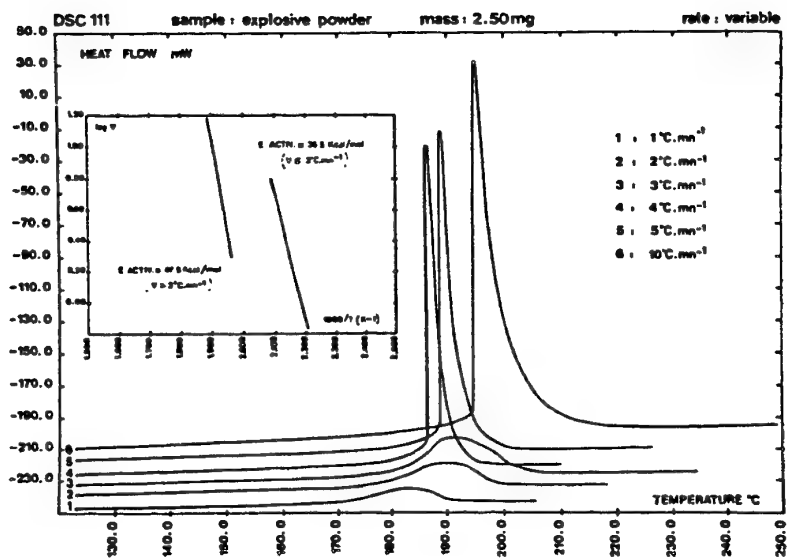


Figure 8 - Influence of the scanning rate on the decomposition of an explosive powder.

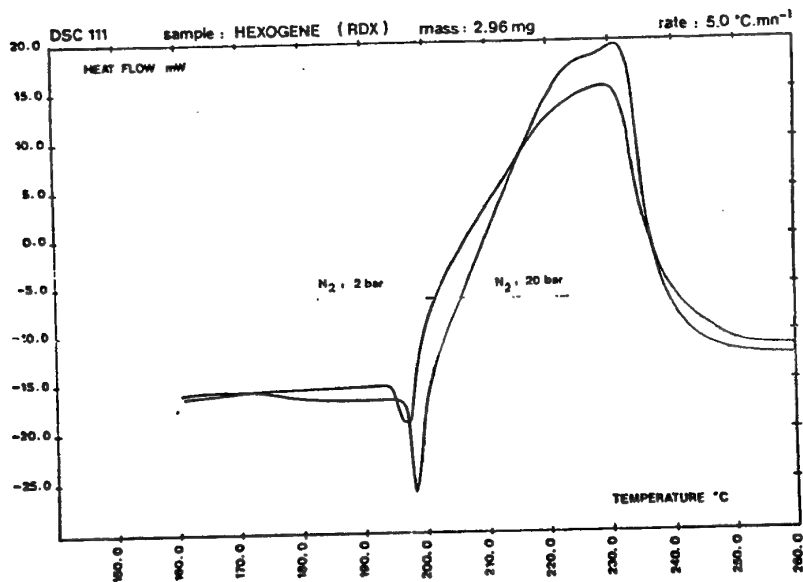


Figure 9 - Influence of pressure (N<sub>2</sub>) on the decomposition of RDX.

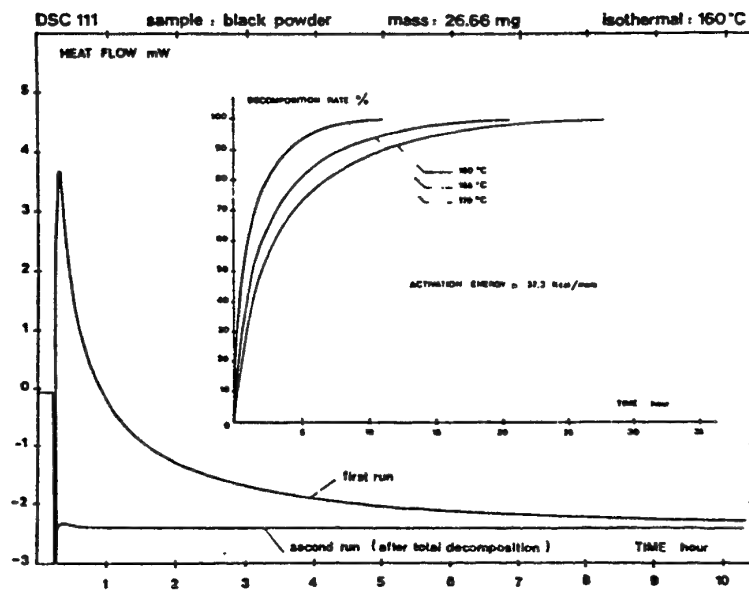


Figure 10 - Isothermal decomposition of a black powder.

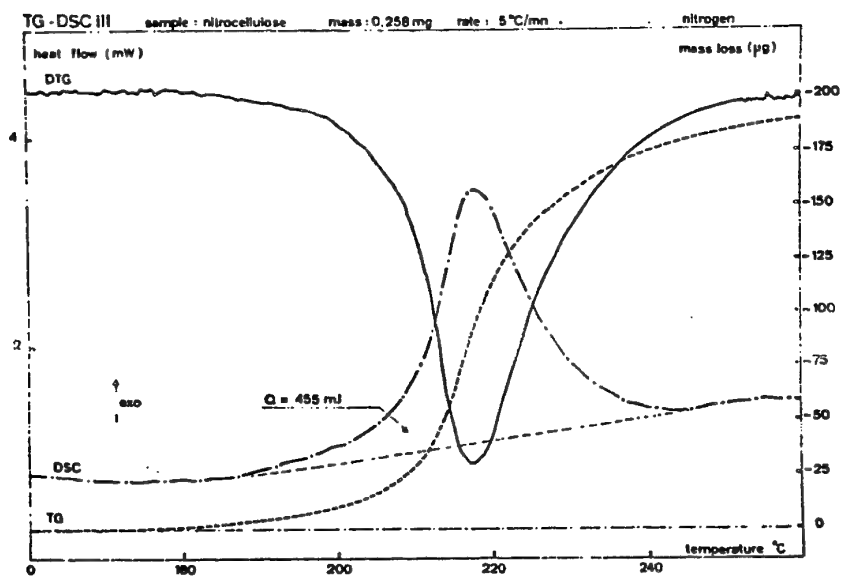


Figure 11 - Decomposition of nitrocellulose.

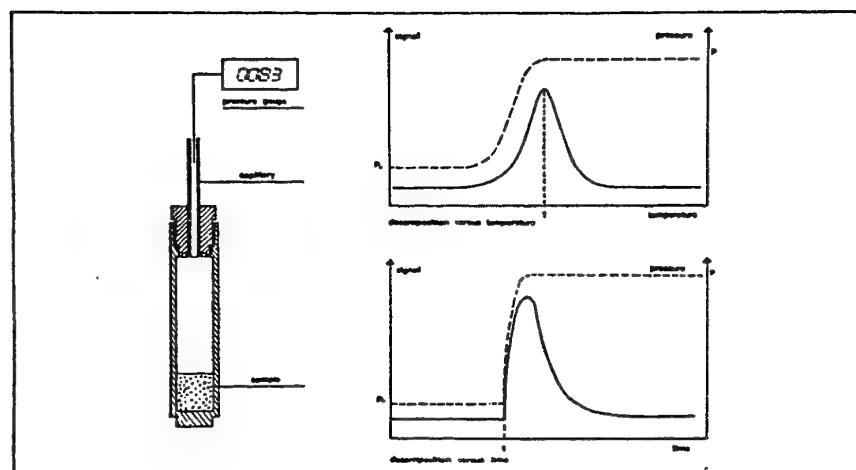


Figure 12 - Heat/Pressure determination by calorimetry.

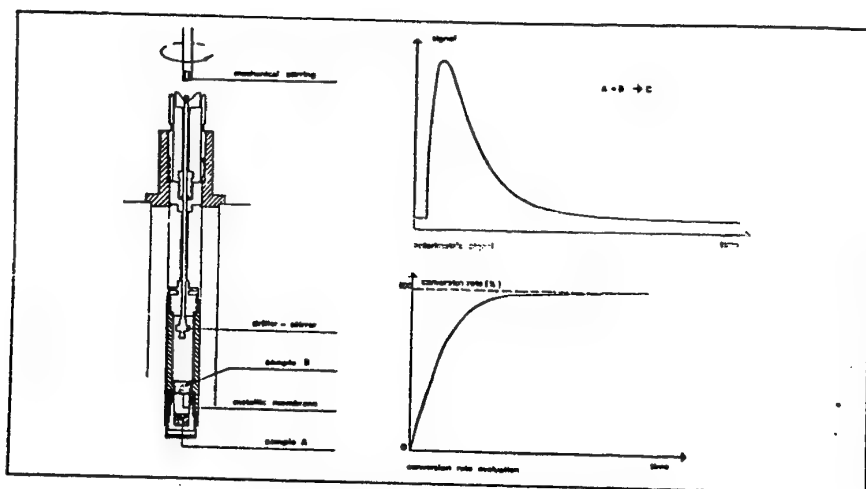


Figure 13 - Mixing calorimetry.

## **Microcalorimetric performance now and in the future: Its use in solid state kinetics**

Jaak Suurkuusk  
Thermometric AB  
Spjutvägen 5A, S-175 61 Järfälla

Thermal Activity Monitor, TAM, represents a tool to accurately predict and validate the quality and safety of a product after storage for more than 10 years at ambient conditions. From heat flow measurements at three or more slightly elevated temperatures, 40 - 70°C, the extracted kinetic information can be extrapolated to ambient temperature by means of the obtained activation energy. The duration of one measurement can be from several hours up to one week. The slow processes and the long measurement time make great demands on the instrument's baseline reproducibility and long time stability.

The longtime baseline stability of a standard TAM,  $< \pm 100\text{nW}$  over 24h, is primarily based on the temperature stability of the surrounding liquid,  $< \pm 100\mu\text{K}$  over 24h, and the signal amplifier of TAM. Introduction of the new Nanowatt Amplifier improved not only the short time noise but also significantly the baseline fluctuation. Stability over 24hour became less than 50nW and over 1hour less than 20nW. By combining the Nanowatt Amplifier with the new 20ml Twin Calorimetric Unit, a baseline stability of 5nW/ml over 24hours and a noise of less than 1nW/ml (0.1Hz) is obtained. Just as for the 4ml calorimeters, the 20ml Twin Calorimetric Unit can be equipped with a reaction vessel with humidifier. This allows for large volume sophisticated gas perfusion experiments with programmable relative humidity over the sample. In the latest version of the Digitam software, version 4.1, most common kinetic analyses can directly be conducted on the experimental data. TAM is also available in a high temperature version, optional, which allows measurements up to +150°C.

The continuous development of calorimetric techniques aims at improving the sensitivity and stability, so that measurements can be made at actual storage temperature. Another goal is to be able to handle different artifacts, such as sample conditioning, relaxation in sealing materials etc. Not before then can this technique fully utilize the potential high sensitivity.

## DISCUSSIONS AND COMMENTS ON PAPERS

MICROCALORIMETRY: AN ANALYTICAL TOOL FOR MONITORING STABILITY, COMPATIBILITY AND AGING.

B E DOUDA

No questions

MICROCALORIMETRIC INVESTIGATION OF ENERGETIC MATERIALS : A REVIEW OF METHODIC DEVELOPMENT AT BICT.

S WILKER

The question was asked why a 3% energy loss was used to determine when a gun propellant had reached an unacceptable ballistic behaviour and where this value came from. The value is on arbitrary one and resulted from research done at TNO, Netherlands. It is possible that this figure relates to no stabiliser left in the composition.

It was remarked that the Activation Energies recorded were high and was this due to ageing of the material.

DETERMINATION OF INTERACTION PROFILES IN COMPATIBILITY TESTING.

L G SVENSSON

The importance of pressure on the experimental results were discussed since the experiments were carried out in sealed ampoules. Changes in pressure will result in changes in concentration of reactive gases within the adhesive, however, for experiments done at low temperatures it was found that the build up of pressure from the propellant was very low.

The comment was made that for accelerated ageing tests carried out at 70 or 80°C large errors could occur because the heat flow profile at this temperature is very different from the profile at 20 or 30°C.

MICROCALORIMETRIC CRITERIA FOR EVALUATION OF CORROSIVE LIQUID PROPELLANT ON METAL CONTAINERS.

A CHIN

No questions.

## PRELIMINARY MICROCALORIMETRY STUDIES OF ADVANCED GUN PROPELLANTS.

PRESENTED BY J ADAMS

The authors White, Kempson and Berry, observed an initial negative slope in unaged samples which was not seen in aged samples but they could not account for this observation. Dr Wilker pointed out that the negative slope is due to initial reactions that have to be completed before a steady state is reached. At the temperature of the experiments quoted (60/65°C) a week would be required to complete the initial reaction but in his laboratory they use 80°C to condition the sample prior to testing, see paper No 2.

## THE USE OF MICROCALORIMETRY IN THE PREDICTIVE SURVEILLANCE PROGRAM.

J A WILSON

The question was raised how much support the surveillance policy was receiving from the US military customer? At first this support was restricted but has improved as the message has got around. It has been proved that estimating ageing can be estimated from kinetic data using microcalorimetry and is effective. The surveillance programme is initially expensive but calculated estimates indicate that the money should be recovered between 7 and 8 years.

## KINETIC DESCRIPTION OF THE AGEING OF GUN AND ROCKET PROPELLANTS FOR THE PREDICTION OF THEIR SERVICE LIFETIME.

M A BOHN

A question was asked regarding the three kinetic equations used when determining the decomposition of stabiliser content vs time curve. A third equation was developed, combining 1st and zero order reactions which represented the type of stabiliser decrease more accurately.

One delegate asked if the reaction products had been determined? The reaction products had been determined and using the method of stabiliser depletion some workers had concluded that an autocatalytic mechanism not applicable.

## 20mm GUN PROPELLANT SAFETY SERVICE LIFE STUDY USING MICROCALORIMETRY/ HPLC CORRELATION DIAGRAMS.

D S ELLISON

Some of the graphs shown had spikes superimposed on the curves and the question was asked if this was the result of a physical process? These spikes were not considered to be due to a pressure leak since the rise of the spike was very reproducible.

To obtain the data for the Arrhenius plot the heating rate at 1 joule was found from the heat flow curve.

AN ASSESSMENT OF THE STABILITY OF NITRATE ESTER BASED PROPELLANTS  
USING HEAT FLOW CALORIMETRY.

R G JEFFREY

It was confirmed that the production of the N-Nitroso compound was obtained for only one propellant.

INFLUENCE OF ENVIRONMENTAL FACTORS ON THE LIFETIME OF GUN  
PROPELLANTS INVESTIGATED WITH HEAT FLOW MICROCALORIMETRY.

N. Van der MEER

Two heat flow curves were shown one run in air and the other in nitrogen and the question was asked if there was any reason why those run in nitrogen gave a smoother heat flow curve. The speaker considered this was not a chemical effect of oxygen on the sample but an instability of the equipment or due to moisture.

MICROCALORIMETRIC DETERMINATION OF THE CURE REACTION IN SOME  
FLUORINATED POLYETHER RUBBERS.

P F BUNYAN

No questions.

USE OF ISOTHERMAL MICROCALORIMETRY IN THE EARLY DETECTION OF  
DRUG FORMULATION INCOMPATIBILITIES.

M A PHIPPS

What criteria was used to choose the mixing ratio of the 50/50 binary components? The choice was an arbitrary one but consideration is being given to other ratio of blends.

The difference in results that can be obtained when samples are high or low energy mixed was highlighted in the presentation. Comment was made that when boron and potassium nitrate are rapidly and thoroughly mixed then high heat flows are observed straight after milling.

The question was asked if all "incompatibilities" ie heat flows are detrimental? The authors said that any degradation product was not acceptable as it could lead to toxic substances.

COMPARISONS OF PYROTECHNIC WHISTLE COMPOSITIONS BY DIFFERENTIAL  
SCANNING CALORIMETRY

J A DOMANICO

Were other safety tests used, for example, ESD or friction. Yes these other tests were used and when a third component was considered the values obtained changed for the loose composition but not for the pressed.



Electrostatic sensitivity of the composition was reduced by addition of carbon black and the total heat output from the DSC experiments was obtained by measuring the total area under the curve.

#### MICROCALORIMETRY: PRELIMINARY INVESTIGATION OF DICHROMATED MAGNESIUM AND COMPATIBILITY STUDIES OF THE ENERGETIC BINDER POLYNIMMO.

D BLAZER

It was confirmed that for both studies the microcalorimeter was run at a temperature of 55°C. Comment was made that under the conditions of the experiment that not enough time was allowed for sample to equilibrate and this would lead to difficulty in making the thermodynamic measurements.

It was asked if after the boron/polyNIMMO experiment whether the sample had solidified ie cured. The author said it was hard to tell from visual examination and the sealed ampoule had not been opened after the experiment.

#### AGEING STUDIES ON THE BORON-POTASSIUM DICHROMATIC SYSTEM.

E L CHARSLEY

It was confirmed that in the experiments in air and argon only one relative humidity was used, that is , 69%.

In dry atmosphere the heat flow level was 30 microwatts a small but significant amount. Under very dry conditions the effect of oxygen was very low.

It was stated that the main modification in the gas flow cell was the introduction of a heated outlet capillary and replacement of the peristaltic pump by a mass flow controller.

#### PHENOMENON OF AUTOCATALYSIS IN DECOMPOSITION OF ENERGETIC CHEMICALS.

S CHERVIN

Why didn't the ageing affect the 1st order rate reaction?

The reaction rate is a function of the concentration of the reactant but because a catalyst is being created then the 1st order reaction cannot be affected.

#### THE DECOMPOSITION OF BRANCHED GAP BY THERMOANALYTICAL TECHNIQUES.

D E G JONES

No questions.

THERMAL STABILITY OF AMMONIUM DINITRAMIDE AND AMMONIUM DINITAMIDE CONTAINING VARIOUS TABILIZERS.

R F BOSWELL

No questions.

COMMON FACTORS THAT MAY AFFECT THE ACCURACY OF MICROCALORIMETRIC DATA.

D S ELLISON

In studying the pressure increases of propellants was a different instrument used? The Setaram C80 fitted with a high pressure cell was used in the pressure measurements. The authors noted that no big pressure changes occurred in the system during oscillations and no fuming was observed.

PRACTICAL APPLICATION OF MICROCALORIMETRY TO THE STABILITY STUDIES OF PROPELLANTS.

P GUILLAUME

The author confirmed that work was done on double base propellants with a nitroglycerine content of around 20%.

The question was asked if DPA was a better stabiliser than N-NO-DPA but it was thought that they were as good as each other, however, this needed confirming by other techniques but work done previously suggested this to be the case.

APPLICATION OF MICROCALORIMETRY AND GAS FLOW AMPOULE SYSTEM TO STUDY THE SHELF LIFE OF PYROTECHNICS.

A CHIN

No questions.

ADVANCES IN MICROCALORIMETRY.

E A LEWIS

The paper had highlighted the lack of suitable standards for calibration of microcalorimeters. One delegate asked why the heat of fusion of metals could not be used. Cannot be used because the heat of fusion of metals is a phase change and can only be used with a scanning instrument, such as DSC, DTA, whereas a microcalorimeter is an isothermal instrument.

## VARIOUS CALORIMETRIC TECHNIQUES APPLIED TO THE CHARACTERISATION OF ENERGETIC MATERIALS.

S MOREAU

A question was asked regarding the measurement of pressure in high pressure cells and the time that the pressure could be held constant. The author could not give a definitive answer since the experiments had been done on a energy/temperature axis and not a time axis. Mr Ellison said he had run experiments for 200 days and that he had noticed some oscillation in the pressure.

## MICROCALORIMETRIC PERFORMANCE NOW AND IN THE FUTURE: ITS USE IN SOLID STATE KINETICS.

J SUURKUUSK

Questions centred around the observed baseline for a flow rate for a given RH which should be zero. Relative humidity values quoted are these published in the literature and obtained from saturated salt solutions. The reliability of the published data was not known but the measured values are within  $\pm 1\%$  RH of the published values.

## FINAL DISCUSSION

LEAD BY DR PETER LAYE.

This final section of the Workshop consisted of a discussion session lead by Dr Laye supported by a panel of experts consisting of Dr Chin, Dr Wilker and Mr Svennson. Dr Laye opened the discussion by highlighting the importance of microcalorimetry to the study of energetic materials and that the aim of the session was to draw together ideas, to assess the present situation and to consider the future. As a starting point he suggested that three areas had been covered during the presentations and that discussion should consider these in turn. The three areas were:

SAMPLES  
INSTRUMENTAL  
INTERPRETATION

## SAMPLES

The first point made was that to obtain satisfactory or meaningful results the samples needed to be conditioned prior to testing. Dr Douda was curious to know if anyone had any experience of testing complete devices in large sample cavities. He suggested that squibs, igniters, cartridge activated devices (CADS) and pressure activated devices (PADS) could be examined in this way. He had heard that the French had a microcalorimeter with a 30mm sample cavity and had also evaluated a complete 105mm round. As yet nobody had any data on samples being tested in large cells but it was pointed out that if the amount of energetic material in the device is small than the heat flow signal will also be small. Dr Chin was

designing a large cavity cell to look at devices, larger samples and systems such as the breakdown of propellant in the presence of black powder. With this system he wanted to study the breakdown of the propellant to produce water and the effect this would have on the black powder such as the recrystallisation of the nitrate. He hoped to age devices in the microcalorimeter so that the ageing process could be studied then to remove the device and determine its performance. Examples of devices to be studied in this way would be boosters and detonating cord. The advantage of using large samples of material is that more heat flow will be observed and so long as there are no safety implications then useful information will be obtained.

A question was asked if anyone had compared the results from powder and compacted samples. DERA, Bishopton had observed that autocatalysis started earlier in compacted pieces of propellant. The explanation put forward was that the gases produced on decomposition and which cause autocatalysis were contained within the compound.

Hercules who manufacture nitrocellulose indicated they had damaged the microcalorimeter cell due to NO<sub>x</sub> gases escaping passed a Viton O ring. Therefore when studying materials that produce corrosive gases on decomposition, then a protective device such as a glass ampoule within the stainless steel container should be used. Dr Chin referred to his paper where he had designed a cell to contain a corrosive liquid propellant.

## INSTRUMENTAL

A considerable part of this topic was devoted to discussion on the calibration of the microcalorimeter for temperature humidity and energy output. The accepted standards, common for other thermal techniques, can not be used since they are only suitable for scanning instruments. The microcalorimeter is a isothermal instrument.

The workshop agreed that the main problem is to identify a compound or chemical reaction that can be used for instrument calibration. It appeared that a number of different methods were favoured by different workers and they are associated with the technical area in which they work. One method which had proved successful for solution calorimetry is to measure the heat of solution of a compound such as TRIS, (tris [hydroxymethyl] aminomethane). The reaction between two compounds has also been used. Within the pharmaceutical industry the reaction between triacetin and imadazol has been favoured. Currently there is an exercise running within the pharmaceutical industry with eight microcalorimeters, throughout the world, using this reaction to measure heat flow, enthalpy, rate constants and kinetics. The results are not due until September. There are a variety of test reactions that have been used but the question still arises, "What is the best reaction?" Collaborative work requires to be done to establish the best reaction compounds. A disadvantage of using a chemical reaction is that the result obtained is very temperature dependent, therefore temperature needs to be accurately controlled and calibrated.

For the purpose of calibration, radioactive probes using americium have been used in Sweden for the past 10 or 12 years and found to give a stable signal. The problem with this method is the safety factor and the difficulties of handling radioactive materials. An external heater, independent of the microcalorimeters electronics has been used and this has been found to

give good results for experiments carried out in ampoules but is not so good for open system experiments.

Dr Wilker suggested to the delegates a "round robin" comparison exercise using the propellant used by himself, Rat, Guillaume and Pantel since it was already well characterised and their work had confirmed good reproducibility. There were problems with this suggestion in that only laboratories with explosive licenses could participate and there would be difficulties in transporting the material between laboratories and across international boundaries. Dr Wilker invited anyone interested in the proposal to contact him. Delegates were interested in the idea of a "round robin" exercise but could not agree on a suitable reference for the study.

The question was asked if it made any difference on the results by not having a reference sample. Most delegates used reference samples and these could be kept for a long time eg purified sea sand. Also the effect of heat capacity and the problems of crimping the ampoule were mentioned by some delegates.

Humidity can be a problem in microcalorimetry experiments and there is a case for a change in the design of cells to overcome the problems. When studying pyrotechnics the humidity experienced by the sample can have a large effect on the results obtained. It was reported that in microcalorimetric experiments on ADN (Ammonium Dinitramide), which is very hygroscopic, that vacuum drying the sample increased the activation energy.

A number of papers reported that the work had been carried out at a relative humidity (RH) of 69% and the reason for this was questioned. An RH of 69% is used because this is the RH of a saturated sodium nitrate salt solution. A query was raised about the use of a salt solution since it was believed that sodium nitrate might decompose giving rise to  $\text{NO}_x$  gases. This however, was not thought to be the case.

The question was asked that in the paper by Rat, Guillaume, Wilker and Pantel on the stability of propellants whether humidity was a factor in the results obtained. It was confirmed that moisture/humidity had a huge effect on the heat flow curves. The excellent correlation between the different laboratories was only obtained by either fixing the moisture content or by carefully preconditioning the sample. The work was done on double base propellant but similar precautions had to be taken with single base propellants. It was also stated that when filling the sample ampoule that it should be filled as full as possible since this was representative of a filled cartridge with regards to the atmosphere surrounding the propellant.

Dr Laye asked "Where are we going with the technique of microcalorimetry and has DSC been used for long term studies?" Generally DSC has not been used for long term studies since the signal just goes to zero after a short time. This is because the DSC is less sensitive than a microcalorimeter, the difference in sensitivity being about 10,000 times. Kodak have used DSC for screening and run it for 1000 hours. Professor Charsley said that for long term studies heat treatment of samples could be carried out in a furnace prior to transferring the samples to the DSC for measurement of the amount of reaction remaining.

Dr Chin wished to see modifications to the cooling system for the TAM because it was open to the atmosphere and evaporation was continuously occurring. Long term experiments could not be left as the water level required frequent topping up. He suggested a sealed unit. A simple solution was suggested which used a secondary reservoir with a tube coming from the bottom and dipping just below the surface of the cooling water. When evaporation occurred the level of the cooling water fell, air entered the reservoir and water flowed out thus maintaining the level of the coolant water.

Dr Wilker highlighted the difficulty in crimping the lids onto glass ampoules. In some cases this can take a long time (15 minutes) and how can you define how tight is tight. Even with extreme care being taken, when crimping a lid, leaks can still occur.

## INTERPRETATION

Discussion on interpretation centred round the kinetics of reactions and in particular the kinetics of decomposition of double base propellants. Some delegates had observed a change in slope of the Arrhenius plot at 60°C. Dr Wilker said this change in slope did not occur in every instance but when it did the activation energy and pre-exponential factor used to calculate the service life of the propellant should be the one derived from the slope at lower temperatures. If the slope at higher temperatures, ie above 60°C is used then the kinetics would predict an unrealistic service life. He could not explain why the change in slope occurred but suggested it could be a change in mobility of small molecules within the nitrocellulose matrix. Workers at DERA, Bishopton reported they had obtained a linear relationship with samples examined at 50, 60 and 70°C.

Mr Svennson suggested that an apparent activation energy be used since activation energy relates to a single reactant. He stressed the importance of diffusion processes and thought that non-linear relationships in Arrhenius plots were due to differences in activation energy between diffusion and the chemical reaction contributions to the decomposition process.

Dr Bohn commented that in the study of kinetics of reactions the triacetin reaction was simple whilst the decomposition of propellants was difficult and complex.

Again the importance of moisture/humidity was stressed in obtaining satisfactory and repeatable results. Dr Wilker suggested a value of 0.68% moisture in the propellant and expected that in a glass ampoule the equilibrium between moisture and the sample to be achieved however he doubted if with larger cells that equilibrium would be reached.

Dr Laye asked what progress did delegates see in the future and did they want another meeting?

There was general agreement that a similar meeting to the Workshop should be held in 2 or 3 years. The reasons for this were that the technique was developing fast with new developments in hardware such as a microcalorimeter with a sensitivity of nanowatts becoming available. Also the problems experienced with the Relative Humidity Perfusion Unit should be overcome.

The use of microcalorimetry in the study of propellants is now routinely used but as this Workshop showed there are still problems to be overcome and understood. In the field of pyrotechnics, microcalorimetry is just starting to be used and it was felt that although some lessons can be learnt from the work on propellants the problems will need a different approach. Dr Chin thought adsorption/desorption studies would be a way forward and Mr Svensson thought diffusion would be important in the study of pyrotechnics.

On calibration and techniques it was felt that microcalorimetry was at the stage that DSC was 10 years ago and that there was a need for more study of experimental variables such as sample weights and gas flow rates. These should be sorted out in the next 2 years.

Dr Laye closed this session by thanking all the delegates for taking part in the discussion and making the Workshop a success by their active participation.

#### FOOTNOTE

Following the Workshop, agreement has been obtained in principle for a second Workshop, under the auspices of TTCP, to be held in the UK in 2 years time.

## LIST OF ATTENDEES

### AUSTRALIA

Dr Jerry Adams                      DSTO

### BELGIUM

Dr Pierre Guillame                P B Clermont SA

### CANADA

Dr David Jones                      Canadian Explosives Research Laboratory  
Dr Louis-Simon Lussier            Defence Research Establishment, Valcartier

### DENMARK

Mr Niels Frederiksen              Naval Materiel Command Denmark

### FINLAND

De Maija Hihkio                    Finnish Research Centre of Defence Forces  
Dr Irmeli Tuukkanen              Defence Materiel Establishment Headquarters

### FRANCE

Dr Corrine Bales                    ETBS  
Mr Stephan Moreau                SETARAM  
Ing Mauricette Rat                SNPE

### GERMANY

Dr Manfred Bohn                    Fraunhofer-Institut Fuer Chemische Technologie  
Dr Robert Heger                    BASF AG  
Dr Thomas Kroehl                  BASF AG  
Dr Stephan Wilker                  BICT

### THE NETHERLANDS

Mr Win de Klerk                    TNO - PML  
Dr B J van der Meer                TNO - PML



## NORWAY

Ms Inger Haaland	Royal Norwegian Navy Material Command
------------------	---------------------------------------

## SWEDEN

Ms Veronica Andersson	Nitro Nobel AB
Ms Anneli Lidmar	Nitro Nobel AB
Dr Jaak Suurkuusk	Thermometric AB
Mr Lars-Gunnar Svensson	Celcius Materialtekuik

## UNITED KINGDOM

Dr Peter Barnes	CESO (NAVY)
Mr David Blazer	DERA, Fort Halstead
Dr Paul Bunyan	DERA, Fort Halstead
Mr Tony Cardell	DERA, Fort Halstead
Prof Ted Charsley	Leeds Metropolitan University
Mr Jim Dodds	DERA, Fort Halstead
Dr Stephen Elsby	Royal Military College of Science
Dr Colin Fairclough	Unilever
Miss Heidi Fieldhouse	Leeds Metropolitan University
Dr Trevor Griffiths	DERA, Fort Halstead
Dr Nick Hudson	AWE, Aldermaston
Mr Ronald Jeffrey	DERA, Bishopton
Dr Peter Laye	University of Leeds
Miss Vicki Norris	DERA Chorley
Mr Jim Queay	Leeds Metropolitan University
Dr Daniel Read	Chloride Industrial Batteries
Mr Jim Rooney	Leeds Metropolitan University
Dr Satvinder Singh	CESO (Navy)
Mr Robert Taylor	Thermometric Ltd
Mr David Tucker	DERA, Fort Halstead
Mr Neil Turner	CESO (Navy)

## UNITED STATES

Mr Robert Boswell	NSWC, Indian Head
Dr Sima Chervin	Eastman Kodak Company
Dr Anton Chin	NSWC, Crane Division
Mr Joseph Domanico	ERDEC
Dr Bernie Douda	NSWC, Crane Division
Mr Daniel Ellison	NSWC, Crane Division
Dr Bill Hubble	NSWC, Crane Division
Dr Edwin Lewis	Calorimetry Science Corp

Dr Mark Phipps  
Mr H M Swett  
Dr Albert Tompa  
Mr James Wilson  
Dr Richard Winnike  
Mr Michael Zinn

Glaxo Wellcome  
NAWCWD, Chine Lake  
NSWC, Indian Head  
NSWC, Crane Division  
Glaxo Wellcome  
NSWC, Indian Head

## Distribution List

Mr P Twardawa (National Leader and Chairperson, WTP-4)  
Defence Research Establishment Valcartier  
2459 Pie - XI DIVD North  
Val-Beliar QC  
G3J 1X5 Canada

Dr J S Adams (National Leader, WTP-4)  
Aeronautical and Maritime Research Laboratory  
Weapon Systems Division  
PO Box 1500  
Salisbury SA5108 Australia

Dr H J Buswell (National Leader, WTP-4)  
Defence Research Agency  
Fort Halstead, Sevenoaks  
Kent TN14 7BP United Kingdom

Commander  
OL-AC PL/CA-R  
Attn: Dr Robert C Corley (National Leader, WTP-4)  
5 Pollux Drive  
Edwards Air Force Base  
CA93524 - 7048 USA

Dr P Barnes (Chairperson KTA 4-21)  
CINO, Ensleigh, Bath United Kingdom

Dr Bill Hubble  
NSWC Crane  
Indiana, USA

Mr Leo de Yong  
AMRL, Melbourne,  
Australia

Dr G Hooper  
VP(SS)  
Ordnance Board  
Abbey Wood  
Bristol  
United Kingdom

Dr J Platt  
DSc(Land)1,  
Main Building  
Whitehall  
London SW1A 2HB  
United Kingdom

Mr A E Cardell  
Defence Research Agency  
Fort Halstead, Sevenoaks  
Kent TN14 7BP United Kingdom

Dr T T Griffiths  
Defence Research Agency  
Fort Halstead  
Sevenoaks  
Kent TN14 7BP  
United Kingdom

Dr G Manton  
Defence Research Agency  
Royal Ordnance, Euxton Lane  
Chorley, Lancs United Kingdom

Dr K Smit  
AMRL, Melbourne,  
Australia

Mr R. Hancox  
AMRL, Melbourne,  
Australia

Mr J Wilson  
NSWC, Crane  
Indiana, USA

Dr B Douda  
NSWC, Crane  
Indiana, USA

Dr A Chin  
NSWC Crane  
Indiana, USA

Mr M Lateulere  
NSWC Indian Head,  
MD, USA

Mr F Valenta  
NSWC Indian Head  
MD USA

Document Exchange Centre  
DISNO  
Department of Defence  
Campbell Park Offices (CP2-5-08)  
Canberra Act 2600  
Australia

Director Scientific Information Services  
National Defence Headquarters  
Major General George Pearkes Building  
Ottawa K1A 0K2, Canada

Defence Research Information Centre  
Kentigern House  
65 Brown Street  
Glasgow G2 9EX, United Kingdom

Defence Technical Information Center  
(Attention: DTIC - OCC)  
Cameron Station (Bldg 5)  
Alexandria VA 22304-6145  
USA

Dr T T Griffiths  
Defence Evaluation and Research Agency  
Bld R47  
Fort Halstead  
Sevenoaks  
Kent, TN14 7BP

Attendees of the Workshop.